Microfiltration of micro-organisms: the effect of the extracellular matrix on fouling

Stec, Lara Zoe

Award date:
2001

Awarding institution:
University of Bath

MICROFILTRATION OF MICRO-ORGANISMS:
The Effect of the Extracellular Matrix on Fouling

Submitted by Lara Zoë Stec

for the degree of PhD

of the University of Bath

2001

ProQuest LLC
789 East Eisenhower Parkway
P.O. Box 1346
Ann Arbor, MI 48106-1346

Acknowledgements

There are many people who without their help I could never have completed this mammoth task. There are still more who have helped me improve on its content by helping me to make links between different research areas I would never otherwise have made.

I would like to thank my supervisor, Robert Field for having the patience to support me and giving me encouragement throughout the long process of completing my thesis.

I am also greatly indebted to Frank Podd, for his help in many aspects of my PhD, from beginning to end, from helping with my computer programs to being my chauffeur in the middle of the night!

My mother, Kate Stec has contributed in many ways to the existence of this thesis, from giving birth to me to scrutinising every page of writing to ensure contextual consistency and dead good English.

I would also like to thank all the technicians who helped me, Fernando Acosta, John Bishop and Richard Bull in particular.

The work on measuring the zeta potentials was made possible by Richard Bowen and the kind and generous donation of time by Paul Williams at the University of Swansea.

Finally, my thesis, my ability to carry out experiments and my time at Bath was enhanced by knowing the other postgraduates, especially Matthew Bennett, who was a very thorough proof reader, Chris Shorrock, Nayar Zahir, Meloney Bartlett, Jauhr Usman, Samantha Platt and Torsten Brinkman.

Summary

The microfiltration of micro-organisms is often treated as equivalent to the filtration of inorganic colloids. The presence of extracellular matrices means that microbial fouling is actually more complex, since its macromolecular constituents broaden the scale of relevant interactions.

This thesis attempts to gain a better understanding of how the extracellular matrix of a cell contributes to the balance between hydrodynamic and physicochemical factors that determine filtration behaviour.

Three gram negative bacteria of similar size and shape but distinctly different extracellular properties were selected for this purpose. *Sphingobacteria multivorum* NM1B 12558 is encased in a smooth polysaccharide capsule. *Pseudomonas putida* NM1B 9494 has many flagella, while *Pseudomonas elodea* NM1B 31461 is patented for its production of copious amounts of slimy polysaccharide, known as gellan gum. These bacteria were filtered under conditions of constant temperature, crossflow rate and crossmembrane pressure. The suspension conditions varied in valency (NaCl or $CaCl_2$), ionic strength and presence of BSA.

The resulting fouling behaviour was analysed both experimentally and theoretically; using blocking models derived from Hermia's equations using modifications for crossflow filtration.

Both methods demonstrated that cell deposition of *S.multivorum* was dominated by hydrodynamic effects; early rapid pore blocking kept cell deposition low. The exceptions to this rule were the high ionic strengths alone, particularly calcium. Addition of protein reversed these exceptions, and all proteinaceous suspensions had a uniform resistance value. Protein had a similar effect for *P.putida* suspended in NaCl solutions.

P.elodea exists in aggregate form under all conditions, and was therefore fundamentally affected by physicochemical conditions as they determined the type of aggregate formed. For example, increasing the ionic strength solution increased the cake density.

The cell deposition for *P.putida* was also controlled by hydrodynamic effects, except for solutions with high $CaCl_2$. This bacterium proved the most difficult to clean, postulated to be a result of flagella-pore bonding.

1 Introduction

Crossflow microfiltration (CFMF) is increasing in popularity, as the advantages become clearer and the disadvantages diminish. CFMF can offer continuous processing without a change of phase and nothing need be added (e.g. a flocculent) which then needs to be removed at a later stage.

CFMF is especially good for biological separations, since the system can be easily controlled and the risk of aerosol production is avoided. Shear stresses tend to be lower than with other methods such as centrifugation, so disruption of delicate biological material is reduced. Other processing conditions, such as pH, pressure and temperature, also tend to be mild.

In order to make CFMF a financially competitive prospect, fluxes have to be maximised to 100-150 $lm^{-2}h^{-1}$ or LMH (Kroner, 1984). Below these flux values the membrane areas required are very large and costs are high.

Therefore an understanding of which forces and parameters dominate the filtration behaviour of biological suspensions must be improved in order to attain this goal. There are several ways particles can foul a membrane. The contribution of each type of fouling to the overall decrease in flux is dependent on: -

- the operating conditions
- the membrane properties
- the particle properties
- the properties of the liquid in which the particles are suspended, including the solutes present.

At present many experiments and iterations need to be performed to find satisfactory operating conditions; an improved understanding of the mechanisms involved for each type of fouling can help to speed up this process.

Understanding of how cell parameters at a macroscopic scale affect fouling by their interaction with the hydrodynamics of a system has improved greatly in the past decade. Parameters such as particle size and size distribution has been the focus of much attention (Altmann and Ripperger, 1997; Li, Fane, Kostner, Vigneswarin, 1998; Field, Wu, Howell & Gupta, 1995; Foley, Malone & MacLoughlin, 1995b).

Results are consistent, whether bacteria or particles such as silica or mineral colloids are examined, because particle size is a parameter independent of material type. On the other hand, characterisation of particle shape effects using colloids as a model is difficult, as colloids differ in shape considerably (Tarleton and Wakeman, 1993). However, examination of the effects of bacteria cell shape is a simpler prospect, and progress has been made in this area (Tanaka, Usui, Kouda & Nakanishi, 1996).

The effects of pH and ionic strength on filtration of large colloids is not a popular research topic as physicochemical forces are subsumed by hydrodynamic forces at around 0.5 μm and above (Tarleton and Wakeman, 1994). On the other hand, their effect on proteins has been a source of frequent examination (Marshall, Munro & Tragårdh, 1993). Although most bacterial particles are above 0.5 μm, they are surrounded by an extracellular matrix of macromolecules such as carbohydrates and proteins. Therefore, physicochemical factors and their effect on bonding are much more important for micro-organisms than colloids.

The presence of this extracellular matrix may also affect filtration behaviour at a more mechanical level, as it is often compressible, even when the cell itself is not. Hodgson, Leslie, Schneider, Fane, Fell and Marshall (1993a) demonstrated the importance of this compressible layer by studying the effects of its removal. However, they ignored the precise properties of the extracellular coating (or matrix).

This thesis attempts to elucidate how hydrodynamic forces on one level compete with physicochemical effects on another level to influence the filtration behaviour of three bacteria with different extracellular matrices. The three species of rod-shaped bacteria selected are listed below:

1) *S.multivorum* - smooth capsule

2) *P.elodea* - copious slimy gellan gum

3) *P.putida* - numerous flagella at each end

These three bacteria were filtered under similar crossflow velocity and longitudinal pressure conditions. The first few experiments were conducted with the cells in broth. However, for the majority of experiments, the cells were suspended in various salt solutions, differing in ionic strength (high and low) and valency (Na^+ and Ca^{2+}). The pH was kept constant at 6.6 for all experiments. To investigate the effect of protein on filtration behaviour, most experiments were repeated with 1g/l BSA added to the suspensions.

This report begins with a literature review on the microfiltration of cells and their separation from broth and the proteins they produce. It describes the effect of operation conditions on the flux, with a brief discussion of the models available that attempt to explain these effects. The interaction of cells and proteins with each other and the membrane surface is discussed, and the observed effects of these interactions are recounted. The importance of shear on filtration behaviour is also detailed, along with factors affecting specific cake resistance and the development of cake structure over time, particularly with respect to rod-shaped organisms.

The next chapter reviews the current knowledge of the three cells selected, including their industrial uses, and describes the criteria for their selection. This chapter also describes the BSA protein utilised in these experiments.

Chapter 4 contains the materials and methods employed in this thesis. The first part covers the cell surface characterisation studies. These involved experimental tests to ascertain cell sizing, hydrophobicity, zeta potential, viscosity and the presence of polysaccharides. The latter part of this chapter lays out the materials and methods for the filtration experiments. It describes the rig, the experimental conditions and the cleaning regime. The initial experiments were carried out while the cells were suspended in broth, but the majority of experiments were undertaken in the salt solutions or salt/protein solutions described above. They were performed at constant crossmembrane velocity and longitudinal pressure. The transmembrane pressure (TMP) was 0.5 bar for the majority of each experiment, i.e. after the initial steep flux decline had taken place.

Chapter 5 contains the results for the cell characterisation described in the first part of the materials and methods section.

The experimental results for the filtration studies are laid out in Chapter 6, where they are analysed in terms of resistance, relative increase of cell deposition to resistance, specific cake resistance (SCR) and cell deposition in terms of cell layer equivalents. The effect of the different conditions on final flux, irreversible fouling, protein transmission, and deposition are also presented. Distinct trends, both for each organism and for each type of solution can be discovered by these examinations.

Chapter 7 analyses these same results by fitting them to three model approaches, all derived from Hermia's dead-end filtration model. The model approaches suffer, to different extents, from assumptions that are not fully met by the experimental conditions (i.e. the transmembrane pressure fluctuates). However, one model approach fits all of the

experimental results well, while another fits the *P.putida* and some of the *P.elodea* results well.

The subsequent chapter discusses the results from the experimental and theoretical chapters and compares the trends found.

Finally, chapter 9 contains the overall conclusions and a discussion of further work.

2 Background literature

2.1 Introduction

Crossflow microfiltration is an important separation method for a variety of applications including wastewater treatment and nuclear waste. It is a particularly useful for biological systems for the following reasons: -

a) The low-density difference between liquids and solids do not matter (Kroner, Schutte, Hustedt & Kula, 1984).

b) Modest operating conditions with respect to temperature, shear etc.(Brown & Kavanagh, 1987)

c) Good containment to satisfy GMP (good microbiological practice) (Lojkine, Field & Howell, 1992)

d) Unlike dead end filtration, it can be operated for long periods of time without the flux decreasing to zero.

e) The permeate from CFMF tends to be cleaner than a centrifugal supernatant (Le, Spark & Ward, 1984a)

f) Higher purity means processing may be reduced to one step in some cases (Mourot, Lafrance & Oliver, 1989).

Crossflow microfiltration has many applications as a result of its particular pore size range (10^5 Dalton to 1μm) such as:

- Separation of whole cells from extracellular products (Le, 1987), (Sims and Cheryan, 1986)
- Biomass concentration (Mourot *et al.*, 1989),
- Separation of cell debris from intracellular products (Le *et al.*, 1984a, Le, Spark, Ward & Ladwa, 1984b).
- Cell recycling when a microfiltration membrane is coupled to a fermenter (Defrise & Gekas, 1988).

CFMF can be operated in more than one mode. Traditionally, pressure or crossflow velocity is kept constant throughout the duration of the run. If the system volume is constant (e.g. retentate is returned to the feed). This leads to a flux pattern similar to that shown in Figure 2.1, where there is an initial dramatic fall in flux, followed by an elbow as the rate of flux decline slows, and finally a period of gradual flux decline (quasi-steady state) until a steady state is reached.

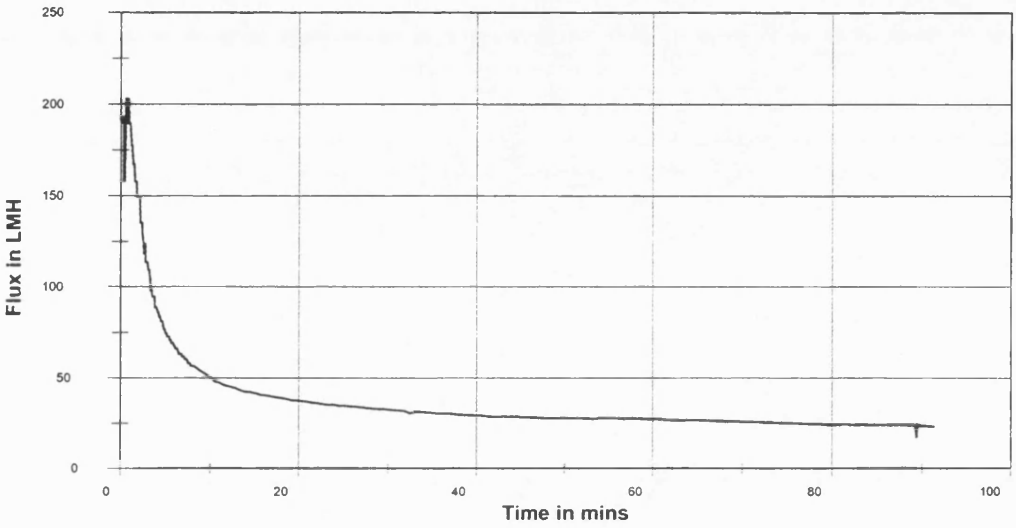

Figure 2.1 Typical flux reduction curve (*P.elodea* in high $CaCl_2$)

This flux behaviour is due to fouling. The different types of fouling in microfiltration and a description of experiments to visualise fouling are described in section 2.2. The parameters that affect fouling and filtration performance are detailed in section 2.3.

Recently, constant flux operation has been recommended (Field, Wu, Howell, and Gupta, 1995) since below a critical flux value, particular to each system, fouling will not occur. However, pressure and crossflow velocity must be dynamically changed to maintain this constant flux. Since flow conditions within the pores are constant, this mode of operation is useful for investigation of membrane performance. The learning from operation at critical flux is expanded in section 2.3.3

The probability of a particle contributing to overall fouling depends not only on forces linked to hydrodynamic considerations, but also on physicochemical forces. Both of these types of forces, and modes for their resolution, are described in section 2.4. Models for microfiltration and cell adhesion as a result of these forces are discussed in sections 2.5.2 and 2.5.1.

Modelling of bacterial cell filtration is often closely linked to that of colloids. Although colloids are slightly smaller than most bacterial cells, they are simpler and therefore easier to study when discovering the effect of hydrodynamic forces on particles. On the other hand, proteins are one or two orders of magnitude smaller than bacteria, but offer more of an insight into the complexity of filtration of biological entities. Therefore section 2.7 expands upon research into microfiltration of proteins, which is a more broadly studied topic than that of cells. Preceding this, section 2.6 summarises how pH and ionic strength conditions might influence cells.

Finally, section 2.8 provides examples of how cells and protein interact during experimental research.

2.2 Fouling

Reduction in flux due to fouling can occur by a variety of mechanisms. One or more of these mechanisms may occur for a given system depending on the system conditions, and are illustrated in Figure 2.2 to Figure 2.7.

1) Pore blocking may occur only when the membrane surface is relatively clear i.e. the cake layer is less than one cell thick. It occurs when the relative dimensions of a pore and particle are close (see section 2.3.7). If a particle completely blocks a pore then there is no flux through the pore, pictured in Figure 2.2. If the particle is slightly smaller than the pore, it may rest just inside the pore and reduce the effective pore area

2) For particles much smaller than the pores, such as macromolecules, deposition inside the pores throughout a pore is possible, also reducing the effective pore area, Figure 2.4. A single adsorptive layer of protein, known as ***conditioning***, is believed to affect binding of the cells to the membrane.

3) For cake filtration (Figure 2.5 to Figure 2.7), flux is reduced due to the tortuosity of the path that the liquid must take through the cake as well as the size of the channels. Both elements depend partly on the size of the particles in the cake and partly on the compressibility, since both of these determine the voidage. Compressibility of cells depends partly on their water content, (Shimuzu, Shimodera & Watanabe, 1993) and partly on the polymers belonging to the extracellular matrix of the cells or adsorbed macromolecules (Hodgson *et al*, 1993a). Figure 2.6 and Figure 2.7 compare filtration of cells with uncompressed and compressed extracellular layers respectively. When the layers are compressed, the voidage is reduced. Most

bacterial cells are incompressible themselves, but may have compressible extracellular matrices (see section 2.5.2.3).

4) Finally, there is a mechanism akin to concentration polarisation of macromolecules. The particle concentration gradient will tend to be higher closer to the membrane rather than at the middle of the tube. When the density of the particles is great enough, this may result in a "flowing cake" which contributes to the cell path tortuosity and inhibits particle transport to the membrane surface. Hsu (1988) found that taking this layer into account, and assuming particles were free to diffuse between the bulk and the membrane wall via the diffusion boundary layer, modelling accuracy was increased.

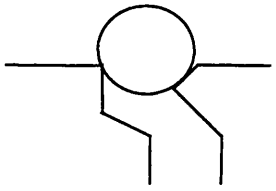

Figure 2.2 pore blocking

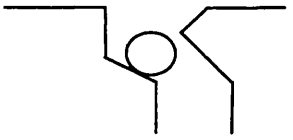

Figure 2.3 Partial pore blocking

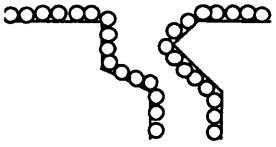

Figure 2.4 standard blocking and conditioning

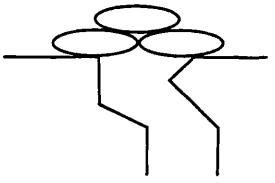

Figure 2.5 cake filtration for a colloid

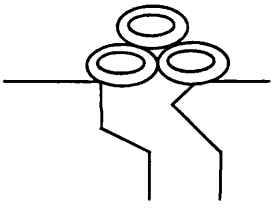

Figure 2.6 cake filtration of cells and uncompressed polymer

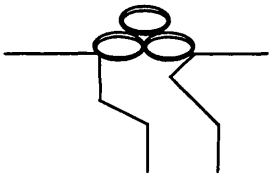

Figure 2.7 cake filtration of cells and compressed polymer

Murase, Ohn and Kimata (1995) tried to explain the curvilinear relationship illustrated in Figure 2.1 by attributing the first part to pore blocking, while the quasi-steady state part is due to cake filtration. The time for the initial phase is reduced at lower transmembrane pressures (TMP) or larger solids concentrations. As soon as these

parameters pass a critical level, cake filtration sets in. Huang and Morrisey (1998) also found this type of fouling behaviour.

Kuruzovich and Piergiovanni (1996) suggested that the same curvilinear relationship seemed to be due to cake deposition for the first phase, followed by compression and a few additional layers at the quasi-steady state.

Shimuzu, Matsushita & Watanabe (1994) found that when filtration of whole baker's yeast cells was compared with filtration of homogenate of the same cells, the main type of fouling on the same membrane changed from pore blocking to cake filtration. Pore blocking is dominated by membrane properties while cake filtration is dominated by the operating parameters such as TMP and crossflow velocity.

Gekas and Hallström, (1990) pointed out that the type of fouling to predominate affected the ratio of reversible fouling to irreversible fouling; reversible fouling disappears when the operation conditions are made less stringent, reversed or if the membrane is rinsed. Flowing cake and pore blocking are reversible, while dense cakes are irreversible and require chemical cleaning. The most extreme case of irreversible fouling is when increasing shear has no effect on the fouling or the flux (Taddei, Aimar, Howell & Scott, 1990). This is common for tightly bound protein fouling.

2.2.1 Fouling of protein and cells together

Gekas & Hallström (1990) and Foley, MacLoughlin & Malone (1995a) found that fouling due to particles (silica for the former, yeast for the latter reference) and proteins is non-additive. If protein fouling on its own is by cake filtration rather than adsorption, the presence of the particles prevents the protein from fouling the membrane surface, therefore the typical tightly bound irreversible proteinaceous cake cannot be formed and flux reduction is attenuated with respect to protein alone.

When filtering protein and silica particles in the same system, Gekas & Hallström (1990) found that protein feeds fouled irreversibly, while silica feeds had a degree of reversibility. This was accounted for by considering that the balance of fouling mechanisms was different for each feed. Photography of the membrane, post filtration, verified that the protein formed a dense, gel-like cake, while the particles either blocked the pores or formed a diffuse cake.

Often when proteins and particles are filtered together, a secondary layer is formed by the particles and it is this, and not the microfiltration membrane that controls

the filtration behaviour of the proteins (Datar 1985). See section 2.8 for further details. The actual pore size thus becomes smaller than the rated pore size.

Therefore, although flux will always decrease with a curvilinear relationship with steady transmembrane pressure operation, the mechanisms for this decrease will not always be the same and the dominant parameters must be ascertained on a case by case basis.

2.2.2 Observation of Particles

Over the past decade there have been increasingly sophisticated visualisation studies of how particles behave in a CFMF system. Video cameras were used to observe the particles during filtration for all papers.

Mackley and Sherman (1992) carried out particle visualisation experiments on polyethylene beads of size 125-180 μm to observe how system hydrodynamics affect particle deposition.

They found that when filtrate flux dominates at the beginning of the run, particles approach at steep angles and attach to the membrane where they impact. This results in random packing. Later on when crossflow (CF) velocity dominates, particles will approach at shallow angles and roll along the cake until an energetically favourable site is reached. This means that packing becomes very selective. Voidage fractions are expected to be between 0.44 for random loose packing and 0.26 for highly ordered hexagonal close packing of spherical particles.

Eventually particles may roll along the cake without being captured at all. The angle of impact due to the CF velocity to flux ratio seems to be a deciding factor for cake build-up. The limiting angle depends on particle size.

This work endorses the particle adhesion models (see section 2.5.2), although the probability of capture decreases gradually rather than there being a sharp cut-off point. No evidence for back-flow was seen, although this may have something to do with the large size of the particles investigated.

Hodgson, Pillay & Fane (1993b), observed that for yeast of around 10-21 μm and resin particles of around 21 μm, a flowing cake layer appeared only during a transition phase from one pressure to another. Li *et al*, (1998) found a more complex situation; for yeast at around 5 μm and latex particles of 6.4 and 11.9 μm, single particle rolling was observed at or above the critical flux. For 3 μm particles however, a flowing cake was

observed under the same conditions. The general trends observed were the slower the crossflow, the more sluggish the movement of the particles, and the smaller the particles, the more mobile they were. Particle deposition probability increased with the number of particles already deposited, as particles were more likely to deposit behind each other. Local variations in membrane characteristics affected the local flux, so some areas of the membrane attracted more particle deposition than others did.

2.3 Factors affecting performance

2.3.1 Transmembrane pressure

Transmembrane pressure is one of the most significant factors in cross-flow microfiltration (CFMF), because it provides the driving force for the mass transfer of permeate through the membrane pores. The most common mode of operation is to conduct experiments keeping the transmembrane pressure constant. Nevertheless, keeping the flux constant and below a critical value to avoid irreversible fouling is increasing in popularity. This is managed by gradually increasing the pressure from an initial low value. The transmembrane pressure (TMP) is defined as: -

$$TMP = \frac{P_1 + P_2}{2} - P_3 - \Pi$$

i.e. the transmembrane pressure is the average of the inlet and outlet pressure (P_1, P_2 respectively) minus the permeate pressure (P_3) and osmotic pressure difference (Π). The osmotic pressure difference is not relevant for cells.

Early work on ultrafiltration membranes showed that an increase in TMP leads to a linear increase in flux up to a pressure independent region. The critical pressure value increases with increasing wall stress and decreasing cell suspension (Porter, 1972).

The picture for microfiltration is similar (Le *et al.*, 1984a), (Le, 1987) but, above the pressure-independent region, the relationship between flux and pressure seems very variable, due to other factors such as increased viscosity and compression complicating the issue.

As the pressure increases, the layers may be compressed. Hence flow through the cake becomes more difficult, especially when the particles are forced into the pores (Hodgson *et al*, 1993a). This leads to a reduction in flow through the pores and reduces the positive effect of the increase in pressure driving force. During concentration

experiments, the increase in viscosity requires an increase in pressure to maintain flux. Once the pressure limit for the membrane is reached, cell concentration must stop.

Sometimes if the pressure is too high, breakthrough of cell matter can occur and the permeate becomes turbid (Le, 1987). However, working near, but not at, the pressure independent zone can give a good flux (Hodgson *et al*, 1993a). A well chosen transmembrane pressure is required for an effective scale up operation (Rusotti, Göklen & Wilson, 1995).

2.3.2 Crossflow Velocity

This is another important parameter for effective control of filtration and fouling, since this affects the rate of removal of particles from the membrane/cake surface back into the retentate, and thus helps to prevent particle deposition. Generally, the flux varies with crossflow velocity raised to the power n. The value of n is system specific and is partly dependent on the flow regime. Le (1987) found that the geometry of the system was crucial for laminar flow estimations. Duddridge and Pritchard (1979) pointed out that an increase in crossflow velocity decreased the thickness of the boundary layer across which mass transfer must take place. With the onset of turbulence, the resultant eddies help to transport both fluid and particles to the membrane. This increase in transport of particles to the membrane is balanced by an increase in shear (see section 2.3.10).

The effect of increasing crossflow velocity is usually positive, i.e. flux increases with crossflow velocity. This is because the shear rate also increases, thereby removing particles from the surface (Riesmeier and Kroner, 1987). The benefits of increasing crossflow however can be reduced by problems occurring as the result of a concomitant increase in TMP. Sometimes n may be negative, as increasing crossflow velocity means a higher proportion of smaller particles forming more densely packed cakes (Kroner *et al*, 1984), (Mackley, 1987). Le Berre and Daufin (1996), using a particle deposition model (see Table 2.1), explained how an increase in crossflow velocity might lead to removal of larger particles, leaving a denser cake of smaller particles, with a greater resistance to flux.

Lojkine, Field & Howell (1992) pointed out that once fouling is established, a change in crossflow velocity has no effect. The word 'established' refers to irreversible types of fouling, rather than the length of time filtration has occurred. For example, if

the cake formed is very dense and well bonded together, an increase in crossflow velocity will not affect it.

Increasing the crossflow usually increases both initial flux and steady state flux over time (Gatenholm, Fell & Fane, 1988a). Shimuzu *et al* (1994) found that initial feed velocity has a linear-log relationship with the steady state flux.

For critical flux operations, crossflow velocity can affect the fouling mechanisms (Field *et al*, 1995), (Li, Fane, Kostner & Vigneswarin, 1998). Operating at a higher crossflow velocity increases the critical flux.

2.3.3 Constant Flux

Microfiltration is usually carried out at a constant transmembrane pressure, which results in a flux decline over time with a similar shape to Figure 2.1. Flux changes result in other conditions such as concentration, solubility and rheology of the boundary layer also changing.

By using constant flux and keeping the transmembrane pressure as a dependent variable, the convective flow of both particles and solute towards the membrane is kept constant (Aimar, Howell & Turner, 1989).

The flux selected should be below the critical flux, that is the flux below which irreversible fouling does not occur (Field *et al.*, 1995). The critical flux value for a system depends on the geometry and hydrodynamics of a system. The initial TMP must be carefully selected; it must be low enough to ensure the critical flux is not exceeded. At an optimum initial flux, the TMP may gradually be increased to values higher than the start-up TMP values that cause blockage.

These phenomena may be explained in several ways. If the start-up flux is low enough, the mechanisms may change from pore blocking to cake build-up. Fouling becomes reversible once the cake has built up. This leads to a higher limiting flux. The nature of the cake is also important. If the TMP is low at start-up time, a flowing cake may result. At a higher initial TMP, the cake is believed to be a combination of stagnant and flowing cake that makes the cake resistance higher.

Considering the results of Mackley and Sherman (1992) it may be seen that the resistance to flux is dependent upon the initial TMP and therefore the initial flux, since particle capture probability increases as flux increases. There is evidence to suggest that if the velocity of flux through the pores is much smaller than the membrane surface

velocity (due to crossflow), a vortex is generated, which minimises pore blockage. Such is the situation for sub-critical flux operation.

Under normal start-up conditions, the surface and pore velocities are close in value. In this case streamline flow occurs which leads to greater blockage of pores. With regard to crossflow velocity effects, cake build-up may be retarded by high shear stress (see section 2.3.10).

2.3.4 Temperature and viscosity

Temperature effects are quite significant, because of the changing viscosity of the liquid filtered. The liquid viscosity controls flow through the pores. Scott (1988) noted a fivefold increase in flux when filtering yeast cells over a temperature range of 13-30.5^{o}C. This effect is more than one would expect from a consideration of the temperature dependency of viscosity alone. It suggests the cake itself has changed. Such changes may be due to macrosolutes being more soluble at high temperatures, or, according to Defrise & Gekas, (1988) it may also be due to the change in viscosity of the cell coatings.

Shimuzu *et al* (1993) found the flux at steady state to be inversely proportional to the viscosity of the suspension. This can be explained in part by an observation of Defrise and Gekas (1988); that cake layer thickness increases with the viscosity of the cake layer.

2.3.5 Cell Concentration

The effect of cell suspension concentration is particularly difficult to study since many other factors are involved which derive from the dramatic increase in viscosity. Wall stresses may change from turbulent to laminar. The situation is simpler for ultrafiltration where the flux is inversely proportional to the log of the cell concentration.

For microfiltration however, the relationship between flux and time during concentration is usually sigmoidal (Kroner *et al.*, 1984), (Mourot *et al*, 1989), (Scott, 1988). The first two sections follow a typical fouling pattern over time as seen in Figure 2.8. The third section, where flux suddenly decreases is due to the exponentially increasing viscosity which means that the operation parameters such as crossflow velocity and pressure can no longer be controlled (Belfort, 1989). With higher viscosity suspensions this loss of control occurs at a lower cell concentration. Rossotti *et al*

(1995) found that when filtering *S. griseofuscus* cells, the cell slurry behaved like a high viscosity Bingham plastic at cell concentrations beyond 60% w/v.

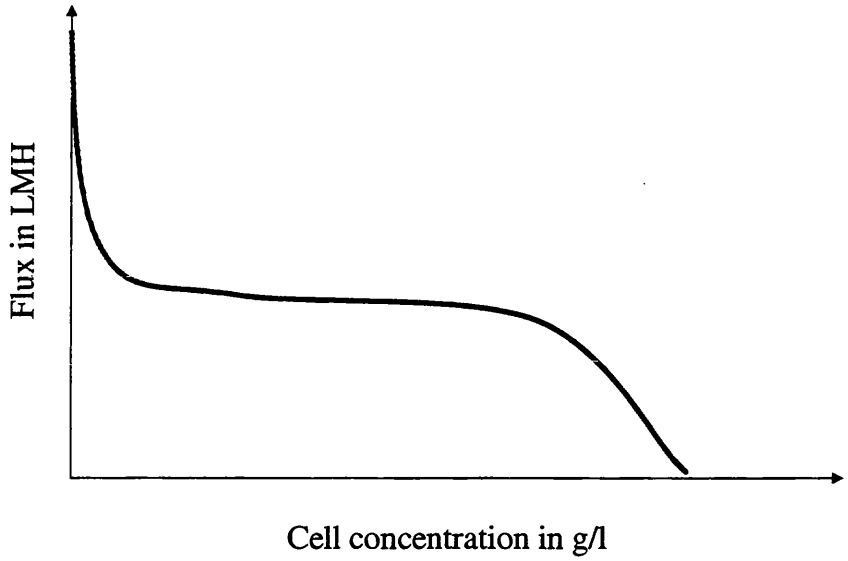

Figure 2.8 Effect of increasing concentration on flux

The point at which the viscosity suddenly increases seems to be independent of membrane type; Scott, (1988) found the critical concentration after which flux suddenly decreased was the same for both UF and MF membranes. This suggests hydrodynamic considerations are very important here.

The sudden drop in flux may be due to a transition from turbulent to laminar flow. Consideration must also be given to the transition of the cell suspension from Newtonian to Non-Newtonian behaviour as concentration increases. Both Le *et al.*, (1984b) and Gatenholm, Patterson, Fane & Fell, (1988b) found two distinct areas for mass transfer coefficients with respect to increasing cell concentration. At low concentrations, the mass transfer coefficient is very high; but at a critical cell concentration, the mass transfer coefficient decreases dramatically; Le *et al.* (1984b) reported a decrease of a factor of five above a cell concentration of 1% dry weight.

This lower mass transfer coefficient remains quite steady up to a high value, however, Le (1987) also found that the effects of the membrane were diminished; membranes with pore sizes of 0.45μm and 0.8μm had similar mass transfer coefficients above a critical cell concentration.

2.3.6 Growth conditions

Growth conditions such as temperature and oxygen supply can affect the rate of growth. The slower the growth rate, the more varied the age of cells in a population. Cell age seems to affect the filtration behaviour of bacteria.

Powell & Slater (1982) noticed that bacterial cells taken in stationary phase are not removed by shear so easily as those that are taken at the beginning and end of the log phase of growth. They suggested that this might be due to cell lysis occurring with the older cells, or that extra proteins or polymers may be secreted during stationary phase.

Taddei *et al* (1990) studied the filtration of yeast, and found that log phase cultures had a higher attachment to the membrane than stationary phase cultures. They explained this phenomenon in terms of the higher oxygen concentration for log phase yeast. Yeast produces unsaturated acids and sterols only in the presence of a high oxygen concentration.

Tanaka *et al* (1996) also noted the difference in filtration rate between gram negative bacteria of different ages. Sonak & Bhosle (1995) discovered that the bacterial cell surface hydrophobicity changes during different phases of growth, which may also help to explain this phenomenon.

2.3.6.1 Media

Media can affect filtration behaviour in several ways; the ionic strength of the medium may be important, since lower ionic strengths may minimise protein aggregation (Forman, De Bernardes, Feldberg & Swartz, 1990) or maximise flux by expanding the fouling cake (Hodgson *et al*, 1993a). Any polymers may attract ions and increase the local ionic strength (Defrise & Gekas, 1988). A further discussion of the effects of ionic strength can be found in section 2.6.

The choice of nutrients in the broth must be chosen carefully. Different proteins may adsorb either to the cell or cell debris or to the filtration membrane, thus affecting the flux (Kroner *et al.*, 1984). For example, Göklen, Thien, Ayler, Smith, Fisher *et al*, (1994) found that a peptonised milk-based broth adversely affected both the flux and the transmission of other proteins, which was avoided on scale up by changing the type of broth. Different broth nutrients may also affect the properties of the cells. For example, the hydrophobic properties of *Acinetobacter calcoaceticus* are affected by the carbon source, while an increase in sugar content of a broth for *Candida* strains helps their ability to attach to surfaces (Defrise & Gekas, 1988).

However, the broth ingredient with the most profound effect is antifoam (Kroner *et al.*, 1984, Riesmeier *et al.*, 1987). Antifoams are surfactants that accumulate on the membrane surface, usually by hydrophobic interaction. Some antifoams may improve

flux (Field *et al*, 1994) but most do not. Flux reductions of hydrophobic membranes are more pronounced than hydrophilic membranes, although both types are affected (Jönsson & Jönsson, 1991).

Silicone based surfactants seem particularly bad for all types of membranes (Fane, Kim, Hodgson, Leslie, Fell, Franken, Chen & Liew, 1990). Their effect is immediate and does not vary with alteration of crossflow velocity, showing mass transfer above the membrane is not an important mechanism for fouling in these cases (Field *et al.*, 1994).

2.3.7 Membranes & Pores

Membranes and their modules can be classified by their: -

- Geometry
- Pore shape
- Mean pore size
- Pore size distribution (range of pore sizes on the surface)
- Porosity (percentage of membrane voidage)
- Chemical properties

2.3.7.1 Geometry

Tubular or capillary membranes have the advantage of well-defined flow conditions (Schulz & Ripperger, 1989). When utilising flat sheet membranes, using small channel heights with high velocities can increase fluxes. This gives a high wall shear rate for both laminar and turbulent regions (Hodgson *et al*, 1993a). Pleated membranes can concentrate solutions effectively (Tanny, Mirelman & Pistole, 1980). Permeate-side geometry is important, since a complicated permeate-side geometry may result in a higher backpressure and therefore a lower TMP (Hodgson *et al*, 1993a).

Filter length is important for both types of membrane. As distance from the membrane entrance increases, the pressure gradient decreases due to frictional energy losses. Thus as the thickness of the fouling layer increases, the flux decreases along the membrane length (Riesmeier *et al*, 1987). This means that shorter lengths of membrane give higher overall fluxes, but have a disadvantage in that their low-pressure gradients inhibit the ability to decouple TMP from shear generation. The average wall

concentration is lower in short channels, so pressure-independent regions may not exist if filtration units are short enough (Aimar *et al.*, 1989).

Laminar flow conditions in cross flow microfiltration are not ideal, since there is poor mass transfer and mixing within the vessel. If the viscosity is low enough, operating in the turbulent regime can reduce this problem. Even then the radial velocity components are approximately only 1/10 of the axial velocity.

By choosing the correct type of oscillatory motion and equipment geometry, it is possible to obtain a flow where radial velocity is comparable to axial velocities, so that better mass transfer and better scouring are obtained (Mackley, 1987).

Neither the use of baffles nor oscillatory motion alone can lead to a significant increase in flux (Wu, Howell & Field, 1993; Field *et al*, 1995; Mackley, 1987; Mackley & Sherman, 1992). However, the use of both techniques can lead to an improvement of flux of up to 30% when centre baffles are used (Mackley & Sherman, 1992).

Mackley & Sherman (1992) performed a flow visualisation study to demonstrate the mechanisms by which the membrane is scoured. Only by oscillating the flow can the eddies formed be swept into the bulk flow. Wall baffles shield the cake from the crossflow more than centre baffles, so they are less efficient.

At optimum oscillation amplitudes, each space between the baffles acts like a well-stirred tank. If there are several continuous stirred tanks in a row then plug flow will result. The oscillation amplitudes required are small so that energy consumption is kept to a minimum. Performance may be further improved by differential pressure switching, which gives the crossflow the opportunity to scour the membrane.

Considering the results of Mackley and Sherman (1992) it may be that the resistance is dependent upon the initial TMP and therefore the initial flux, since particle capture probability increases as flux increases. There is evidence to suggest that if the velocity of flux through the pores is much smaller than the membrane surface velocity, a vortex is generated which minimises pore blockage. Such is the situation for sub-critical flux.

Under normal start-up conditions, the two velocities are close in value. In this case streamline flow occurs which leads to greater blockage of pores. With regard to cross-flow velocity effects, cake build-up may be retarded by high shear stress.

2.3.7.2 Membranes

There is a range of methods and materials available to manufacture microfiltration units, each with their distinct characteristics.

Most microporous polymeric membranes have anisotropic pores, which are narrow at one surface, then expand below the surface into a sponge-like structure, with interconnecting pores (Hodgson *et al*, 1993a). Their porosity is in the 70-80% range. The pore density tends to be quite high and pore size distribution tends to be quite wide (Fane *et al.*, 1990).

Nucleopore or nucleation track membranes however, have cylindrical or isoporous pores: their pore size distribution is very narrow and in the microfiltration size range. They have a low pore density and hence a low porosity, and are therefore inappropriate for applications where maximising flux is important (Brock, 1983).

Ceramic membranes are also available, with variable pore densities and wide pore-size distributions. This makes filtration of small particles inefficient (Mourot *et al*, 1989). These are essentially depth filters; i.e. they do not have a proper pore structure.

Sintered filters are generally made from glass, porcelain or metal. They are made by fusing small particles of material together. They have a restricted use because both the pore density and the porosity are very low and therefore the filtration rate is low. The pore size distribution is narrow however (Brock, 1983).

Finally, there are membranes made from anodised metal. They have a narrow pore-size distribution, cylindrical pores and a high pore density. According to Fane *et al* (1990), these membrane properties are the optimum for minimising fouling.

2.3.7.3 Membrane selection according to material properties

Many organisms prefer to adsorb to low energy hydrophobic surfaces (Defrise and Gekas 1988) and are negatively charged. Therefore as a rule of thumb, to minimise fouling on a crossflow microfilter, hydrophilic and/or negatively charged membranes are the best for downstream processing of biotechnology products. However, these are not always the most appropriate criteria; other factors such as pressure tolerance, or resistance to chemicals may be more important.

Sometimes hydrophilic membranes increase fouling. If the surface tension of a particle (a measurement of surface energy) is higher than that of the liquid in which it is suspended, adhesion favours hydrophilic (high-energy) surfaces over hydrophobic

surfaces (Defrise and Gekas, 1988). This principle also applies the other way round, which is the more usual situation (see section 2.4.6.2).

The decrease in flux for some systems, such as that described in Göklen *et al* (1994) is not affected by this property of the membrane. Göklen *et al* (1994) attributed the decrease in flux for this system either to concentration polarisation or a flowing cake; they did not observe any deposition on the membrane. Therefore this observation is only to be expected, as the cake does not come into direct contact with the membrane.

2.3.7.4 Pores

Pore size and distribution are the critical factors for initial fouling, and, if fouling is less than one layer thick, for the whole run. Microfiltration membranes have cut-off points ranging between 10^5 daltons-1μm (Brown, 1987), although between 0.1 and 0.6μ m is more usual (Schulz & Ripperger, 1989).

Pores should be big enough to prevent macromolecules from getting stuck in them, but too small to risk cell debris or particles from entering the pores and getting blocked.

A description of how the relative sizes of particle/macromolecule and pore determine the types of fouling encountered has already been discussed in section 2.2. It is important to note that although these interactions may be easily classified, a combination of types of pore/particle interaction is likely to be encountered in any given system (Fane *et al*, 1990).

Spacing between the pores is important; the specific resistance of the cake layer is greater for less porous membranes. Fane *et al* (1990) suggested that this was due to longer path lengths. Ethier & Kamm (1989) demonstrated that the hydrodynamic resistance of the rejecting membrane becomes significant when filter cake thickness is smaller than or comparable to the pore separation. Under these circumstances, the effect of increasing velocity and therefore resistance around pores becomes significant; the flow of permeate is two dimensional rather than one-dimensional. Hodgson *et al* (1993b) filmed the fouling of 10 μm yeast and 20 μm silica particles on a lower pore density 0.2 μm membrane and a high pore density 0.02 μm membrane. Under the same operating conditions, the initial flux was higher for the 0.2 μm membrane. Both membranes had fouling less than a layer thick, but the 0.2 μm membrane had more complete coverage as a result of a higher initial flux.

Le *et al*, (1984b) compared cell harvesting data for *Erwinia carotovora* using 1.2μm, 0.6μm and 0.45μm membranes. They found that the membrane that gave the highest fluxes was the intermediate 0.6μm membrane. This was explained by comparing the particle size with the membrane surface dimensions. If the particle size is less than the interpore distance and greater than the pore size, total plugging of a pore is possible, since the particle can completely cover the pore. If the particle size is greater than both pore size and interpore distance, total plugging of pores cannot occur.

2.3.7.5 Microsieves

Kuiper, Van Rijn, Nijdan and Elwenspoek (1998) have reported a new type of microfilter, named a microsieve. These membranes have a very low flow resistance, due to a membrane thinner than the pore size, with a low resistance support. The porosity is as high as possible and the pore size and distribution are uniform over the membrane. All these features mean the flow resistance is low, so it can operate at a low transmembrane pressure.

The microsieve is made of chemically resistant silicon nitride with a roughness below 10nm. Beer has been filtered with a flux of 4,000 LMH without an increase in TMP for at least 5 hours.

Despite this catalogue of advantages, microsieves have yet to become a panacea for all of industry's filtering needs; at the moment they can be made only in a clean room with specialised expensive machinery.

2.3.8 Particle size effects and particle size distribution

The behaviour of a cake is generally dominated by the largest particles present (Lojkine *et al*, 1992). However Schulz & Ripperger, (1989) were among the first to point out that at higher crossflow velocities, particle size distribution at the membrane is shifted towards smaller particles. Larger particles have a lower specific resistance and pack more loosely. This means that the cakes made up of large particles flow more easily than small particle cakes (Romero & Davis, 1988a).

Foley *et al*, (1995b) and Chang & Hwang (1995) attempted to allow for particle polydispersity in their modification of existing models. The model described in Foley *et al* (1995b) correctly predicted some experimental observations, such as an increase in transmembrane pressure leads to an increase in final flux. This is because an increased proportion of large particles is presented at the membrane, resulting in a higher cake

voidage. It could not however explain the fact that a higher crossflow velocity can either increase or decrease the final flux. At higher crossflow velocities, the cake is made of smaller particles; therefore the cake voidage is low. On the other hand, the number of layers is reduced. The relative importance of these two phenomena affects the outcome.

The model of Hwang and Chang (1995) concentrated on the effect of particle size distribution. They tested their model on latex particle suspensions and found that as predicted, the quasi-steady state flux increased as the average particle size in suspension increased.

These models seem to contradict the results found by Sims & Cheryan (1986) when concentrating *Aspergillus niger*. They noticed that when the concentration increased above a factor of 1.4, the long thin mycelia broke down into smaller (by up to 85%), rounder particles and the flux increased. They attributed this to an increased ease of sweeping away smaller particles from the surface, contradicting subsequent observations. However it is likely that the improvement in flux was due a change in morphology rather than a change in size.

2.3.9 Particle Shape Effects

The results for *Aspergillus niger* may be explained partly by the change in particle shape. Tanaka *et al* (1996) found that the longer cells of *L.delbrueckii* fouled sooner and to a greater degree than the shorter rods of *E.coli* and *B.subtilis*. Tanaka, Abe, Asakawa, Yoshida and Nakanishi (1994) demonstrated that *Bacillus* rod shaped cells tended to reduce flux more than ellipsoid *C.glutamicum* cells. This can be attributed to the fact that the ellipsoidal cells are deposited randomly throughout the run, whereas the rod shaped cells are more subject to hydrodynamic forces such as shear. At the beginning of the run the flux is relatively high compared to the crossflow velocity, and the rods are deposited randomly. After initial deposition however, the flux is relatively low and the rods are deposited parallel to the surface.

This development over time probably occurs because at the start of filtration, dominant drag forces move the cells vertically to the membrane. Later on when the flux is low, the angle of approach is close to the horizontal (Mackley & Sherman, 1992; Tanaka *et al.*, 1996). The balance of flow may affect the orientation of the rods (see section 2.3.1.2 for a further description).

2.3.10 Shear

While crossflow velocity is the parameter that is measured and / or controlled, it is shear that actually affects the fouling of the membrane. The most common and simplest way to calculate shear at the membrane surface is given by the equation:

$$\tau_w = \frac{\Delta P_L D}{4L} \qquad \textbf{Equation 1}$$

Where:-

τ_w= shear stress

ΔP_L= longitudinal pressure drop

L=length of filter

D= hydraulic diameter of membrane tube

An equation directly relating crossflow velocity to shear, which takes viscosity into account via the fanning friction factor f is given by:

$$\tau_w = \frac{1}{2} f \rho v^2 \qquad \textbf{Equation 2}$$

Where:

f= fanning friction factor

ρ = density of retentate

v = crossflow velocity

Holdich *et al* (1995) pointed out that the shear inside a membrane tube relies partly on the cake thickness. If the cake deposit is large, the actual shear stress τ_w will be larger than predicted according to Equation 1. Therefore, they suggested that pressure sensors just inside each end of the tube could help predict the shear stress more accurately.

In the early 1980s there was much interest in the topic of how cells behaved when adhering to a solid surface; the problem of biofilms growing in water pipes, heat exchangers and cooling towers had come to the fore. Information from these studies can help in the understanding of the role of shear in microfiltration.

Duddridge, Kent & Laws (1982) investigated the effect of shear stress on *Pseudomonas fluorescens* attached to stainless steel. They found that adhesion was at a maximum at shear stresses below 6-8 Nm^{-2}. Significant detachment of cells was

observed at shear stresses over 10-12 Nm^{-2}, although a few cells were still attached at 120Nm^{-2}. Duddridge *et al* (1982) claimed that the figure of 10-12 Nm^{-2} seemed to represent the shear stress required to break irreversible bonds. The shear stress required to remove the majority of cells from a surface is called the critical shear stress.

Powell & Slater (1982) reviewed the critical shear stresses required to remove bacteria or blood cells from various surfaces. The results for blood cells were all very low (0.24-1.05 Nm^{-2}), but for bacteria, the range was much wider (between 1.1 and 53 Nm^{-2}) for different species adhering to glass. In their experiments they found that the critical shear stress increased with the length of time a cell was allowed to settle onto the surface before shear was applied. This effect increased up to a time cut-off point, specific to each species of bacterium. This is taken to be the time taken for irreversible bonding due to polymer production to happen (see section 2.4.6.4).

The amount of shear stress needed to break a cell is relatively large at 1-2kNm^{-2} (Shimuzu *et al* (1994) but proteins are much more sensitive to shear. Enzymes are active only if their tertiary structure remains intact, or they will become denatured. Charm and Wong (1970) found that denaturation of enzymes increased with the number of passes of feed through the system. Bowen and Gan (1992) observed that this occurred particularly when membranes with a particularly high affinity for protein were used. Therefore it is possible that it may be the shear within the pores and the cycles of attachment and dissociation rather than the shear across the membrane surface that causes problems for proteins in the filtrate. For proteins on the surface however, denaturation due to crossflow shear is an issue. Denaturation can also affect the bonding of the proteins.

Le Berre and Daufin (1996) found that measuring the ratio of J/ τ_w was useful to measure process performance, as the flux (J) governs transport to the membrane, while τ_w governs transport along the membrane. They found that as the cake builds up, the cake absorbs some of the energy imparted by the shear stress. Therefore the effective shear stress τ_{weff} should be used instead, and is given by:

$$\tau_{weff} = \tau_w - \tau_w^* \qquad \textbf{Equation 3}$$

τ_w^* is the critical erosion shear stress, below which there is no transport of particles away from the surface. The value depends on the membrane and solute and/or particles to be transported. Above this critical value the erosion rate is found to be directly proportional to τ_w raised to the power of 1.24.

Le Berre and Daufin found that operation of skimmilk crossflow filtration above a J/τ_{weff} value of 1 LMH/Pa gave satisfactory performance with a gradual increase in fouling and decrease in protein transmission through the membrane. Below this figure, the membrane was quick to foul and the protein transmission decreased rapidly. However, not all conditions of J/τ_{weff} =1 were equally as good; flux has a quantitative effect on separation performance through the critical flux, but does not affect permeability or selectivity. Shear stress, on the other hand, affects deposit thickness and porosity by removal of larger particles from the membrane. Although the research described in this work was performed at a smaller scale than cells (0.1-0.3μm), the results are relevant to this present study.

Subsequently Yamamoto, Periasamy, Donovan & Ensor (1994) studied the force required to remove 10 μm polystyrene/latex spheres. Using a video camera attached to the flow cell, they found that single cells detached at the lowest stresses followed by doubles, triplets and finally large aggregates. This contradicts the experience of Le Berre and Daufin (1996) and the generally accepted view that large particles are the easiest to remove. However, since these agglomerates are only one sphere thick, this phenomenon may be explained in terms of greater contact area and therefore greater adhesion.

Hodgson *et al* (1993b) used a similar technique to study filtration of agglomerates. They found that no agglomerates on the membrane, but noticed that this was because the agglomerates could not deposit on the membrane (as a result of shear) rather than being easily sheared away once deposited.

The influence of shear stress will be different for situations where fouling is less than a layer thick and those where deposition of cells is cumulative.

Surface roughness can also complicate the issue of shear, since a rougher surface offers protection from shear for some of the cells.

2.4 Intermolecular Forces and Forces Acting on a Single Particle

In order to get a more comprehensive picture of cell/macrosolute filtration it is necessary to study forces and interactions on a scale relevant to a single cell. The forces acting on a particle and surface during microfiltration can be divided into three categories:

1) Forces due to externally applied fields

2) Hydrodynamic forces

3) Conservative forces arising out of natural proximity

Forces of type 1) and 2) are responsible for transport of the particles to the membrane, where type 3) forces may result in particle-surface or particle-particle bonding.

2.4.1 Hydrodynamic Forces

Micro-organisms are often treated as colloidal particles when considering the forces they are subject to. This is because they are of a similar size (between 0.8μm - 5.0 μm diameter approximately), have negatively charged surfaces and low density (Gatenholm *et al.*, 1988b).

This is an oversimplification, partly because micro-organisms are large enough to be hydrodynamically active and can affect fluid flow even when in bulk flow (Belfort, 1989). Their size means that they interact with fluids differently from macromolecules; Brownian motion contributes little to particles over 1μm, and shape has a significant effect on their movement.

All particles in a crossflow membrane filtration are subject to a force towards the membrane wall, as a result of the flux. This is called the convective force.

Particles in turbulent flow may also approach the membrane surface by two other main mechanisms. Eddy diffusion can bring the particles from the bulk to the laminar boundary layers. Frictional forces slow the particle before it reaches the surface (Kent, 1988). Spontaneous down-sweeps of fluid may penetrate the sublayer and bring the particles directly to the membrane surface (Marshall, 1986). However, the main mechanism with respect to convection to the membrane is caused by the flux. The balance of forces on a spherical particle is illustrated in Figure 2.9.

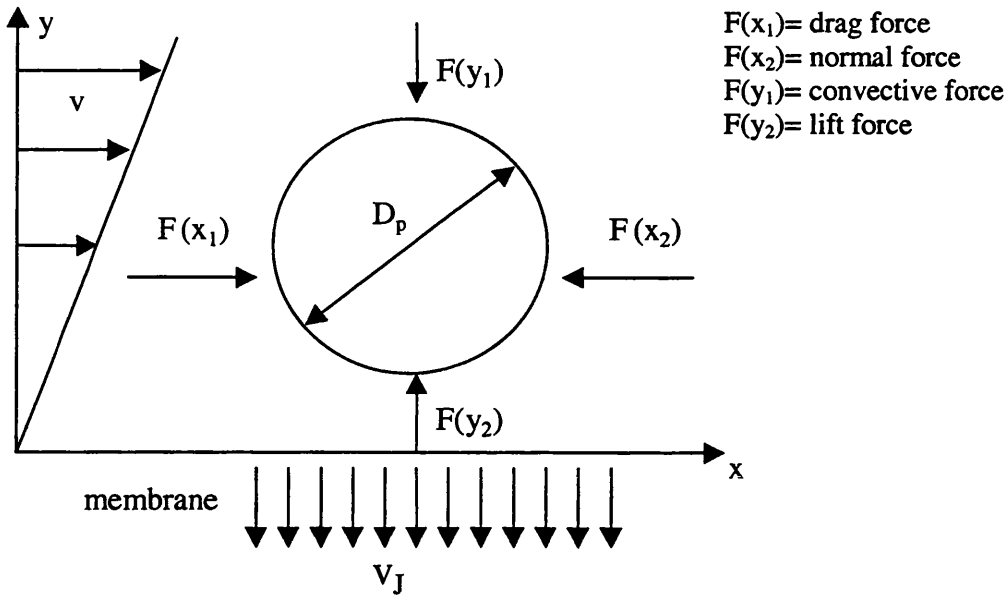

Figure 2.9 Force balance on a particle at the membrane

The convective force due to flux $F(y_1)$ can be calculated thus,

$$F(y_1) = 3\pi\mu D_p J \qquad \textbf{Equation 4}$$

Where

D_p= particle diameter

μ = viscosity

J = flux

If the fluid flow is laminar, the crossflow gives rise to a pressure difference in fluid velocity on either side of a particle. This in turn results in forces and couples being set up. As the particle approaches a surface, the net force is away from the wall. This force is called the lift force and is calculated by:

$$F(y_2) = \frac{0.761\tau_w D_p^{\,3} \rho^{0.5}}{\mu} \qquad \textbf{Equation 5}$$

The balance of these two forces determines how close a particle can get to a membrane.

Since the lift force depends upon the cube of the particle diameter while the convective force is directly proportional to the particle diameter, lift forces for larger particles tend to be high, thus discouraging deposition on the membrane. Lift forces are less important for particles less than 1μm (Buffham and Cumming, 1995), and for high viscosity fluids.

The force parallel to the membrane $F(x_1)$ is a result of the shear stress induced by the crossflow velocity, known as the drag force. As the flux decreases, the balance between the lift force and drag force starts to favour deposition of smaller particles.

Field *et al* (1995) suggested that this balance of forces could be explained in terms of critical flux. Below this critical flux, no fouling can occur, (i.e. the lift force and drag force are greater than the convective force). At the beginning of a constant TMP experiment, fluxes are high and the convective force exceeds the other forces. As the flux decreases, Field *et al* (1995) postulated that the flux drops below the critical flux for the largest particles, thus they cannot be deposited as the convective force is now less than the other two forces. As the flux decreases further, a greater proportion of particle sizes will exceed their critical flux. Hence they cannot be deposited, and the cake is made of increasingly finer particles.

Before deposition, the most significant forces on a particle may be assumed to be hydrodynamic (i.e. drag, convective and lift). Once the particle is deposited, adhesive forces and frictional forces become important. The action of the forces normal to the membrane (adhesive forces and convective forces) cause a friction force opposite to the drag force of the crossflow i.e. $F(x_2)$ in Figure 2.9.

Thus, the friction force F(f) is related to the normal force F(n) or $F(x_2)$ by a friction coefficient ϕ, which has a grinding and a rolling part and takes adhesive forces into account (Altmann & Ripperger, 1997).

$$F(f) = \phi F(n) \qquad \textbf{Equation 6}$$

2.4.2 Forces due to Externally Applied Fields

Gravitational fields do not normally contribute significantly to microfiltration, especially when the microfilter is vertical, since the relative density of the cells is so low. The significance increases if the cells are flocculated and the filter is orientated horizontally. The relative temperature of the bulk suspension and the material at the membrane itself is important; warm material will tend to drift towards cooler areas. If the cell has flagella or other means of movement, taxis can be also a significant factor.

2.4.3 Conservative Forces

There are four main forces involved in adhesion.

1) Electrostatic interactions
2) Van der Waals forces
3) Hydration forces
4) Steric forces

Electrostatic interactions occur when ionogenic groups such as COO^-, PO_4^{3-} and NH_3^+ which are on the cell surface attract their counter-ions, so cells are surrounded by a charged electric double layer. The potential energy of the double layer can be estimated by using zeta potentials. The isoelectric point of most cells is at pH 2-3.5 (Mozes, Amory, Leonard et Rouxhet, 1989) so they are negatively charged above this value. The membrane surfaces they attach to are also usually negatively charged, so frequently electrostatic forces are repulsive when ionospheric atmospheres overlap (Ho, 1986). This is particularly true for hydrophilic cells.

Van der Waals Forces or dispersion forces are a result of coupling of electromagnetic fluctuations throughout the radiation spectrum (Israelachvili, 1994). The dispersion energy between two non-polar molecules varies with R^{-6} where R is the distance of separation. With two flat surfaces, interactions are more complicated and the resultant energy varies with l^{-2} where l is the separation distance. These forces are generally attractive, but are generally overestimated at large separation distances. Van der Waals forces often lead to a preferential attractive force between cells in a mixed population. Thus they are useful for the initial stages of aggregation (Bell, 1978).

Hydration Forces or hydrophilic forces are short-range repulsive forces (on bacteria they are due to the repulsion of the phospholipid bilayers). Their strength depends on the energy needed to dehydrate surfaces with hydrophilic groups as they come together. Associated with hydration forces are hydrophobic interaction forces, where two non-polar groups adhere to each other - mainly due to the strong attraction of water molecules for each other rather than any direct attraction between the two molecules themselves. This force is frequently shown to be important in microbial interface reaction, for example the perpendicular orientation of bacteria when they attach

to a surface is ascribed to this phenomenon (Dahlbäck, Hermansson, Kjelleberg & Norkrans, 1981).

Steric Forces: These are the result of the interactions of polymers in the extracellular matrix. The glycocalyx of a micro-organism is species-specific and can take many different forms. They are made predominantly of either homo- or heteropolysaccharides (Wilkinson, 1958), but glycoproteins, proteins and nucleic acids are also present and usually contribute to a lesser degree. The structures they form vary from slime to clearly defined gel-like capsules to diffuse fibrillar strands of soluble slime (Harbron & Kent, 1988). Polymer bonding is thought to be either ionic, hydrogen bonding, or occurring through interaction of hydrophobic groups (Le & Gollan, 1989).

If the polymers are soluble, strong attraction may occur between the polymers and between the polymers and surfaces. One polymer may have parts attached to two surfaces. This is known as polymer bridging. If the polymer is insoluble, the necessity of removing the solvent between two surfaces in such close proximity is thermodynamically unstable, so repulsion occurs and further movement of polymer is restricted (Ho, 1986). These are known as osmotic factors, because there is an osmotic tendency for the water to return to the space. The size of these forces depends on polymer coverage; they can be larger than the electrostatic forces and have a large range. When these forces are attractive, they are considered to be a major element in irreversible bonding. For a more detailed description, see section 2.7.4.

Steric interactions all take place at a much slower rate than the previously listed conservative forces. There are two reasons for this:

1) Some polymers useful for adhesion are stimulated by contact with another surface, but take time to be secreted (Ho, 1986).

2) For the extant polymers, diffusion due to Brownian motion needs to take place (Marshall, 1986).

Naturally the second mechanism takes a longer period of time than the first. Defrise and Gekas (1988) described the theory that macromolecular conditioning on a surface encourages polymer secretion (see section 2.2.1). Polymers may enhance adhesion to a surface by changing the electrokinetic potential of the surface. The presence of ions is important in this mechanism, since it is essentially a result of electrostatic forces.

2.4.4 Biofouling

Clues to how cells interact with each other and with flat surfaces can be obtained from looking at naturally occurring biofilms, for example, those in heat exchangers (Harbron & Kent, 1988), (Kent, 1988). There is a tendency for both organic and inorganic species to accumulate at solid/liquid interfaces, leading to the membrane surface being coated with a thin film of molecules, proteins in particular. This is called conditioning. The layer is seldom more than 0.1μm thick. It is generally thought that the properties of this layer determine subsequent cell deposition. However, there seems to be experimental evidence both supporting (Gekas & Hallström, 1990; Dewanti & Wong, 1995) and refuting (Hallab, Bundy, O'Connor, Clark & Moses,1995; Duddridge & Pritchard, 1979) this opinion.

Naturally occurring biofilms are generally a mixture of bacteria, aquatic fungi and protozoa embedded in a loose matrix of mostly polysaccharide and glycoprotein. The matrix forms aqueous gels of 85-96% water with the help of calcium, magnesium and iron. The negatively charged surfaces of the cell form polar bonds with these cations (Costerton, Geesey & Cheng, 1978). 1-10% of the structure is actually cells. These biofilms are viscoelastic, so they can stand temporary deformation. Even so, re-entrainment of small parts of the biofilm due to scouring action is almost continuous, especially with thicker, denser films in laminar flow.

Biofilms can withstand forces over 1-1.5 Nm^{-2} but biofilms developed under high velocity/shear conditions may adhere to surfaces more firmly than those at lower velocities may. The presence of ions is very important for adhesion. Cations, especially divalent ones, are important to counteract the negative charge of the cell. It is possible that there is involvement in divalent cations in bridge formation between the negatively charged substratum and the cell (Kent, 1988).

2.4.5 Specific Bonding of Gram Negative Bacteria

As well as non-specific bonding through Van der Waals forces, electrostatic attraction or hydration forces, it is important to remember that specific bonding may also occur between the cells. The previously mentioned lipopolysaccharides are a definite part of the Gram negative cell wall for example. They serve partly as strain-specific antigenic determinants and so may be involved in cell-cell adhesion. Specific bonding occurs not only between any ligand and receptor, (such as an antigen and antibody) but also between identical strain specific ligands (Bell, 1978). However, an opportunity for

this to occur could come about only if non-specific temporary bonding already existed, since the length of these lipopolysaccharides is only around 30nm, and time for diffusion is relatively slow.

These can be attached to protein that is quite free to move around in the phospholipid bilayer, towards an area already in contact with another surface, for example.

Their movement and activity can be restricted by attachment to other molecules in the cytoplasm (Bell, 1978) or if the cell is bound to other molecules. Since these bonds are at close range, they will be competing with repulsive electrostatic reactions.

Another factor to be considered is that the cell-cell bridges have an optimum length corresponding to a minimum internal energy (Bell, Dembo & Bongrand, 1984). Like a spring, if the bonds are too compressed or too stretched, the chemical potential will be too high. The intercellular bonds tend to be broken by shearing rather than tensile forces. Once broken, they may re-form again, especially under conditions of high viscosity.

Specific bonds are usually energetically favourable and therefore are considered to make a significant contribution to the overall irreversible bonding (Cozens-Roberts, Quinn and Lauffenberger, 1990).

2.4.6 Resolution of Forces

Traditionally there are two main ways of resolving the forces mentioned above, Derjaguin-Landay-Verwey-Overbeek (DVLO) theory and thermodynamic analysis. Neither can resolve all the relative forces simultaneously.

2.4.6.1 Derjaguin-Landay-Verwey-Overbeek DVLO Theory

This theory assumes that micro-organisms can be considered as hard bodies with well-defined surfaces and no biochemical interactions. Water is taken to be a continuous fluid, so hydration and steric forces are ignored. The only forces considered are Van der Waals and electrostatic interactions. In fact the size of both these forces depends on particle shape and roughness, as both these factors affect the number of possible contact points (Altmann & Ripperger, 1997).

The theory relates the stability of the colloidal dispersion to the total potential energy of interaction between the particles. The total energy of interaction is the sum of the attractive and repulsive forces.

Usually cells do not have enough energy to get beyond the potential barrier, which is at about 1 nm for objects the size of cells (Defrise & Gekas, 1988). There is a secondary minimum at 5-10 nm where there are weak attractive forces that may halt the cell long enough for other attractive forces to occur. The secondary minimum is strongly dependent on the system, especially on electrolyte concentration of the solution (Defrise & Gekas, 1988).

DVLO theory makes many false assumptions. For example, the forces arising from glycocalyx interactions (i.e. steric forces) are ignored; the forces that actually result are a combination of all the conservative forces together. The approach of a cell is governed initially by the strength of the electrostatic repulsion, but as the separation decreases, Van der Waals forces start to dominate. At very small separations, short range forces are dominant over DVLO forces. Short-range forces include covalent bonds, dipole and solvation forces (i.e. hydration and hydrophobic interactions). These forces prevent cell fusion (Defrise & Gekas, 1988).

Attachment in cells by the forces considered here can occur by hydrogen or ionic bonding of cell protrusions such as flagella (4-35 nm x 10 μm), fimbriae or pili (0.01-0.2 μm x 10μm) (Harbron & Kent, (1988)). Their potential barrier is much smaller than the cell's and easy to overcome due to their fineness. Once the cells are at the secondary minimum, lipopolysaccharides (30nm) can also participate in specific bonding.

2.4.6.2 Thermodynamic Approach

This model predicts that bacterial adhesion occurs when the free energy of adhesion is minimised. It assumes that the effect of electrical charges can be neglected. Surface energies can be estimated by measuring the relative surface tensions, or by measuring contact angles. The equation for Gibbs free energy, ΔG is given by

$$\Delta G = \gamma_{cs} - \gamma_{cl} - \gamma_{sl} \qquad \textbf{Equation 7}$$

Where

γ = interfacial tension

c = cell

l = liquid

s = surface

These measurements can only be relative to each other. Evaluation of γ_{cs} relies on experiments concerning solid-liquid rather than solid-solid interactions, therefore the thermodynamic approach does not take electrostatic interactions into account (Mozes *et al.*, 1987).

There seems to be at least a qualitative link between relative surface energies of bacteria and adherence to surfaces. Hydrophilic materials with low critical surface energies (20 - 30 ergs cm^{-2}) exhibit minimal biological adhesion (Defrise & Gekas, 1988). Cells have a free surface energy of around 68 erg cm^{-2} (Dahlbäck *et al*, 1981). Thermodynamically, cells should adhere best to high-energy (hydrophobic) surfaces, but in reality bacteria can adhere to a whole range of surfaces, with some surfaces at an optimum energy for attachment. This is because it is the relative surface tensions of the liquid and solid that determines attachment. If the surface tension of the bacteria is greater than that of the liquid, adhesion will be more extensive on hydrophilic, high surface energy materials. If the relative surface tensions are reversed, adhesion will be lower on these materials.

For crossflow microfiltration (CFMF), ideally, hydrophilic membranes should be used to deter adhesion (Fane *et al.*, 1990). In reality a membrane may be used, as long it is neither too hydrophobic nor hydrophilic.

2.4.6.3 Application of Theories

Mozes, Marchal, Hermesse, Vanhecht, Reuliaux, Leonard & Rouxhet, (1987) tested the adhesion of two hydrophilic micro-organisms and one hydrophobic micro-organism on various supports. Adsorption of the hydrophilic cells was mainly controlled by electrostatic interactions. Overall, the hydrophobic micro-organism favoured adsorption to hydrophobic supports; a thermodynamic approach was used to describe this. However there was still an electrostatic influence noticeable in some of the bonding. This behaviour is analogous to that observed in protein bonding in section (2.4.4).

Cells with an intermediate degree of hydrophobicity adhered to polystyrene only near the isoelectric point if suspended in a low ionic strength solution. In a high ionic strength they adhered strongly over a range of pHs. Therefore adhesion depends on both the hydrophobic and electrostatic properties of the surfaces. Thermodynamic and kinetic factors may have a combined influence.

DVLO theory predicts that cell-supported electrostatic interactions are acting at a rate equal to that of cell deposition. On the other hand, surface energy will influence the

equilibrium between attached and non-attached cells, i.e. the depth of the primary potential well.

De Weger, Van Loossdrecht, Klaassen & Lugtenberg (1989) found that both the cell electrophoretic mobility and the cell hydrophobicity influenced adhesion of bacteria to polystyrene. The degree of coverage increased with the cell hydrophobicity under the following conditions: -

- Where cell retention was reversible
- Adhesion was considered to take place in the 2° minimum.

In this case only long-range forces are expected to be important; cell hydrophobicity can act through Van der Waals forces.

2.4.6.4 Micro-organism attachment

Ho *et al.* (1986) developed a previous model by Marshall, Stout & Mitchell, (1971) which attempted to explain micro-organism attachment to surfaces. He suggested that it occurred in three stages.

1) Weak reversible adhesion at secondary minimum. This bonding is reversible i.e. cells can be washed off.
2) Firmer, non-specific adhesion by fimbriae and pili.
3) Bonding by extracellular material (polymer bridging etc.). This stage is irreversible; i.e. cells resist being washed off.

They suggested that stages 1 and 2 occurred within seconds, whereas stage 3 occurred more slowly. Others have pointed out (Harbron & Kent, 1988; Duddridge *et al*, 1982) that the third step may depend on whether suitable polymers exist on the surface already, or whether they need to be synthesised (Kent, 1988).

Powell and Slater (1982) reported that the time taken for biologically stable irreversible links took only fifteen to thirty minutes for *E.coli* and *B.cereus*, but took up to an hour for *S.typhimurium.*

Duddridge *et al* (1982) assessed the effects of shear stress on *Pseudomonas fluorescens* attached to stainless steel. The number of bacteria attached decreased with increasing shear stress, but even at very high shear stresses, there were still a few bacteria attached. The number of bacteria attached decreased rapidly with increasing shear stress, reaching a plateau of 6-8 Nm^{-2}. Duddridge *et al* (1982) postulated that this

critical surface stress might be a measure of maximum initial stickiness of the bacterium (reversible adhesion stage).

They also measured the shear stress required to remove a film deposited under static conditions. This was around 10-12 Nm^{-2}, which could be an indication of the force required to break polymer bonding from either surface.

2.5 Models

2.5.1 Cell adhesion models

A group of models designed to understand specific attachment of cells in blood vessels or onto biological surfaces have been developed. These were created to help in understanding how white blood cells attach to a site in inflammation for example, or how bacteria colonise the gut of an animal, but may be relevant to filtration too.

Many models are derived from the original model by Bell (1978) designed to estimate the reaction rates of ligands binding to receptors. Microvilli are also considered to be capable of specific bonding. The model allows the deduction of macroscopic forces from microscopic bond properties. From this model, it was demonstrated that specific bonds tend to be stronger than non-specific bonds, and the force required to break an antigen-antibody or lectin-carbohydrate bond is equal to that required to extract a receptor molecule from the cell membrane.

Hammer and Lauffenburger (1987) developed this model into the "point attachment model", so named because it assumes that the adhesion area is small. They discovered that stress distribution of bonds is small. Torque cannot be counteracted by a narrow band of bonds in the middle of the cell; it is resisted if the specific bonds are diffuse and is counteracted predominantly by the stress of the bond at the back edge of the cell. Therefore it is not advantageous for a cell to have localised potential points of attachment if adhesion to a surface is necessary.

Figure 2.10 demonstrates the balance of forces for this model. Although it is quite similar to Figure 2.9, it would be inappropriate to model microfiltration as it stands. Since the model underestimates the forces in the y direction (by ignoring the convective force), the force per bond, θ, is overestimated at separation distance, S. θ is calculated to counterbalance only the torque set up by the fluid, τ, and that set up by the bonding force, $F(x_2)$.

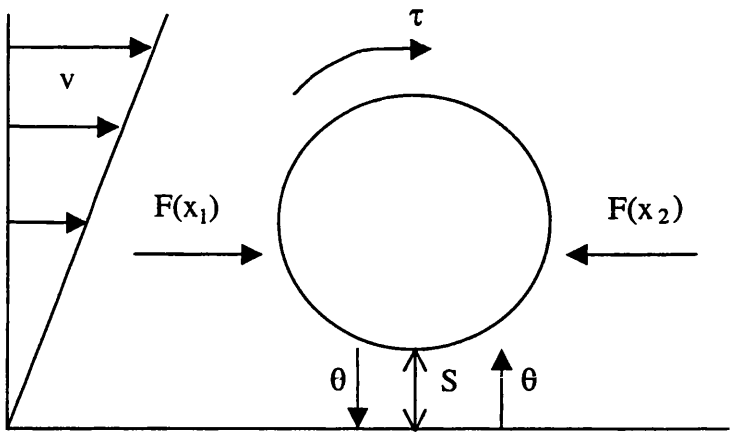

Figure 2.10 Force balance on a particle with specific bonding to a surface

Hammer and Apte (1992) showed that different adhesion molecules had different types of bonds; some promote rolling, others promote adhesion, and others adhesion strengthening. Bonds formed differ in their rates of forward and reverse reaction, their affinity and their resistance to stress. It is shear rather than tension that breaks these bonds.

Hammer and Apte (1992) simplified the adhesion forces; instead of distinguishing between different types of interaction using the DVLO and thermodynamic theories, adhesion force was taken to be additive. For each microvillus the net colloidal force is a sum of

- Van der Waals
- Gravitational
- Electrostatic interactions
- Steric stabilisation forces.

One of the greatest problems with these models is that values for the parameters required, such as forward and reverse reaction rates for each ligand-receptor and their affinities are extremely difficult to measure all at once. Therefore values to fit these models have been collected from disparate sources.

2.5.2 Microfiltration models

2.5.2.1 Backflux models

In order to understand the operation of microfiltration systems better, it has been essential to develop models to account for the following phenomena:

1) When TMP is constant, the flux drops rapidly at the start of a run, coming to a quasi-steady state for a much longer time period before steady state is reached.

2) Although many particles are presented at the membrane during the course of a run, the cake formed is much thinner than for dead-end filtration. At steady state no net deposition of particles occurs. Therefore mechanisms for transport away from the membrane must exist.

3) The effects of increasing and decreasing both TMP and crossflow velocity.

4) Different types of fouling can occur (see section 2.2).

Fouling in these models is ascribed to the increased hydrodynamic resistance of either a flowing layer above the membrane, or a static cake deposited over the membrane, or both. The idea of a state of equilibrium being reached when the cells reach maximum concentration near the membrane is common.

Crossflow microfiltration (CFMF) developed from a combination of crossflow ultrafiltration and dead end microfiltration practices. Therefore it is not surprising to find that the first attempts to model the fouling of microfiltration systems applied models suitable for describing the flux reduction due to concentration polarisation of macromolecules (known as film theory). However, the local mass transfer coefficient, calculated by using the Leveque equation, depended on employment of the Stokes-Einstein equation, which describes Brownian motion diffusivity. Brownian motion does not affect particles above about 0.3μm (Rautenbach and Schock, 1988), so use of this equation is inappropriate for particles above this size.

Therefore a set of models has been designed to account for the fact that not all particles presented at the membrane remain there. These are presented in Table 2.1.

Model	Principle	Appropriate for	Disadvantages
Particle deposition theory, Green & Belfort (1980)	If the drag force is greater than the lift force a cell will deposit (see section 2.4.1)	Laminar flow of particles less than 10μm.	No consideration of non-hydrodynamic effects such as influence of other particles
Particle adhesion model, Rautenberg & Schock (1988)	Cells will deposit if crossflow velocity is equal to the flux velocity multiplied by a friction factor see section 2.4.1	Small particles in dilute suspension	Some high values show more than just friction forces involved (Schulz and Ripperger 1989). Assumes infinite dilution.
Particle adhesion model modification, Altmann and Ripperger (1997)	Same as above but considers adhesive forces as well as friction forces.	Proving that smaller particles adhere at membrane at a wider range of conditions than larger particles. Therefore at low CFV, cakes are finer	Only considers individual particles, not their interaction.
Particle adhesion model modification Stamatakis and Tien (1993)	Looks at cake deposition in terms of protrusion of an existing cell of a minimum height preventing further rolling of another particle.	Cake build-up description. Accounts for particle size distribution and compressible cakes.	Acknowledges Van der Waals forces but ignores them due to their complexity. The model cannot predict start up conditions.
Pure convection model, Leonard and Vassilief (1985)	Particles are deposited on the membrane by the convective force caused by the flux, and this is balanced by the drag force caused by the crossflow velocity.	Dilute suspensions	Model is concentration independent and does may not consider viscosity. Layer height prediction may thus be very high.
Shear enhanced model Zydney and Colton (1986)	Brownian motion diffusivity enhanced by particle-particle interactions.	When decrease in flux is due to a very thin layer of cells adjacent to membrane; for that is what the model predicts.	Assumes velocity profile and therefore viscosity uniform throughout boundary layer. Not good for non-Newtonian fluids.
Shear induced hydrodynamic diffusion model, Davis and Leighton (1987) Romero and Davis (1988a), (1988b)	Hydrodynamic interactions of particles cause shear (Phillips, Armstrong & Brown, (1992))	Predicting position and time taken for stagnant layer to develop (flowing layers predicted to start first). Predicts both transient and steady states	Does not consider adhesive forces or pore blocking therefore predicts reversible cake formation only. Parameters are difficult to measure.

Table 2.1: Microfiltration model summary

The earliest models concentrated on balancing two competing forces at a time, lift force versus drag force for the particle deposition theory (Green and Belfort 1980) convective force versus drag the pore convection model (Leonard & Vassilief 1985). These models do not take particle-particle interaction into account.

The models to consider shear (Zydney and Colton, 1986; Davis and Leighton 1987; Romero and Davis, 1988a, 1988b) take particle interaction into account insofar as they affect the mechanisms of removal. They do not however consider how particle interaction aids deposition.

Chellam and Wiesner (1998) claimed that shear induced diffusion brought theoretical and experimental data into better agreement than some particle adhesion models, but cake morphology was still not accounted for.

A few years earlier, Stamatakis and Tien (1993) had tried to consider how particle-particle interaction might affect the settling of particles rather than their removal, by modifying the particle adhesion model. They calculated a critical cake protrusion height. Above this value, a rolling particle meeting the protrusion will cease its lateral migration and settle on the membrane. Their model also included another factor usually neglected in these back flux models - compressibility. Although they acknowledge the existence of adhesive forces such as Van der Waals, they could not be incorporated into their model.

Altman and Ripperger (1997) also took the particle adhesion model and tried to modify it with respect to these adhesion forces. However, again they concentrated on the forces on a single particle and not on cell interaction or cake morphology.

Since these models concentrate on back transport, it is difficult to incorporate cake morphology, particle interactions, or fouling due to adhesion into a single model. Membrane structures are idealised and there is often no differentiation between reversible and irreversible fouling.

Another way of modelling fouling is by using the cake resistance models. These models do not consider back transport, but can help to improve understanding of cake morphology and describe different types of fouling.

2.5.2.2 Cake resistance models

Green and Belfort (1980) were one of the first teams to use Darcy's law (Equation 8) to try to describe CFMF. Darcy's law is traditionally used in dead end microfiltration.

$$J = \frac{TMP}{\mu R_T} \qquad \textbf{Equation 8}$$

Where:

R_T= total resistance

R_T comprises the sum of resistances due to the membrane plus the resistance due to the cake, which can be between about 2 and100 times higher.

The resistance of a layer of particles is given by the Carman-Kozeny equation:

$$R_L = \frac{180(1-\varepsilon)^2 \delta_c}{\varepsilon^3 (2r_p)^2} \qquad \textbf{Equation 9}$$

Where:

R_L= resistance to particle layer

ε = voidage of layer

δ_c = thickness of layer

r_P= particle radius

The cake resistance increases when cake thickness increases, voidage decreases or average particle size decreases. Steady state flux occurs when all three remain constant - the filtrate flux convecting particles to the surface is balanced by particle lift velocity away from the cake.

Green and Belfort (1980) found that although the results from experiments were of a similar order of magnitude to those predicted by the model, for one particular set of data the cake would have to occupy 70% of the channel for it to be viable. This model does not predict a pressure independent zone or bulk particle concentration dependence, nor does it consider the particle interactions.

This apparent failure of the model may be accounted for by the modification to the equation by Shimuzu *et al* (1993,1994)

$$J = \frac{TMP}{\mu(R_m + R_{p+} + R_c)}$$ **Equation 10**

Where:

R_m= resistance of membrane

R_P = resistance due to pore blocking

R_c = resistance due to cake

At the beginning of a run, R_c does not exist; therefore any increase in resistance is attributed to pore blocking. Shimuzu *et al* (1994) believe R_p is entirely dependent on membrane characteristics, such as pore size and membrane charge. This may be oversimplistic, as it also depends on particle properties (e.g. whether the particles aggregate).

Shimuzu *et al.* (1993,1994) used the particle adhesion model to explain how different flow conditions during the course of a run might affect the predominant type of fouling. A lift velocity specifically for membrane filtration balances out the flux in their interpretation of the model.

They believed that initial pore blocking was independent of hydrodynamic conditions and was dependent on membrane characteristics.

Once the flux had reached a critical level however, the hydrodynamically dependent cake filtration mechanism took over, until the flux was equivalent to the lift velocity; and steady state was reached. If the flux drop due to pore blocking decreased beyond the lift velocity however (i.e. if a high resistance membrane is used or pores are large in relation to particles) a cake layer would not form. This model is therefore useful in differentiating between these types of fouling.

However differentiating between specific fouling mechanisms is difficult. A more pragmatic approach to splitting R_T is to divide it into reversible and irreversible fouling, as observed in Le Berre and Daufin (1996). This is not only easy to measure, but of practical interest when trying to maximise flux by periodic backflushing through the membrane (Kroner *et al* 1984) or crossflushing across the membrane (Stamatakis and Tien 1993).

These two operations help to increase the flux during an operation by removing the reversible fouling.

2.5.2.3 Specific cake resistance

The historical legacy of assessing resistance by employing equations derived from dead end filtration is that many sources are confident that the specific cake resistance or cake resistance per layer can be measured for a given particle type (Shimuzu *et al,* 1993). The specific cake resistance can be found by employment of the steady state method. Compressibility can be estimated by varying the pressure, also by using dead end filtration figures.

Since specific cake resistance is a measure of porosity, these values can then be applied to crossflow filtration of the same particles. Voidage is a property of particle size and compressibility.

Shimuzu *et al* (1993) calculated the specific cake resistances for particles of between 0.15 and 3.8μm using this method. They found that the mean specific cake resistances lay between 10^{12} and 10^{15} mkg^{-1}, with yeast and bacterial cells being two to three orders of magnitude higher than latex particles. The difference was attributed to the greater percentage of water in the cells, leading to the increased compressibility.

Tanaka *et al* (1994, 1996) also used this method to find the specific cake resistance for a group of bacteria. This value was then put into the equation below to calculate the theoretical flux:

$$J = \frac{TMP}{\mu(R_m + \alpha W)} \qquad \textbf{Equation 11}$$

Where:

R_m = resistance of membrane

W = weight of cake deposit

α = specific cake resistance

μ = viscosity

For ellipsoidal *C. glutamicum* cells, the theoretical and experiment fluxes correlated very closely. However for the rod shaped bacteria of *B. subtilis, B. brevis* and *B.cereus*, the

calculated and actual fluxes were only in agreement for the first few minutes before they diverged (the model underpredicts the flux loss).

Visualisation of these cake formations by Mackley & Sherman (1992) explained how this phenomenon occurred (see section 2.2.2). At the beginning of the filtration, transmembrane flux is high compared to crossflow velocity; cells are deposited in a random orientation, as for dead end filtration. Later on as the flux declines, crossflow dominates and the shear stresses align the rod-shaped bacteria in parallel with the membrane, thus causing a smaller average voidage and the actual α is higher than predicted. This phenomenon was independent of compressibility, as a change in pressure did not affect the specific cake resistance.

Chellam and Wiesner (1997) had further evidence that cake morphology affected specific cake resistance. Specific cake resistances for a variety of particles were all higher in crossflow filtration than dead end filtration. Operation conditions also fundamentally affect the specific cake resistance, which increased for: -

1) an increase in shear rate

2) a decrease in the initial permeation rate.

Finally, Tanaka, Usui & Nakanishi (1998) observed that a high initial flux at the start of filtration encouraged higher protein deposition, which decreased the cake voidage and thus increased α (specific cake resistance).

It must be noted however that for systems encouraging significant pore blocking, this specific cake resistance can be considered only as an apparent value, as it is difficult to separate out resistance due to pore blocking and cake build-up.

2.5.2.4 Blocking filtration laws

Hermia derived models to describe four different types of fouling for dead end filtration. A further description of three of these models may also be found in section (7.1).

a) **Complete pore blocking.** This mechanism assumes that each particle arriving at the membrane surface participates in blocking a pore.

b) **Standard blocking.** Each particle arriving at the membrane is deposited onto the internal walls, which reduces the pore volume.

c) **Intermediate blocking.** Each particle arriving at the membrane surface may settle either on top of an already present pore-blocking particle, or may directly cover some part of the membrane.

d) **Cake filtration.** A particle arriving at the membrane must settle on another that is either already blocking a pore or covering a membrane area.

Field and Arnot (1995) and Field *et al* (1995) have since modified models a, c and d to allow for back diffusion. Model b is not affected by back diffusion, so does not need to be modified. In deriving the standard filtration model, it is assumed that the permeate volume decreases in proportion to the filtrate volume by particle deposition on the pore walls. Assuming straight cylindrical pores and laminar flow, and taking classical filtration equations, they show

$$\frac{t}{V} = \frac{1}{v_0} + k_s \frac{t}{2}$$ **Equation 12**

Where:

t = elapsed filtration time

V = filtrate volume

v_0 = initial flow rate

k_s = filtration constant

Thus a linear plot of t/V versus t indicates that the standard blocking model is valid (Lojkine *et al*, 1992).

2.5.2.5 Growth of layers

Altman & Ripperger (1997) summarised the processes thought to govern the build up of cake to its equilibrium state under constant transmembrane pressure in diagrammatic form. Figure 2.11 is an adaptation of their diagram.

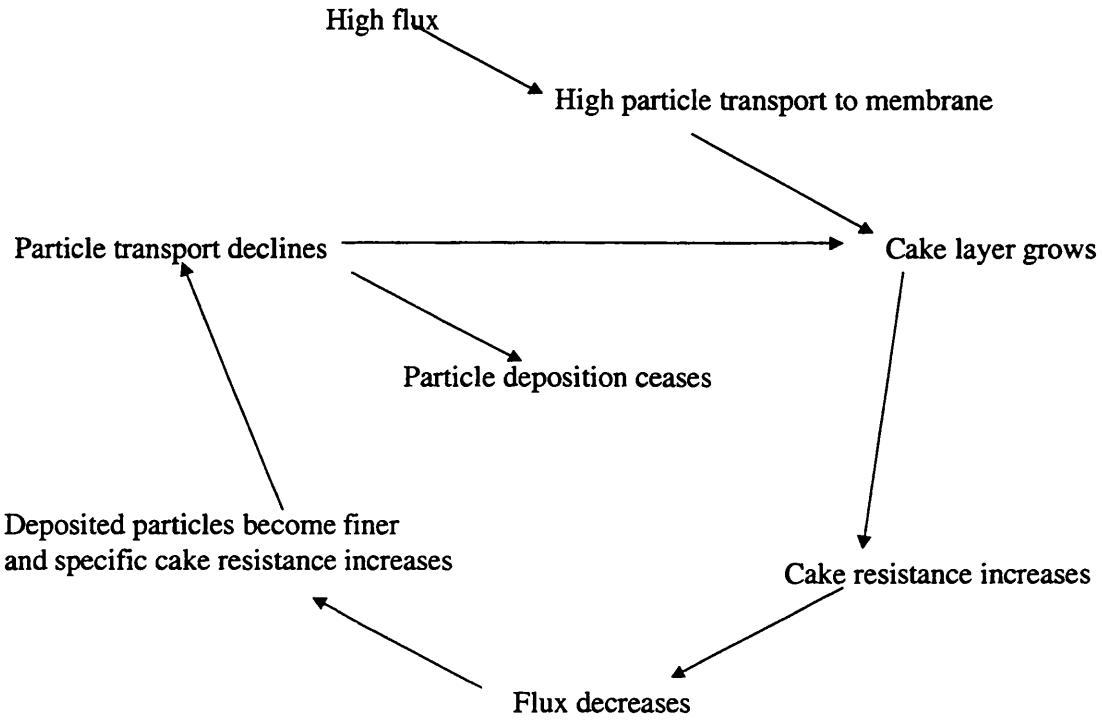

Figure 2.11 Growth to an equilibrium state of a cake.

It is important to note that the growth of cake to equilibrium for a given system is determined by the influences of flux, particle size and cake resistance on each other.

2.6 Effect of pH & ionic strength on cell interactions

Recently there has been much interest in understanding how particle size, especially particle polydispersity (Chang and Huang, 1995: Foley *et al,* 1995b; Tarleton and Wakeman 1993) and particle shape (Tanaka *et al* 1994,1996,1998) affect the flux. However, the main investigations into how physicochemical conditions affect the flux of cells with different extracellular properties has yet to be investigated thoroughly.

There have been many investigations into the effect of pH and ionic strength on protein filtration (see section 2.7.4), but there has been relatively little research on cells so

far. This is probably because they are slightly larger than colloids. Filtration of larger colloids is not expected to be dominated by hydrodynamic effects, since physicochemical effects are expected to be quite small for these colloids. Tarleton and Wakeman (1994) investigated the effect of pH and ionic strength on calcite particles of about 0.5μm, and found the physicochemical effects to be small.

For smaller particles however, such as proteins and macromolecules, physicochemical effect will be more important. Since biological particles are larger particles covered in small macromolecules, the net results cannot be as simple for a biological entity as for a colloid.

The work of Hodgson *et al.* (1993a) found that removal of the extracellular matrix from the gram negative bacterium SW8 proved that the extracellular matrix does indeed have a fundamental effect on filtration performance.

Even in the presence of extracellular proteins, complex interactions can occur. Le *et al*, (1984a) found that adsorption of amidase onto *Pseudomonas fluorescens* cell debris increased with decreasing pH in the range from pH 5 to pH 9. Similar behaviour was found when different cell debris and a different enzyme were tested.

Below is a summary of factors relevant to assessing the filtration behaviour of different cells with different extracellular matrix characteristics.

2.6.1 Effect of physicochemical conditions on whole cells and macromolecules

The pH and ionic strength of an electrolyte is critical for determining the interactions of the particles and molecules in which it is suspended; this determines the electrostatic contribution to the force balance. At low ionic strengths away from the isoelectric point, the surfaces are exposed and net repulsion may occur if entities of the same net charge sign come close, especially if the particles are relatively large. At high ionic strengths and close to their isoelectric points, ions are closely packed against the surface. This brings the net charge close to 0 and shortens the Debye length. For a large, smooth highly charged particle, the opportunity for other attractive forces to contribute to binding may only occur under these conditions. For a smaller, rougher particle, especially with long thin polymers attached to its surface, bonding is easier under less extreme conditions; local interactions may occur more easily since macromolecules may overcome repulsion. Fu and Dempsey

(1998) give an example of this. For colloids of about 0.1μm, they found that filter cakes were most stable at a low surface potential (≈30meV). They also noted that the potential that gives the lowest cake porosity increases with particle size.

2.6.2 Types of ions

Adding divalent ions to a salt solution is up to 100 times more efficient at reducing the surface potential than increasing the concentration of monovalent ions; surface potential is determined by the divalent ions if they make up more than 3% of a salt solution. They often bind chemically to negative surface sites, thus also decreasing the surface charge density (Israelachvili, 1994).

Often attractive short range forces in the presence of Ca^{2+} exceed that predicted by Van der Waals forces. This is attributed to the additional attractive Van der Waals type forces between the highly polarisable divalent ions in the double layer, known as ion-correlation force (Israelachvili,1994).

Divalent ions, especially Ca^{2+} and Mg^{2+} appear to be necessary for efficient bonding. They increase the stability of the polymer matrix and in their absence, polymer bonding is easily disturbed (Duddridge and Pritchard 1979). One of the main mechanisms of yeast flocculation is believed to be due to Ca^{2+} binding the charged groups on cell surfaces (Bowen and Ventham, 1994).

Ho (1986) described how the effects of both physicochemical parameters depend on:

- the polymer coverage
- the liquid the cells are suspended in
- separation distance of the cells.

As previously mentioned, when the polymers are insoluble, and the cells are close together, osmotic factors dominate and the net steric effect is repulsive.

There is a range of possibilities if the polymers are soluble in the liquid in which they are suspended.

For cells with relatively long macromolecules, polymer bridging, (i.e. a polymer may have sections attached to both cell surfaces) is common for cells relatively far apart,

especially if the polymer coverage is low. This is especially favoured in the presence of smaller colloids.

Incipient flocculation of cells occurs at a pH near the isoelectric point and a very high ionic strength, and may be viewed in terms of the short range bonding between segments. Hydrogen bonding, ion pair bonding (e.g. $COO^- NH_3^+$), and triple ion bonding are considered to be the most important short range reaction for biopolymers.

A similar effect is found for cells with a relatively low polymer coverage under the same physiochemical conditions, but this classical coagulation is naturally less dependent on steric forces.

Flocculation can occur due to entrapment of cells in a viscous polymeric matrix or polymeric gel, but this is independent of any thermodynamic considerations and seems to be a means of cell dispersion, rather than aggregation.

2.6.3 Effect on specific bonding

Cozens-Roberts *et al* (1990) found that the strength of bonding with respect to pH had a Gaussian distribution for immunoglobulins (antibodies/lectins/ligands). The value of the bonding maximum (pH 7.6) was particularly interesting. This is the pH of blood (Samson Wright's Applied Physiology, 1983), which is the normal environment of these immunoglobulins. When investigating the effect of ionic strength on bonding, it was found that the bonding strength decreased up to 0.15M and then remained the same for higher strengths. 0.15M is also the molarity of blood. Since non-specific bonding is thought to be suppressed at high ionic strengths (Doig and Trust, 1993), this plateau value is considered to indicate the strength of the non-specific bonds.

The significance of specific bonds must depend on the type of bacteria. For pathogens and opportunistic pathogens it is highly advantageous to have the ability to bond specifically to host surfaces, and is one sign of potential virulence (Doig & Trust, 1993). For cells adapted to other environments, it may be less useful. For all types of cells though, the ability to bind to cells of a similar type can afford the advantages of protection from a harsh environment.

2.6.4 Electroviscous effects

A high ionic strength may also reduce flux through a membrane due to electroviscous effects (Nazzal & Wiesner 1994). A flow of water displaces ions accumulated near the walls. This sets up a potential that produces an additional resistance to flow. Back migrating ions exert a drag force on the water moving through the capillaries. This is known as an electroviscous effect. This effect may also occur in fouling cakes.

At very high ionic strengths however, flux can increase once more as the Debye length decreases and the viscous effect is reduced.

Nazzal and Wiesner (1994) recommended that for colloid cakes, particle size can be manipulated by inducing aggregation i.e. changing the pH and ionic strength. However, if electroviscous effects dominate, the lowest cake resistance will be at low ionic strengths and high particle surface charge.

2.7 Protein fouling

The balance of hydrodynamic forces acting on a protein molecule is different from that acting on a bacterial cell, because they are one or two orders of magnitude smaller. One very important difference is that Brownian motion has a significant effect on the movement of a protein particle. Andrade (1985) listed the four main transport mechanisms for a protein:

1) Diffusion (different mechanisms from cells)
2) Thermal convection (not very important in cells)
3) Flow or convective transport (same as cells)
4) Coupled transport such as convective diffusion processes (different mechanism from cells).

Proteins and cells are subject to similar bonding forces, especially since cells have proteins attached to their surface, so the influence of parameters such as pH and ionic strength on protein is of interest. The most popular protein used in protein fouling experiments is BSA, so the results have a direct relevance to this thesis.

This review concentrates on protein microfiltration, mentioning ultrafiltration only as a point of contrast.

2.7.1 Fouling order

The simplest traditional explanation for the typical fouling curve can be explained in three steps shown in Figure 2.12.

I. Concentration polarisation

II. Protein deposition

III. Further deposition and consolidation

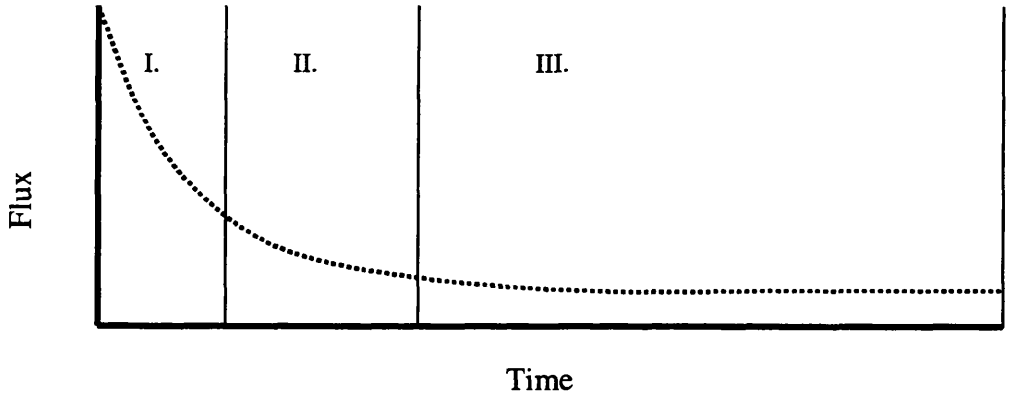

Figure 2.12: Traditional explanation of protein fouling

Concentration polarisation occurs very quickly and provides a reservoir of proteins from which deposition can occur. Deposition can occur both on the face of the membrane and inside the pores. The degree to which these occur depends on the relative sizes of the protein and membrane pore size, (Marshall, Munro and Trägårdh, 1993). Bowen, Calvo and Hernandez, (1995) identified three main types of filtration fouling:

1) When the proteins are much larger than the pores, as in ultrafiltration membranes, there is no intrapore fouling, but complete retention of proteins by the membrane. The reduction in flux is due to concentration polarisation, and the flux reduction is almost instantaneous.
2) When the protein is of a similar size to the pore size, pore blocking can occur, leading to an exponential decrease in flow.
3) If the pore size is much greater than the protein size, two distinguishable steps of long term adsorption and cake filtration occur. These steps may occur both within the pores and on the membrane surface. These two steps may also occur when the proteins are much larger than the pores; in this case fouling would be on the membrane surface only. This follows on from concentration polarisation.

The phenomenon of adsorption must be distinguished from that of deposition (the mechanism responsible for conditioning). Adsorption involves partition of a protein molecule between the solute and a surface. Therefore the maximum adsorption thickness must be that of a monolayer, but it may be significantly less (Bowen and Gan, 1991a). Further deposition of molecules remaining in solution is likely. This may continue up to 400 layers (Marshall *et al.* 1993). Generally the term "deposition" includes both of these phenomena.

Adsorption of proteins seem to fit Langmuir isotherms satisfactorily, even though they assume that protein adsorption reaches the equilibrium state of:

$P+A \leftrightharpoons PA$ Where P represents the protein and A represents the membrane surface.

In reality protein adsorption to a surface seems to be irreversible, but the fact that it tends to fit these isotherms demonstrates that the bonding is predominantly due to electrostatic attraction.

The Langmuir adsorption relationship can be expressed as

$$1/[PA]=1/K[A_T][P]+1/[A_T]$$

Where A_T is the amount of protein adsorbed if a single protein occupies each available site, and K is the binding constant.

Thus 1/[PA] versus 1/[P] can be plotted, where the gradient equates to the bonding constant. There tend to be two types of adsorption site, exhibiting high and low affinity for the surface as shown in Figure 2.13. Bowen and Hughes (1990) and Bowen and Gan, (1991b) assert that the higher bonding constant represents the strength of the adsorption bond, while the shallow gradient represents an average deposition bond. The cell deposition tends to be close together with a high bonding strength close to the membrane and a looser, weaker cake further away from the surface (Bowen and Gan, 1991b).

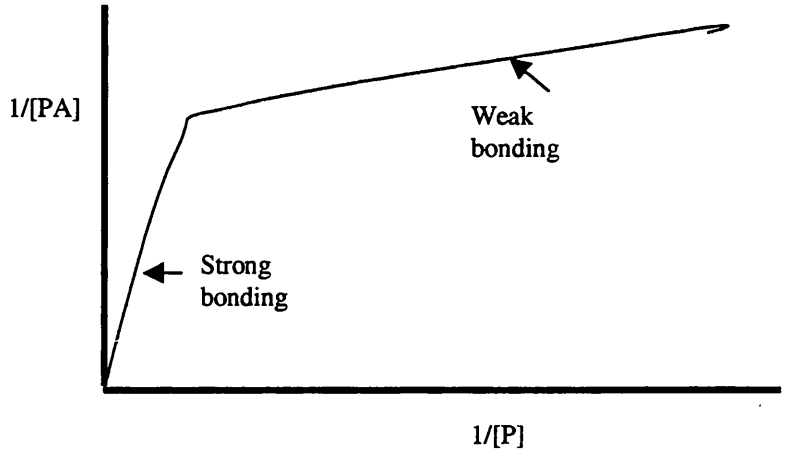

Figure 2.13: Strength of Adsorption bonds

Bowen and Jenner applied Hermia's models (see section 2.5.2.4) to describe four different types of fouling for dead end filtration:

- Complete pore blocking,
- Standard blocking,
- Intermediate blocking,
- Cake filtration.

A further description of three of these models may also be found in section 7.1.

Bowen and Jenner, (1995) studied how the four fouling models varied over time for filtration of BSA in 0.1 and 0.2 μm membranes. They found that the most dominant mechanism throughout the run was the standard blocking model, but all the other types of fouling existed concurrently. This is because the membrane used had a wide pore size distribution, so different fouling mechanisms were occurring at different pore sizes.

Foley *et al.* (1995a) found that pore blocking was affected by the pore size and pore size distribution of the asymmetric membranes used; the pressure difference was different across each pore.

2.7.2 Transmission

The standard blocking model, which is common at the beginning of a run, assumes that pore size is only slightly reduced, therefore transmission is still high. As time goes on, other mechanisms such as cake filtration start to dominate and protein transmission can be significantly reduced (Güell and Davis, 1996). This is a particular problem if the membrane is being used for fractionation. Molecules of lower molecular weight start to be retained, and selectivity between molecules is reduced.

There is also a risk that even if transmission is good, the activity of the protein may not be 100%. Bowen & Gan (1992) found that, for high affinity membranes and/or long filtration times, much of the protein in transmission was denatured. They postulated that this was due to protein denaturation either to many adsorption/desorption cycles or increased shear in the pores as a result of increased deposition narrowing the pores.

2.7.3 Importance of aggregates

Protein may build up gradually, molecule by molecule, or may deposit as aggregates. The presence of aggregates may make cake formation much quicker and easier. Aggregates can block the larger pores, causing a disproportionate loss of flux and they can also act as seeds for further deposits. Marshall *et al.* (1993) found that prefiltration can improve flux, as it removes the aggregates.

Some proteins are more prone to aggregation than others - Güell and Davis (1996) found that ovalbumen had a greater tendency to aggregate and therefore tended to foul more than either BSA or lysozyme. One of the main types of bond involved in aggregation is believed to be of the intermolecular thiol-disulphide variety. Ovalbumen has four thiol groups, BSA has one and lysozyme has none. Intermolecular thiol-disulphide is believed not to be the only type of bond to encourage aggregation however; disulphide bonds between cysteine residues are also thought to fulfil this function. A high initial flux may encourage aggregation as it may result in a supersaturation of protein molecules near the pore entrances.

2.7.4 Effect of pH and ionic strength

Analysis of the effect of pH on protein deposition can reveal which type of bonding dominates (Bowen and Hughes, 1990). At the isoelectric point, the protein has no net charge, so any deposition is due to hydration effects. As the pH moves further away from the isoelectric point, the protein becomes more charged. Therefore if the cell deposition is at a maximum at the isoelectric point, hydration effects dominate. If the maximum deposition is at a pH higher or lower than this value, electrostatic effects dominate.

Electrostatic effects are profoundly affected by the ionic strength of the solution. The charge on proteins increases either side of the isoelectric point and electrostatic repulsion enlarges the molecules at a low ionic strength. Ions in a high ionic strength solution shield the charges, thus decreasing the protein size and therefore voidage/permeability. It has been postulated that it is the charge on the protein rather than the difference in charge between the membrane and protein that affects fouling. This is attributed to the fact that when a protein is charged, the solubility increases and so the affinity for the membrane decreases.

The presence of some ions however may help adsorption, as both anions and cations are adsorbed to a molecule when it adsorbs to a membrane. It is especially true that cations are taken up when a negatively charged protein is adsorbed to a negatively charged surface (Bowen and Gan, 1991b).

2.7.5 Protein Concentration

Güell and Davis (1996) and Marshall *et al*, (1993) have reported an increase in deposition at the membrane surface when the concentration of BSA is increased. The former experiments were done below the isoelectric point at pH 3 and the latter experiments were done at the isoelectric point of pH 4.8. Therefore this phenomenon appears independent of net charge.

2.7.6 Membrane characteristics affecting fouling

Under static (dead end conditions) hydrophilic membranes tend to adsorb fewer proteins than hydrophobic ones. Hydrophobic membranes may denature adsorbed protein, causing them to expose different sites, thus encouraging further protein fouling. However, the membrane material is not the only consideration. It has been found that pore size and pore size distributions are more important parameters. Güell and Davis (1996) demonstrated that if the protein is much smaller than the pore size, it is the membrane morphology, especially the pore size distribution, which is important. In this case it is because the primary cause of flux decline is protein aggregation (affected by morphology) rather than individual protein adsorption (affected by surface chemistry). This contrasts with ultrafiltration membranes where the relative dimensions are comparable, so protein adsorption dominates, and surface chemistry becomes important.

Surface roughness may also affect protein fouling. Adhesion of surface-active molecules onto a surface results in a decrease in surface energy. An increase in surface roughness increases the surface free energy, and so can increase the adhesiveness of certain particles.

2.8 Separation of Solids and Macromolecular Solutes

When separation of cells or cell debris and macromolecules such as enzymes or proteins is required, complications arise with transmission of all the proteins through the

membrane (Le & Atkinson, 1985). This problem is particularly bad with cell debris (Kroner *et al.*, 1984, Le *et al.*, 1984a).

2.8.1 Effect of Physical Parameters on Enzyme Transmission

The effect of pressure on enzyme transmission is not clear, but enzyme transmission seems to increase at high pressures (Le *et al.*, 1984a). There seems to be evidence to show that this increase is due to better axial mixing within the pores (Hodgson *et al*, 1993a).

When whole cells or cell debris are present, there is a definite correlation between crossflow (CF) velocity and transmission. Le *et al.* (1984a) found:

$$\text{Transmission} \propto \text{CF velocity}^{0.18}$$

This is contrary to the concentration polarisation theory, which predicts that as CF velocity increases, wall concentration should decrease and transmission should therefore decline. When no cell debris is present, no such correlation exists.

It seems that at low pressures, CF velocity is important whereas at high pressure, the pressure effects dominate.

2.8.2 Mechanisms of Transmission Impedance

Various studies have linked protein inactivation and subsequent aggregation as a source of fouling (Le *et al.*, 1984b), (Hodgson *et al.*, 1993a). This theory is endorsed by the fact that macromolecules present in diluent such as antifoam and proteins cause enhanced flux decline compared to microfiltration of washed cells (Brown & Kavanagh, 1987). It is also well known that proteins have a great affinity for solid/liquid interfaces (Kent, 1988). The retention behaviour of macromolecules depends on the molecular weight, concentration and solution properties, e.g. pH and salt concentration (Datar, 1985). The retention of enzymes and total protein increases as an operation is prolonged (Kroner *et al.*, 1984).

Kroner *et al.* (1984) pointed out that the flux/transmission pattern of a separation of formate dehydrogenase and yeast cell debris seems to indicate a formation of thin but dense sublayers of suspension particles. These sublayers have permeabilities comparable to that of low cut-off ultrafiltration membranes so limiting macrosolute transmission through microporous membranes. This observation is endorsed by other papers (Datar, 1985; Hodgson *et al.*, 1993a; Defrise & Gekas, 1988). Le *et al.* (1984a) studied the separation of

aryl acylamidase from *Pseudomonas fluorescens* cell debris. They observed a transmission pattern that started off low for the first five minutes, then increased to a maximum level before falling again. They postulated that the initial low transmission was due to conditioning. Once the membrane surface was saturated, transmission increased until a formation of a secondary layer reduced it once more. The secondary layer characteristics have been found to depend primarily on the pore structure of the membrane (Le & Atkinson, 1985).

Hodgson *et al.* (1993a) carried out a study on the influence of the extracellular matrix on filtration and protein transmission. Using scanning electron microscopy they showed that less than 1 layer of SW8 bacteria was needed to reduce flux dramatically. Further studies by Hodgson *et al.* (1993b) on yeast confirmed this phenomenon.

They compared the fluxes obtained for untreated SW8 with those for SW8 treated with either pronase or EDTA. They then went on to compare this data to that for similar cell suspensions with BSA added. The final resistance to flux on addition of BSA was 2 orders of magnitude higher than that for cells only. Transmission profiles differed according to cell surface treatment; transmission decreased significantly after 60 - 70% coverage for untreated and pronase treated bacteria but it hardly affected the transmission for EDTA-treated cells. It is postulated that enmeshment of the surface polymers to form a matrix is the cause of the resistance and the reason that BSA had reduced transmission. For SW8 these polymers are mainly lipopolysaccharides with a few proteins. Costerton *et al.* (1978) pointed out the presence of lectins in the glycocalyx of most bacteria. Lectins bind very specifically to a particular molecular species in the glycocalyx of a cell of the same species (they are the plant equivalent of an animal antibody). This is probably one of the major mechanisms of enmeshment under these circumstances.

The Leva correlation which estimates cake voidage with particle bed pressure drops does not apply, since it is the matrix between the cells, not the cells themselves that compresses; and it also cannot apply because the particle beds are very thin. Sometimes flux enhancement with increasing crossflow velocities may arise due to the re-entrainment of macrosolutes rather than particles themselves (Le *et al.* 1984a).

2.9 Summary

A large body of research exists on the forces a biological entity is subject to during microfiltration. These forces are too numerous and complex to be able to derive a universal equation to fit all circumstances, especially when the dominant fouling mechanisms are system specific. Factors such as the relative sizes and shapes of the particles to be filtered, the operating conditions, the properties of the membrane selected and the physicochemical conditions all contribute to the balance of forces. Therefore, in order to understand a given system, it is important to understand the dominant forces and fouling factors at work for that particular system.

3 Cell and Extracellular Matrix Studies

3.1 Rationale

The aim of this work was to study the effects of the extracellular matrix on fouling. Therefore it was important to find three types of bacteria which were as similar as possible in other respects, but with extremely different extracellular matrix physiologies. This chapter describes how the three bacteria were chosen, and reviews the current knowledge about these bacteria and their close relatives. A short review of the protein utilised in some of the experiments, bovine serum albumin, is also included.

3.1.1 Extracellular matrix characteristics for consideration

Extracellular polysaccharide can occur in two forms, either as loose slime or as a well defined capsule (Wilkinson, 1958). They are usually both made up of only one type of polysaccharide, although this is not always the case, and they are usually hydrophilic, giving the cell a characteristic charge. Presence of a glycocalyx has been associated with initial colonisation of surfaces (Marshall *et al.*, 1971). It was decided that for this study, one of the cells selected should have a well-defined capsule, and one should be covered in slime.

Bacteria may also have flagella, fimbriae or pili that extend out from the cell wall. Flagella are up to 10μm long and 0.01-0.2μm thick (Dyson, 1978). They are made up of several strands of homogenous protein flagellin, which are wound about each other in a rope-like structure and secured to the cell membrane with a basal body. They are used for motility - the cell moves by whipping its flagella. When a cell uses its flagella to move towards a stimulus, this is known as ***taxis***. Pili (0.01μm by<10μm) are much smaller than flagella and cause bacteria to adhere to one another and to other cells. Fimbriae are even shorter, measuring 2μm, and are also thought to be involved in adhesion. It was important to find a third bacterium that had one or more of these types of structures on the exterior.

The following additional criteria were set down: -

1) They had to be Class I micro-organisms in order to minimise the risk of opportunistic pathogenicity.
2) They had to be of comparable size and shape.
3) They had to be Gram negative.
4) They had to be easy and fast to grow.
5) They must not occur in long chains naturally - bonding had to be due to interactions in the suspension or within the microfiltration unit.
6) If possible they had to be non-proteolytic, so that the amount of protein in the feed would remain constant.

These criteria were outlined to The National Collections of Industrial and Marine Bacteria Limited, who advised on three possible micro-organisms. The properties of the three micro-organisms selected are described in Table 3.1.

Organism	*Pseudomonas putida* NCMIB 9494	*Pseudomonas elodea* NCMIB 31461	*Sphingobacterium multivorum* NCMIB 2735
Shape	rod-shaped with rounded ends	rod-shaped with rounded ends	rod-shaped with rounded ends
Optimum growing temperature.	*28° C	#30° C	*25° C
Extracellular Matrix Type	Large number of Flagella Possibly fimbriae no capsule	High polysaccharide slime producer	Capsule only
Proteolytic	*Yes	*Not Known	*No
Pathogenically All three Category 1	^Colonisation more frequent than infection. Resistant to β-lactates	^Not known - never seen in hospital samples	^Occasionally found in hospital samples - but not a proven pathogen

Table 3.1: Summary of bacteria characteristics

References:

* = Bergey's Manual of Systematic Biology (1989), Bergey's Manual of Determinative Biology (1994).

^ = Topple and Wilson's Principles of Bacteriology, Virology and Immunity (1990) (Parker. & Collier (eds.)

= Kang and Veeder, (1983)

Other information – NCMIB catalogue

3.2 Cell review

3.2.1 Names

Both the genus and species of the same organism can be reclassified as more of its properties are discovered. For example, the bacterium originally named *Flavobacterium multivorum* (Holmes, Owen & Weaver, 1981) was renamed *Sphingobacterium multivorum* when sphingophospholipids were found to exist in this organism (Yabuuchi, Kaneko, Yano, Moss & Miyoshi, 1983). *Pseudomonas putida* has always been known by this name, but the bacteria referred to in this thesis as *Pseudomonas elodea* has been renamed several times. It shares many of the same properties of the *Pseudomonas* genus, but has poorer motility (hence *paucimobilis as a species name*) and also has sphingophospholipids in the cell wall (hence *Sphingomonas* for a genus name). In fact this bacterium seems to have distinctive properties in common with both of the other two, since it was originally classified as a *Pseudomonas* and two of its strains were once mistakenly classified as *Flavobacterium multivorum* (Holmes *et al*, 1981). Below is a catalogue of alternative names for *Pseudomonas elodea* 31461. This name is retained for this thesis, since this is the name it is supplied under in the NMIB catalogue. The current accepted name however is *Sphingomonas paucimobilis.*

- *Pseudomonas elodea* (Fialho, Monteiro & Sá-Correia, 1991)
- *Pseudomonas paucimobilis* (Smalley, 1982)
- *Auromonas paucimobilis* (Sutherland, 1994)
- *Sphingomonas paucimobilis* (Kawahara, Seydel, Motohiro, Hirofumi, Rietschel & Zähringer, 1991)

3.2.2 Pathogenicity

According to the WHO risk group system, a risk Group 1 micro-organism is one that is unlikely to cause human or animal disease of veterinary importance. All three bacteria are classified in this group, but *S.multivorum* and *P.elodea* are both common around hospitals, where they are opportunistic pathogens (Smalley, 1982). *S.multivorum* in particular has been known to cause septicaemia (Areekul, Vongsthongsri, Mookto & Chetanadi, 1996) and both display endotoxin activity on infection, causing such problems as leg ulcers, bacteria and peritonitis (Smalley and Bradley, 1983).

3.2.3 Methods of adhesion

3.2.3.1 Glycosphingolipids

P.elodea and *S.multivorum* are now both defined by their production of sphingophospholipids, which are usually only found in eukaryotic cells. However, *S.multivorum*, like *P.putida*, still maintains a conventional Gram negative outer cell wall which can be simplified as predominantly a phospholipid bilayer with lipopolysaccharides and protein embedded into this structure (Stanier, Adelberg and Ingraham, 1985). The lipopolysaccharides are the major hydrophilic antigenic determinant of the bacteria, and the O-side chains may extend out as much as 30 nm from the wall surface. A schematic diagram of a typical Gram negative outer cell wall is given in Figure 3.1. Lipopolysaccharides contain about six molecules of fatty acids, which are tightly gathered and stretched to the inside of the membrane. This part is known as the 'lipid A' section.

The outer wall of *P.elodea* does not contain lipopolysaccharides. Their function seems to be replaced by sphingophospholipids (Kawahara *et al.* 1991). Both molecules are ampiphilic. The lipid A equivalent part however has no fatty acids and only two hydrocarbon chains, which probably form a much looser bundle with adjacent molecules compared to the fatty acids of lipid A (Kawasaki, Moriguchi, Sekiya, Nakai, Ono, Kune & Kawahara, 1994). This makes the walls less electron dense. Although the cell walls of *S.multivorum* contain sphingophospholipids (Yabuuchi *et al.* 1983) they still contain much higher amounts of fatty acids than *P.elodea* (Smalley, 1982).

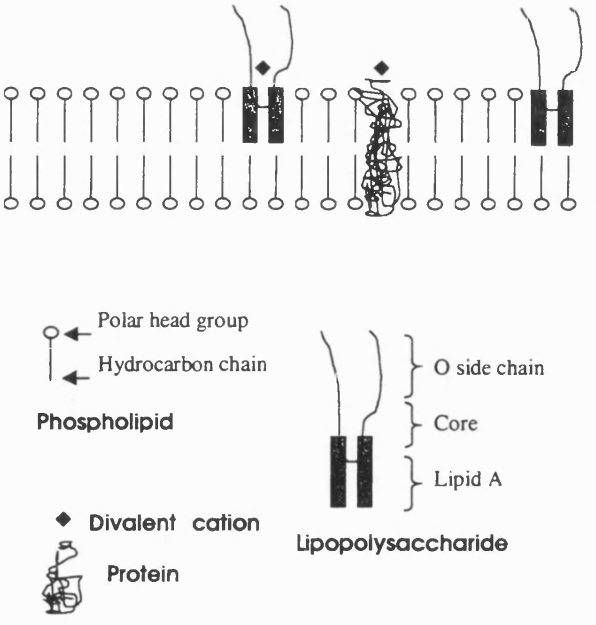

Figure 3.1: Basic structure of a cell wall from a Gram negative bacterium after Stanier, Adelberg and Ingraham (1985)

3.2.4 Specific adhesion mechanisms

Bonding of bacteria can be specific (e.g. receptor- ligand bonds) or non-specific (e.g. hydrophobicity and electrostatic attraction). The long O-antigenic lipopolysaccharides of the cell wall in *Pseudomonas spp.*, such as *P.putida* WCS358 appear to be involved in non-specific bonding, since shortening of these chains does not affect adhesion to surfaces such as sephadex beads. It does affect the adsorption to plant tissue however, since these bonds are specific (De Weger, van Loosdrecht, Klaassen & Lugtenberg, 1989).

The ligands on the surface of *P.elodea* and *S.multivorum* have been compared directly. They appear to have some antigenic properties in common, as they both bind to lectins from *Helix aspersa* (Smalley & Bradley, 1983). Lectins are proteins that act as a plant equivalent to antibodies in animals; therefore they play a role in specific cell adhesion (Dyson, 1978). The antigenic similarity between *P.elodea* and *S.multivorum* is limited, however; as they did not display similar bonding patterns with any of the nine other lectins tested. They also failed to produce antibodies to each other's mouse antisera.

Buell, Whetton, Tari & Anderson (1993) investigated specific cell-cell interactions in *Pseudomonas putida* that resulted in an agglutinable phenotype. These interactions seemed to come from a range of specific proteins in the glycocalyx. The flagella did not seem to contribute significantly to this type of bonding.

3.2.5 Industrial importance

3.2.5.1 Biocontrol

Biocontrol has been an important area for *P.putida* for several years now, and the potential for the other two in this area is starting to be realised. The fact that *P.elodea* and *S.multivorum* have sphingophospholipids on their outer walls is particularly useful, since they are required to adhere to eucaryotic plant cells, which possess cell wall sphingophospholipids by definition (Fenton & Jarvis, 1994). All three are useful at removing toxic compounds from the soil or air. Table 3.2 shows some examples of how they have been applied for this purpose so far.

Bacteria	Purpose	Reference
P.putida	Can reduce soft rot caused *by Erwinia carotovora* or *X.campestris* by up to 80% on fruit and vegetables e.g. tomatoes & peppers. Inhibits their growth by producing antibiotics. It can work for up to 5 weeks.	Liao (1989)
P.putida	A thin bacteria coating can promote plant growth and suppress fusarium wilt.	Buell, *et al*, (1993)
P.putida	Biodegradation of H_2S on an immobilised filter.	Chung, Huang & Tseng (1996)
Pseudomonas aeruginosa	*Pseudomonads* classified on their ability to produce a range of water-soluble fluorescent pigments. At least one of these pigments can improve growth of plants by complexing with iron required for the growth of deleterious micro-organisms.	MacDonald & Bishop (1984)
S.multivorum	Can detoxify corynetoxins up to a critical concentration. These cause Annual Ryegrass toxicity in grazing cattle.	Stuart, Payne, Reyes, Ashton & Edgar (1994)
P.elodea & *A.faecalis* co-culture	Biodegradation of polychlorinated biphenyls (a common environmental pollutant) to H_2O and CO_2	Davison & Veal (1997)
P.elodea	Degrades α, β, γ & δ hexachlorohexanes. These are insecticides commonly used in tropical countries. They are very persistent and can get into water and the food chain	Johri, Dua, Tuteja, Saxena, Saxena & Lal (1998)

Table 3.2: Industrial uses of *P.putida, S.multivorum* and *P.elodea*

3.2.5.2 Plasmids

The properties of these cells may be modified by insertion of genes on a plasmid to enhance their biocontrol abilities. Not all bacteria are suitable for plasmid transfer ; they are a potential energy drain and some strains may lose plasmids more readily than others may (McLoughlin, 1994). Monteiro, Fialho, Ripley & Sá-Correia (1992) found that although *P.elodea* 31641 can accept and retain small plasmids easily, there is a limit of 30-35kb of genetic material that can be transferred successfully. *S.multivorum* has been identified as an organism that accepts and retains naturally occurring plasmids such as the *sym* plasmid from *Rhizobium.* This plasmid confers the ability to nodulate leguminous plants, but not to fix nitrogen (Fenton & Jarvis, 1994). Therefore a successful retention of plasmids is easy to identify.

3.2.5.3 Gellan gum

The production of gellan gum, the copious extracellular polysaccharide from *P.elodea* 31461, has been patented (Kang & Veeder, (1983)) and it is mainly because of this product that interest in *P.elodea* has been increasing in recent years. The clarified polysaccharide can be prepared by filtering the hot fermentation liquor (Morris, Tsiami & Brownsey, 1995). It is built up of a linear chain of a tetrasaccharide unit of D-glucose,

D-glucuramic acid and L-rhamnose in the proportions 2:1:1. In its native form it forms weak elastic gels in the presence of cations when heated and cooled (Moorhouse, 1987). The L-glyceryl groups prevent co-ordinated interaction of ions and carboxyl groups required for strong gelation. The deacylated conformation however, can form much harder gels in the presence of cations.

The properties of the gels depend on the cation used. The presence of Calcium at relatively low concentrations produces particularly hard gels. The degree of deacylation also affects the gel properties, making it suitable for a wide range of products (Sutherland, 1994). Gelrite is already on the market as an agar substitute, which is clearer than traditional agar and stronger, so it can be spread thinner. Kelcogel is also a registered trademark, and is designed for a whole range of food products such as a thickener for ice cream and mayonnaise. However, it is awaiting a licence from the FDA. This is proving difficult because of the stigma attached to microbiological products.

High ionic strength of calcium ions has an interesting effect on the acylated form, shown in Figure 3.2.

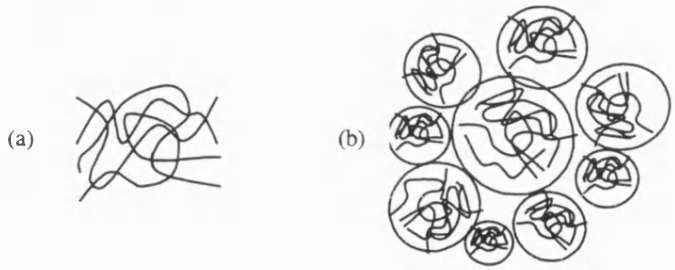

Figure 3.2: Comparison of gellan gum structure at a) low ionic strength b) high ionic strength $CaCl_2$

At low ionic strengths the polysaccharide forms an elastic network. At high ionic strengths it forms a microgel, where the inter-microgel forces are very weak and the microgel forces are strong. This gives the gel the potential for particularly interesting taste release properties (Morris, *et al*, 1995).

3.2.6 Effects of growth conditions

Gellan production is clearly an energetically expensive activity for *P.elodea*: Non gellan producing mutants grow faster than their slimy parents when incubated at 30°C (Fialho, Monteiro & Sá-Correia, 1991). At 30°C the parents produce an intermediate amount of polymer, between the amount they produce at 35°C (optimum cell growth, minimal gellan production) and 20°C (poor cell growth, greatest amount of high molecular weight gellan gum produced). Gelrite grade gum is produced at the lower temperature (Martins & Sá-Correia, 1993).

Dewanti & Wong (1995) found that restricting the nutrients available during growth of E. coli 0157 affected the type and amount of polysaccharide produced. Low nutrients produced smaller cells that produced more polysaccharide, and formed a stronger biofilm more quickly as a result. They also reported that a strain of *Pseudomonas putida* produced two sorts of polysaccharide – one for covering the surface and one produced after attachment to a solid surface. The growth medium affected the proportions of production. Buell *et al.* (1993) also found that the degree of cell agglomeration for two strains of *P.putida* mainly depended on the growth medium.

3.3 Bovine serum albumen (BSA)

This protein was chosen because it is one of the most commonly studied proteins, and so is well characterised. Its isoelectric point is at pH 4.8 and it has a molecular weight of 67,000 Daltons with dimensions of 11.6 x 2.7 x 2.7 nm (Güell and Davies, 1996). Albumins can bind both anions and cations. It has been proposed that cations and ions are absorbed or released when a protein attaches itself to a surface (Bowen & Gan, 1991b). For example, it appears that when a negatively charged protein adheres to a negatively charged surface, cations are taken up by the protein to balance the effect. The titratable ionic groups on BSA, such as carboxyl groups, number around 100, with pK values of around 4, so the effect of salts on BSA properties should be significant. Albumins are particularly affected by the presence of calcium ions, as one of their functions is to bind calcium for transport in the blood (Samson Wright's Applied Physiology, 1982). Human serum albumin, a close relative of BSA, has a weak affiliation ($K=100M^{-1}$) for calcium at 16 different sites.

3.4 Conclusions

Three gram negative rods were found that had similar size and shape specifications, but dramatically different extracellular matrix characteristics. The bacteria chosen were:-

1) *Sphingobacterium multivorum* (a smooth capsulate bacteria).

2) *Pseudomonas elodea* (with gellan gum, known to be affected by calcium ions).

3) *Pseudomonas putida* (with many flagella encompassing the cell wall surface).

BSA was also chosen as it is one of the most commonly studied proteins and one of its primary functions in blood is to bind well to calcium.

4 Materials and methods

4.1 Introduction

Three bacteria with different extracellular properties but of a similar size and shape were filtered under similar conditions to see how the extracellular matrix affected fouling factors. In the first few experiments the three micro-organisms were filtered in broth. The majority of experiments, however, were carried out with cells suspended in solutions of NaCl and $CaCl_2$ of known ionic strength, both with and without BSA. All of these solutions were filtered for 90 minutes under identical conditions. This chapter describes the materials and methods involved in characterisation, growth and maintenance and filtration of the bacteria. It is divided into three main sections.

The first section describes the materials and methods employed to characterise the three bacteria in terms of: -

- Surface charge (Zeta potential measurements)
- Hydrophobicity (BATH, SAT and adhesion to a hydrophobic surface)
- Cell sizing and cell size distribution (optical microscope, conventional SEM, cryogenic SEM
- Mass (dry weight)
- Polysaccharide levels (precipitation in alcohol)
- Viscosity (viscometer)

The second section covers the materials and methods for growth and maintenance of the bacteria. It also includes a description of how the suspensions for the filtration experiments were prepared, and how the cells were counted for growth and calibration purposes.

The materials and methods for the filtration experiments can be found in the final section of this chapter, covering: -

- Experimental apparatus (the rig, the membrane, the computer and its program, the bubble flowmeter)
- Experimental procedure
- Cleaning
- Safety and disposal

4.2 Characterisation of cell properties

Characterisation of the three species of bacteria selected was necessary to help to understand the filtration behaviour, and to verify the dimensional similarity of the three types of cells. See chapter 5 for further details.

4.2.1 Zeta Potential

A Zetamaster from the University of Swansea was used to calculate the Zeta potentials of the cells. The zeta potential for a bacterium can be calculated from the data obtained using Smoluchowski's equation as described in the equation below. This version of the equation is used when the double layer thickness (the Debye length) is significantly less than the diameter of the particle (Hunter, 1981). The cross beam mode was set to F(m)=1.5 to ensure conditions compatible with the Smoluchowski equation as described below.

$$u_E = \frac{\varepsilon_r \zeta}{\mu}$$ **Equation 13**

Where: -

u_E = electrophoretic mobility

ε_r = relative permittivity to a vacuum (water=79)

ζ = zeta potential

μ = viscosity of suspending liquid

It was necessary to measure the Zeta potential of the bacteria and protein at each of the ionic strengths used in the filtration experiments. Cells were grown up in 250 ml shaker flasks, washed and resuspended, as described in section 4.3. Time did not allow the measurement of the combined effects of bacteria and BSA on the zeta potential value, but the order of magnitude for these results can be inferred from the others.

4.2.2 Hydrophobicity measurements

It is a well accepted fact that one hydrophobicity test done in isolation does not give a good indication of the hydrophobicity of different types of particles. More than one must be undertaken to build up a more comprehensive picture and the results can only be taken to be relative to one another (Lee & Yii, 1996; Bunt *et al*, 1995). This is partly because conditions such as ionic strength or ionic species used can affect the results (Jones *et al*, 1996). Another reason is that different tests measure hydrophobicity at different scales. Three types of tests were carried out on the bacteria:

1) BATH (Bacterial Adherence To Hydrocarbons),

2) Adhesion to a surface test (a Petri dish)

3) SAT (Salt Aggregation Test).

For the first two tests, washed cell suspensions of the same composition as in the filtration experiments were used (see section 4.3), while the SAT tests were carried out with washed cells in different concentrations of $(NH_4)_2SO_4$ solution

Most of the cell concentrations for the BATH and Petri dish test were measured using a spectrophotometer. However, some of the *Pseudomonas elodea* suspensions, especially those above 9 x 10^8 cells per ml, needed to be counted using the haemocytometer.

All the SAT suspensions had to be counted by haemocytometer, since all cell concentrations had to be approximately 5 x 10^9 cells per ml for this test. A detailed description of assessment of cell numbers is given in section 4.3.1.

4.2.2.1 BATH test

The BATH test was a modification of the test first described in Rosenberg *et al* (1980). This method is based upon measuring the degree of partitioning of the bacteria between solutions of electrolyte and hydrocarbon. It detects specific hydrophobic sites on the cell surface.

There are several possible hydrocarbons that can be used, but n-octane was selected, since this seems to be the most sensitive to hydrophobicity across a range of cell types and hydrocarbon concentrations Rosenberg *et al.* (1980), and is the one most frequently recommended (Rosenberg, (1984), Lee & Yii, (1996)). The BATH Procedure was carried out as follows: -

1) Before the tests were carried out, the test tubes were cleaned using chromosulphuric acid, as recommended in Rosenberg *et al* (1984).

2) The cells were suspended in the same ionic solutions as for the filtration experiments, since it is known that ionic strength affects the results (Bunt *et al*, 1995). Bacteria suspensions both with and without BSA were tested.

3) The initial cell density (C_b) was measured at 330 nm and the suspensions adjusted to be between 2 and 6 x 10^8 cells per ml.

4) 6 ml of each cell suspension was aliquoted into a 10 ml test-tube and 0.48 ml of n-octane was added to each tube.

5) The contents of the test tubes were then vortexed on a whirlimixer for 2 minutes and allowed to settle out into an aqueous and organic phase for 15 minutes.

6) The cell concentration in the aqueous phase was then re-measured (C_a).

Hydrophobicity is expressed as the inverse of the ratio of the bacteria in the aqueous phase post emulsification of the bacteria, to the bacteria in the aqueous phase prior to partitioning, i.e.

$$CSH = 100\left(\frac{C_a}{C_b} - 1\right) \qquad \textbf{Equation 14}$$

Where: -

CSH= Cell surface hydrophobicity rating

$C_{b=}$ Cell concentration in aqueous phase before test

$C_{a=}$ Cell concentration in aqueous phase after test

4.2.2.2 SAT test

Lindahl, Faris, Nadström & Hjerten (1981) outlined this technique to test for the overall hydrophobicity of a surface, based on cell aggregation due to 'salting out'. The procedure is laid out below.

1) The cells were suspended in 0.002M sodium phosphate buffer (pH 6.8).

2) The cell density was measured at 330 nm, to check that the cell concentration was in the order of 5×10^9 cells/ml. The cell concentration needed to be as high as this in order for the effects to be seen clearly (Lindahl *et al*, 1981).

3) Serial dilutions of an $(NH_4)_2SO_4$ solution of between 0 and 4M were made up. Further details of the SAT solution concentrations are given in Table 5.2 in Chapter 5.

4) 25 µl of cell suspension was mixed with 25 µl of each of these $(NH_4)_2SO_4$ dilutions on a slide pre-cleaned with alcohol.

5) After 2 minutes, each slide was examined for signs of agglutination under a stereo microscope under a low power. The presence of agglutination is regarded as a positive result.

Lee and Yii (1996) also suggested guidelines for grading hydrophobicity measurements for this test, dependant on the minimum strength of solution to cause aggregation. These thresholds are outlined in Table 4.1

Molarity in moles per litre	Hydrophobicity definition
0-1	Strongly Hydrophobic
1-2	Medium Hydrophobicity
2-4	Weak Hydrophobicity
>4	Not Hydrophobic

Table 4.1 Definition of hydrophobicity for The SAT test.

4.2.2.3 Adhesion to plastic test

This test is based upon the probability of cells attaching to a hydrophobic surface to determine the cell hydrophobicity. Therefore it also is a test of overall hydrophobicity.

1) The same cell suspensions as for the BATH test were also used for this test.
2) 6 mls of each cell suspension was aliquoted into a 100 x 10 mm Petri dish which provided a hydrophobic surface as described by Buell, Whetton, Tari and Anderson, (1993).
3) Two sets of dishes were incubated for 4 hours at 6°C before being gently shaken (50 rpm) at room temperature. One more batch was incubated for 4 hours at 28°C to test for temperature effects.
4) After 20 minutes the cell suspensions were poured into cuvettes and the cell densities re-measured at 330nm.

The lower the turbidity of the final cell suspension: the greater the number of cells deposited, and the higher the level of hydrophobicity demonstrated. The results in Tables 5.3 to 5.5 are again categorised into ranges of 10%. All sets of results were within this 10% margin for each test.

4.2.3 Cell sizing and cell size distribution

In order to determine the effects of the extracellular matrix, it was important to establish that the cell dimensions were comparable.

Initial experiments were carried out in which cells were stained with crystal violet and carbolfuchsin (Collins, Lyne & Grange, 1995). A coverslip was then placed over part of the stain and sealed. The stained cells were examined under a light microscope at a magnification of ×70, with a C.C.D. camera connected to a video recorder. The disadvantage of this technique is that the cells are dehydrated when stained and will undergo shrinkage, so the actual size of the cells in the suspension feed cannot be measured this way. Nevertheless, this is a suitable method for measuring the cell size distribution, assuming that the shrinkage factor is consistent, as a large sample size can be taken. A total of one hundred cell size measurements for each species of bacteria was deemed a satisfactory sample size. These measurements were made from printed stills from the video.

The most accurate way to measure the cell dimensions was cryogenic SEM. Since the sample was frozen rapidly to avoid the formation of crystals, all the water was retained in the sample. As stated by Graham *et al.* (1991) this procedure could give an accurate image of the actual dimensions of the cell, but the sample size could not be very large- only 40 cells for each species.

Images of the cells were also taken using the more conventional SEM with gold sputtering in order to define the cell shape. This gave an indication of the dimensions of the cell with the cell 'coating' removed; loose polysaccharides and proteins are stripped from the wall during preparation. The sample size could only be 50 or less.

TEM images were also taken, in an attempt to record any fimbriae, pili or flagella present.

For all electron microscope images, photographs were taken and developed, and it is from these photographs the cell dimensions were measured.

4.2.4 Mass

The mass per cell was deduced as follows; 2×250 ml shaker flasks of each bacterium were grown up to stationary phase (see section 4.3.2.2). They were then washed once in buffer, in 1/3 of the original broth volume. The cell concentration for this buffer suspension was then measured using a diluted sample of the cell suspension where the absorbance was less than 1.7. The sample was then poured into pre-weighed weighing boats and dried in an oven below 100 degrees for 2-3 days, then re-weighed.

4.2.5 Polysaccharide levels

Extraction of polysaccharide was carried out using the method detailed in Kang & Veeder (1983). This involved precipitating the polysaccharides by adding 2 parts isopropanol to 1 part cell suspension. This precipitate was emptied onto pre-weighed filter paper and dried in a tray drier.

4.2.6 Viscosity

Cell samples were grown in a 250 ml shaker flask then washed with buffer (see section 4.3.2.2). They were then resuspended in solutions of the same composition as the filtration experiments, at a concentration of approximately 7-7.5 x 10^8 cells/ml, as for the filtration experiments, both with and without BSA. BSA alone in the different solutions was taken to be the control. The viscometer used was a Brookfield Digital Viscometer (model DV-II). It was set up for 30 and 60 rpm at 23-24°C, in order to check for non-Newtonian behaviour.

The readings were left to settle for a couple of minutes with each change in shear before three readings were taken and averaged. Each set of readings was within 6% of one another. Most of the viscosities were too low to register at 30 rpm, so the rheology could not be determined. However, the only suspension likely to reveal a degree of non-Newtonian behaviour would be *P.elodea* with its copious gellan gum production (Kang & Veeder, 1983). None of the viscosity measurements changed significantly with time.

4.3 Growth and Maintenance

4.3.1 Calibration and measurement

One of the most crucial measurements both for ensuring similarity of experimental conditions and understanding cell deposition is that of cell counting. A quick, simple method to measure the cell concentration of a suspension was required.

4.3.1.1 Most probable number method

In order for the results to be comparable, it was essential for the cell concentrations to be equivalent in these experiments. It was also necessary to be able to follow cell growth to stationary phase. There are several methods of counting viable cells. The first to be tried was the "Most Probable Number" method (Isaac & Jennings, 1995). This method is one of the more accurate ways to ascertain the number of viable cells present and initially seemed most suitable for the growth curve calibration. It is based on the assumption that bacteria follow a Poisson distribution in liquid media. That is to say that repeated samples of the same volume and media will contain a comparable average number of micro-organisms. If the cell number is large, as for example, at the end of the log phase, the differences between samples is small.

The most probable number of bacteria in a sample is deduced by taking a sample of a given volume, and growing it up in nutrient broth, together with a tenfold and hundredfold dilution of the same sample. The most dilute sample with signs of growth indicates that this is the dilution at which at least one bacterium was present. Tables have been prepared for samples of 10 ml, 1 ml, and 0.1 ml using three or five tubes of each sample size (Isaac and Jennings, 1995). These give the most probable number per 100 ml. This method cannot give rapid results since it relies on cell growth of 24 to 48 hours before the results can be known (Smalley and Bradley, 1983). This was the first method to be tried, but was discontinued since filtration is affected by the total number of cells, rather than the number of viable cells, and a more rapid assessment method needed to be found.

4.3.1.2 The Haemocytometer

The total number of cells can be estimated by counting samples under a light microscope.

A haemocytometer, illustrated in Figure 4.1, was used for this method. The overall grid scored on the surface of the glass is 3mm x 3mm. This is divided up into

nine squares of $1mm^2$. It is usual to count yeast cells at a magnification of x 45 in these squares, but the bacteria were hard to discern on this scale. The centre square is divided up into 25 squares of 0.2 x 0.2mm. Therefore the bacterial cells were counted in the 0.2mm x 0.2mm squares (highlighted in yellow in Figure 4.1) at a magnification of x 60. The coverslip was raised 0.1mm above the glass, so each square represented the number of cells in 4×10^{-6} cm^3.

1) The cells were diluted with Ringer's, so that the number of cells per square was around 100. 1% formalin was added to the cell suspension as part of the dilution process. This helped to preserve the cells intact.

2) The number of cells in several squares was counted until the total number of cells recorded was just above 500; the number of squares counted was usually between four and seven.

3) This counting procedure was repeated with two more samples. The determination of the number of cells per ml was achieved as follows.

Cells per ml = cells counted/(squares counted x 4.6×10^{-6} x dilution factor)

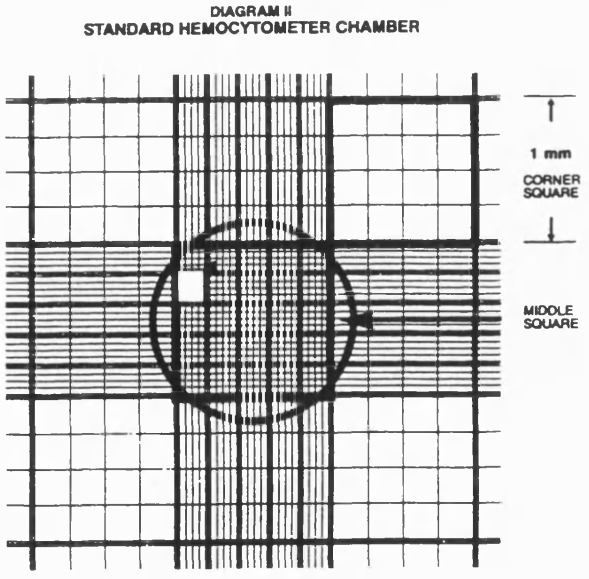

Figure 4.1: Representation of a Haemocytometer

The reproducibility of these cell counts depended on the dilution factor and number of cells present in one square, i.e. the higher the cell concentration to be assessed, the more difficult it was to estimate the cell concentration accurately. Standard deviations ranged between 4 and 18%, with a mode of 11%.

4.3.1.3 Spectrophotometer

Counting cells under a microscope is still not a very rapid method of assessment, as several counts must be carried out. It was therefore necessary to relate the haemocytometer figures to an even quicker method of analysis. One appropriate method is spectrophotometry; cell concentration can easily be related to the turbidity or absorbance of the sample. The optimum wavelength is the one that gives the maximum absorbance. Samples of all three bacteria suspensions were taken and a scan was performed on a CECIL Aurius Spectrophotometer. It was shown that absorbance remains high until around 350nm, then drops rapidly. Calibration curves for the same cell sample were drawn for the different bacteria in both broth and buffer at 330, 480 and 550 nm, using the same spectrophotometer as for the experiments- a CECIL CE 1020. A sample selection of these calibration curves, including all the calibration curves used, can be seen in appendix A. A wavelength of 330nm was selected as appropriate for both the broth and Ringer's calibrations. The disadvantage of using this wavelength is that plastic cuvettes absorb some of the light, and therefore it is more usual to use a higher wavelength. The problem is not too serious however, since the offset of the control (water in a cuvette) had an absorbance reading of approximately 0.12, equivalent at worst to an offset of approximately 8% of the original cell concentration for *S.multivorum*. This is less than the mode of error for the haemocytometer cell counts.

Another necessary compromise was with the cell concentration range measured. At low turbidities, there is a direct correlation between the light scattered and its concentration. At high cell concentrations, there is secondary scattering (Kleizen *et al*, 1995) and the relationship between the two is more complicated. A typical shape of a calibration curve is given in Figure 4.2.

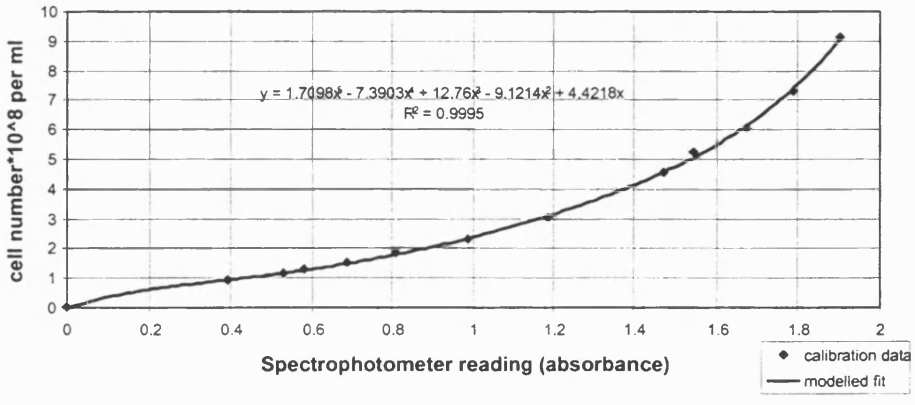

Figure 4.2: Absorbance calibration curve for *S.multivorum* in Ringer's at 330 nm

Eventually the curve flattens off or becomes too steep, and readings become too inaccurate to rely upon. It is usual to attempt to work only in the linear part of the curve, but most experiments were carried out at a cell density of around 7-7.5 x 10^8. Looking at the calibration curves, it can be seen that working in this range would entail diluting down these samples several times to get into the linear part of the curve.

Since dilution will result in its own errors, and is difficult for broth, it was deemed best to set an absorbance limit of 2 (as recommended by the manufacturers) for calibration purposes and 1.85 for experimental purposes. Because of its high turbidity, *P.elodea* samples had to be diluted at least 1:2 every time. For samples containing calcium chloride or BSA, samples had to be diluted 1:4. Samples of *P.putida* and *S.multivorum* in calcium chloride solution also had to be diluted 1:2.

As can be seen by the calibration curves in appendix A, the 480 and 550 nm curves had linear plots over a wider range of cell concentrations. This advantage was offset by a greater disadvantage; the CECIL CE 1020 was not very sensitive to change in absorbance at these wavelengths. This problem was compounded by the fact that at higher wavelengths the calibration curves revealed much lower gradients. Thus a small error in absorbance caused a greater uncertainty over the value of the cell concentration at these higher wavelengths. Back checks on cell concentration readings at 330 nm, using the haemocytometer, demonstrated that the standard deviation for these readings were less than the 11% standard deviation for the haemocytometer counts.

It is interesting to note that one sample of *P.putida,* estimated at 5.02×10^8 cells per ml using the calibration curve/cell count method, was estimated to be 4.4×10^8 cells per ml using the Most Probable Number method for viable cells. Thus there is only 14% difference between the two methods. For *S.multivorum*, the estimated cell density of a sample was 2.2×10^8 cells per ml for both methods. The fact that both methods gave rise to similar numbers was encouraging. However the cells were in nutrient broth until sampled, so they had a good chance of remaining alive. Therefore similarity was expected.

4.3.2 Growth, Maintenance and Cell preparation

4.3.2.1 Bacteria Maintenance

All three bacteria were obtained from the NMIB catalogue in the form of freeze-dried cultures: *Pseudomonas putida* (NMIB 9494), *Pseudomonas elodea* (NMIB 31461) and *Sphingobacterium multivorum* (12558). After rehydration they were maintained on

Oxoid nutrient agar slants and plates. 300 ml of Oxoid nutrient broth in shaker flasks were inoculated with bacteria from these plates and grown up for 48 hours at 25°C and 170 rpm.

These three cultures were sub-cultured every six weeks onto two nutrient agar slopes and three 10 x 100 mm Petri dishes in order to maintain viable, fast -growing stocks. They were grown for 48-72 hours at 28-30° C, before being stored in the refrigerator at 4°C.

Originally *P.elodea* NMIB 12171 was used, but the growth of this strain was very poor, and a switch to NMIB 31461 was made.

4.3.2.2 Growth of cells for characterisation

Bacterial cells from the Petri dish sub-cultures were inoculated into 200 mls of nutrient broth in a 250 ml flask using a sterile loop. They were grown up in a shaker bath at 170 rpm until stationary phase was reached. Conditions were as described in Table 4.2, except for the growth times. Stationary phase was reached at 18-24 hours for *P.putida*, 18-30 hours for *S.multivorum* and 42-54 hours for *P.elodea*. The cells were then decanted into 20 ml test tubes and spun down for ten minutes at 4,000 rpm using a Burkard Koolspin centrifuge. The broth was poured away and the cells resuspended in buffer (see section 4.3.2.5) before re-centrifuging. The cells were then resuspended in the appropriate medium.

4.3.2.3 Fermentation

2× 250 ml seed flasks of Oxoid nutrient broth were inoculated from the Petri dish sub-cultures and grown up in a shaker bath at 170 rpm. At first all the cell cultures were grown until mid-stationary phase (around 18 hours for *P.putida* and *S.multivorum*), but it was found that inoculation of the seed at early to mid-exponential phase resulted in a more rapid increase in cell density rate in the main fermentation. The final cell density at stationary phase also tended to be higher. The *Pseudomonas elodea* shaker culture on the other hand, was grown until early stationary phase. This was necessary because *P.elodea* displays slow growth and is easily contaminated. At stationary phase, it is easy to see if there is contamination; a pure *P.elodea* culture is bright orange, but any likely contaminants will be paler. The conditions for each seed culture are laid out in Table 4.2.

160 ml of seed culture was inoculated into 1600 ml of nutrient broth in a 2 litre Quickfit fermenter jar. This operation was performed using a 50ml sterile syringe and sterile rubber tubing under a sterile hood. The two-litre fermenter was immersed in a water bath at the appropriate temperature (Table 4.2) and aerated using either an aquarium pump (30 litres per hour) or service air. Cell samples were taken every 4-8 hours until two consecutive cell density measurements had similar values, indicating early stationary phase. This was chosen as the most appropriate time to harvest the cells, since this is when the cell density has reached a maximum, but nearly all the cells are still alive. It is important to harvest the cells as young as possible, as the harvesting process is time-consuming. Fermentations were stored in a cold room at 4 °C until the centrifuge equipment was available.

Bacteria	broth type	seed culture times	Temperature	fermentation times
P.putida	N.B.	4-8 hours	28 °C	36-72 hours
S.multivorum	N.B. + 1% glucose	5-10 hours	25 °C	48-72 hours
P.elodea	N.B. + 2% glucose	36-48 hours	30 °C	72-96 hours

Table 4.2: Fermentation conditions

N.B.= Oxoid nutrient broth

It is important to note that the glucose solutions described in Table 4.2 were originally vacuum filtered into the autoclaved nutrient broth through a 0.45 μm Mempore filter. This led to frequent contamination problems, even though the filter was autoclaved. It was therefore decided to include the glucose in the broth before autoclaving. At these glucose concentrations, the problem of caramelisation was not found to be severe.

Initial experiments were undertaken on cells in broth. The more concentrated suspensions were diluted into nutrient broth in order to make the concentrations of the bacterial suspensions as similar as possible. In these particular experiments the cell concentration was 2×10^8 cells per ml. This is about an order of magnitude lower than at stationary phase.

4.3.2.4 Harvesting

For the rest of the experiments, the bacterial cells were decanted into 300 ml centrifuge pots and spun down under the conditions listed in Table 4.3. The broth was then decanted off and autoclaved (section 4.4.4), while the cells were resuspended and washed once in phosphate buffer. Washing in Ringer's was not desirable: it contains

salts such as sodium, potassium and calcium chloride, as well as sodium thiosulphate pentahydrate. The presence of these salts would compromise the ionic strength and valency of the experimental solutions. Therefore phosphate buffer, as defined in section 4.3.2.5, was preferred.

The difference in the necessary centrifugation conditions between the cells may be due only in part to cell density. It appeared to be also due to the strength of the intercellular bonds, as the hard pellet formed by *P.putida* was extremely difficult to resuspend, diffuse *P.elodea* started to resuspend with a small shake, while *S.multivorum* resuspended with even the slightest movement.

Bacteria	**Centrifugation time in minutes**	**Speed in rpm**
Sphingobacterium multivorum	40	10,000
Pseudomonas elodea	25	10,000
Pseudomonas putida	15	6,000

Table 4.3 Conditions for cell centrifugation

The washed cell pellets were suspended in 500-900 mls of electrolyte of the appropriate ionic strength (see section 4.3.2.5), and the cell density estimated using the CECIL CE1020 spectrophotometer. The cell suspension was diluted into a 2 litre Quickfit vessel to give a suspension as close to 7.5×10^8 cells per ml and 1800 ml as possible. The absorbance was remeasured as a check. A leeway of 0.5×10^8 cells per ml was permitted.

Some of the experiments were undertaken with BSA in the diluent. This fraction VIII BSA was obtained from Sigma. For experiments with protein, 1g/l was stirred into the electrolyte before the cells were suspended in it.

4.3.2.5 Media Ionic Strength definitions

The simplest way to make up solutions of particular ionic strengths is to adjust the strength of a sodium or potassium phosphate buffer. The buffer used in this case was a Na_2HPO_4/KH_2PO_4 buffer of pH 6.6 0.005M (1.875×10^{-3} mol/l and 3.125×10^{-3} mol/l respectively). The buffer pH was selected to be well away from the isoelectric point of BSA of 4.8 (Bowen & Williams, 1995) and the molarity needed to be low, since the lowest concentration of NaCl to be added was 1.725×10^{-3}M, or 0.1 g/l. The high concentration of NaCl was set at 40 g/l (0.68M). To contrast with the effect of the

monovalent Na^+ ion, 29.5 g/l $CaCl_2$ –an equivalent ionic strength to 40 g/l NaCl was also tried.

Experiments with these three solutions were run both with and without BSA. Finally experiments with 0.6 g/l $CaCl_2$ (5.4 x 10^{-3}M) were also run. The equation to estimate the ionic strength of a solution is given as:

$$I = \frac{1}{2}\sum c_i z_i^2 \qquad \textbf{Equation 15}$$

Where:

c_i = concentration of ions in moles per litre

z_i = valency

The cells were tested for their ability to remain intact in all of these solutions. Each species of bacteria was suspended in each type of electrolyte for three days in a cold room at 4 °C and the absorbance measured before and after the three days. A change of reading might be due either to a change in number of cells, or to a change in size due to osmotic effects. Three sets of each test were taken. The cells in low ionic strength electrolytes did not seem to degenerate significantly; the absorbance of the cell samples after three days represented only a 1-2.5% drop in cell concentration. The high ionic concentration cell suspensions on the other hand recorded a drop of 7-7.5% for NaCl and 7.5-8% for $CaCl_2$ at the end of three days. The drop after only one day was between 1 and 2%. The control cells suspended in Ringer's revealed no change in absorbance throughout the three days.

4.4 Microfiltration Experiments

4.4.1 Experimental Apparatus

Figure 4.3 shows the experimental rig set-up. All tubing was silicon, attached to the apparatus via solid plastic tubing and snap ties. The inside diameter of the permeate line was 2 mm, while the rest of the tubing had an inside diameter of 10mm and a thickness of 1.5 mm. A centrifugal pump (Volumation micropump, 11 amps, 50 Hz) forced the water/feed suspension from one of the 2 litre feed tanks through the apparatus. The temperature of the feed was kept constant by a water bath (23 °C for all experiments). The flowrate of the retentate was measured by a rotameter (maximum scale 2 litres per minute) and an approximate value for the inlet/outlet pressures for the transmembrane pressure was taken from the pressure gauge readings. A more accurate

TMP (Transmembrane pressure) reading could be calculated from the data relayed from the pressure transducers to the computer. Thus the inlet, outlet and permeate pressures were displayed on screen. The bubble flowmeter also logged data to the computer, which displayed the permeate flux on screen (see section 4.4.1.3).

Diverter valves were required on the feed lines, since a rapid switch from water to feed was required while the bubble flowmeter was running (see Computer program section). They were simple plastic roll on/off valves fitted to the outside of the silicon tubing. Without these valves, air got into the pipes when the pump was turned off, which could damage the pump when it was turned on again.

There were also two valves of the same type on the retentate lines to enable the choice of retentate return to the feed vessel or waste vessel. This was important both at the beginning of an experiment when the pipe contents change from water to cell suspension and during cleaning, when changing from flush to recycle mode. It was also important to contain the bacteria in the rig for safety reasons.

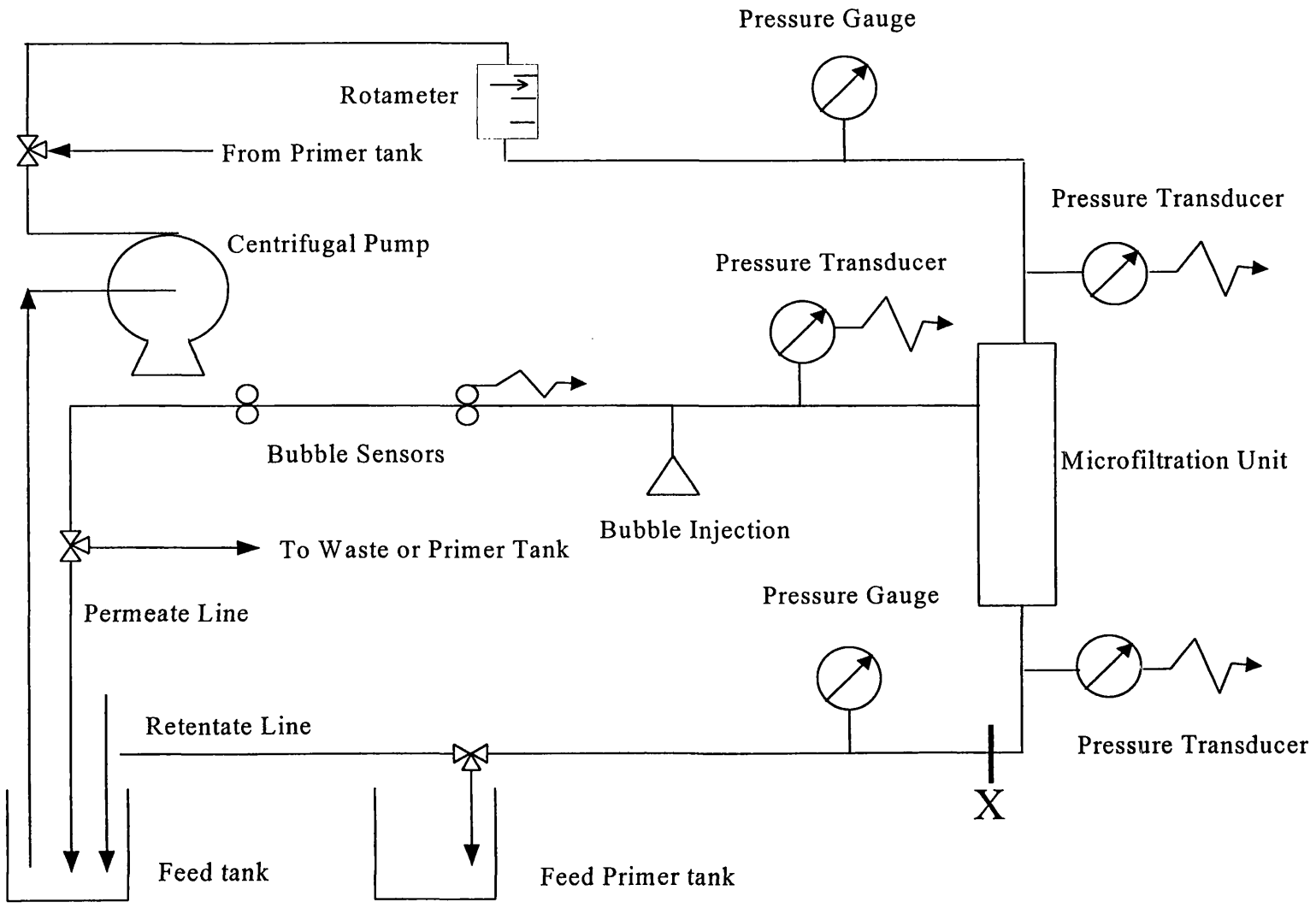

Figure 4.3: Plan of the rig layout

4.4.1.1 The Membrane

An Optimem-E300 microfiltration module was used for all the experiments. This houses a capillary membrane with the retentate remaining within the tube, and the permeate entering into the shell. Below is a table of the membrane specifications.

Name	Optimem-E300 Microfitration module
Company	Acumem (North West Water)
Pore size	0.2 μm
Maximum Pressure	3 bars
No. of fibres	40
Length	29.9 cm
Diameter of Fibres	1.5 mm
Total area	0.0565 m^2
Water Flux at 1m/s crossflow velocity,1 bar TMP, 25° C	286 l/hr
hydrophobic/hydrophilic	very hydrophilic

Table 4.4: Details of the membrane used in the experiments

When the membrane was out of use for a few weeks, it was filled with a solution of 0.05% w/v sodium azide to prevent growth of any micro-organisms.

Unfortunately, attempts to characterise the hydrophobicity by surface angle measurements and the charge by streaming potential analysis were unsuccessful, since the membrane was not a flat sheet.

4.4.1.2 Pressure Transducers

Three Druck PDCR 900 pressure transducers were purchased. Their positions in the rig are marked in Figure 4.3. All three transducers relayed signals to the 286 computer for logging. The TMP could then be calculated after the end of the experiment using a spreadsheet.

Transducer number	**0**	**1**	**2**
Offset	-26	-1	-24
Scale	99.02	99.76	100.13
Range (bar)	1	2	2

Table 4.5: Pressure transducer calibration

Pressure Results- (Offset x 100 x Range/Scale x 2048)

4.4.1.3 Bubble flowmeter

A bubble flow meter was used to measure the permeate flux. This method is useful for microfiltration experiments, as it has a high turndown ratio. The flow rate was measured by allowing a bubble to be generated and released into the permeate liquid (see

Figure 4.1). The permeate and bubble then flowed through a glass tube past three infrared sensors. The first sensor controlled the rate of generation of bubbles. The difference in refraction index of infrared light for liquid and gas means that a signal is generated when the trailing edge of the bubble passes the sensor. The time taken for the bubble to travel between the other two sensors can thus be measured. These measurements were calibrated to give an equivalent flux. A more detailed description of how the bubble flow meter was made and the principles behind it can be found in Bishop & Sanders (1989).

The calibration equation was used to calculate the flow rate and its coefficients were found by comparing the time it took a bubble to travel between the sensors and the value of the flow rate obtained by using a measuring cylinder. The bubble flow meter was not accurate above a flux of 140 LMH^{-1}, the reasons for this were twofold:

1) the transit time measurement was discretised to steps of only 1 millisecond
2) this inaccuracy was scaled up because the flux versus transit time graph increased exponentially.

The calibration equation was as follows: -

flux = 3.77 + (25.83 / transit time).

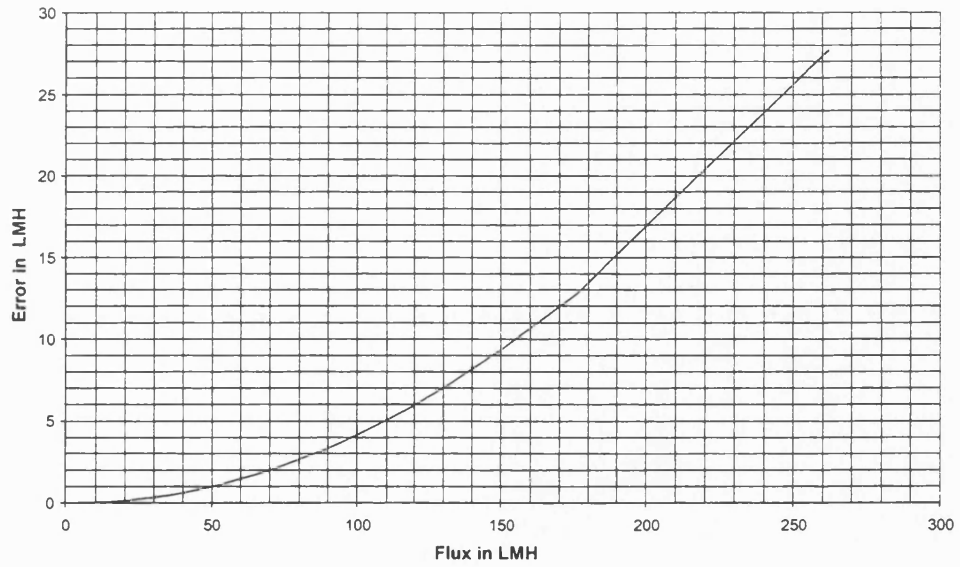

Figure 4.4 Estimation of bubble flow meter error

Figure 4.4 illustrates how the error increases with increasing flux. From this graph, it can be seen that at 140 LMH the error is 8 LMH, equivalent to a 5.7 % error. These calculated errors were of a similar magnitude to the experimental errors found by

comparing the calculated flux with the flux found by using a measuring cylinder. For example, comparison between the bubble flow meter values and the measuring cylinder values show a 4% difference at 122 LMH.

4.4.1.4 The Computer and its Program

Originally, a program was written to log the permeate flux only; there were no pressure transducers on the rig. After the addition of the transducers, a new program was written to include pressure readings. The authors of this program are J.T. Bishop and F.J.W. Podd. The program can be seen in appendix B.

The program was designed with three specific requirements in mind: -

1) Data for the first few minutes might be particularly important, where the initial rate of change was high. Therefore as much data as possible had to be logged during this period.

2) As the rate of change decelerated, the data could be averaged to minimise the amount of data written to file.

3) The computer had to convert the data from the bubble flow meter and pressure transducers to figures that were easy to comprehend.

It was found that the program was prone to crashing without warning, so two more criteria were added.

a) The data should be saved direct to disk, rather than a buffer memory

b) There had to be a quick way to continue the program if it stopped in mid-experiment.

The bubbles for the flowmeter were produced from a cell which hydrolyses water. The cell was switched on automatically by the program and it had to run for several minutes before the bubbles reached the bubble flowmeter. The addition of a few drops of sulphuric acid to the cell could increase the rate of bubble production. By pressing 'R', the timer was reset to 0 and the program continued. This was useful both at the beginning of the experiment (when there was a change from recording of the CWF to recording experimental data), and when the program crashed.

The program could be customised to alter the time elapsed before the data was averaged, and the number of data points over which the average was taken. Optimum values depended on the bacteria being used. This facility was also useful because the rate of bubble production varied with the concentration of ions present, therefore some

experiments had more data than others did. The minimum time between data points might be as little as 2 seconds.

Sometimes the bubble flowmeter would erroneously send a transit time value of zero. If this zero value was used to calculate the flow rate, a "divide by zero" error would result. This problem was resolved by enforcing a lower limit of 0.001 on the transit time value.

4.4.2 Experimental Procedure

Distilled water was used in the rig for both the experiments and cleaning processes in order to prevent blocking of the membrane by salt precipitates. Below is a description of the experimental procedure.

1) The clean water flux was taken before each experiment under the same conditions as the experiment. Since the bubble flowmeter is inaccurate above 140 LMH, and the clean water flux was between 180 and 190 LMH, the clean water flux was measured using a 200ml plastic measuring cylinder. This inaccuracy is irrelevant for the experiment itself, since all experiments soon fall quickly to a flux value easily measured by the bubble flow meter.

2) Before the start of the experiment, the cell suspension was weighed using Sartorius Isocal scales, pre-tared for the weight of the vessel.

3) Before the experiment could start, the bubbles in the bubble flow meter had to be stabilised. Therefore a pattern for bubble production had to be established, before a rapid changeover from water to cell suspension and the start of the timing of the experiment for the data collection. Therefore the bubble flowmeter was primed with a distilled water run before switching to the cell suspension. This switch marked the start of the experiment. Some of the cell suspension ran to the waste vessel before switching to recycling mode. This was to ensure that the rig contained cell suspension only, and no distilled water from the previous operation remained in the rig to dilute the cell suspension. The time taken for the first few mls of suspension to travel from the feed vessel, through the rig and back to the waste vessel helped to estimate the total rig volume.

4) Experiments were run at an equilibrium value of 0.5 bar transmembrane pressure, 0.23 m/s crossflow velocity equal to 0.95 $lmin^{-1}$ flowrate (laminar flow) and 23°C for 90 minutes. It is important to note that at the start it was the crossflow velocity and crossmembrane pressure, i.e. the difference between the inlet and outlet pressure

at 0.45 bars, that were kept constant. This meant that the TMP values started at around 0.13 and rose to the equilibrium of 0.5 bars in the first few minutes.

5) 0.3ml samples were taken from the feed at 0, 1, 6, 12, 30, 60 and 90 minutes from one third of the way below the suspension surface using a 1 ml syringe and 2.5 mm silicon tubing. Their absorbance was then measured using a CECIL CE 1020 spectrophotometer to determine the cell concentration (see section 4.3.1.3). When the feed contained BSA, extra samples were taken and their protein contents were assessed using the Merck Bioquant Bradford assay and measuring the absorbance at 330 nm. Other wavelengths were also tested, but again this wavelength proved to be the easiest to interpret for the machine. The Biorad protein assay was also considered, but proved unreliable.

6) After the end of the experiment, the pump was switched off and the cell suspension reweighed. This figure, combined with the estimate for the total rig volume (taken to be 226.5 ml), provided a basis from which to calculate the total number of cells deposited on the membrane, once the cell concentration was estimated from the absorbance readings. This value was necessary to calculate the specific cake resistance and cell layer equivalent described in chapter 6.

7) After the end of each experiment, the rig was rinsed out with 6 litres of water and a clean water flux taken with the 200ml measuring cylinder. This is referred to as the second CWF (clean water flux). The second CWF was then compared with a reading taken before the start of the experiment (the first clean water flux). This gives a good indication of the proportion of reversible fouling, given as a percentage recovery in chapter 6.

4.4.3 Cleaning

Since three different micro-organisms were filtered through the same rig, it was very important to avoid contamination. Sims and Cheryan (1986), Mourot *et al.* (1989) and Datar (1985) all found that rinsing with water at 50-60 ^{o}C both before and after using detergent proved to be effective.

Shorrock & Bird (1998) found that the length of time required for an effective cleaning agent such as Ultrasil 11 to contact the membrane was only a few minutes at similar temperatures to this. At Ultrasil 11 concentrations above 0.002 w/v%, they found flux recovery was complete after 10-20 minutes. Ultrasil 11 is composed of 43.6% NaOH, which is an effective cleaning agent, able to remove the majority of foulants

alone, but it also contains more than 30% EDTA, as well as small amounts (less than 5%) of non-ionic and anionic surfactants. EDTA is known to have a deleterious effect on adhesion of biofilms to surfaces. For example, Wustman (1998) described polysaccharides present in a diatomaceous extracellular matrix that were soluble in EDTA. Micro was also tried on this rig, but proved to be difficult to remove from such narrow diameter tubes after cleaning.

The permeate line was closed for parts of the cleaning program in order to minimise the debris being forced into the pores. The cleaning regime performed at the end of each experiment is described below.

1) The rig was rinsed through by pulsing with six litres of water, two litres at a time. Extra scouring occurred as a result of the pump being switched off then on again between rinses. The permeate line was kept open throughout. The second clean water flux was then taken at 23 °C, 0.5 bar TMP and 0.95 l/min (0.23 m/s) crossflow velocity.

2) The permeate line was then closed and two litres of water at room temperature was recycled for 3 minutes while being pulsed. This was repeated four times. A closed permeate line ensures that loose foulant does not enter the pores, but leaves the rig through the retentate line.

3) Two litres of 0.1% w/v Ultrasil 11 at 50 °C was recycled for 10 minutes with the permeate line still closed. The first 500 mls of cleaning solution was diverted to the waste vessel. Pulsing was done for the first three minutes only, then the permeate line was opened, to ensure the pores were also cleaned.

4) Six litres of water at 60 °C, then four litres of water at room temperature were rinsed through the rig, and then the final clean water flux was measured.

5) Another clean water flux was then performed under the same conditions as before. This flux was taken to be the first clean water flux measurement for the next experiment, to be compared to the second clean water flux in order to obtain a percentage recovery value.

6) On some occasions, either the clean water flux was unsatisfactory or there was foulant still visibly emerging from the membrane module. When either of these phenomena occurred, the procedure was repeated from step 4.

Pulsing was achieved by altering the conditions between 0.45 bar, 0.23 m/s and 0.825 bar TMP, 0.3 m/s manually, by altering the pump speed every 4 seconds. Originally the pulsing was done by fitting an on/off valve in the position marked X in Figure 4.3 but this weakened the silicon tubing, causing it to burst after a while. However, both methods seemed to be equally effective despite the absence of baffles. Both methods produced a scouring effect when the permeate line was closed. This often resulted in foulant removal being visible in the retentate pipe returning to the feed. This also happened frequently when the pump was turned on in between rinses.

Sometimes this procedure was not enough to clean the membrane adequately. It is often suggested that a recovery of flux to within 10% is adequate to assume a clean membrane, but nearly all of the *S.multivorum* results demonstrated that 90% of the fouling was reversible fouling anyway. Sometimes even when the CWF was high, turning on the pump once more resulted in a visible rush of foulant leaving the membrane module.

In order to get the flux to within 5% of the original value, it was sometimes necessary to immerse the membrane module in a warm ultrasound bath. This was very effective, but shortened the life of the membrane drastically: the membrane started to disintegrate after the second or third ultrasound bath. However, this treatment was required only under very heavy fouling conditions, such as a combination of $CaCl_2$ and BSA with *Pseudomonas.*

It is well known that proteins are attracted to a liquid-air interface by their hydrophobic areas (Dahlbäck *et al.*, 1981). It was therefore decided to include air bubbles at the start of each rinse in an effort to remove this resistant fouling. This can denature protein, but this is not a concern, since the scouring effect and presence of surfactant will have already denatured them. This method did seem to work well, especially where other more conventional methods failed. A visible increase in suspended foulant in the retentate was seen when bubbles were introduced.

Both the pulsing without baffles termed as crossflushing by Kurozovich & Piergiovanni (1996), and the entrainment of air bubbles have been used to improve flux during filtration with some success, but there does not seem to be literary evidence for either method to be used for cleaning. Hadzimajlovic and Bertram (1998) also found that pulsed flow improved flux, even without baffles, but only if the flow was laminar. Since temporary cavitation is often suggested as one of the mechanisms for cake removal, this

would seem a perfect way to combine two of the cleaning mechanisms employed in this study.

4.4.4 Safety and Disposal

Class I micro-organisms are classed as micro-organisms that are unlikely to cause human or animal disease of veterinary importance according to the WHO risk group system (HMSO 1990).

Since these micro-organisms may be opportunistic pathogens at high cell concentrations, the following steps must be taken when handling them: -

1) PVC gloves and laboratory glasses must be worn.
2) Disposable objects such as gloves and paper tissue must be placed in a bin bag for incineration.
3) Containers of broth, cell suspensions and initial rinse water must be autoclaved at 121°C for 20 minutes before disposal down the sink.
4) Surfaces should be wiped down regularly and spillages contained by covering with sodium hypochlorite solution. A concentration of 2,500 ppm is recommended for general use and 10,000 ppm for spillages. These solutions must be made up daily since sodium hypochlorite degrades quickly.

5 Cell and Extracellular Matrix Results

5.1 Introduction

This chapter contains the results for the cell characterisation experiments, detailing the results for: -

- Surface charge (Zeta potential measurements)
- Hydrophobicity (BATH, SAT and adhesion to a hydrophobic surface)
- Cell sizing and cell size distribution (optical microscope, conventional SEM, cryogenic SEM
- Mass (dry weight)
- Polysaccharide levels (precipitation in alcohol)
- Viscosity (viscometer)

5.1.1 Characterisation of the Extracellular Matrix

Measurement of the microbial surface properties is important for understanding the interactions between membrane and cell and between the cells themselves and this can be undertaken in several ways. Qualitative measurements are carried out by binding the cells to specific molecular species, as described by Defrise and Gekas (1988). One of the advantages of these techniques is that they can give information on both the organisation of the outermost surface and the topological distribution of the polymers involved. One such method is the BATH (Bacterial Adherence To Hydrocarbon) adhesion assay. This can give an indication of the distribution of the hydrophobic sites on the cell surface. Other tests for assessing average hydrophobicity are the SAT (Salt Aggregation Test) test and 'adhesion to a hydrophobic surface', i.e. a Petri dish.

Estimation of zeta potentials is also important since they give an estimate of how close the particle can approach to another surface with regard to electrostatic interaction. Zeta potentials give an indication of the average ionogenic nature of the surface. The Zeta potential is a measure of the potential charge at a distance from the particle where the ions are not dragged with the particle when it moves. In other words, it is the potential just beyond the double layer of ions (Hunter, 1981).

Contact angle measurements are used to provide information on the surface free energy of solids. Measurement of the hydrophobic or hydrophilic nature of membrane is

easy by this method, but for interaction between cell and surface the procedures are difficult and unreliable, (Mozes *et al.*, 1987) so they were not attempted in this study.

5.2 Zeta Potential

A Zetamaster from the University of Swansea was used to calculate the Zeta potentials of the cells. The Zetamaster measures the electrophoretic mobility in a charged field. The zeta potential for a bacterium can be calculated from this data using Smoluchowski's equation as described in Chapter 4

5.2.1 Zeta potential results

A summary of the calculated zeta potential results for the three micro-organisms under investigation is presented in Table 5.1. The results for BSA are also included. The potential measured varies in relation to the density of the ionic double layer, which is greater at higher ionic strengths. Each biological particle was tested in electrolyte solutions of the same composition as used for the filtration experiments, with the exception of low $CaCl_2$.

The controls for these measurements were the electrolyte solutions alone. From Table 5.1, and Figure 5.1, it can be seen that the zeta potential for low NaCl is close to zero with minimal variation in the reading. This is proof that there are few detectable ions in this solution. For high $CaCl_2$ however (Figure 5.2), the Zeta potential is definitely positive at 10.02 mV and the scatter of readings is wider, with a standard deviation of 0.85. High NaCl has a similar standard deviation, but is only just positive at 1 mV.

Suspension type	ζ potential (mV)	Standard deviation
low NaCl	0.58	0.1
high NaCl	1.00	0.84
high $CaCl_2$	10.02	0.85
S.multivorum & low NaCl (overall)	-26.71	13.5
S.multivorum & low NaCl lower peak	-38.19	3.39
S.multivorum & low NaCl higher peak	-12.35	2.44
S.multivorum & high NaCl	-5.27	2.75
S.multivorum & high $CaCl_2$	3.75	0.9
P.elodea & low NaCl	-33.2	5.59
P.elodea & high NaCl	-3.52	1.79
P.elodea & high $CaCl_2$	-0.36	1.18
P.putida & low NaCl (overall)	-14.34	3.82
P.putida & low NaCl lower peak	-20.44	1.01
P.putida & low NaCl middle peak	-14.22	1.01
P.putida & low NaCl higher peak	-8.7	0.35
P.putida & high NaCl	-4.2	2.07
P.putida & high $CaCl_2$	0.96	1.04
BSA & low NaCl	-21.62	8.19
BSA & high NaCl	2.15	0.76
BSA & high $CaCl_2$	1.67	1.04

Table 5.1: Zeta potential values for cells and BSA as measured

For the bacterial particles, the measurements at low ionic strength NaCl reflected the charge on the surface most accurately, since there were few ions present to shield their surfaces. Thus the charge distribution is at its most diffuse in this solution.

The surface of *S.multivorum* exhibits two distinct charge areas, as seen in Figure 5.3. The more negative area has a mean zeta potential of -38.19 mV. This is the most negatively charged area found in all the tests. The standard deviation for this area is 3.9 mV. The overall zeta potential is -26.71 mV, with the largest SD (standard deviation) of all at 13.5 mV.

The bacteria with the lowest mean zeta potential is *P.elodea*, at -33.2 mV. The value of the S.D. is slightly larger than for *P.putida* at 5.59, but it can be seen from Figure 5.5 that there are no distinct zones of charge for this organism. BSA shows a similar pattern, as illustrated in Figure 5.6, with no distinct zoning, but a diffuse (SD 8.19) distribution around a mean of -21.62 mV. It is therefore assumed that this trend for zeta potential is typical of a macromolecule. Thus the pattern of zeta potential for *P.elodea* affirms the theory that it is the relatively uniform extracellular matrix (ECM) of gellan gum that is being measured here.

The surface of *P.putida* shows a zeta potential pattern closer to that of *S.multivorum* (see Figure 5.4), with three peak zones, some of them bimodal. This time

the SD of all three of these areas is only 3.82 mV. The overall mean charge is the least negative value at -14.34 mV.

The presence of a high ionic strength of NaCl disguised the effect of these individual sites, as the double layer was compressed and the surface was shielded. There was therefore less negative, very uniform distribution for all three micro-organisms, with *S.multivorum* still exhibiting the most negative zeta potential at -5.27, with the largest SD of 2.75; narrower than any of the measurements in low NaCl.

The presence of a high level of a divalent ion such as Calcium had an even greater effect on the double layer since divalent ions compress the double layer by up to 1.5 times more than Na^+ (Israelachvilli, 1994). Thus all the bacteria displayed a charge close to zero, with *S.multivorum* as the most positive at 3.75mV (SD 0.9). This is still less positive than the charge of the solution alone, at 10.02mV. Since BSA has such a definite affinity for calcium, it is surprising that this suspension did not yield the highest Zeta potential. The Zeta potential for the protein is still more positive than *P.putida* and *P.elodea* though, with a value of 1.67mV (SD 1.04). A graph of the test for BSA in high $CaCl_2$ can been seen in Figure 5.6.

Some of the variation in zeta potential value for all tests must be attributed to the solution. The SDs of the high NaCl and Ca Cl_2 controls were 0.84 and 0.85 mV respectively.

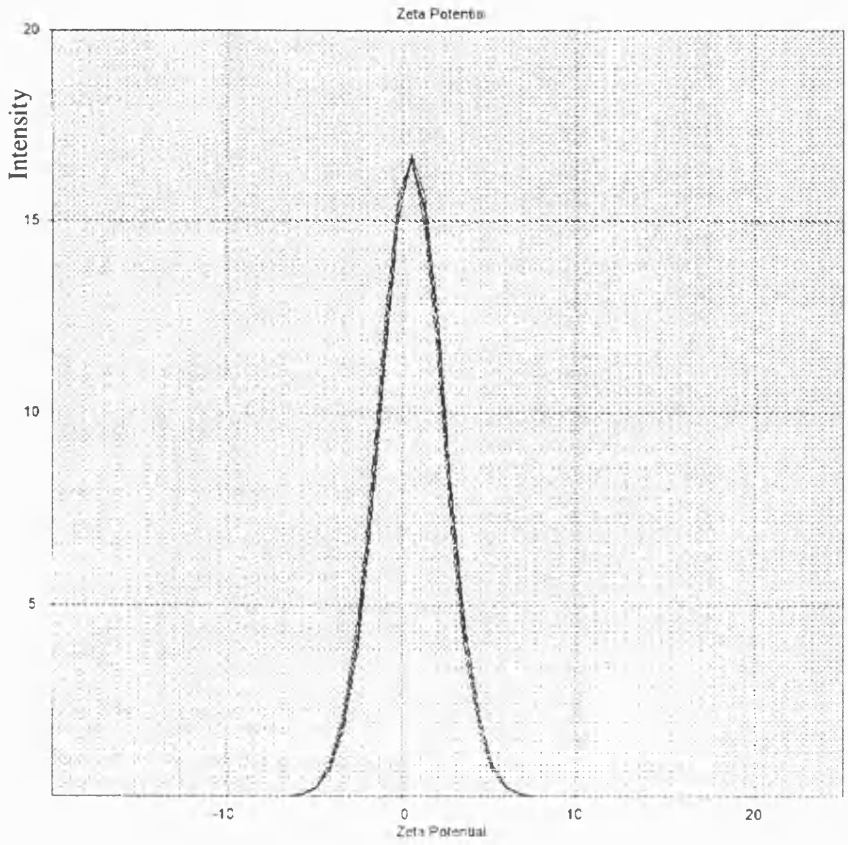

Figure 5.1 Zeta potential for low NaCl solution only

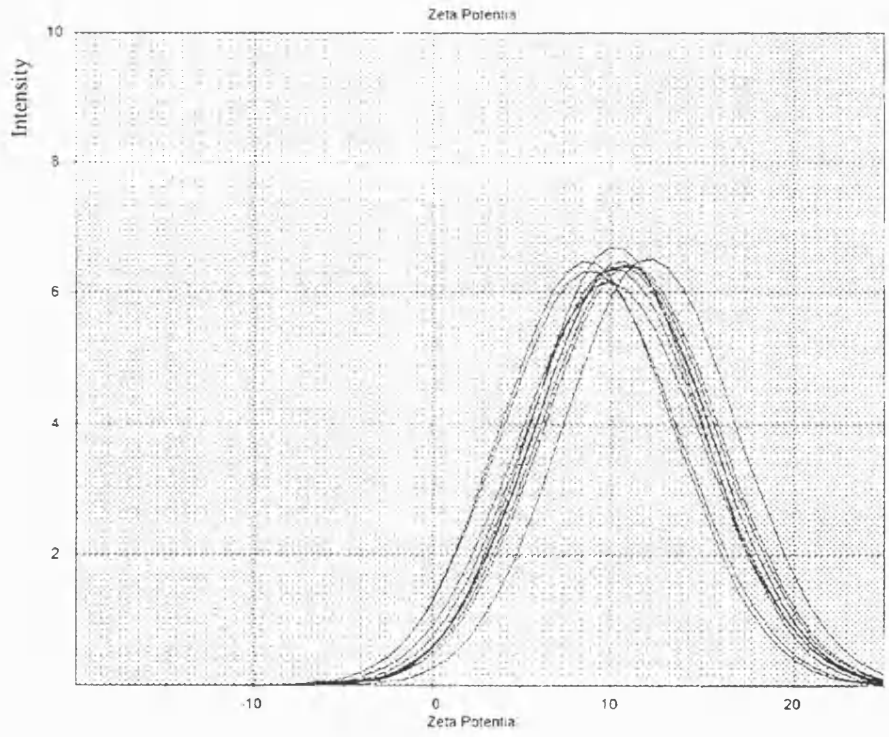

Figure 5.2 Zeta potentials for high $CaCl_2$ solution

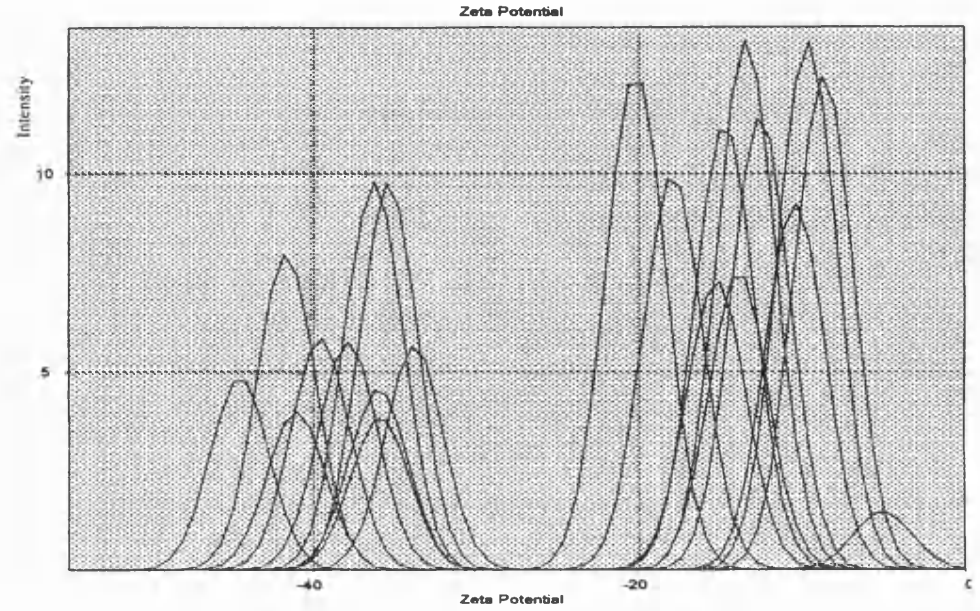

Figure 5.3 Zeta potentials for *S.multivorum* in Low NaCl

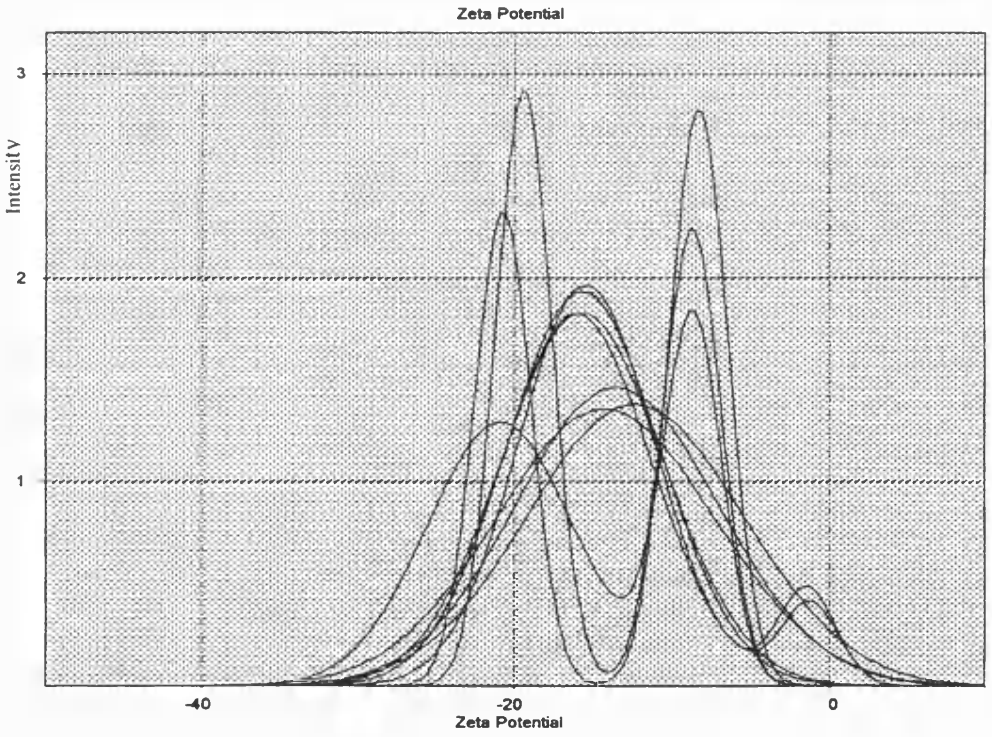

Figure 5.4 Zeta potentials for *P.putida* in Low NaCl

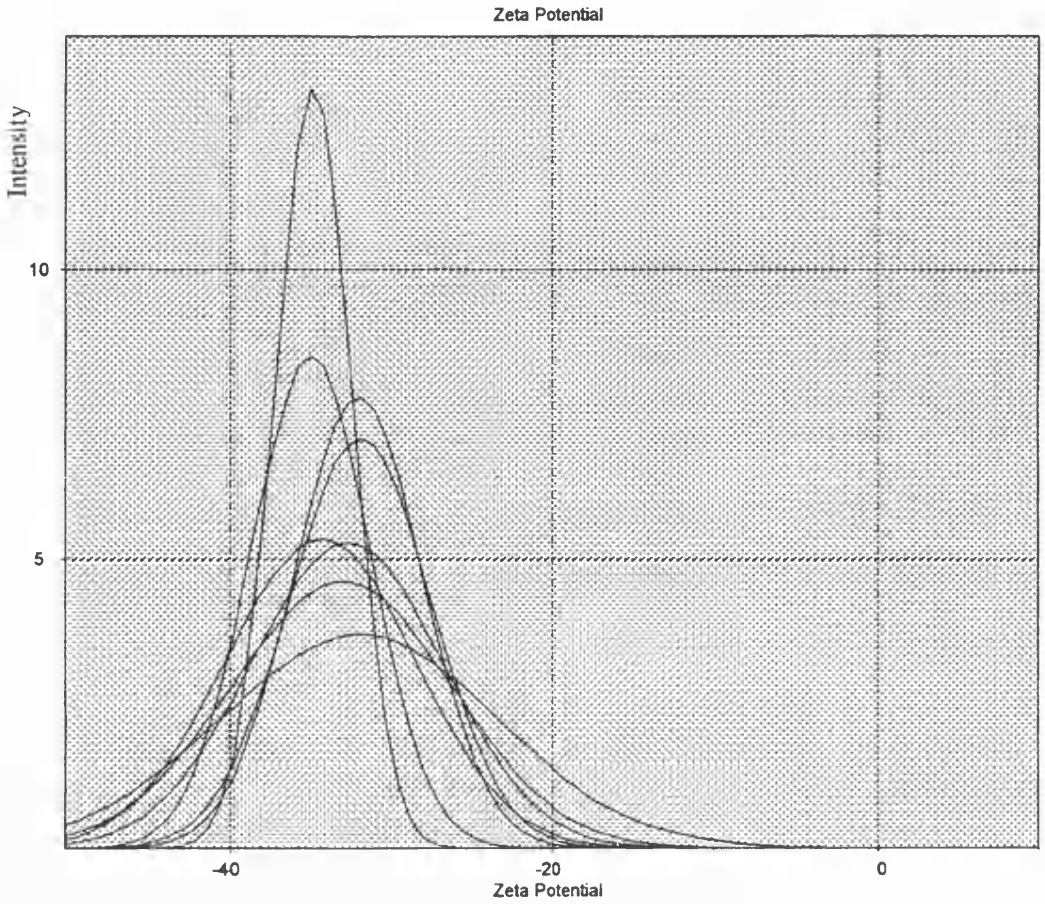

Figure 5.5 Zeta potentials for *P.elodea* in low NaCl

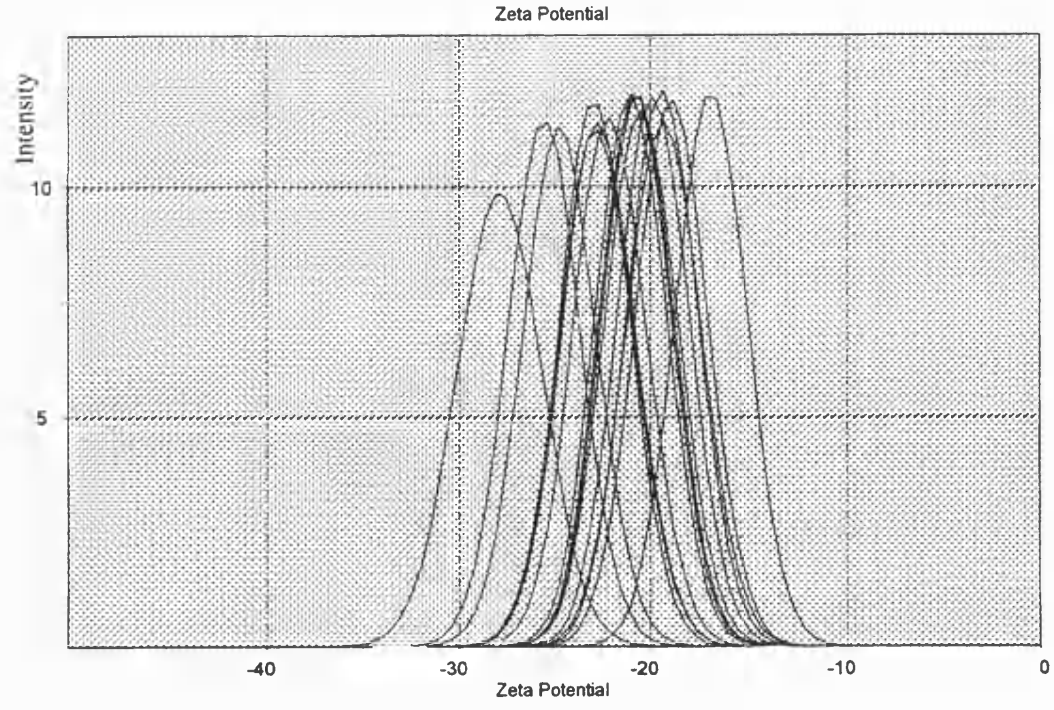

Figure 5.6 Zeta potentials for BSA in low NaCl

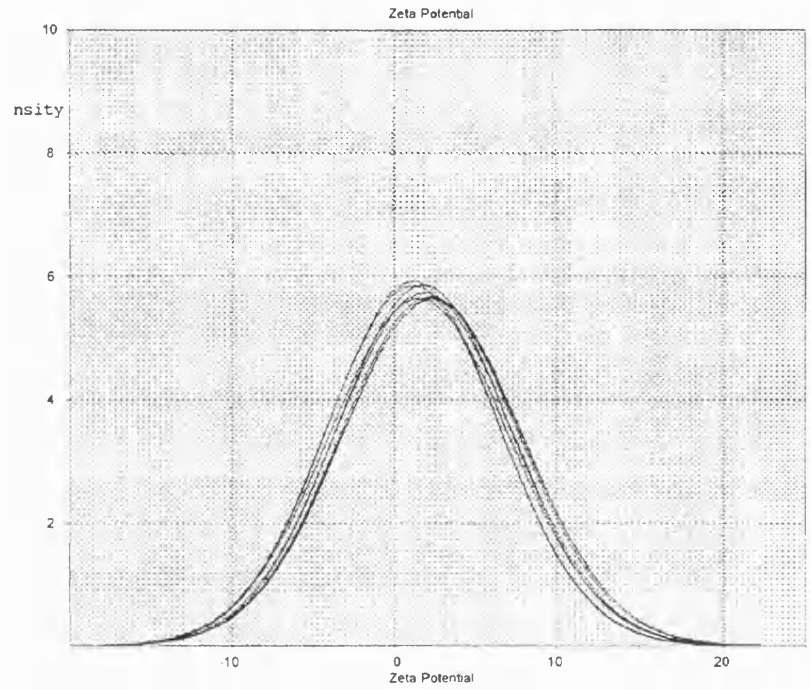

Figure 5.7 Zeta potentials for BSA in high $CaCl_2$

5.3 Hydrophobicity measurements

It is a well accepted fact that one hydrophobicity test done in isolation does not give a good indication of the hydrophobicity of different types of particles. The results are very sensitive to both the anions (Bunt, Jones & Tucker, 1993) and cations (Lindahl *et al*, 1981) in solution, as well as to their ionic strength (Jones *et al*, 1996). More than one test must be undertaken to build up a more comprehensive picture and the results can only be taken to be relative to one another (Lee & Yii, 1996; Bunt *et al*, 1995). Another reason for the need for multiple testing is that different tests measure hydrophobicity at different scales. Each method has advantages and disadvantages according to the principles behind it.

Three types of tests were carried out on the bacteria for this thesis:-

1) SAT (Salt Aggregation Test)

2) BATH (Bacterial Adherence To Hydrocarbons),

3) Adhesion to a surface test (a Petri dish)

The SAT tests were carried out with washed cells in different concentrations of $(NH_4)_2SO_4$ solution, with agglomeration at given ionic strengths as the positive sign of hydrophobicity. For the latter two tests, washed cell suspensions of the same

composition as in the filtration experiments were used (see section 4.3.2), and the percentage removal from the aqueous cell suspension was the marker for the degree of hydrophobicity.

5.3.1 SAT Results (overall hydrophobicity)

Lindahl *et al* (1981) outlined this technique to test for overall hydrophobicity of a surface. It is based on 'salting out' of the cells, analogous to salting out of a protein. The DVLO theory considers the Van der Waals forces (including those of hydrophobic groups) and the electrostatic forces only. Electrostatic repulsion is suppressed in high ionic solution, due to a high density double layer. Above a critical point, agglomeration is believed to be due to hydrophobicity only. See section 2.7.4 for a further explanation. The lowest ionic strength solution to cause agglomeration in this method determines the hydrophobicity of the cell. The test was carried out three times and most of the results were consistent with each other. The sign in brackets for *P.elodea* indicates where one of the tests may have differed slightly from the others.

Lee and Yii (1996) suggested guidelines for grading hydrophobicity measurements for this test. These are interpreted in the last column in Table 5.2

$(NH_4)_2SO_4$ conc. (M)	*P.putida*	*S.multivorum*	*P.elodea*	*Baker's yeast*	*Hydrophobicity definition**
0	–	–	–	–	
1	–	–	–	–	Strong
1.5	–	–	–	–	Moderate
2	–	–	–	–	Moderate
2.25	–	–	–(+)	–	Weak
2.5	–	–	+	–	Weak
2.75	+	–	+	–	Weak
3	+	–	+	–	Weak
3.25	+	–	+	–	Weak
3.5	+	–	+	–	Weak
3.75	+	+	+	–	Weak
4	+	+	+	+	Weak

Table 5.2: Hydrophobicity of bacteria according to the SAT test

+ sign represents salting out

* reference Lee and Yii (1996)

The results in Table 5.2 indicate that none of the three bacteria are very hydrophobic, although *P.elodea* seems to be the most hydrophobic. This result could be affected by a strong tendency for these bacteria to form dispersive aggregates under most circumstances, due to their slimy gellan gum ECM (Jones *et al*, 1996). *S.multivorum* seems to be significantly less hydrophobic than the other two, although this too may be

affected by the fact that this cell type tends not to agglomerate. These results should give an indication of general hydrophobicity, without the specific effect of the ions present in the filtration experiments being demonstrated.

5.3.2 Plastic Adhesion /BATH tests. (Overall/specific site hydrophobicity)

The other two methods on the other hand were carried out with the cells suspended in the same electrolytes as for the filtration experiments; in fact the same set of cell suspensions was used for both methods.

5.3.2.1 BATH test

The BATH test was a modification of the test first described in Rosenberg *et al* (1980). This method is based upon measuring the degree of partitioning of the bacteria between solutions of electrolyte and hydrocarbon when agitated together on a whirlimixer. The hydrocarbon chosen for this experiment was ***octane***. It detects specific hydrophobic sites on an otherwise hydrophilic surface (Sorongon, Bloodgood & Burchard, 1991). Hydrophobicity is expressed as the proportion of the bacteria lost from the aqueous phase post emulsification, measured by adsorption on a spectrophotometer.

The percentage is calculated thus:

$$CSH = 100\left(\frac{C_a}{C_b} - 1\right) \qquad \textbf{Equation 16}$$

Where:-

CSH= Cell surface hydrophobicity rating

$C_{b=}$ Cell concentration in aqueous phase before test

$C_{a=}$ Cell concentration in aqueous phase after test

Lee and Yii (1996) suggested applying the following definitions for hydrophobicity to the final percentages in the aqueous phase. These are taken from Sartos (1990).

- > 50% loss Strongly hydrophobic
- 20-50% loss Moderate hydrophobicity
- <20% loss Not hydrophobic

The data for all the suspensions in Table 5.3 to Table 5.5 are expressed in these terms. Each type of suspension was tested three times and all three sets of results fell within the same category.

5.3.2.2 Adhesion to plastic test

Samples from the same cell suspensions were also pipetted into Petri dishes of dimensions of 10x100mm and incubated. The absorbance of the samples was then measured. The lower the absorbance of the remaining cell suspension, the greater the number of cells deposited, the higher the level of hydrophobicity demonstrated, i.e. equation 16 can be reapplied in a different context. The results in Table 5.3 to Table 5.5 are expressed in ten percent ranges. Each type of suspension was tested three times and all three sets of results fell within the same ten percent range for each type of sample. Even increasing the temperature from 6 to 28°C did not change the results enough to go beyond these 10% ranges. This implies that the results cannot be due entirely to hydrophobic attachment, as hydrophobic interactions are known to be temperature sensitive (Israelachvili, 1994). Plastic adhesion results measure overall adhesion and can only be interpreted relative to one another.

5.3.2.3 Results for the tests

S.multivorum	Plastic Adhesion %	BATH using Octane %
High Calcium	80-90	Moderately hydrophobic
High Calcium & BSA	0-10	Strongly hydrophobic
Low Calcium	20-30	Not hydrophobic
Low Sodium	0-10	Not hydrophobic
Low Sodium & BSA	0-10	Not hydrophobic
High Sodium	30-40	Moderately hydrophobic
High Sodium & BSA	0-10	Not hydrophobic

Table 5.3: Hydrophobicity of *S.multivorum* in different media according to the BATH and Plastic adhesion tests

P.elodea	Plastic Adhesion %	BATH using Octane %
High Calcium	40-50	Not hydrophobic
High Calcium & BSA	0-10	Not hydrophobic
Low Calcium	50-60	Moderately hydrophobic
Low Sodium	50-60	Moderately hydrophobic
Low Sodium & BSA	70-80	Not hydrophobic
High Sodium	30-40	Moderately hydrophobic
High Sodium & BSA	60-70	Not hydrophobic

Table 5.4: Hydrophobicity of *P.elodea* in different media according to the BATH and Plastic adhesion tests

Pseudomonas putida	Plastic Adhesion (%)	BATH using Octane (%)
High Calcium	0-10	Not hydrophobic
High Calcium & BSA	20-30	Moderately hydrophobic
Low Calcium	10-20	Not hydrophobic
Low Sodium	10-20	Not hydrophobic
Low Sodium & BSA	20-30	Not hydrophobic
High Sodium	0-10	Not hydrophobic
High Sodium & BSA	10-20	Not hydrophobic

Table 5.5: Hydrophobicity of *P.putida* in different media according to the BATH and Plastic adhesion tests

5.3.2.3.1 Plastic adhesion results

P.elodea has the highest adhesion results for both the sodium suspensions and the low calcium suspensions. *S.multivorum* has the highest hydrophobicity of the high $CaCl_2$ only suspensions, while high NaCl only suspensions are moderate, and the rest are low. On the other hand, all the results for *P.putida* are very low, increased only slightly by the presence of BSA. BSA increases the hydrophobicity of *P.elodea* suspensions to a greater degree. Since protein seems to have the opposite effect for *S.multivorum*, the sites exposed by attachment of BSA to the cell surface must differ according to the organism.

The plastic adhesion result for *S.multivorum* in high $CaCl_2$ is much higher than in the other solutions and for the equivalent BATH test. This could be because electrostatic effects may be complicating the interaction with the Petri dish, especially because the

zeta potential for *S.multivorum* in $CaCl_2$ yielded the highest positive value of all the bacteria. Electrostatic interference is known to be one of the disadvantages of this type of test (Sorongon *et al*, 1991).

5.3.2.3.2 Comparison of plastic adhesion test and BATH test

There is very good agreement between the two tests for the *P.putida* results, which are universally low for both, with the highest hydrophobicity for high calcium with BSA suspensions. This adds substance to the theory that it is the flagella and not the cell surface hydrophobicity that is being measured. It is common to find that extracellular protrusions dominate hydrophobicity measurements, especially when they surround the cell. For example, Lindahl *et al* (1981) compared *E.coli* with hydrophobic fimbriae with a non-fimbriated mutant, and found the former exhibited hydrophobic properties while the latter tested predominantly hydrophilic.

Flagella are made up predominantly of one protein, flagellin (Dyson, 1978). Therefore no specific sites should be detected for this species and the overall hydrophobicity test (plastic adhesion) and the specific site hydrophobicity test (BATH) should have comparable results.. This is not always the case with the other two bacteria. For *S.multivorum,* calcium obviously has a significant effect on the specific sites that bond to octane, as all three results are very different from the plastic adhesion test results. This effect may also be due to the double layer obscuring the hydrophobic sites. The zeta potential results indicate that there is more than one zone on the surface so particular sites of hydrophobicity may be obscured by the dense charge. The results for the NaCl solutions all correlate with the plastic adhesion tests.

Both methods correlate well with respect to the different effects of ionic strength on the CSH of *S.multivorum* and *P.elodea.* For *S.multivorum,* hydrophobicity increases in stronger solutions, whereas *P.elodea* exhibits the opposite trend. Bunt (1993) suggested that the latter phenomenon might be the result of the thicker double layer for high ionic strengths obscuring the hydrophobic sites.

The high values of cell surface hydrophobicities (CSH) at high salt concentrations for *S.multivorum* may be due to cavity theory, especially for the plastic adhesion test. For two hydrophobic surfaces to come together and bond, work against the surface tension must occur to create a cavity. This requirement for work decreases when hydrophobic sites (e.g. on the Petri dish) bind to a protein or carbohydrate in the presence of high salt concentrations, since the surface tension is lower. Therefore

hydrophobic bonding can be energetically favourable in high salt concentrations. An increase in hydrophobicity with an increase in ionic strength is the most commonly found observation (Bunt *et al*, 1993, Rosenberg, 1984, Lindahl *et al*, 1981). This observation obviously depends on the total energy of the system, which may be different in the *Pseudomonas* species (Bunt et. al., 1995).

One notable observation for the specific BATH test results is that all three of the bacteria have low hydrophobicity with BSA and either of the NaCl solutions. This implies that the BSA also screens the specific sites, which do not expose any hydrophobic sites of their own.

The analysis of these results is comparable with the identification of adhesion mechanisms for protein onto membranes (see section 2.4). Maximum deposition may be at the protein's isoelectric point, or far from it, depending on which forces dominate. A similar statement can be made for ionic strength. Since the membrane used is hydrophilic, but negatively charged, like the cells, maximum adsorption to its surface should be for organisms of low hydrophobicity and low charge. Therefore from these tests, the highest cell adhesion to the membrane should be for *P.putida* in any high ionic strength solution. This appears to be a valid assumption, since the membrane is most difficult to clean after experiments with these suspensions.

5.3.3 Cell sizing and cell size distribution

In order to determine the effects of the extracellular matrix, it was important to establish that the cell dimensions for the three bacteria were comparable.

One method adopted was to observe cells stained by either carbolfuchsin or crystal violet under a light microscope and the dimensions recorded via a CCD camera. This method shrinks the cells during processing and so it is not an accurate way to estimate actual cell size. Nevertheless, it is a good way to measure the scatter of cell sizes (assuming that the shrinkage factor is consistent) as a large sample size can be taken. A statistical analysis of 100 cell measurements can be found in Table 5.7, and stills from the CCD camera can be seen in Figure 5.8, Figure 5.11 and Figure 5.14.

The most accurate way to measure the cells was cryogenic SEM. This technique freezes in all the water present, ensuring shrinkage is negligible (Figure 5.9,Figure 5.12 and Figure 5.15. This method provided an accurate image of the actual dimensions of the cell, but the sample size was lower at only 40.

Images of the cells were also taken using a more conventional SEM technique, using gold sputtering in order to define the cell shape. This gave an indication of the dimensions of the cell with the cell 'coating' shrunken or removed; loose polysaccharides and proteins are stripped from the wall during preparation. Samples of photographs using conventional SEM can be found in Figure 5.10, Figure 5.13 and Figure 5.16. Again the sample size was lower than for the light microscope method at between 20 and 50 measurements. A comparison of the mean dimensions and standard deviations of the measurements for the two SEM techniques can be seen in Table 5.6.

TEM images were also taken, in an attempt to record any fimbriae, pili or flagella present. Only one picture revealed anything- a single flagella for *P.elodea,* which was unexpected. The problem with this method is that although the resolution is high enough to see flagella, the method of preparation encourages the flagella to lie flat against the cell.

5.3.3.1 Cell size and size distribution method

A Comparison of cryogenic and conventional SEM results indicates that the standard deviation values for cryogenic SEM are greater than for conventional SEM, indicating the presence of a variable amount of extracellular matrix. *P.putida* has the greatest SD for both methods. This is because the measurement depends on how the long thin flagella are lying against the cell surface: the measurement is not for a definite mass of polysaccharide glycocalyx, as for the others.

The difference in the mean length for *S.multivorum* and *P.elodea* is close to the SD for cryogenic SEM, but the difference between mean widths is much greater than the SD for either technique. This is consistent with the presence of a polysaccharide ECM, either as a capsule (*S.multivorum*) or as loose, slimy gellan gum. (*P.elodea*).

The difference between the mean values for *P.putida* is less than the SD for either type of measurement, indicating a lack of polysaccharide coating.

The presence or absence of polysaccharide coating can be clearly seen on the cryogenic SEM images in Figure 5.9, Figure 5.12 and Figure 5.15, where cells have been growing on agar clustered together. The cellular shapes of *P.putida* are clearly distinguishable, while the thick coatings of both *P.elodea* and *S.multivorum* make the outline of the cells harder to distinguish.

The extreme sliminess of *P.elodea* is in evidence even in the conventional SEM picture (Figure 5.13), where polysaccharides are stripped and/or shrunken. A

comparison of Figure 5.10 and Figure 5.16 illustrates the relative smoothness of the *S.multivorum* capsule compared to the capsule-free surface of *P.putida*.

	Cryogenic SEM (μm)	Standard deviation (μm)	Conventional SEM (μm)	Standard deviation (μm)	Difference (μm)
S.multivorum	2.39 x 1.017	0.7 x 0.08	1.71 x 0.59	0.59 x 0.06	0.68 x 0.43
P.elodea	2.28 x 0.825	0.65 x 0.11	1.62 x 0.455	0.41 x 0.1	0.66 x 0.37
P.putida	2.42 x 0.61	0.88 x 0.09	1.98 x 0.53	0.69 x 0.11	0.44 x 0.08

Table 5.6: Estimation of cell sizes from SEM images

	S.multivorum				*P.elodea*				*P.putida*			
	area	length	width	ratio	area	length	width	ratio	area	length	width	ratio
average	0.82	1.40	0.58	2.45	0.86	1.74	0.49	3.65	0.99	1.63	0.59	2.82
mode	0.70	1.40	0.50	2.00	0.24	0.60	0.50	1.33	0.40	0.90	0.60	2.50
std	0.33	0.39	0.11	0.71	0.48	0.89	0.10	2.04	0.67	0.88	0.12	1.46
smallest	0.36	0.90	0.40	1.29	0.22	0.50	0.30	1.00	0.20	0.50	0.39	1.00
largest	2.52	3.00	1.20	5.28	2.28	3.80	0.80	9.74	3.96	4.70	0.90	7.40

Table 5.7: Statistics for cell sizing in μm (μm^2 for area) taken from light microscope images.

A sample size of 100 cells was considered to be large enough to enable measurement and analysis of the CCD camera images. It can be seen from Figure 5.8, Figure 5.11 and Figure 5.14 that the clarity of these images leaves much to be desired, especially when analysing such a large sample. It was therefore, especially reassuring to find that the average lengths for the three cell types were within 20% of the conventional SEM values.

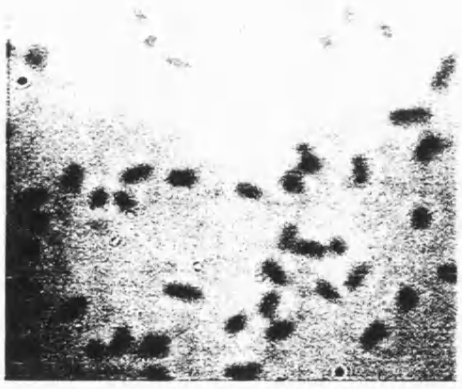

Figure 5.8 Light microscope image of *S.multivorum*

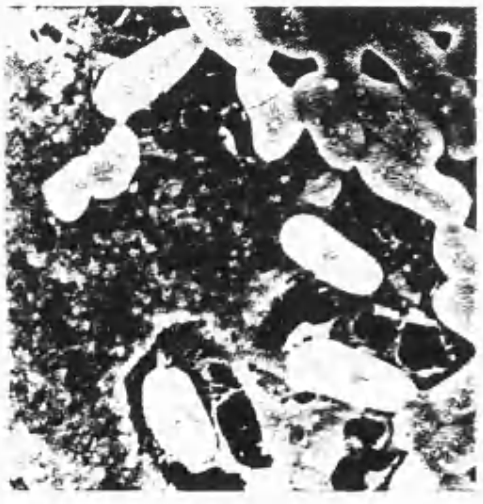

Figure 5.9 Cryogenic SEM of *S.multivorum*

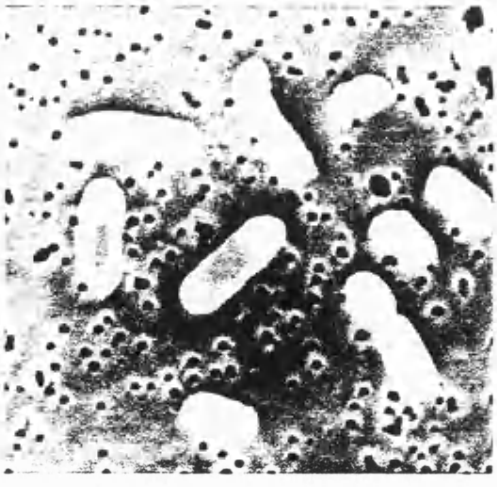

Figure 5.10 Conventional SEM of *S.multivorum*

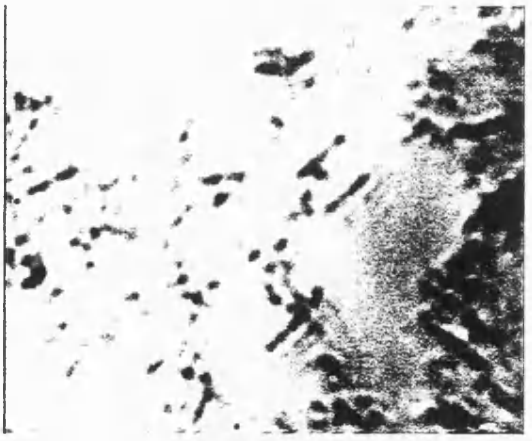

Figure 5.11 Light microscope image of *P.elodea*

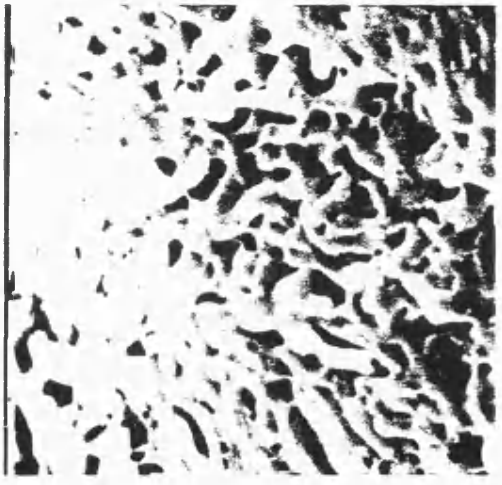

Figure 5.12 Cryogenic SEM of *P.elodea*

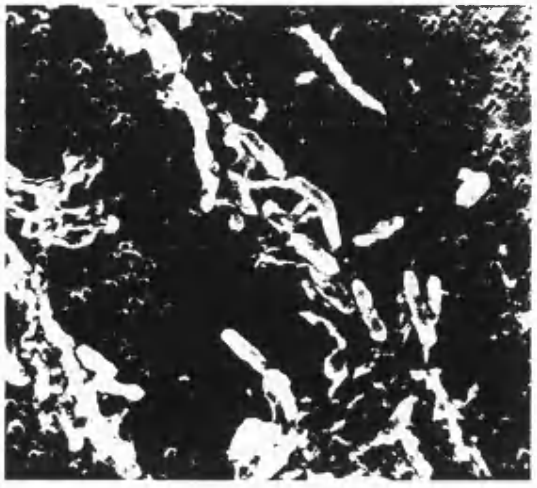

Figure 5.13 Conventional SEM of *P.elodea*

Figure 5.14 Light microscope image of *P.putida*

Figure 5.15 Cryogenic SEM of *P.putida*

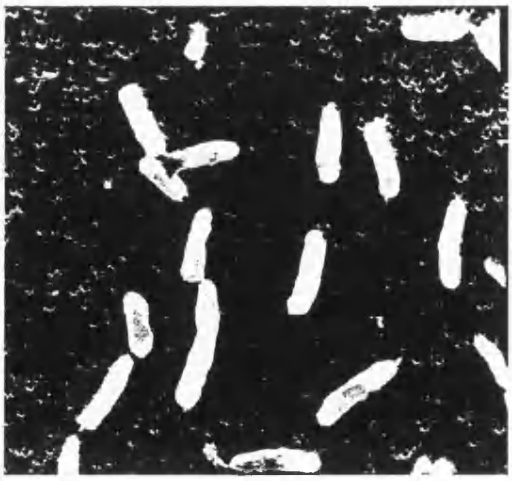

Figure 5.16 Conventional SEM of *P.putida*

The fact that *S.multivorum* has the lowest average length in Table 5.7 is deceptive; the reason for this is that the other two have a wider range of lengths, indicated by the greater standard deviations (0.883 and 0.893) for *P.putida* and *P.elodea,* compared to 0.639 for *S.multivorum*. This explanation is supported by the graph in Figure 5.18, where it can be seen that only 1% of *S.multivorum* cells are above 2.5 μm, while for *P.elodea* and *P.putida*, the equivalent figures are 8 and 10% respectively. It was observed during haemocytometer cell counts that the *Pseudomonas* bacteria have a greater tendency to exist in chains of two or even three for *P.elodea*. Figure 5.13 also has evidence of this tendency for *P.elodea*, and the red arrow in Figure 5.14 indicates an example for *P.putida*. However, Figure 5.17 illustrates that this accounts for only some of the cells measured. Figure 5.15 and Figure 5.13 illustrate there is also a wide range of cell lengths extant in the population.

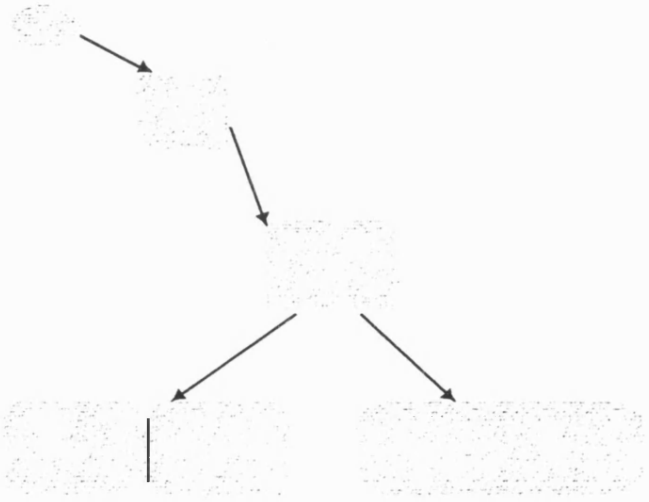

Figure 5.17: Pattern of cell growth for all three bacteria

All three bacteria are approximately spherical when very small, indicated by the 1:1 ratio minimum in Figure 5.21. As the cells grow, they tend to get longer, but not much thicker. This is demonstrated by the relatively low standard deviations for the width compared to those of the lengths. *P.elodea* is the thinnest bacteria, but all three are of roughly similar width (see Figure 5.19).

The most concise evidence that all three species are of comparable size is the close correlation of the cell areas, seen in Figure 5.20.

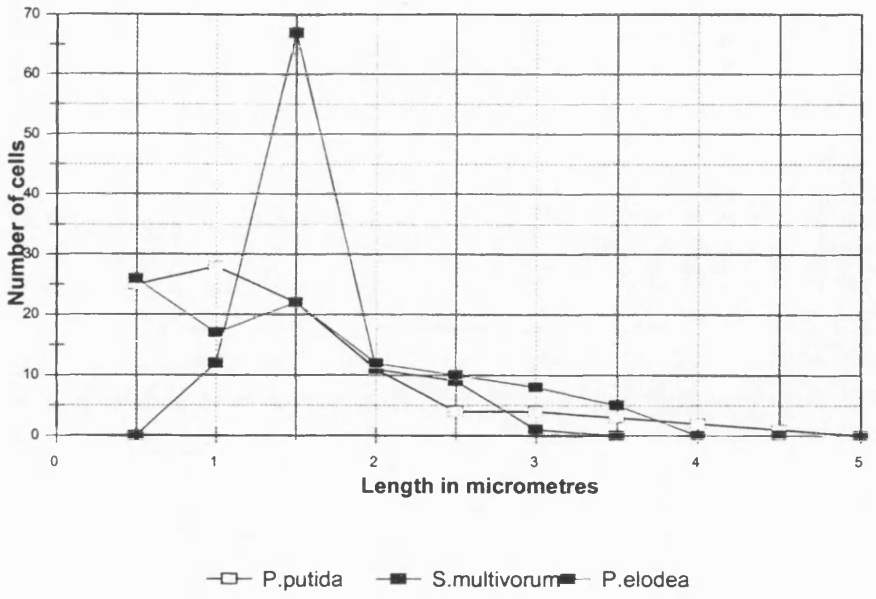

Figure 5.18 Length of cells observed under the light microscope

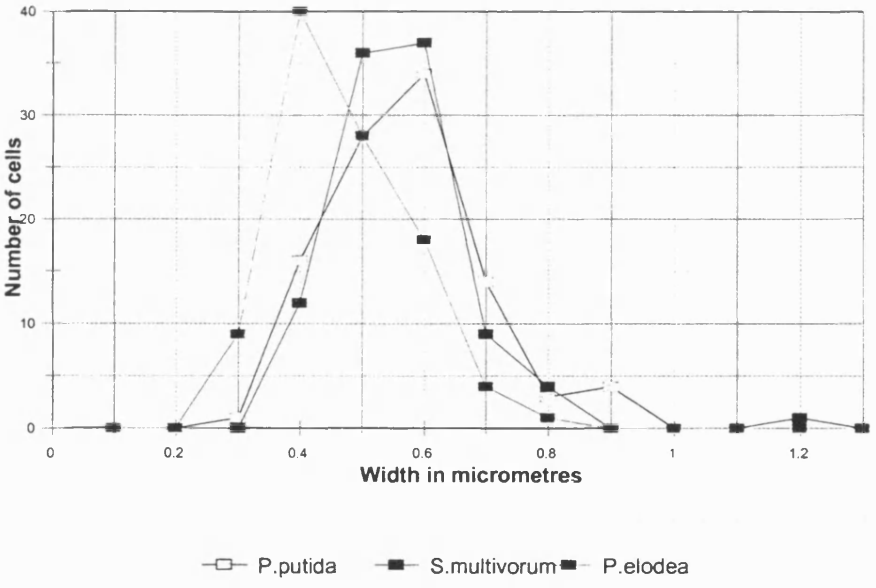

Figure 5.19 Width of cells observed under the light microscope

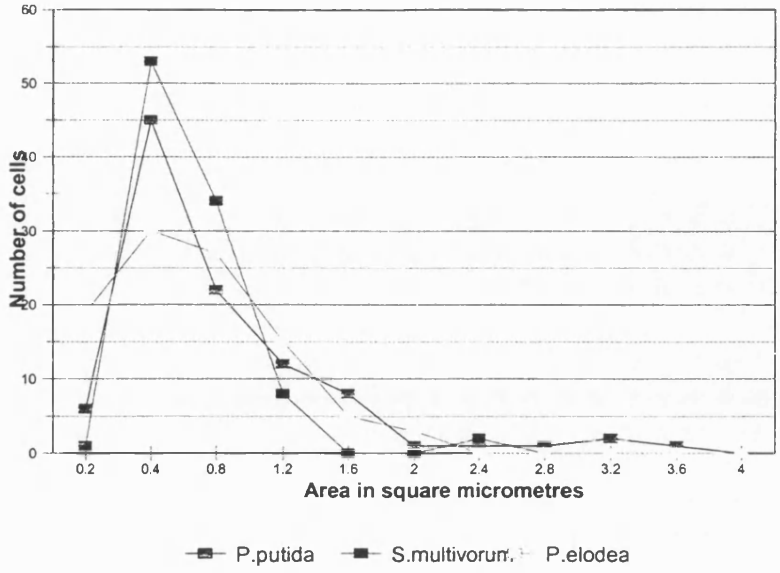

Figure 5.20 Area of cells observed under the light microscope

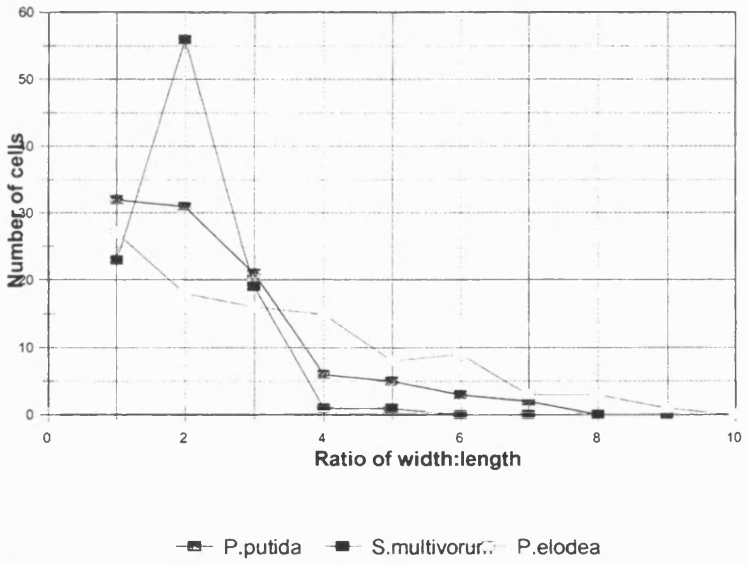

Figure 5.21 Ratio of width to length of cells observed under the light microscope

5.4 Mass

The mass per cell was calculated by taking a known volume of bacteria suspension of a measured cell concentration, which was then dried, in an oven at 90-100 °C. The final weight was used in the following calculation: -

$$M_C = \frac{V_S C}{M_T} \qquad \textbf{Equation 17}$$

Where: -

M_C= mass of one cell

V_S= suspension volume

C= cell concentration of suspension

M_T= total dry mass

5.4.1 Mass results

The mass of each type of bacterium was measured four times and the mean of these values is set out below. These figures are accurate to within 8% for *P.putida* and *S.multivorum*, and 10% for *P.elodea.*

Mass of *S.multivorum* = 2.5×10^{-12} kg

Mass of *P.elodea* cell = 3.2×10^{-12} kg

Mass of *P.putida* cell = 2.1×10^{-12} kg

5.5 Polysaccharide levels

Extraction of polysaccharide was carried out using the method detailed in Kang & Veeder (1983). This involved precipitating the polysaccharides by adding 2 parts isopropanol to 1 part cell suspension. This precipitate was emptied onto pre-weighed filter paper and dried in a tray drier at around 60 °C.

Unfortunately it was very difficult to quantify the amount of polysaccharide; it was easily visible to the naked eye as agglomerates with *P.elodea*, whereas with the other two cell types, nothing was seen. This test clearly worked only for loose polysaccharide, as the smooth *S.multivorum* capsule is also predominantly polysaccharide. Kang & Veeder (1983) state that the polysaccharide levels in *P.elodea* broth should be approximately 1.5%.

Wilkinson (1958) pointed out that the centrifugal conditions must be chosen carefully since the slime of *P.elodea* may be removed from the cell wall if incorrect

settings are used. Unfortunately, due to time and equipment constraints, much of the polysaccharide slime had been stripped away. However, it appeared that enough slime remained to produce a significant effect. Rialho *et al* (1990) washed their *P.elodea* cells twice in Ringer's and still found the effects of agglomeration of the polysaccharides to be strongly in evidence, which is consistent with the findings in this study.

5.6 Viscosity

Viscosity was measured by a Brookfield Digital Viscometer (model DV-II). The results at 60 rpm are laid out in Table 5.8. Most experiments were performed with cell suspensions of 1.5 x 10^9 cells per ml, to ensure a differentiation between tests. Bracketed values are tests done at about half the cell concentration-similar to the cell concentration for the cell suspensions in the filtration experiments.

5.6.1.1 Viscosity results

	P.putida	*S.multivorum*	*P.elodea*	BSA
Broth	1.17	1.22	1.5	
Low Na	1.11	1.16	1.22	
Low Na /BSA	1.2	1.18	1.24	
High Na	1.4 (1.3)	1.49 (1.28)	1.43 (1.27)	
High Na /BSA	1.42	1.42	1.4	
High Ca	1.38	1.42	1.53	1.09
High Ca /BSA	1.56 (1.42)	1.63 (1.48)	1.5 (1.43)	
Low Ca	1.48	1.4	1.46	

Table 5.8 Viscosity of cells and suspensions in mPas or centipoise

The viscosity of cells in Table 5.8 was affected by ion valency and concentration, with high concentrations of ions in the suspension medium, particularly the divalent ion calcium increasing the viscosity. Addition of protein had a negligible effect on the values, except at high calcium concentrations.

The greatest viscosities for all three bacteria were for the protein/$CaCl_2$ solution. This effect was not due to the protein alone. As the test on the protein/$CaCl_2$ solution without cells indicates, it is also due to agglomeration, which is easily visible to the naked eye.

The viscosity of *P.elodea* in broth, where there was a high level of gellan gum, was equal to that of *P.elodea* in $CaCl_2$. This result endorsed the assertion that there is still a significant amount of gellan gum attached to the surface, as the effects could still be seen. It is a well-established fact that gellan gum forms a weak gel in the presence of calcium ions, (Moorhouse, 1987).

The viscosity of the cells must have been much higher near the membrane surface where the cake forms, but the viscosity levels in this area could not be inferred from these results. The effect of halving the cell concentration however can be seen from the bracketed values in Table 5.8. The order of viscosity levels is, however, likely to be the same. At high concentrations *P.elodea* will act as a non-Newtonian fluid, taking on the properties of gellan gum.

5.7 Conclusions

The zeta potentials for all three cells in low ionic strength solutions were negative, with *P.putida* and *S.multivorum* showing evidence of more than one type of site. The effect of high NaCl meant that all three became only slightly negative with a narrow distribution, while $CaCl_2$ brought the zeta potentials close to zero, with *S.multivorum* slightly more positive than BSA or the other bacteria.

This may have had an effect on the hydrophobicity results, which were generally low to moderate. A high ionic strength solution tended to decrease the hydrophobicity for *Pseudomonas putida* and *P.elodea* but not for *S.multivorum*. Measurements for *P.putida* were assumed to be for the flagella surrounding the cell surface.

The cell sizes taken for subsequent calculations, such as the cell layer equivalent values in section 6.4.4 are those measured by cryogenic S.E.M. Therefore the dimensions used in calculations are as follows:-

1) *S.multivorum*- 2.39 x 1.017 μm

2) *P.elodea*- 2.28 x 0.825 μm.

3) *P.putida*- 2.42 x 0.61 μm

There was a tendency for the *Pseudomonas* species to form chains of two or three. *P.elodea* is slightly thinner than the other two are when stripped of slime. Nevertheless, their average areas are all within 19% of each other.

Cell mass values for the calculations in chapter 6 were taken to be:

1) 2.5×10^{-12}kg for *S.multivorum*

2) 3.2×10^{-12}kg for *P.elodea*

3) 2.1×10^{-12}kg for *P.putida*

It was not possible to quantify the polysaccharide levels present in *P.putida* buffer suspensions. However, as expected, this organism was the only one with a positive indication of the presence of loose polysaccharide.

The viscosities of the cell suspensions were low – between 1.16 and 1.6 mPas, the highest viscosities being shown for high $CaCl_2$ for all species and for *P.elodea* in broth. This supports the fact that gellan gum is still present.

6 Experimental results for filtration of bacteria

6.1 Introduction

This chapter contains the results for the filtration experiments. The experiments are described in chronological order, the first ones being those in broth.

The majority of experiments however were performed in suspensions of buffer. These buffers varied in ionic strength, valency of the ions and the presence/absence of BSA protein.

The effects of these three differences on the filtration behaviour of three bacteria were assessed by looking at several filtration characteristics. From these analyses, a picture of how the dominance of either hydrodynamic or physicochemical forces depends on both the filtration conditions and the organism being filtered can be established. The filtration data is assessed in the following ways: -

- Resistance
- Cell deposition
- Comparison of rates of increase of resistance and cell deposition
- Specific cake resistance
- Analysis of repeat experiment data
- Relationship between irreversible fouling and final flux
- Protein transmission

6.2 Filtration conditions

Details of the experimental conditions can be found in chapter 4. All the experiments were performed at a crossflow velocity of 0.23 m/s and a crossmembrane pressure of 0.14 bar (STD 5.2%) at 23°C. The value for the transmembrane pressure had a steady state value of 0.5 bar (STD 5.2%) after the initial fouling had occurred. This was generally within the first few minutes, as can be seen by the sample graphs in Figure 6.5 to Figure 6.7

Initial experiments were performed using the fermentation broths of the three bacteria at cell densities of 4.2-5.6x10^8 cells per ml. This was useful as an initial investigation, but:-

- fermentation proteins for each bacterium were different, and might interact differently
- final cell concentrations were hard to control.

Thus the majority of subsequent experiments were carried out under more controlled conditions; washed cells were suspended in buffer of different ionic strength and the initial cell density was carefully calculated to be within 7% of 7.5x10^8 cells per ml.

6.3 Filtration in broth

The initial experiments were carried out with the bacteria still suspended in broth. The main measured parameter for these experiments was the flux, determined by the bubble flowmeter (section 4.4.1). The proportion of reversible fouling was also measured by measuring the percentage recovery after rinsing. Fouling curves for the three micro-organisms are presented in Figure 6.1. The capsulate *Sphingobacterium multivorum* and the flagellate *P.putida* have similar final fluxes, although their initial fouling patterns vary, with *S.multivorum* having a much steeper initial fouling curve. Even for fermentations with a 33% difference in cell concentration, the final fluxes for both *P.putida* and *S.multivorum* were within 17% of each other. However for a difference in *P.elodea* cell concentration of 30-35%, the corresponding final fluxes differed by as much as 50-60%. Thus *P.elodea* experiments appear to be more sensitive to cell concentration than the others.

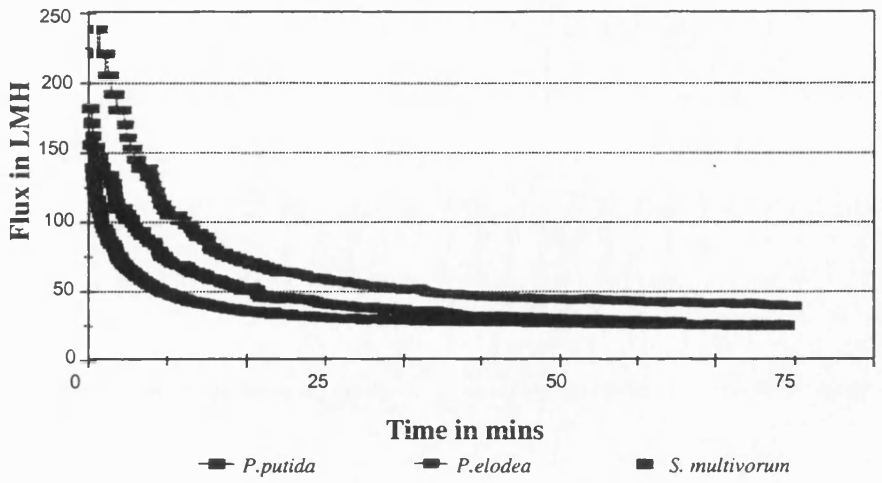

Figure 6.1 Comparison of bacterial fouling curves in broth

Species	**Extracellular Characteristic**	**Percentage CWF Recovery**	**Final Flux ($lm^{-2}h^{-1}$)**
S.multivorum	Capsular	84.4	28.1
P.putida	Flagellate	75	26.4
P.elodea	Slime	70.7	39.2

Table 6.1: Description of Bacteria and Summary of Fluxes Based on 2 runs

The clean water fluxes (CWF) taken after initial rinsing (Table 6.1) endorses the theory that flux reduction is primarily due to reversible fouling, not only in *S.multivorum*, but also for the other two bacteria. All three of the water flux recovery rates are high, but *S.multivorum* produces a particularly high percentage flux recovery. Both these phenomena can be explained by the fact that *S.multivorum* is the only one of the three with no protrusions or surface roughness to aid attachment to the membrane and thus can detach with the greatest ease.

The higher fluxes for *P.elodea* were unexpected, since during cultivation the cells were very prone to agglomeration, and therefore heavy fouling was anticipated. This apparent anomaly may be explained by the fact that extracellular polysaccharides are very negatively charged. Therefore if the cells are surrounded by a large amount of polysaccharide, repulsion may occur between cells and between a cell and the negatively charged membrane. This would result in a looser cake and therefore in attenuated flux decline. If this is the case, then at higher ionic strengths, fouling will be increased and flux reduced for this organism, because the presence of positive ions can help form bonds between two negatively charged surfaces. The combined presence of large amounts of polymer and positive ions in the broth for *P.elodea* could be conducive to the formation of strong irreversible bonds. This may explain the relatively low CWF

recovery for *P.elodea.* This theory is proved and discussed further in section 5.2. The Zeta potential results are also consistent with this assertion; the Zeta potential for *P.elodea* in low ionic strength buffer is –33mV. At a high NaCl ionic strength the *P.elodea* Zeta potential decreases to –3.52mV, while at high $CaCl_2$ it is only –0.36mV.

6.4 Filtration in phosphate buffer with NaCl/$CaCl_2$

For the majority of experiments, the three types of micro-organisms were washed thoroughly and suspended in phosphate buffer of 0.005M and pH 6.6. The effects of high and low ionic strength, and monovalent and divalent ions on filtration were studied by adding the following salts.

- High NaCl (40 g/l)
- Low NaCl (0.1 g/l)
- High $CaCl_2$ (29.5 g/l)
- Low $CaCl_2$ (0.6 g/l)

The ionic strengths of the high sodium and calcium solutions are equivalent (680 mmol/l). The ionic strength of the low calcium solution is ten times that of the low sodium solution at 17.1 mmol/l. Comparison of the two low ionic strength suspensions can demonstrate the sensitivity of the bacterial filtration system to a change in ionic strength.

The effect of a defined amount of a particular protein on each bacterium's filtration behaviour was also of interest. Further experiments were run with 1 g/l of bovine serum albumen (BSA) added to the first three types of solution.

For comparison, it can be noted that nutrient broth contains 5g/l NaCl and approximately 8g/l of a mixture of proteins including peptone.

6.4.1 Fundamental filtration characteristics- flux, TMP and resistance

Pressure transducers were inserted into the rig for this set of experiments, so transmembrane pressure as well as flux, could be measured. This meant that the resistance to filtrate flux could then be calculated, using Darcy's law (Equation 18):

$$R = \frac{\Delta P}{\mu J} \qquad \textbf{Equation 18}$$

Where ΔP= Transmembrane pressure

μ= Viscosity of permeate

J = Flux

The flux/TMP/resistance curves in Figure 6.2 to Figure 6.7 illustrate the simplest methods of filtration behaviour analysis. A full catalogue of these graphs for all experiments in buffer can be found in appendix C.

6.4.1.1 Controls

It was necessary to perform control experiments to assess the interaction of both cells and suspension with the rig, and discover whether these interactions affected the results.

6.4.1.1.1 Controls run without membrane module

Test runs with bacterial suspensions were carried out on the rig with the microfiltration unit removed. Cell adhesion to the inside surfaces of the rest of the rig was found to be negligible for all electrolyte conditions; the cell concentrations before and after 90 minutes of cell suspension recirculation were found to be within 1% of each other.

6.4.1.1.2 Controls with membrane module

It was also necessary to determine how the solutions and protein suspensions affected the flux without the cells, so experiments were run for each of the solutions with and without proteins. Details are given in section 4.4.2.

All four controls (the four different electrolyte solutions alone) showed a steady flux and no increase in TMP, and therefore no increase in resistance throughout a 90 minute run. Therefore no fouling due to the solutions alone was observed.

The flux/TMP/resistance curve for the low NaCl and low $CaCl_2$ solutions with BSA did not change with time. Data for the former is shown in Figure 6.2.

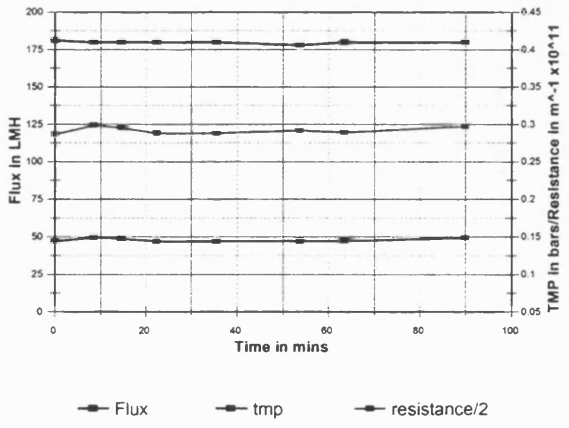

Figure 6.2 Filtration of BSA in low NaCl

Both of the high ionic strength solutions encouraged some fouling of the membrane, resulting in a decrease in flux and an increase in resistance, shown in Figure 6.3 & Figure 6.4. However, this decrease in flux was much less dramatic than for the experiments with the cells. From a starting flux of 188-190 lm^2h^{-1}, the final fluxes were 154 lm^2h^{-1} for high NaCl and 144 $lm^2h^{-1}$for high $CaCl_2$. The highest final flux for the main experiments with bacteria was 49 lm^2h^{-1} (see Table 6.19). The TMP did not reach the equilibrium value of 0.5 bar for either control, but reached only 0.22 and 0.25 bar respectively.

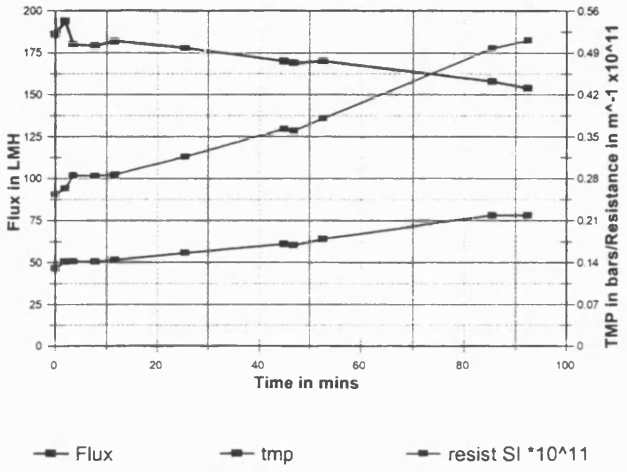

Figure 6.3: Filtration of BSA in high NaCl

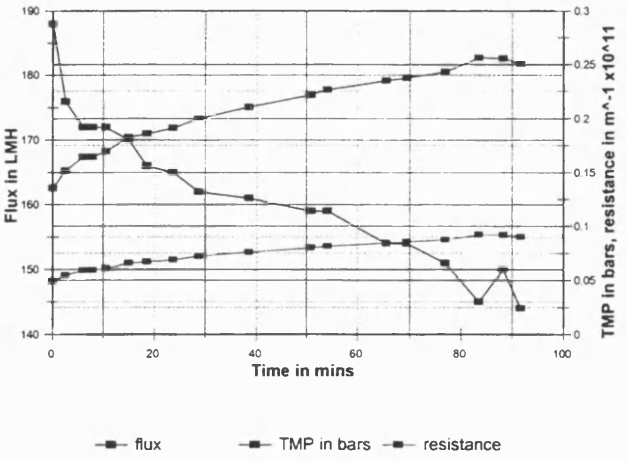

Figure 6.4: Filtration of BSA in high $CaCl_2$

6.4.1.2 Cell suspensions

Figure 6.5 to Figure 6.7 show the changing relationship over time between transmembrane pressure, flux and resistance for three of the experiments with bacteria, and demonstrates the greater variability in the rates and severity of fouling compared to the controls.

These graphs demonstrate that the TMP is not constant from the beginning in these experiments, it starts at around 0.14 bar, rising to the steady state value of around 0.5 bar, at a rate commensurate with the initial rate of fouling. Once at this value, the variation in TMP fluctuated by up to 4.2% with the fluctuation in pump power.

The initial rate of fouling, indicated by the steepest part of all three flux curves in Figure 6.5 to Figure 6.7, differs with the type of bacteria filtered, as in the initial broth experiments. It also differs with suspension conditions. This is discussed in detail in Chapter 7.

It can also be seen that the resistance curves are much more descriptive of the fouling activity than the flux curve after initial fouling, since the change in gradient is easier to observe.

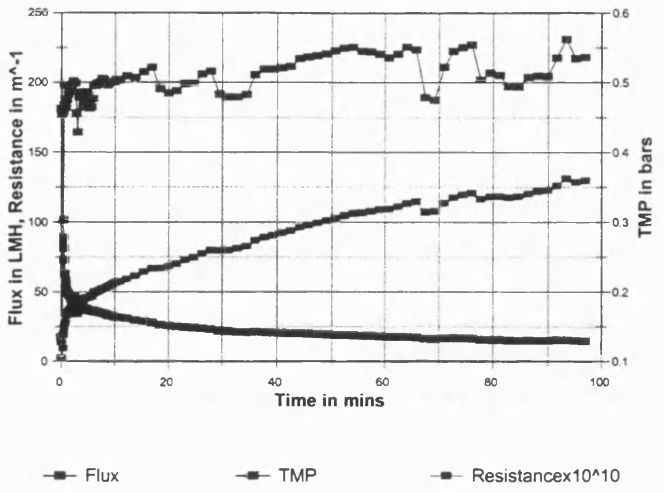

Figure 6.5: Relationship between flux, TMP and resistance for *S.multivorum* in high NaCl

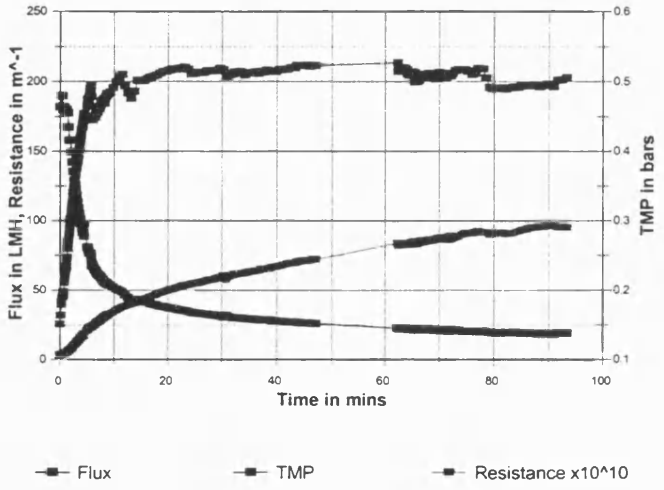

Figure 6.6: Relationship between flux, TMP and resistance for *P.elodea* in high NaCl

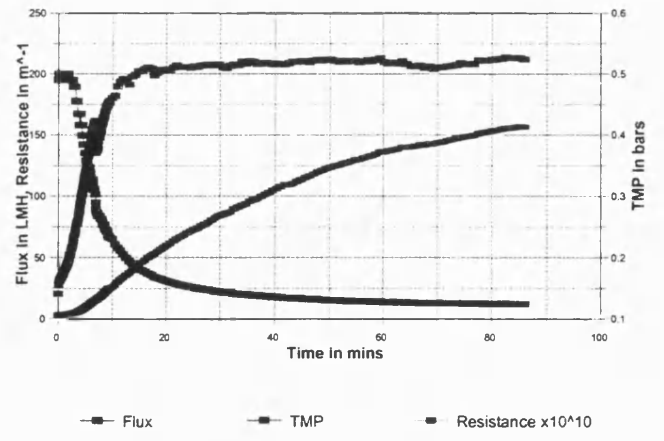

Figure 6.7 Relationship between flux, TMP and resistance for *P.putida* in low $CaCl_2$

6.4.2 Resistance

Since resistance is calculated directly from two direct measurements, and differences between values can easily be interpreted, it is taken to be the primary parameter to quantify filtration and fouling performance in this thesis. The contents of Table 6.2 to Table 6.4 reveal the final resistance after 90 minutes of filtration for all filtration conditions. These figures are accurate to within 7%. The error calculations can be found in appendix D.

S.multivorum in:-	**Solution only** ($m^{-1} \times 10^{10}$)	**With BSA** ($m^{-1} \times 10^{10}$)
Low NaCl	50	82
High NaCl	130	81
Low $CaCl_2$	53	N/A
High $CaCl_2$	106	77

Table 6.2: Final resistances for *S.multivorum*

P.elodea in:-	**Solution only** ($m^{-1} \times 10^{10}$)	**With BSA** ($m^{-1} \times 10^{10}$)
Low NaCl	59	145
High NaCl	162	Not known
Low $CaCl_2$	35	N/A
High $CaCl_2$	77	95

Table 6.3: Final resistances for *P.elodea*

P.putida in:-	**Solution only** ($m^{-1} \times 10^{10}$)	**With BSA** ($m^{-1} \times 10^{10}$)
Low NaCl	124	166
High NaCl	82	164
Low $CaCl_2$	157	N/A
High $CaCl_2$	59	40

Table 6.4: Final resistances for *P.putida*

6.4.2.1 Ionic strength

For the salt solution alone, a higher ionic strength gives a higher resistance for *S.multivorum* and *P.elodea*. Conversely for *P.putida*, it is the low ionic strengths that yield the higher resistance.

6.4.2.2 Addition of BSA

The resistance increase for the high NaCl/BSA control after 90 minutes was only 2.6 x 10^{10} m^{-1}, while for the high $CaCl_2$ control it was 3.7 x 10^{10} m^{-1}. The resistance increase due to the cells and to the protein only was not simply additive, as can be seen in Table 6.2 to Table 6.4. This observation is expected, since it has previously been observed by Hodgson *et al* (1993) and Foley (1995) and by Field *et al.* (1995). In fact, addition of BSA sometimes resulted in a decrease in resistance; both *S.multivorum* in high ionic strength solutions and *P.putida* suspended in high $CaCl_2$ solution follow this trend: *P.elodea*, however, follows the opposite trend of a commensurate resistance increase with the addition of protein.

The results for *S.multivorum* are distinguished by the fact that the final resistance values for suspensions containing BSA are very similar; they are all between $77x10^{10}$ m^{-1} and $83x10^{10}$ m^{-1}. This indicates that either the cell-protein or the membrane protein interaction is very important. Since the effect is independent of ionic strength, the effect must be independent of ionic interactions, indicating that hydrodynamic effects are determining the behaviour.

For *P.elodea*, the addition of BSA increases the resistance by 143% when BSA is added to the low NaCl suspension. The increase for high $CaCl_2$ suspension is much less, only 23%.

The effect of protein on *P.putida* filtration differs according to the valency of the cation. For the two NaCl solutions, the presence of BSA increases the resistance significantly, to a similar value (164 and $166x10^{10}$ m^{-1}). For the high $CaCl_2$ suspension however, the resistance decreases from $58.7x10^{10}$ m^{-1} to $40.2x10^{10}$ m^{-1}.

6.4.2.3 Valency

For all three types of cells, the high ionic strength NaCl solution leads to a greater resistance than the high $CaCl_2$ solution. The effect of valency on the low ionic strength solutions is not so universal however. The fact that low $CaCl_2$ solution has a higher ionic strength than low NaCl must also be taken into account.

The two *S.multivorum* low ionic strength suspensions have similar final resistances, at 50 and $53x10^{10}$ m^{-1} for NaCl and $CaCl_2$ respectively. Thus at low ionic strengths, *S.multivorum* filtration behaviour is not very sensitive either to valency or small changes in molarity, and hydrodynamic effects must dominate.

P.elodea follows the same trend at low ionic strengths as at high ionic strengths, with the resistance in low NaCl being higher ($59x10^{10}$ m^{-1}) than that of low $CaCl_2$ ($35x10^{10}$ m^{-1}). An increase in ionic strength for solutions of the same valency results in an increase in resistance. Thus if ionic strength effects dominated, the low $CaCl_2$ suspension would have the higher resistance. These results imply that valency has a stronger influence than ionic strength on the resistance.

For *P.putida* in low molarity suspensions, decreasing the valency seems to lower the resistance. This is contrary to the trends for both the high ionic strength valency results and the same valency ionic strength results. Therefore other unknown factors must be influencing these results see chapter 8 for a further discussion.

Calcium appears to have a marked effect on all three micro-organisms. This is partly due to the tendency of all three species to experience the greatest agglomeration with high concentrations of $CaCl_2$. See chapter 7 for more details.

6.4.3 Shear

Throughout these experiments, the crossflow velocity and thus the crossmembrane, or longitudinal, pressure drop is kept constant. The shear stress is calculated using Equation 16. Thus a constant longitudinal pressure drop should result in a constant shear stress.

$$\tau_w = \frac{\Delta P_L D}{4L}$$ **Equation 19**

Where:-

τ_w= shear stress

ΔP_L= longitudinal pressure drop

L=Length of filter

D= hydraulic diameter of membrane tube

Figure 6.8 shows that, using equation 19, the calculated shear stress is approximately constant after the flux elbow, and is similar for each experiment. The standard deviation of 5.2% from a value of 1.55 Nm^{-2} is due to the fluctuation in the

power of the pump, which was unpredictable. However, in reality cake build up affects the effective hydraulic diameter. Therefore the actual shear rates are greater than calculated, especially for conditions encouraging large cake build up, such as aggregation. For aggregates of a critical size and density, this shear may be sufficient to remove them from the surface. If the cell cake builds up to a critical size, parts of the cake may be sheared cyclically (see section 6.4.4)

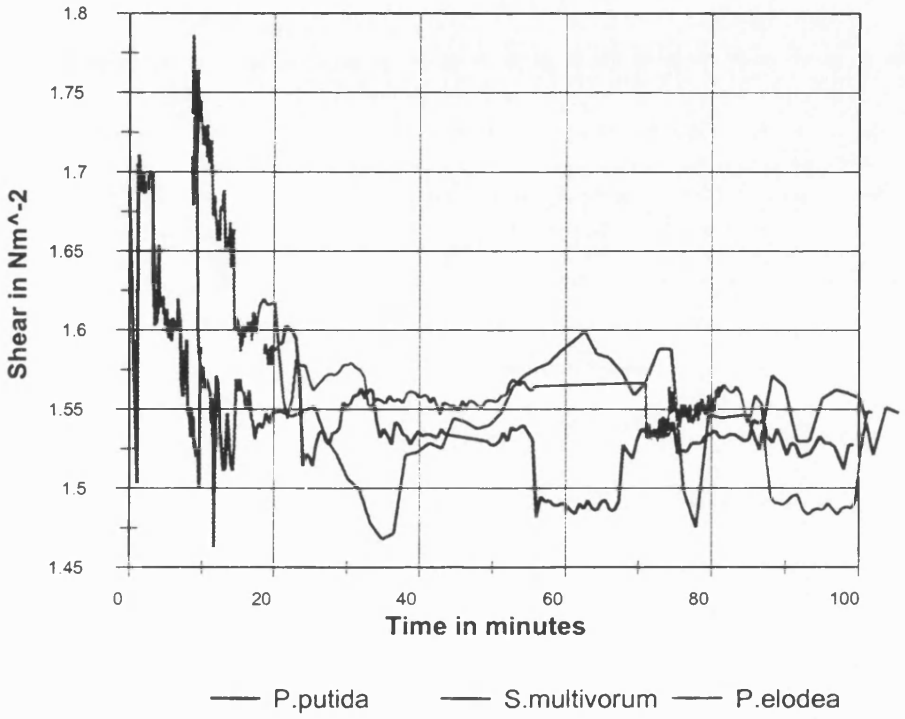

Figure 6.8 Shear values during experiments of all three bacteria in high NaCl.

6.4.4 Cell deposition and cell layer equivalents

It was not possible to find a way to determine the actual number of cell layers, because the structure of the module precluded visualisation techniques. The results for the amount of cells deposited have been expressed as 'cell layer equivalents' to allow a direct comparison between the cells. These figures are an underestimation of the actual number of cell layers, since they do not assume any voidage at all between the cells. The assumption that all the cells lie flat seems valid, judging from the observations of Tanaka *et al.* (1996).

Cell layer equivalents (C.L.E) are calculated by employing the following equation:

$$C.L.E = \frac{aC_d V_s}{A}$$ **Equation 20**

Where:

a = area of 1 cell

C_d = cells per ml lost from retentate

V_s = total volume of feed

A = area of membrane

A summary of the C.L.E. values is given below in Figure 6.9. Details can be found in Table 6.5 to Table 6.7. The accuracy of these figures is to within 11%, i.e. the accuracy of the cell counts (see section 4.3.1).

The *P.putida* runs have, with one exception, values of 16-19 C.L.Es., whilst the final *S.multivorum* results are typically around 5 C.L.Es., with two exceptions. The *P.elodea* results are very scattered however.

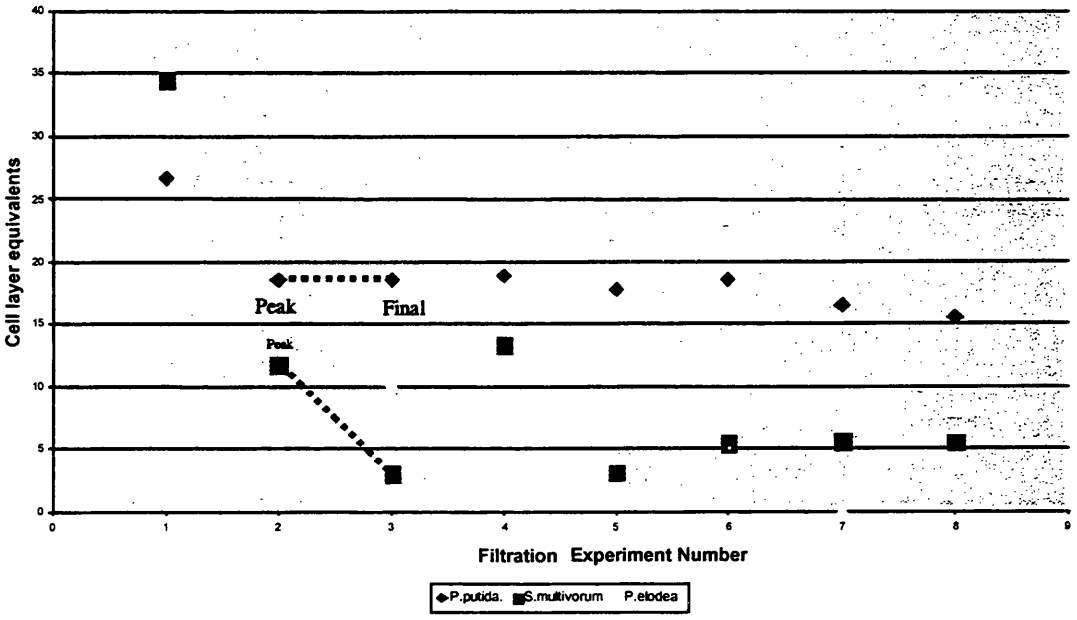

Figure 6.9 Cell layer equivalent scatter plot

S.multivorum in:-	Solution only (C.L.E.)	With BSA (C.L.E.)
Low NaCl	5.4	5.5
High NaCl	13	5.6
Low $CaCl_2$	3.1	N/A
High $CaCl_2$	34	*12/3

*The first number is the peak C.L.E. and the second one shows the final C.L.E.

Table 6.5: *S.multivorum* cell layer equivalents

P.elodea in:-	Solution only (C.L.E.)	With BSA (C.L.E.)
Low NaCl	24	8.1
High NaCl	3.8	N/A
Low $CaCl_2$	22	N/A
High $CaCl_2$	11	*14/10

*The first number is the peak C.L.E. and the second one shows the final C.L.E.

Table 6.6: *P.elodea* cell layer equivalents

P.putida in:-	Solution only (C.L.E.)	With BSA (C.L.E.)
Low NaCl	19	16
High NaCl	19	17
Low $CaCl_2$	18	N/A
High $CaCl_2$	27	19

Table 6.7: *P.putida* cell layer equivalents

6.4.4.1 Effect of ionic strength on values

For both *S.multivorum* and *P.putida*, C.L.E. is highest in the high ionic strength $CaCl_2$ solution. For *S.multivorum*, this type of suspension has the greatest cell deposition of all the experiments in this study at 34 C.L.E. A figure of 13 CLE for the high NaCl solution is much lower, but is still high for this bacterium, since it can be seen from Figure 6.9 that the majority of results for *S.multivorum*, are at 5.6 CLE or below.

For *P.elodea*, ionic strength has the opposite effect to *S.multivorum*; for both NaCl and $CaCl_2$, the higher cell deposition is in the low ionic strength suspensions, with similar figures, 26 CLEs and 22 CLEs for NaCl and low $CaCl_2$ respectively. The high

$CaCl_2$ cell deposition is much higher than the high NaCl deposition, at 11 compared to 4 CLEs. This is to be expected, since the presence of high $CaCl_2$ caused higher agglomeration in all bacteria. Since agglomeration is lower in low ionic strength solutions, it may seem surprising that the cell deposition is highest for these suspensions, but these forms of agglomerates appear large and diffuse to the naked eye. See chapter 8 for a further discussion.

The results for *P.putida* are very similar for all conditions except for high $CaCl_2$, as shown in Table 6.7. At a value of 27 C.L.E., the cell deposition is around 50% higher than that for the others. This too can be explained by the high tendency for all cells to agglomerate in the presence of Ca^{2+}. Some agglomeration does occur at high sodium concentrations too, but this does not affect the cell deposition equilibrium, as the figures for low NaCl and high NaCl are both around 19. This indicates that the cell deposition is determined more by hydrodynamic factors than physicochemical factors.

6.4.4.2 Effect of BSA

For *S.multivorum*, the effect of BSA on high ionic strength suspensions is significant for high NaCl; the cell deposition is brought down from 13 CLEs to 5.6 CLEs, similar to both the low ionic strength suspensions and low NaCl with BSA. Thus the presence of BSA does not change the cell deposition for low NaCl. For high $CaCl_2$ with BSA however, the cell deposition is very erratic, as shown in Figure 6.10. This variation is far greater than the estimated 11% experimental error. Table 6.6 shows how the peak cell deposition for this suspension at 1 minute (12 CLE) is close to that of high NaCl (13 CLE), but the final cell deposition is the lowest for all the conditions at 3 CLEs.

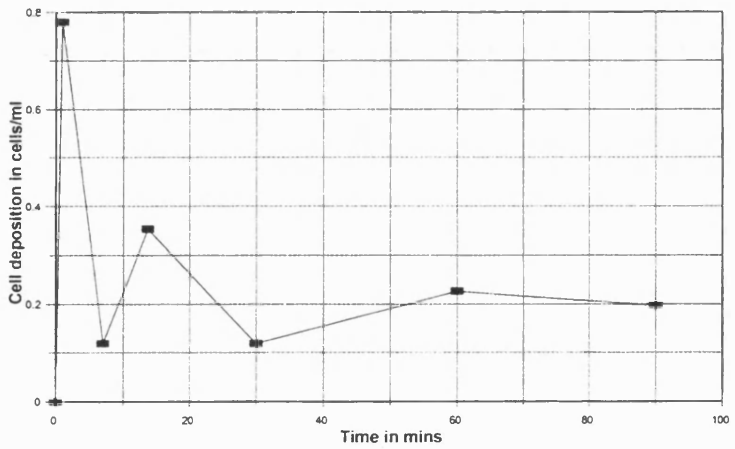

Figure 6.10 Cell deposition for *S.multivorum* and BSA in High $CaCl_2$ solution

The effect of BSA on *P.elodea* in high $CaCl_2$ is similar to that of *S.multivorum*. The cell deposition fluctuates dramatically, the time peaking at 14 CLEs at 30 minutes, but with a final figure of 10 CLEs. This is close to the value for the final CLE without BSA. For low NaCl, the addition of BSA decreases the cell deposition from 24 CLEs to 8.1 CLEs.

BSA has a negligible effect on the cell deposition of *P.putida*. The results for both NaCl suspensions are similar, both with and without the addition of protein. The addition of protein has a significant modifying effect on high $CaCl_2$ – the cell deposition is brought down from 27 to a similar figure to all the other *P.putida* experiments at 19 CLEs.

6.4.4.3 Cell layer equivalents and resistance

6.4.4.3.1 *S.multivorum*

S.multivorum has similar values for the low ionic strength suspensions (3.1 & 5.4 CLEs), although this time the resistances are very similar too (50 & $53x10^{10}$ m^{-1}). The lowest final resistances give rise to the lowest CLE for the solutions without protein, which is in direct contrast to *P.elodea*. Even though the final resistances are approximately $30x10^{10}$ m^{-1} greater for the two NaCl/BSA suspensions than for the low ionic NaCl suspension, the cell depositions are very similar (5.5 CLEs). This also applies for the final figure for the $CaCl_2$/BSA suspension. Once again the presence of protein dominates the fouling behaviour, possibly because the presence of protein brings the system to equilibrium more quickly.

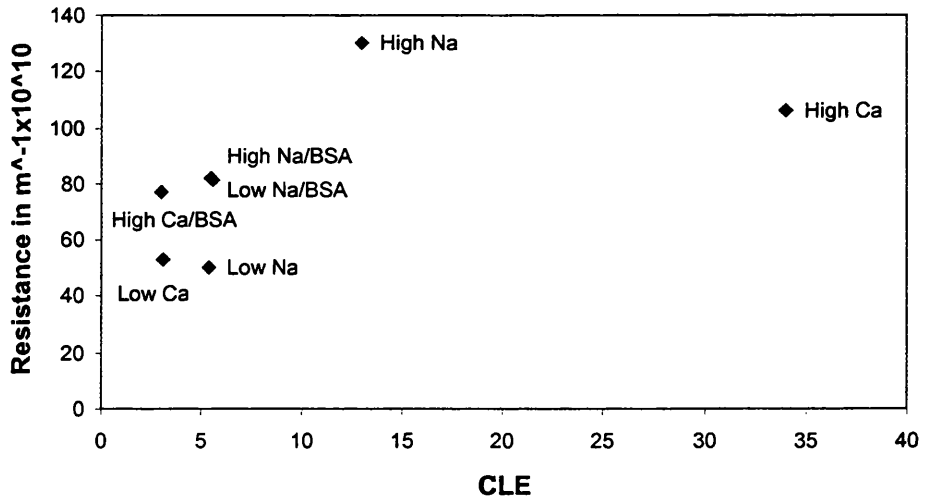

Figure 6.11 Scatter plot of C.L.E. versus final resistance values for *S.multivorum*

The high NaCl only suspension has both a greater resistance and greater cell deposition than these aforementioned suspensions, but the C.L.E. of the high $CaCl_2$ still remains the highest at 36, even though the resistance is lower than for high NaCl. These similarities and differences are illustrated in the scatter plot in Figure 6.11

6.4.4.3.2 *P.elodea*

A comparison of Figure 6.11 and Figure 6.12 helps to emphasise the difference between the fouling behaviour of *P.elodea* and *S.multivorum*. Like *S.multivorum*, the resistances for *P.elodea* in low NaCl and low $CaCl_2$ are quite close together- 59 and $35x10^{10}m^{-1}$,which again are the lowest values. However, unlike *S.multivorum*, the C.L.E. values are much higher than for the other electrolyte suspensions. Generally, the higher the resistance, the lower the cell deposition. High ionic strengths and the presence of BSA tend to increase the resistance.

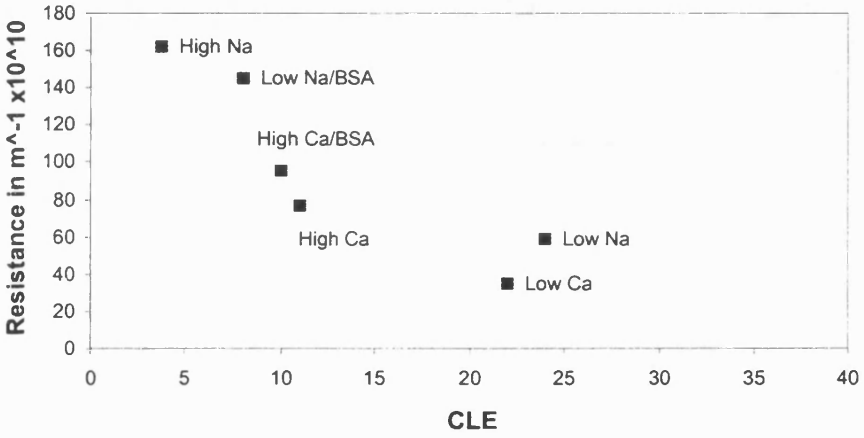

Figure 6.12 Scatter plot of C.L.E. versus final resistance values for *P.elodea*

6.4.4.3.3 *P.putida*

For *P.putida*, the resistance is independent of the CLE number since the resistances vary widely, while the CLEs for all the conditions except high $CaCl_2$ (27 C.L.E.) are all close to a value of 18 CLE.

6.4.5 Comparison of the relative increase of resistance to cell deposition during filtration

A more sophisticated means of comparing resistance and cell deposition is to observe the timing of their respective increases. Figure 6.13 to Figure 6.15 illustrate the distinct differences in the relative increase of resistance and cell deposition to their final

values. These three graphs are characteristic for each organism; plots for the rest of the experiments can be seen in appendix C.

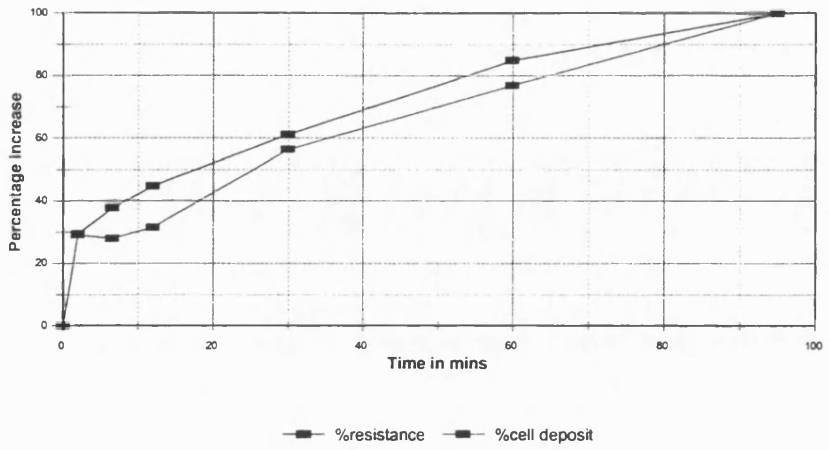

Figure 6.13 Cell deposition and resistance comparison for *S.multivorum* in high NaCl

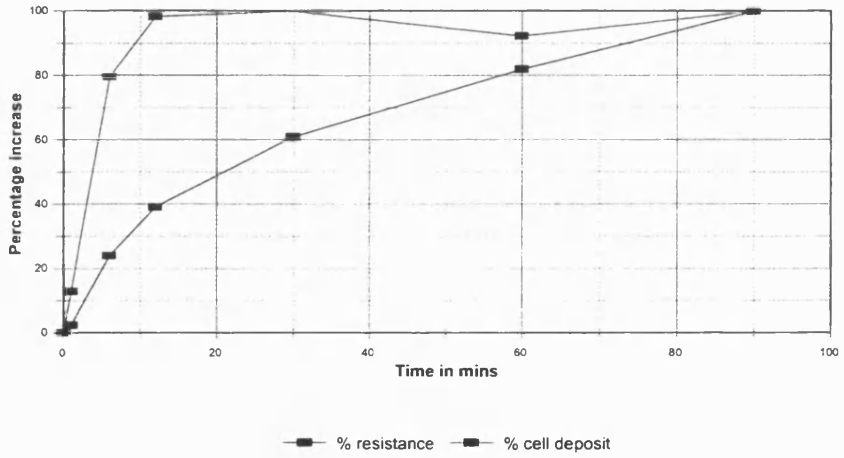

Figure 6.14: Cell deposition and resistance comparison for *P.elodea* in low $CaCl_2$

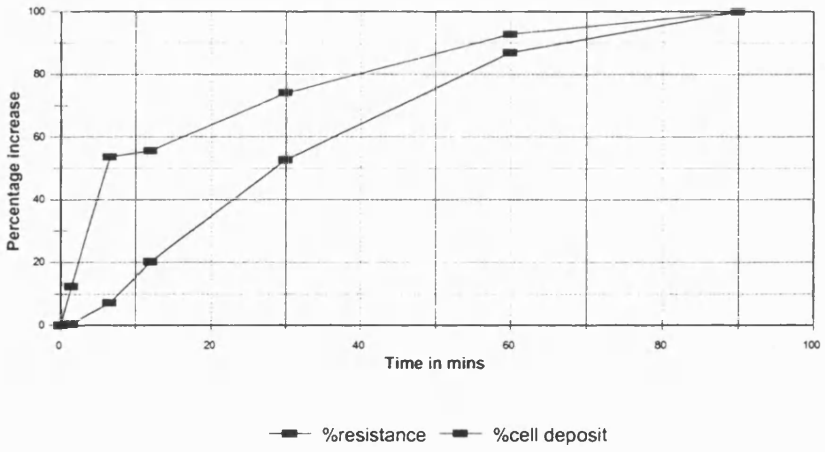

Figure 6.15: Cell deposition and resistance comparison for *P.putida* in low $CaCl_2$

It can be seen that *S.multivorum* tends to have a resistance percentage level higher than that for the cell deposition until the very end of the run. This supports the theory that this organism is prone to a significant level of pore blocking.

P.putida on the other hand, has a resistance increase well below that of the cell deposition, with both values increasing gradually up to 90 minutes.

The cell deposition for *P.elodea* tends to increase up to over 90% of the final value in the first 12-30 minutes (12 minutes for Figure 6.14), but the resistance increases much more gradually. This gives strong support to the theory that the cells rearrange themselves once the cake is deposited (Altmann and Ripperger, 1997, Fu and Dempsey, 1998; Foley, Malone and MacLoughlin, 1995). A further catalogue of plots for experiments can be seen in appendix C.

The cell deposition results for *S.multivorum* and *P.elodea* suspended in high calcium/BSA and *P.elodea* in high calcium solutions all display very irregular deposition results. Since these conditions encourage agglomeration, this may be because there is sporadic complete blocking, which is then suddenly cleared by the increasing crossmembrane pressure.

Another possible explanation is that the cell aggregates are subject to removal due to crossflow shear. Altmann and Ripperger, (1997), Fu and Dempsey, (1998), Foley, Malone and MacLoughlin, (1995) all demonstrate that as the balance of forces on a particle near the cake surface changes, conditions for adhesion of larger particles become less favourable. For *S.multivorum* especially, the resistance seems to be mainly due to only a few cells settling, while other aggregates are being swept off and resettling on the membrane without contributing significantly to the overall resistance.

6.4.5.1 Effect of initial conditions on cell deposition and resistance increase

The protein results verify the theory that it is the first few minutes of operation that determines fouling for the rest of the run. Figure 6.16 compares the rate of resistance increase for three *S.multivorum* runs. The figures in the centre of the plot denote the final values. This graph illustrates the phenomenon that a high initial rate of fouling will continue until the end of the experiment, as for the high NaCl run. This will result in a high final resistance, in this case 130×10^{10} m^{-1}. For a low initial rate of fouling, as for the low NaCl suspension, the final resistance is only $50 \times 10^{10} m^{-1}$. Protein involvement results in an intermediate rate of fouling hence an intermediate resistance value of around 81×10^{10} m^{-1}.

This rate of increase of resistance has its parallel in the rate of cell deposition, shown in Figure 6.17. Again the final values are present in the graph, this time in CLEs. *S.multivorum* in high NaCl, has a characteristic lull in the cell deposition for the first few minutes, before cell deposition starts to increase more quickly (see Figure 6.21). This was found in all three repeat experiments. In this case, this lull results in a higher overall cell deposition than the other two, at 13 C.L.E.s.

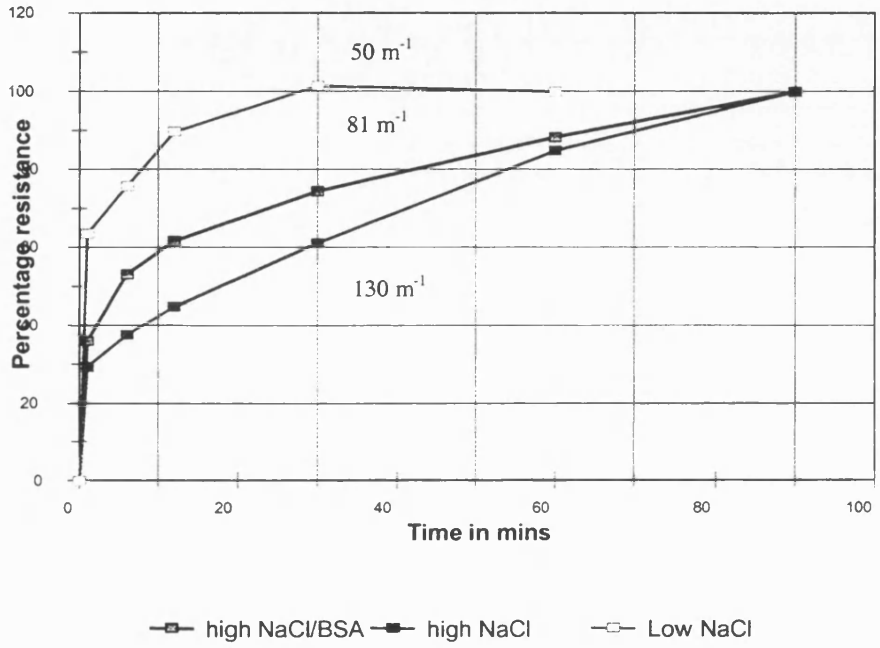

Figure 6.16: Rate of increase of resistance for three *S.multivorum* experiments

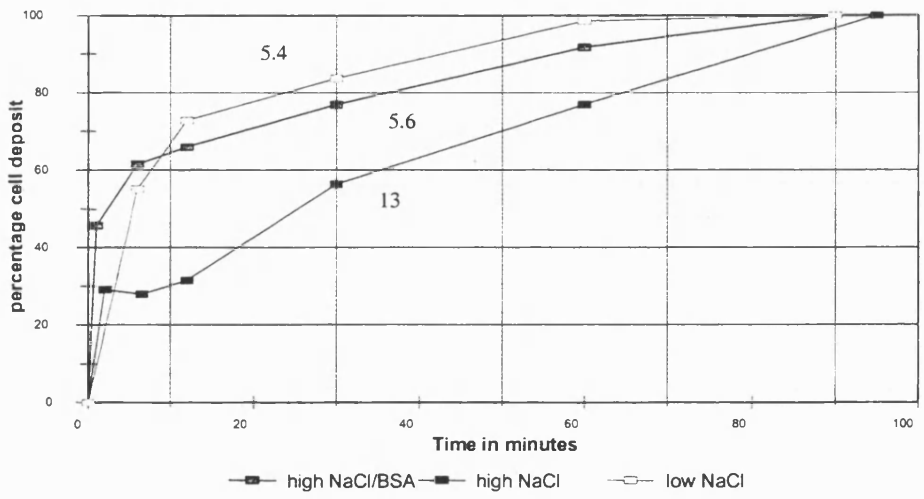

Figure 6.17 Rate of increase of cell deposition for three *S.multivorum* experiments.

6.4.6 Specific cake resistance

Specific cake resistance is often traditionally measured under dead end filtration conditions and taken to be constant. Foley (1994) showed how fouling factors in crossflow filtration complicate the specific cake resistance. Tanaka *et al* (1994,1996) demonstrated that estimation of specific cake resistance by using dead end filtration proved particularly inaccurate for rod-shaped cells. This was because the cell orientation is different in dead end filtration compared to crossflow filtration (see section 2.3.9).

In this thesis the specific cake resistance (SCR or α) is calculated from the cell deposition as follows.

$$\alpha = \frac{R_c}{\frac{C_d V_s M_c}{A}} \qquad \textbf{Equation 21}$$

Where :

C_d = cells per ml lost from retentate

V_S = total cell suspension volume

M_C = mass of 1 cell.

Rc =cake resistance ($R-R_m$).

A=area of membrane

This equation describes the overall specific cake resistance. Since the actual number of layers is not known, a resistance per layer cannot be calculated. However, clues to the relative magnitude of the resistance of layers laid down early and late in each run can be deduced from knowledge of the C.L.E values and the shape of each SCR graph.

There were three main trends observed in the graphs drawn for the specific cake resistance change over time.

- *Trend 1.* The specific cake resistance increased throughout the run.
- *Trend 2.* The specific cake resistance increased steadily during the first part of the run, reaching a plateau value for the second part.
- *Trend 3.* The specific cake resistance reached a peak early in the experiment, from 1-12 minutes, then it started to fall (sometimes to a plateau).

Three experimental graphs exhibiting these trends can be found in Figure 6.18 to Figure 6.20. The graphs for the other experiments can be found in appendix C.

Tables 6.8 to 6.10 summarise the trend exhibited and the final SCR value for each experiment.

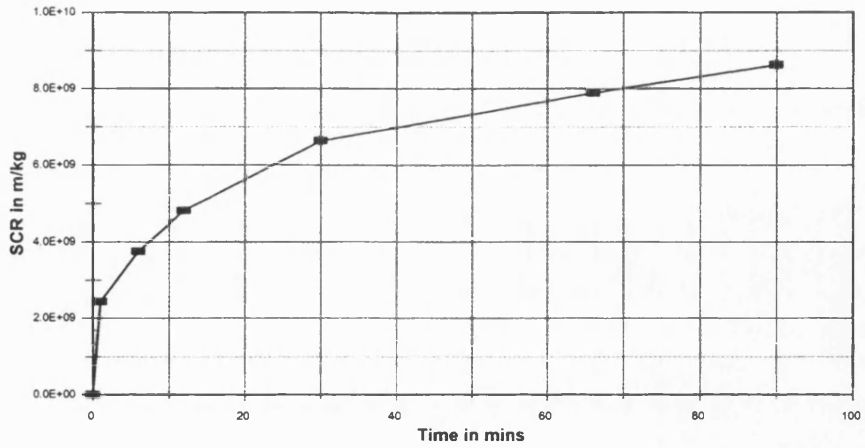

Figure 6.18: SCR trend 1- *P.elodea* in low $CaCl_2$

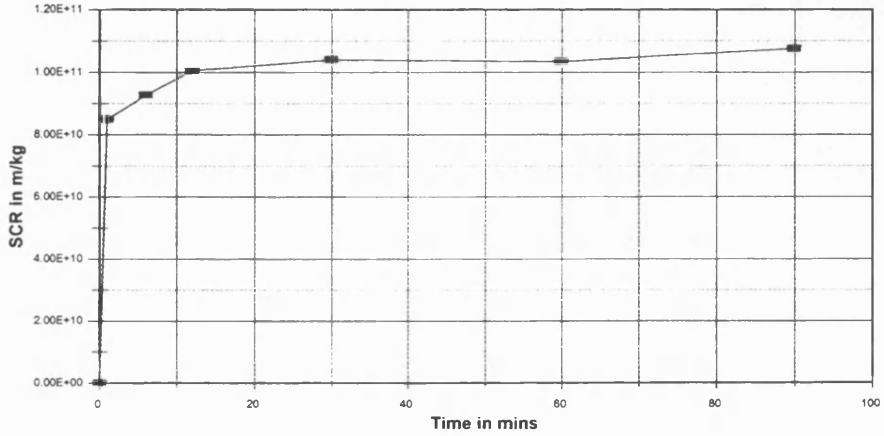

Figure 6.19: SCR trend 2- *S.multivorum* in high NaCl &BSA

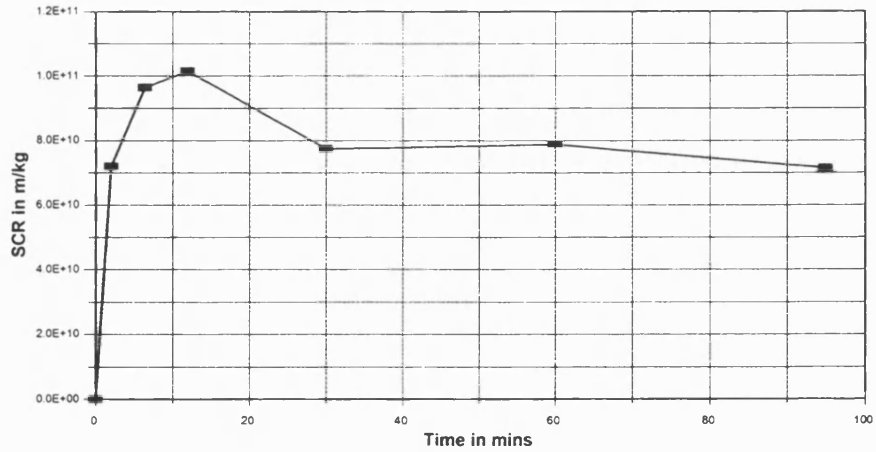

Figure 6.20: SCR trend 3-*S.multivorum* in High NaCl

6.4.6.1 Specific cake resistance values

6.4.6.1.1 *S.multivorum*

In the absence of BSA, the SCR-time relationship is trend 3. In the presence of BSA, the trend varies with ionic strength and valency. Table 6.8 summarises these results.

S. multivorum in:-	**Specific cake resistance**	**Solution only**	**With BSA**
Low NaCl	SCR graph shape	Increases to a max at 6 mins, then a fall to 12 mins, then plateaus	Increases to a max at 6 mins, then a fall to 30 mins, then plateaus
	Max/final SCR value (in mkg^{-1})	7.5/6.5	15/11
High NaCl	SCR graph shape	Increases to max 0-12 mins then decreases to 90 mins	Plateaus around 12 mins
	Max/final SCR value (in mkg^{-1})	10/7.2	11/11
Low $CaCl_2$	SCR graph shape	Max at 1 min, decreases 60-90	N/A
	Max/final SCR value (in mkg^{-1})	9.4/8	N/A
High $CaCl_2$	SCR graph shape	N/A	Wild fluctuation- max at 30-60 mins then a steep fall
	Max/final SCR value (in mkg^{-1})	N/A/2.3	48/19

Table 6.8: Specific cake resistance description for *S.multivorum* experiments

Apart from the high calcium suspension (which has a very high cell deposition value), the specific cake resistance for *S.multivorum* tends to be quite high, between $4.8x10^{10}$ and $15x10^{10}$ m/kg. This is due in part to the early flux decline for this bacterium, which in turn leads to a low CLE equivalent of 3 to 6 CLEs. The specific cake resistance for high NaCl is similar to the other *S.multivorum* experiments despite a higher cell deposition (13 C.L.E.) than for the other conditions.

The early peak in SCR for most of the experiments indicates that pore blocking makes a proportionately high contribution for the first part of the experiment. This emphasises the fact that the quoted SCR is not entirely due to cake resistance, since pore blocking makes a contribution. Therefore the SCR calculated is an apparent SCR, particularly for *S.multivorum*.

Pore blocking appears to make a significant contribution to the overall resistance in the high $CaCl_2$ suspension results; even though the total cell deposition is ten times higher than low $CaCl_2$, the apparent SCR is four times lower.

Comparison of high and low NaCl on the other hand reveals a different bias. Early on in the experiments the SCR peak is higher for high NaCl, even though the cell deposition is also higher. However, although the final high NaCl cell deposition is 2.6 times greater than that obtained in the low ionic strength solution, the final apparent SCRs are similar. Thus the relative contribution by the cells to the overall resistance is similar from the first to the final cell layer, indicating a true SCR.

The final specific cake resistances are similar for low NaCl and $CaCl_2$, the slightly higher figure for $CaCl_2$ can be accounted for by the higher ionic strength for this experiment.

The lower SCR for high $CaCl_2$ compared to high NaCl can be explained by the relatively low contribution of the high $CaCl_2$ cake to the overall resistance, as mentioned above.

The effect of BSA on the SCR seems to be to increase the SCR slightly. The final values for low and high NaCl are close (11.2×10^{10} & 10.7×10^{10} m/kg); although pore blocking is more dominant early in the experiment for low NaCl only.

6.4.6.1.2 *P.elodea*

In the absence of BSA, the SCR-time trends are mainly of type 1. The most noticeable result is the difference between low and high ionic strength solutions.

The two low ionic strength *P.elodea* suspensions have a very low SCR ($0.87x10^{10}$ m/kg for $CaCl_2$ and $1.4 x10^{10}$ m/kg for NaCl). This behaviour accords with a loose cake with many layers. The final SCRs for the high ionic strengths are significantly higher, at 4.1 and $25x10^{10}$ m/kg, in agreement with stronger intercellular bonds, leading to a tighter cake. Other effects are summarised in Table 6.9.

P.elodea in:-	**Specific cake resistance**	**Solution only**	**With BSA**
Low NaCl	SCR graph shape	Steep increase	Steep increase
	Max/final SCR value (in mkg^{-1})	1.4/1.4	9.8/9.8
High NaCl	SCR graph shape	Rapid increase to 6 mins, 6-30 slower, then a drop.	N/A
	Max/final SCR value (in mkg^{-1})	29/24	N/A
Low $CaCl_2$	SCR graph shape	Steep increase.	N/A
	Max/final SCR value (in mkg^{-1})	0.86/0.86	N/A
High $CaCl_2$	SCR graph shape	Steep increase	Steady increase, slow to 60 steeper to 90 mins
	Max/final SCR value (in mkg^{-1})	4.1/4.1	5.38/5.38

Table 6.9 Specific cake resistance description for *P.elodea* experiments

The presence of BSA in low NaCl suspensions appears to increase the SCR by a factor of 7. This is to be expected if the protein embeds itself in the extracellular matrix of gellan gum. Addition of BSA reduces the final CLE; from 24 to 8.1, therefore it shifts the equilibrium balance for cell deposition. For high $CaCl_2$ solution, the presence of BSA has only a small effect on both the SCR values and the CLE values.

6.4.6.1.3 *P.putida*

The suspensions of *P.putida* show no maximum; the trends were either of type 1 or type 2.

P.putida -	Specific cake resistance	Solution	With BSA
Low NaCl	SCR graph shape	Steady increase to 90 mins, 0-6 mins. steepest increase.	Plateaus around 30 mins
	Max/final SCR value (in mkg^{-1})	3.2	6.1
High NaCl	SCR graph shape	Steep increase	Steady increase to 90 mins. 0-1 steepest increase
	Max/final SCR value (in mkg^{-1})	2.3	4.7
Low CaCl	SCR graph shape	Steady increase to 90 mins-0-30 mins. steepest increase	N/A
	Max/final SCR value (in mkg^{-1})	4.32	N/A
High CaCl	SCR graph shape	Not known	Plateaus around 30 mins
	Max/final SCR value (in mkg^{-1})	0.97	0.95

Table 6.10 Specific cake resistance description for *P.putida* experiments

The SCRs for low and high NaCl are relatively close, at 3.15 $x10^{10}$ and $2.3x10^{10}$ m/kg respectively. The CLEs for these two runs are also very similar. On the other hand, the SCR value for high $CaCl_2$ is 4.5 times lower than that for low $CaCl_2$, although the cell deposition is 1.5 times higher. This is partly because high $CaCl_2$ encourages agglomeration, leading to a much higher cell deposition than all the other conditions. Agglomeration may also ensure that the SCR measured for high $CaCl_2$ is a true SCR without any contribution from pore blocking to increase the value disproportionately. The SCR for high $CaCl_2$ with and without BSA are very close, while addition of BSA to the two NaCl suspensions results in an approximate doubling in SCR, this effect is less than for *P.elodea.*

6.4.6.2 Specific cake resistance graph shapes

The typical SCR shape over the course of the *S.multivorum* experiments exhibits a distinctive peak early in the experiment, then a drop as the experiment continues. This suggests the dominance of pore blocking early on, with cake build-up contributing to different degrees as time goes on. The two exceptions for this are high Ca^{2+}/BSA, for

reasons explained earlier in section 6.4.4, and high NaCl & BSA, for which the SCR plateaus at around 12 minutes.

The *P.elodea* graphs exhibit a steep SCR increase. This suggests that most of the cells are deposited in the first 12-30 minutes, and do so randomly and loosely. It is only as the cake settles that the resistance increases. The cake may settle either by compression or by a rearrangement of cake, or a combination of the two. For a discussion of the nature of the cake change, see chapter 8.

The steady increase of the SCR for the *P.putida* suspensions is due in part to the fact that the cells are laid down gradually. It is also because some of the resistance is due to intermediate pore blocking, as demonstrated in chapter 7, where it is demonstrated that *P.putida* follows the intermediate blocking filtration law. The addition of BSA to High Ca^{2+} and low Na^{+} cell suspensions seems to result in a plateau. This is because later in the experiment, the cell deposition is directly proportional to the increase in resistance, i.e. the SCR is constant, so that the cake deposited cannot have been rearranged or compressed. For the same reason, there is also a plateau at the end of the two *S.multivorum* experiments suspended in low NaCl.

6.4.6.3 Compressibility

All the *S.multivorum* SCR results have a peak early on in the run, then the SCR value either decreases or plateaus. This equates with no compressibility of the cake. The same conclusions can be made for *P.putida* with BSA, in both high $CaCl_2$ and low NaCl, and for *P.elodea* in high NaCl.

All of the other SCRs for *P.elodea* have a steady increase right to the end. Since most *P.elodea* cells are deposited in the first 12-30 minutes of a run, this phenomenon suggests either cake compression, or reduction of porosity due to rearrangement of cells within the cake.

P.putida continues to deposit cells right until the end, but the SCR behaviour varies. Some cakes are incompressible, as mentioned above, but some cakes continue to increase their SCR up until the end. This may be because the layers laid down later in the run reduce the mean porosity. See section 2.3.9 for a further discussion of this phenomenon.

6.4.7 Repeat experiments

Some of the experiments were performed more than once to assess reproducibility. Others were performed more than once because the previous runs were unsatisfactory in some way. These latter type were not expected to give the same results as the successful experiments, but by noting the differences, some understanding of how the known variations in conditions affect the results may be derived.

6.4.7.1 S.multivorum

The three experiments for *S.multivorum* in high NaCl were successfully carried out using cells from the same batch. They display extremely high reproducibility. The results for all three experiments are detailed in Table 6.11.

High NaCl	**Main results**	**Repeat experiment 1**	**Repeat experiment 2**
Difference	N/A	Variable crossflow velocity at start	1 day older
Resistance (m^{-1} x10^{10})	130	132	132
C.L.E.	13	13	15
Final SCR(mkg^{-1})	7.2	7.8	6.4
Final flux (LMH)	15	15	14
% recovery	89	96	93

Table 6.11 Repeatability of *S.multivorum* in high NaCl suspension

All three runs exhibit a distinctive cell deposition pattern; a small cell deposition right at the beginning, a pause between 1 and 12 minutes, then the cell deposition increase resumes. (Figure 6.21).

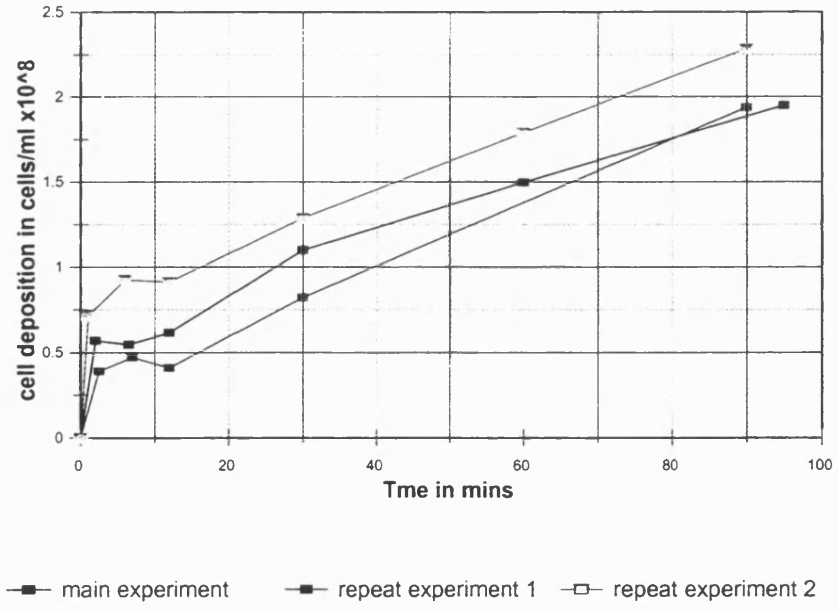

Figure 6.21 Cell deposition trends for three *S.multivorum* in high NaCl experiments

The final flux values are within 3.5% of each other, and the resistance increase rates are very similar in all three experiments, as seen in Figure 6.22. The slight difference in the final flux values can be accounted for by the small differences in TMP, reflected in the small variation in the resistance curves.

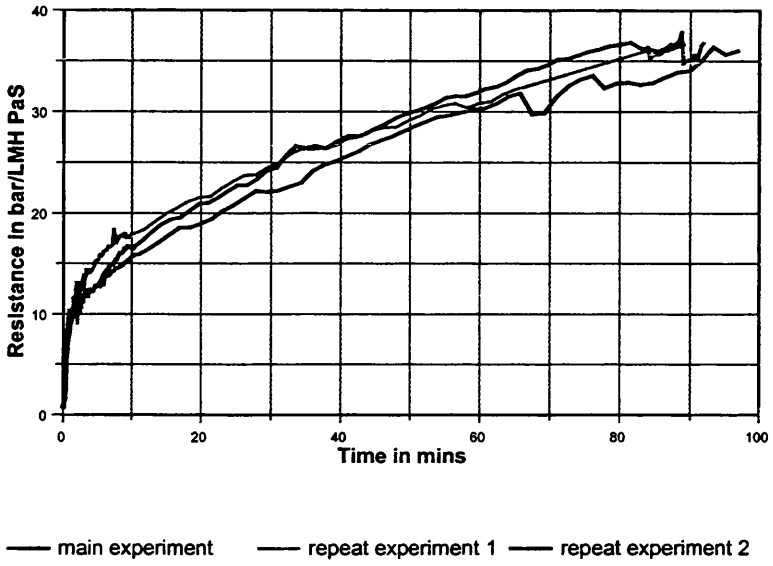

Figure 6.22 Comparison of resistance curves for three *S.multivorum* in High NaCl experiments

Figure 6.24 illustrates the tight clustering of the final flux/percentage recovery values for *S.multivorum* in high NaCl.

Low NaCl	**Main results**	**Repeat experiment 1**	**Repeat experiment 2**
Difference		Low crossflow velocity at start (for 2.5 mins)	Crossflow velocity and pressure low & fluctuating for first 20 mins
Resistance ($m^{-1}x10^{10}$)	50.	32	39
C.L.E.	5.4	5.7	7.5
Final SCR(mkg^{-1})	6.5	4.2	3.9
Final flux (LMH)	37	56	46
% recovery	100	96	97

Table 6.12 Repeatability of *S.multivorum* in low NaCl suspension

Figure 6.24 also shows that there is a broader spread in values for the three low NaCl results for *S.multivorum*, although the tendency for high final flux/high percentage recovery is clear for all 3. The reason for this variation lies in the low starting pressure, as detailed in Table 6.12. This will reduce the pore blocking phenomenon, and thus the decrease in flux is more gradual. The final resistances are thus reduced by 64% and 78% for experiments 1 and 2 respectively. In the case of experiment 2, the cell deposition is

also increased from 5.4 to 7.5 CLEs. This value strays away from the normal value of around 5 for *S.multivorum*, probably because the TMP is irregular and low for as much as the first 20 minutes of the experiment. It therefore can be deduced that cell deposition is dominated predominantly by the hydrodynamic rather than the physicochemical forces.

High NaCl & BSA	**Main results**	**Repeat experiment 1**	**Repeat experiment 2**
Difference		Old cells	Lower TMP (22-77 minutes only)
Resistance ($m^{-1}x10^{10}$)	81	159	61
C.L.E.	5.6	Not known	4.9
Final SCR(mkg^{-1})	11	Not known	9.4
Final flux (LMH)	22	12	29
% recovery	95	81	72

Table 6.13 Repeatability of *S.multivorum* in high NaCl with BSA suspension

Table 6.13 compares the main results for the successful high NaCl and BSA results with two others. The old cells in repeat experiment 1 yield a 96% increase in resistance, and a lower recovery than the successful experiment. Repeat experiment 2 has a resistance and flux within 25% of those of the main experiment (the error margin is 12%), while the cell deposition is only 12.5 % lower; just outside the normal error margin. Therefore, it seems that the lower TMP in the middle of the experiment (a mean of 6.3% lower) has reduced the cell deposition and thus the resistance slightly. However the results are still close, unlike the experiments previously described where it is the starting conditions that differ.

6.4.7.2 P.elodea

Low NaCl	**Main results**	**Repeat experiment 1**	**Repeat experiment 2**
Difference		Under-oxygenated cells	High starting pressure and low cell concentration
Resistance ($m^{-1}x10^{10}$)	59.3	110.3	30.24
C.L.E.	23.5	Not known	12.37
Final SCR(mkg^{-1})	1.4	Not known	1.35
Final flux (LMH)	30.57	17	53.6
% recovery	84.5	35.92	64.37

Table 6.14 Repeatability of *P.elodea* in low NaCl with BSA suspension

Table 6.14 contains the results for the experiments for *P.elodea* in low NaCl. Under-oxygenation of cells reduces the slimy gellan gum production (Fialho *et al*, 1991). This in turn means that the cake formed should be less diffuse than a cake containing significant amounts of gellan gum. Gellan gum can help cell aggregation while keeping the cells apart, especially at a low ionic strength, where ionic repulsion predominates.

This theory is in accordance with the results, where the resistance is increased by 86% when the cells are under-oxygenated. The flux recovery for repeat experiment 1 is the poorest of all the experiments; therefore it seems that the shortage of gellan gum encourages cell adhesion to the membrane, resulting in the unusual domination of irreversible fouling.

The high starting pressure in experiment 2 should result in a greater fouling and thus a higher C.L.E. Although the flux recovery is lower than that for the main results, the cell deposition and resistance are both halved. Therefore the higher resistance matters less than the fact that the initial cell concentration was only $5x10^8$ rather than the usual $7.5x10^8$ cells/ml. The fouling mechanisms for the main experiment and experiment 2 must be similar however, since the values for the specific cake resistance are very close.

High $CaCl_2$	**Main results**	**Repeat experiment 1**
Difference		Old cells
Resistance ($m^{-1}x10^{10}$)	77	124
C.L.E.	11	7.7
Final SCR(mkg^{-1})	4.1	3.4
Final flux (LMH)	24	14
% recovery	65	51

Table 6.15 Repeatability of *P.elodea* in high $CaCl_2$ with BSA suspension

A comparison of the results for experiment 1 with the main results (Table 6.15) indicates a tendency for old cells to increase the resistance and decrease the flux recovery. However, the values for the cell layer equivalents and specific cake resistance seem to be quite close, with a 29% and 16% decrease respectively for experiment 1.

6.4.7.3 P.putida

Three runs were successfully carried out for *P.putida* in 40 g/l NaCl under similar TMP conditions (Table 6.16).

High NaCl	**Main results**	**Repeat experiment 1**	**Repeat experiment 2**
Difference		Fouled membrane, same cell batch	Experiment lasts 240 mins
Resistance ($m^{-1}x10^{10}$)	82	120	158
C.L.E.	19	12	19
Final SCR(mkg^{-1})	0.64	1.5	0.99
Final flux (LMH)	22	15	11
% recovery	91	80	77

Table 6.16 Repeatability of *P.putida* in high NaCl with BSA suspension

The main results and experiment 1 were performed with the same batch of cells on consecutive days, but the repeat experiment 1 was with an imperfectly cleaned

membrane, since it had proved difficult to clean after the first run. Extra chemical cleaning and rinsing was performed before the second experiment. Nevertheless, as the experiment started, some white solid impurities were seen to flush out of the membrane module.

It can be seen from Figure 6.23 that the initial increase in resistance is identical for these two runs (see section 7.6 for a comparison of the models and resistance). Yet after 8 minutes the flux patterns start to diverge, with a higher final resistance for the dirty membrane (120 x 10^{10} instead of 82 x 10^{10} m^{-1}).

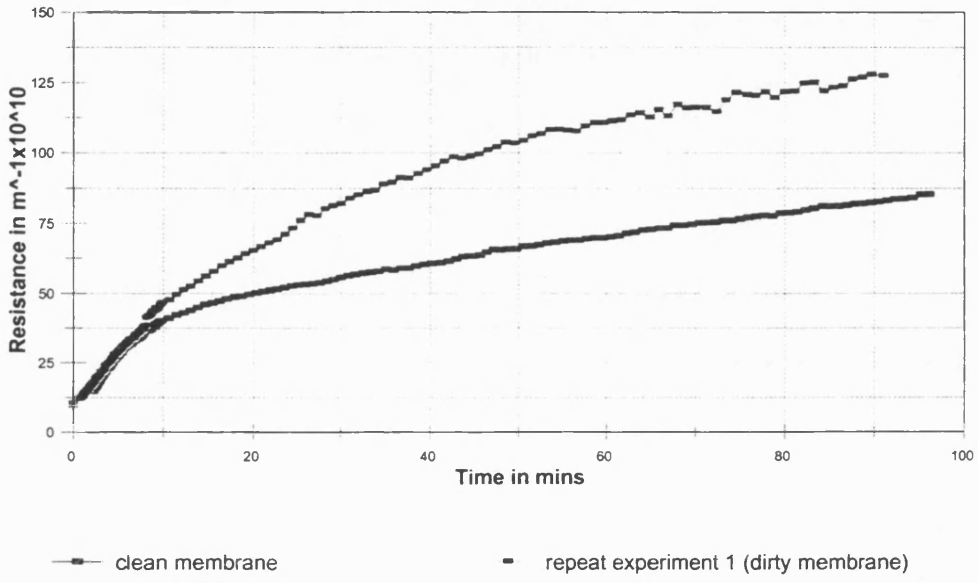

Figure 6.23: Reproducibility of resistance for *P.putida* in 40g/l NaCl

The final cell layer equivalent value is lower for the dirty membrane, 12 compared to 19 CLE. The cells were 1 day older for this experiment, but this is regarded as unlikely to affect the results significantly.

Repeat experiment 2 ran for 240 minutes, rather than the 90 minutes for all other experiments. The final flux at 240 minutes was slightly below that of the dirty membrane (12 compared to 15 LMH), but at 90 minutes the flux value for experiment 2 was in between the value of experiment 1 and the main experiment (18 compared to 22 LMH respectively).

The percentage recovery for experiment 2 was close to that of experiment 1 (77% compared to 81% for the dirty membrane and 91% for the clean membrane.) At 90 minutes, the cell layer equivalent value for experiment 2 was similar to the main experiment at around 19 C.L.E., and only 1 C.L.E. higher at 240 minutes.

At 240 minutes, the cell layer equivalent was only slightly higher. It therefore seems that there are two sorts of equilibrium, a physicochemical cake equilibrium, demonstrated by the cell layer equivalent values, and a hydrodynamic equilibrium, demonstrated by the final flux value. The lower rate of fouling may be because of the greater age of the cells.

It can be seen by the figures in Table 6.17 that the combined effect of a high starting crossflow velocity/low transmembrane pressure results in a decrease in resistance of 30% and greatly reduced reversible fouling. It is likely that it is the low TMP that is responsible for the former, and the age of the cells that is responsible for the latter.

Low NaCl & BSA	**Main results**	**Repeat experiment 1**
Difference		High starting crossflow velocity and old cells
Resistance (m^{-1} x10^{10})	166	116
C.L.E.	16	16
Final SCR(mkg^{-1})	6	4
Final flux (LMH)	11	16
% recovery	96	58

Table 6.17 Repeatability of *P.putida* in low NaCl with BSA suspension

The old cells for all species seem to be more of a challenge to remove from the membrane, regardless of the ionic conditions, perhaps because they are more leaky. Despite the change in pressure conditions, the cell layer equivalent of repeat experiment 1 is the same as the main results at 16 C.L.E. The fact that these values are comparable, while the resistance figures are so different, concurs with the concept of a hydrodynamic and a physicochemical equilibrium.

6.4.8 Relationship between irreversible fouling and final flux

If the contribution of irreversible fouling to the overall resistance were high, the relationship between final flux and either reversible fouling or irreversible fouling would be linear. Figure 6.24 to Figure 6.26 depict the relationship between final flux and percentage flux recovery with respect to clean water flux. This percentage recovery is equivalent to the proportion of flux decline due to reversible fouling. The method used to determine percentage recovery is described in section 4.4.3.

Although none of the relationships are directly proportional, there are nevertheless discernible patterns to be found; for example, the best flux recoveries are for the low ionic strength solutions for all three bacteria.

6.4.8.1 S.multivorum

S.multivorum in:-		Solution only	With BSA
Low NaCl	**% recovery**	100%	97%
	Final flux (LMH)	37	22
High NaCl	**% recovery**	89%	72%
	Final flux (LMH)	15	22
Low CaCl	**Recovery**	96%	N/A
	Final flux (LMH)	35	N/A
High CaCl	**% recovery**	91%	92%
	Final flux (LMH)	17	23

Table 6.18 Comparison of final flux figures and percentage recovery for *S.multivorum*

It can be seen from Table 6.18 that *S.multivorum* shows a high percentage flux recovery (i.e. high reversible fouling) for all conditions.

Figure 6.24 illustrates the clustering of *S.multivorum* in relation to the suspension conditions: For low ionic strength solutions for both NaCl and $CaCl_2$, the percentage recovery is high (96-100%) and the final flux is high (35-37 LMH). The percentage recovery is slightly lower for both high ionic strength suspensions (89-91%), and the final fluxes are significantly lower (15-17 LMH).

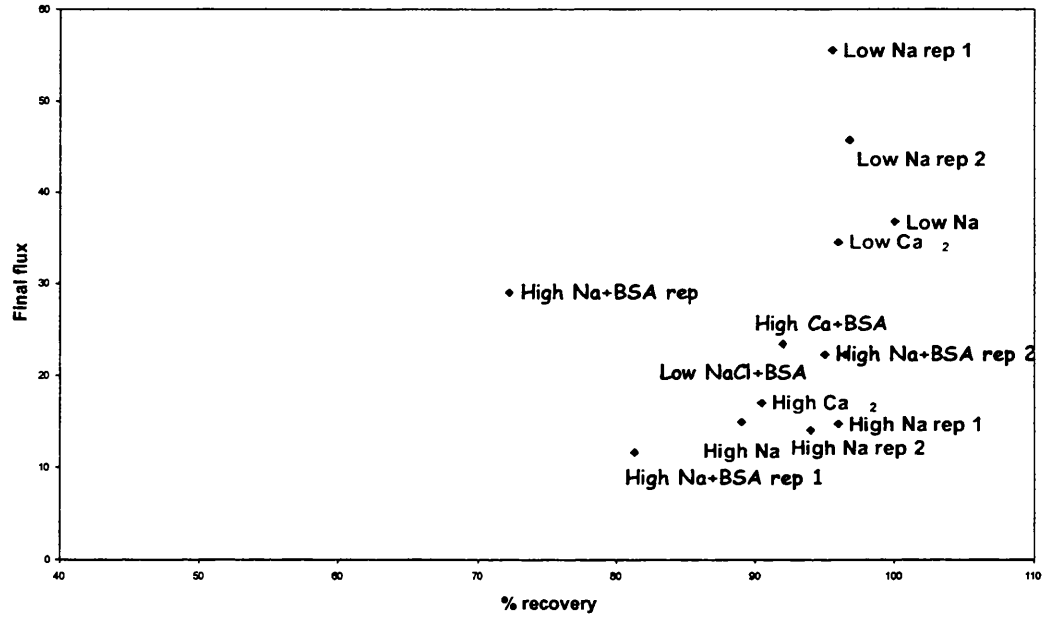

Figure 6.24: *S.multivorum*: Final flux versus % recovery

All the suspensions containing protein occupy a flux band between the high and low ionic strength suspensions, including the broth filtration, which is closest to the High NaCl & BSA point. These results can be explained by the fact that a significant proportion of the fouling is due to pore blocking. For the low ionic strength suspensions, both the cells and the membrane are very negatively charged. (see sections 3.5.1 and

4.1.2). With few positive ions present in the solution to modify the repulsion between the two, the cells are less likely to block the pores. On the other hand, with high ionic suspensions, there are plenty of positive ions to encourage Van der Waals/electrostatic bonding between the cells and the membrane pores, so the final fluxes are lower.

When protein is present, the blocking of the pores may be less absolute, since bonding of the proteins to either the cells or the membrane could result in an incomplete seal between the pores and membrane. The greater importance of pore blocking for *S.multivorum* may also account for the relatively high percentage recovery average for *S.multivorum* compared with the other two; pore blocking may rely entirely upon the pressure applied across the membrane; when that is released, the cells may be flushed from the surface. In fact at the end of some *S.multivorum* experiments, there was a visible rush of cells when the pump was turned on, and the flux recovered to within 10% of the clean water flux during the first rinse. This did not occur with either of the other cells.

6.4.8.2 P.elodea

P.elodea in:-		**Solution only**	**With BSA**
Low NaCl	**% recovery**	85%	74%
	Final flux (LMH)	31	13
High NaCl	**% recovery**	48%	N/A
	Final flux (LMH)	12	N/A
Low CaCl	**Recovery**	91%	N/A
	Final flux (LMH)	49	N/A
High CaCl	**% recovery**	65%	78%
	Final flux (LMH)	24	19

Table 6.19 Comparison of final flux figures and percentage recovery for *P.elodea*

These results for *P.elodea* agree with the theory stated in section 6.3, i.e. reversible fouling and flux decreases at high ionic strengths. The highest fluxes and flux recoveries are for the low ionic strengths, followed by the two protein experiments. The lowest recoveries are for the high ionic strength suspensions. As in the initial broth experiments, the lowest recoveries tend to be for this bacterium. High fluxes tend to equate to high recoveries, but this trend is finite, and below approximately 24 LMH, recovery is low (less than 60%) but not directly linked to the flux. Figure 6.25 contains a polynomial trendline, to help to illustrate this pattern.

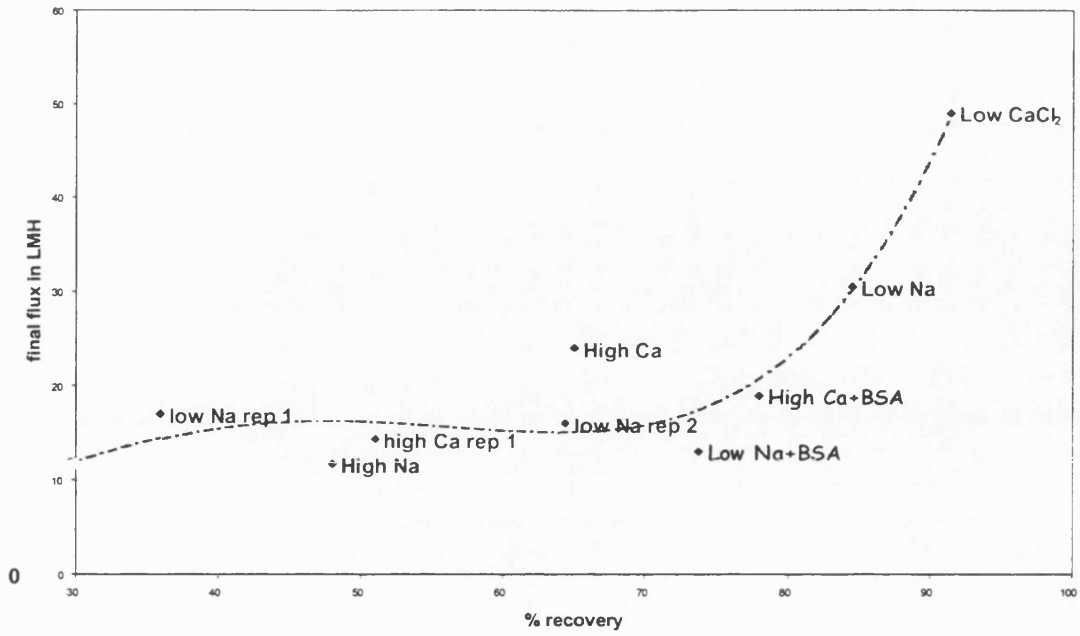

Figure 6.25: *P.elodea*: Final flux versus % recovery

6.4.8.3 P.putida

P.putida in:-		Solution only	With BSA
Low NaCl	**% recovery**	94%	96%
	Final flux (LMH)	16	11
High NaCl	**% recovery**	80%	89%
	Final flux (LMH)	18	11
Low $CaCl_2$	**Recovery**	95%	N/A
	Final flux (LMH)	13	N/A
High $CaCl_2$	**% recovery**	54%	90%
	Final flux (LMH)	31	43

Table 6.20 Comparison of final flux figures and percentage recovery for *P.putida*

The *P.putida* results also exhibit high reversible fouling (80-95%). The exception was high $CaCl_2$ at 54% recovery. Even when the percentage recovery was high, *P.putida* proved the most difficult to clean chemically back to 100% clean water flux, especially at high ionic strengths or if BSA is present. It is more difficult to discern an overall pattern between final flux and percentage recovery for *P.putida,* although the following points are clear.

- The presence of BSA tends to increase the flux recovery. Addition of BSA to a low sodium solution results in a reduction in percentage recovery, with little change in final flux. Addition of BSA to high ionic strengths, on the other hand, results in higher percentage recovery
- High calcium concentrations increase the final flux, over all the other results.

- Low ionic strengths result in low final flux and high percentage recovery

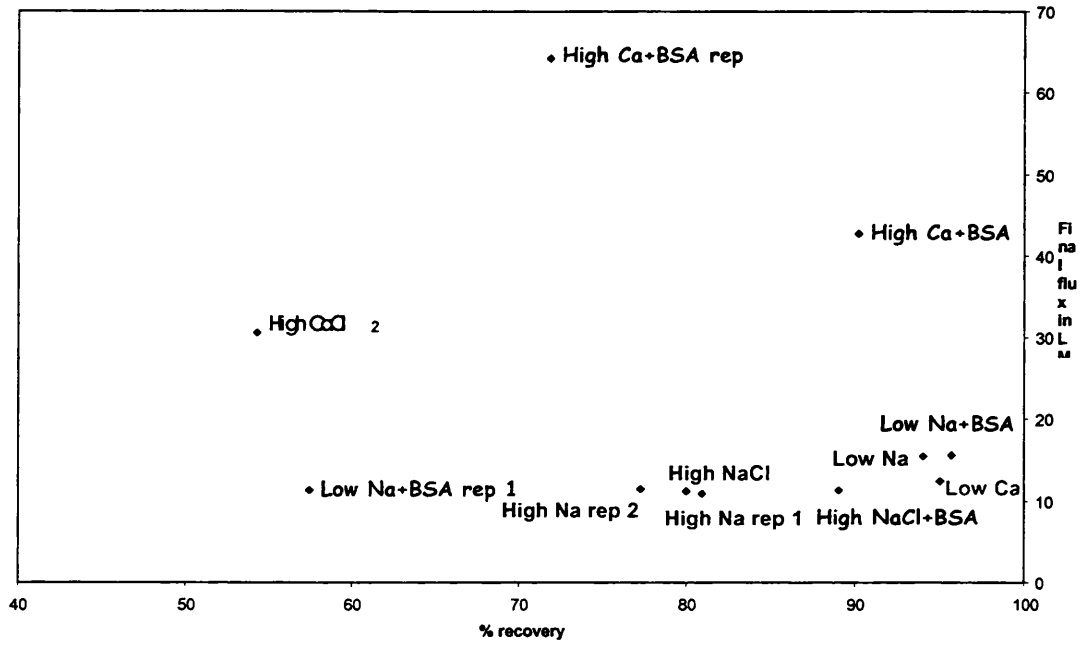

Figure 6.26: *P.putida*: Final flux versus % recovery

6.4.8.4 Effect of bacterial age on flux recovery

As well as the experiments where the parameters were properly controlled, those experiments where some of the parameters were imperfect have also been marked on Figure 6.24 to Figure 6.26.

For both *P.putida* and *P.elodea*, there are experiments in low NaCl where the final flux and the percentage recovery are both lower than for the successful experiments. This is probably due to the increased age of the cells, since both these experiments were performed when the cells were 2 to 3 days older than the rest. *P.putida* suspended in NaCl + BSA suspension has a similar final flux, but the percentage recovery for the old cells is much lower.

For *S.multivorum* in low NaCl, older cells seem to have a higher final flux, although the percentage recovery remains high.

6.4.9 Protein transmission

For the experiments involving protein, BSA levels in the retentate and permeate were measured for all experiments containing BSA at 1, 30 and 90 minutes, with couple of experiments (*S.multivorum* in low NaCl and High $CaCl_2$) having extra points measured. See section 2.7 for a further discussion on protein fouling and section 4.5.2 for a description of the method.

It was hoped that this method would yield not only the transmission patterns, but also the total weight out of the target quantity of 1 g/l w/v of BSA in suspension to be deposited in the cake and on the membrane walls. However, this method of protein measurement did not prove to be very accurate. A repeat measurement on the same sample might reveal a difference of 8-20% in the absolute value, although the relative values within one set of measurements only varied by up to 4%. Thus the values in Table 6.21 to Table 6.28 are presented as percentages, to avoid having to take the former larger error into account. The first four of these tables contain protein loss information for all the experiments, while the latter three summarise the protein rejection behaviour (i.e. reduction in transmission) of all the experimental conditions.

Control solution with BSA	**Final protein loss**
Low Na^+	14.1%
High Na^+	1%
High Ca^{2+}	4.1%

Table 6.21: Protein lost during control experiment

S.multivorum	**Protein loss at 1 min.**	**Protein loss at 30 mins.**	**Final protein loss.**
Low Na^+	0%	8%	7%
High Na^+	Not known	1.4%	12%
High Ca^{2+}	2%	8%	9%

Table 6.22 Protein lost during *S.multivorum* experiments

P.elodea in:-	**Protein loss at 1 min.**	**Protein loss at 30 mins.**	**Final protein loss.**
Low Na^+	0.6%	3%	2.5%
High Na^+	Not known	Not known	Not known
High Ca^{2+}	2.7%	6.2 %	13%

Table 6.23 Protein lost during *P.elodea* experiments

P.putida in:-	**Protein loss at 1 min.**	**Protein loss at 30 mins.**	**Final protein loss.**
Low Na^+	2%	13.5%	12%
High Na^+	6.5%	4.5%	6.6%
High Ca^{2+}	3%	3%	8.8%

Table 6.24 Protein lost during *P.putida* experiments

It is a commonly accepted phenomenon that cells act as an ultrafiltration membrane for protein molecules, and thus there are two filtration mechanisms coming to equilibrium when protein is present in a cell suspension: -

a) Protein deposition

b) Cell deposition

Protein deposition is important for both transmission/rejection and protein loss in an experiment. As expected, there is a dramatic increase in the rejection levels in the first minute for all the experiments; this must be due to adsorption of a single layer of

protein onto the membrane, as the drop is independent of cell deposition volume. This adsorption is known as conditioning when it on the membrane surface, and standard blocking when inside the pores. This adsorption is responsible for a significant proportion- a minimum of 15%- of the overall protein loss, with the exception of *S.multivorum* in low NaCl/BSA which does not display a detectable protein loss at all in the first minute.

After adsorption of a monolayer of proteins, the kinetics change and rejection may decrease once more. Protein aggregation at higher ionic strengths means that standard blocking inside the pores cannot occur. The aggregates may either block the entrance to the pores or become involved in cake build up on the membrane surface. The rapid deposition of cells on the membrane surface means that pore blocking due to both protein and cells will only be noticeable at the beginning, and will not increase later on in the experiment. Build up of cake involving both cells and protein will occur, leading to greater protein loss, until both systems come to equilibrium. At equilibrium, both the protein loss and the transmission will be constant. If all available deposition sites for BSA are occupied, both on the cake surface and inside the pores, rejection may be close to zero.

However there is no direct correlation between the final cell deposition volume and the total protein loss for any of these experiments.

In this set of experiments, the retentate protein loss usually increases steadily throughout the run, while the pattern for rejection is more variable. While it is common for rejection to be reasonably constant after the first minute, it may also rise or fall on some occasions, for the reasons outlined above.

Control solution with BSA	**Final protein rejection**
Low Na^+	5.8%
High Na^+	0.7%
High Ca^{2+}	1.25%

Table 6.25 Protein rejection for control experiments

S.multivorum	**Protein rejection at 1 min.**	**Protein rejection at 30 mins.**	**Final protein rejection.**
Low Na^+	21%	18%	20%
High Na^+	Not known	14%	0.6%
High Ca^{2+}	13%	11%	12%

Table 6.26 Protein rejection during *S.multivorum* experiments

P.elodea in:-	**Protein rejection at 1 min.**	**Protein rejection at 30 mins.**	**Final protein rejection.**
Low Na^+	11%	12.5%	15.5%
High Na^+	Not known	Not known	Not known
High Ca^{2+}	7%	5.2%	0.3%

Table 6.27 Protein rejection during *P.elodea* experiments

P.putida in:-	**Protein rejection at 1 min.**	**Protein rejection at 30 mins.**	**Final protein rejection.**
Low Na^+	4%	14.5%	31%
High Na^+	12%	11.5%	13.5%
High Ca^{2+}	0.6%	0.1%	0.1%

Table 6.28 Protein rejection during *P.putida* experiments

6.4.9.1 Low NaCl

All three bacteria experiments in low NaCl follow a similar protein loss pattern; they have a significant loss from 1 to 30 minutes, but a minimal change from 30 to 90 minutes. The experiments in low NaCl prove that the relationship between cell deposition and protein loss is not directly proportional; the final protein losses for all three bacteria are significantly higher for low NaCl than for the other solutions (Table 6.22 to Table 6.24), while the cell deposition levels are similar. The control experiments also reveal low NaCl as the medium with the highest protein loss (see Table 6.21). This loss of protein did not result in a fall in flux during the control (section 6.4.1.1). Therefore this fouling is likely to be an internal pore blocking mechanism. See figure 2.4 and section 2.2 for further descriptions of this phenomenon. This may be an indication that the amount of single, unagglomerated BSA able to adsorb/ deposit inside the pores is much greater than the amount of agglomerated protein able to settle as cake on top of the membrane. This is quite possible due to the disparity of the relative surface areas.

The loss of protein from the retentate is independent of the cell deposition only at the start of the runs. The loss seems to occur in three distinct phases for *S.multivorum* in low NaCl (Figure 6.27). Although protein rejection is at a maximum in the first couple of minutes, the retentate protein concentration is unaffected. The steepest decrease for the retentate protein loss is at 6-12 minutes, after which the protein levels do not change significantly. The protein rejection on the other hand does not change between 1 and 6 minutes but decreases slightly from 6-12 minutes, after which any change is within the 4% variation due to the method of measurement. This is despite the fact that 29% of the total cell deposition occurs within the last hour. The apparent specific cake resistance peaks at 6 minutes, then decreases until 30 minutes, but then does not change after 30 minutes for this experiment. This can be explained by the early dominance of pore blocking, while cake filtration is the dominant type of fouling later in the experiment. The protein loss/rejection behaviour may be partly explained by this change in fouling behaviour.

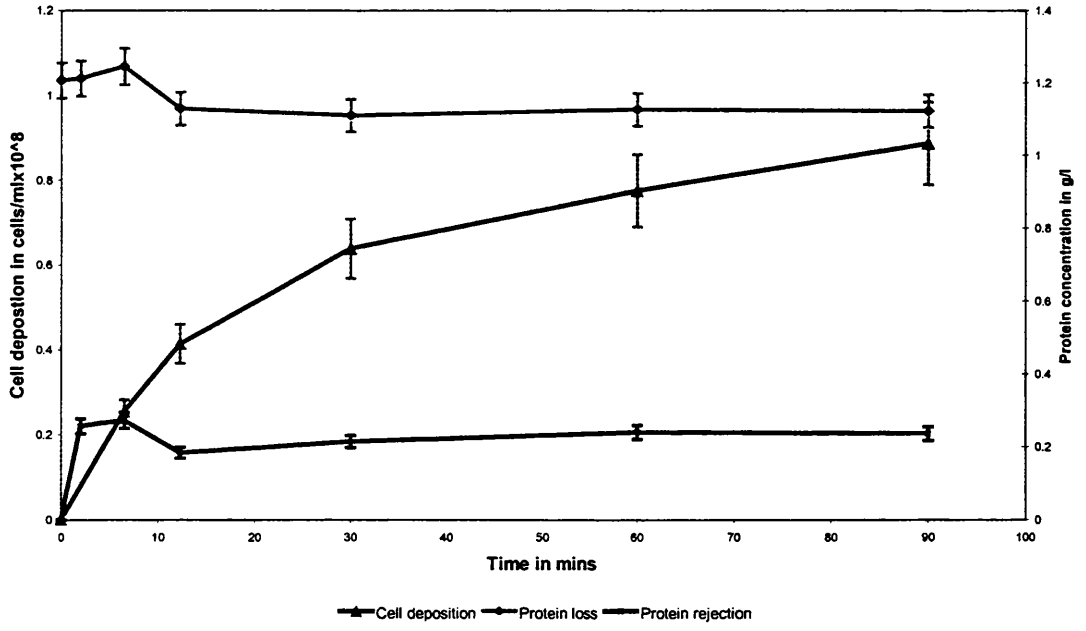

Figure 6.27 Protein deposition for *S.multivorum* in low NaCl

For *P.elodea* (Figure 6.28), the relationship between cell deposition and protein loss seems to be much more direct, especially for the protein rejection. Protein loss is greatest between 1 and 30 minutes, when the cell deposition is greatest, after which the retentate protein, like the cell concentration, remains stable. Protein rejection increases the most in the first minute, to 11%. It increases only slightly thereafter to a final value of 15%: the lowest rejection value of all 3 bacteria in low NaCl. This is not surprising, since the cake formed by *P.elodea* in NaCl appears from the resistance results to have a

diffuse, open structure. Therefore, the secondary membrane formed by this cake should not inhibit protein transmission.

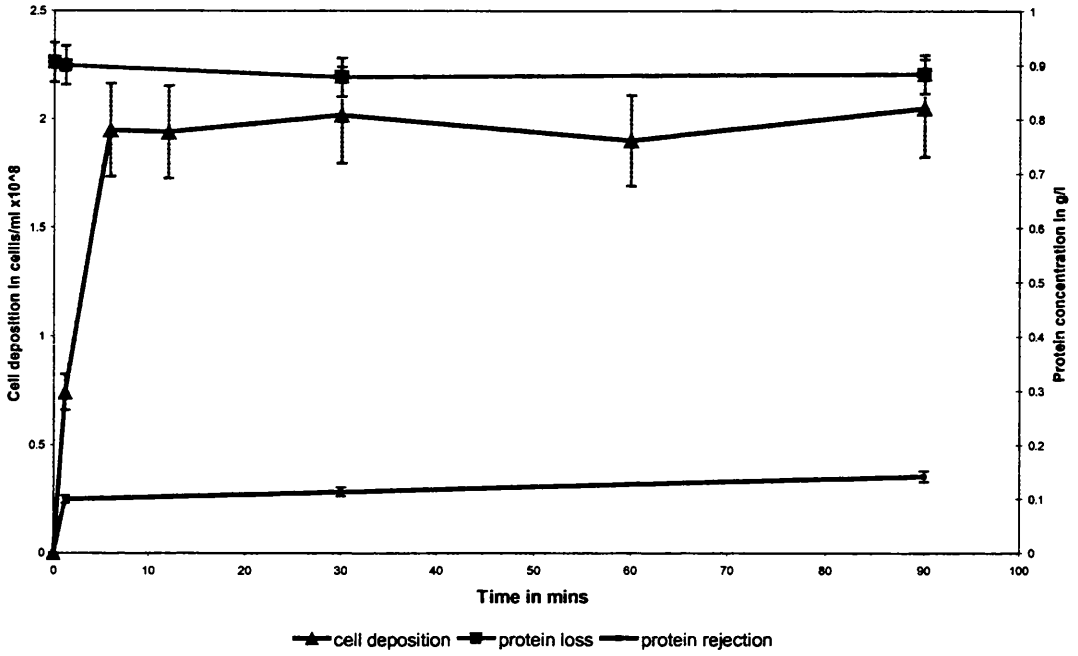

Figure 6.28 Protein deposition for *P.elodea* in low NaCl

From Table 6.22 to Table 6.24, It can be seen from that for low NaCl suspensions, the overall protein losses are the greatest for *P.putida* at a final value of 12%. The rejection is also the highest of all the experiments, at a final value of 31%. Hodgson *et al* (1993) found that enmeshment of proteins in the extracellular matrix affected protein transmission significantly. The surface of *P.putida* is covered in long thin flagella, so the probability of protein enmeshment is greatest for this species.

The pattern for retentate protein loss for *P.putida* is similar to that for *P.elodea*, with the greatest loss between 1 and 30 minutes, after which the protein concentration stabilises. However, this time the cell deposition continues to increase until the end of the run, as indeed does the rejection. Thus the protein deposition continues well into the experiment, while the cells are forming a secondary membrane to increase protein rejection as the experiment progresses. At 30 minutes, the cell deposition has reached 72% of its final amount, while the protein loss is complete and the rejection is only 47% of its final value. This figure and the others not shown in the main text but can be seen in appendix E.

6.4.9.2 High NaCl

The trends for protein loss for high NaCl again do not have a direct correlation with the cell deposition for either *S.multivorum* or *P.putida.* Table 6.22 reveals that the majority of the protein loss (88%) occurs between 30 and 90 minutes. At the same time, only 21% of the total cell deposition is laid down. On the other hand, protein rejection is at a maximum at 30 minutes, becoming negligible by the end of the 90 minutes. Therefore the protein deposition is at equilibrium before the end of the experiment. The maximum at 30 minutes may well be affected by a 6% fluctuation of the transmembrane pressure at the time that the 30 minute sample was taken.

The protein loss at 30 minutes for *P.putida* also changes noticeably in the middle of the run, with the values for 1 and 90 minutes for retentate both at around 6.5%, while it is only 4.5% at 30 minutes. A slight drop in rejection also occurs contemporaneously, but this is within the 8% error margin for protein rejection. Again the TMP changes around the time of this reading; having drifted to 7% above the average, the pressure was corrected manually around this time. See appendix C for these TMP plots.

6.4.9.3 High $CaCl_2$

As seen in Figure 6.29, the protein rejection for *S.multivorum* in high $CaCl_2$ fluctuates, with the variation in values mirroring the cell deposition fluctuation. The protein loss however is less dramatically affected by the fluctuations, but seems to have distinct phases of behaviour throughout the run, some of them converse to the cell deposition. The first minute involves: -

- a small drop in the protein levels
- followed by a plateau until 6 minutes,
- followed by a further drop until 30 minutes
- then a constant protein concentration until the end of the run

These phenomena may be explained by an observation of Le *et al* (1994). They noticed that in the presence of cells or cell debris, transmission was proportional to the crossflow velocity raised to the power of 0.18. As cell agglomeration is noticeable in this experiment, the effective hydraulic diameter of the shear equation (equation 19) is reduced and thus the crossflow velocity is increased. With a fluctuation in cake deposit, both the protein loss and protein rejection are affected.

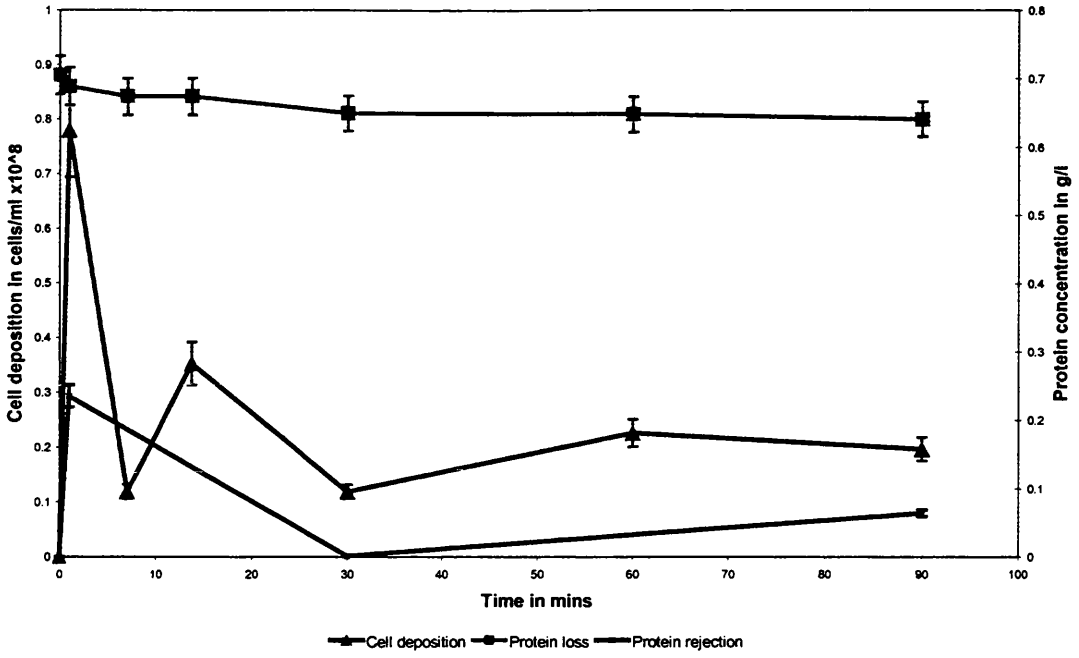

Figure 6.29 Protein deposition for *S.multivorum* in high $CaCl_2$

The effect of $CaCl_2$ on protein and *P.elodea* systems also results in a variation in cell deposition, but this time the fluctuation is less. The protein filtration system seems to come to equilibrium nevertheless, with the final protein rejection at only 0.3%, despite a value of 7% at 1 minute. On the other hand, protein loss rises constantly to a final value of 13%. This is the highest protein loss found for the three *P.elodea* experiments, due to a cake from very tight agglomerates.

For *P.putida* in high $CaCl_2$, the protein rejection is very low throughout the experiment, while the protein loss does not change from 1-30 minutes, but increases dramatically from 30 to 90 minutes, from 3 to 8.8 %. This may be due to cake compressibility, since the cell deposition is quite low during the last hour of the experiment, but the SCR increases exponentially.

6.4.10 Conclusions

Each of the bacteria was affected by ionic strength and by protein presence in different ways. The fouling mechanisms, rate of fouling and cell deposition patterns were unique to each bacteria, and could be explained in terms of how the extracellular matrices affected the influence of hydrodynamic and physicochemical effects on fouling for each. A summary of the main experimental findings can be found in Table 6.29 and Table 6.30

	S.multivorum	*P.elodea*	*P.putida*
Effect of ionic strength increase on resistance	Increase in resistance due to more cell deposition	Increase in resistance due to a tighter cake	Decrease in resistance due to more random aggregates
Effect of valency increase on resistance	Greater resistance for high NaCl than high CaCl2 Resistance for low ionic strengths similar valency and ionic strength difference has no effect.	Greater resistance for high NaCl than high CaCl2 Resistance for low NaCl greater-follows valency not ionic strength trend.	Greater resistance for high NaCl than high CaCl2 Resistance for low CaCl2 greater-contradicts other ionic/valency trends
Effect of protein addition on resistance	All three experiments with BSA have a similar resistance (increase for low NaCl, decrease for high ionic strength)	Resistance increases	Both NaCl experiments increase to similar resistances For high CaCl2, resistance decreases
Effect of ionic strength increase on cell deposition	Increase in cell deposition for both salts	Decrease in cell deposition, particularly for NaCl	Increase in cell deposition for CaCl2 only. NaCl stays the same.
Effect of valency increase on cell deposition	Slight decrease for low CaCl2 Increase for high CaCl2	Similar values for low ionic strengths High CaCl2 higher than high NaCl	Similar values for low ionic strengths High CaCl2 higher than high NaCl
Effect of protein addition on cell deposition	No change for low NaCl. Decrease to same value as low NaCl for high NaCl. Decrease to same value as low CaCl2 for high CaCl2	Decrease for low NaCl Values similar for high CaCl2	Slight decrease for both NaCl experiments Decrease to same value as other experiments for high CaCl2.
Effect of ionic strength increase on SCR	SCR similar for the NaCl suspensions Decrease for CaCl2	Increase in SCR for both types of salt, particularly NaCl	Decrease in SCR for both types of salt, particularly CaCl2.
Effect of valency increase on SCR	Slight increase for low ionic strengths Decrease for high ionic strengths	Slight decrease for low ionic strengths Sixfold decrease in high ionic strengths	Slight increase for low ionic strengths Decrease for high ionic strengths
Effect of protein addition on SCR	Increase to same value for both NaCl experiments Increase to slightly higher value for high CaCl2.	Sevenfold increase for low NaCl 30% increase for high CaCl2	Approximate doubling of SCR for both NaCl experiments For High CaCl2, SCR remains the same.

Table 6.29 Effect of changing conditions on the main parameters measured.

	S.multivorum	*P.elodea*	*P.putida*
Compressibility	No compressibility for any of the cakes.	All cakes compressible	Low NaCl/BSA and high CaCl2/BSA have incompressible cakes. Other cakes unconfirmed.
Cleanability	Easy to clean	Medium	Hard to clean, especially after high ionic strength and/or protein experiments.
Final flux versus reversible fouling	Low ionic strength suspensions highest for both parameters. All suspensions with protein in the middle, high ionic strengths are the lowest. All reversible fouling very high, i.e. membrane fouling least significant.	Order of reversible fouling same as *S.multivorum*, but CaCl2 always has the higher value. Correlation between parameters follows an approximate polynomial trend, with only small changes in flux, but reversible fouling values spread out, i.e. membrane fouling most significant.	No correlation between the two parameters. High CaCl2 has by far the highest fluxes, with and without protein. Low ionic strengths have low final fluxes and high recovery. All reversible fouling quite high, therefore membrane fouling can be noticeable.
Factors affecting fouling rate	Difficult to determine- all fouling rates are rapid	Increase in ionic strength increases fouling rate Increase in valency decreases fouling rate Addition of protein increases fouling rate	Increase in ionic strength increases fouling rate Increase in valency decreases fouling rate Addition of protein increases fouling rate

Table 6.30 Main trends for the three bacteria

7 Fouling Mechanisms

7.1 Introduction

This chapter takes the basic data (in particular the flux data) collected for analysis of experimental data and applies it to some theoretical models to help to understand the relative importance of the following fouling mechanisms throughout each experiment:-

1) Complete pore blocking

2) Intermediate/incomplete pore blocking

3) Cake filtration

Understanding the difference in these modelling results helps to interpret the experimental results, particularly with respect to the differences between the fouling behaviour of each bacterial species.

7.2 Background to models

Hermia (1982) described the different types of fouling on a membrane in dead end filtration mode by a set of equations. An increase in resistance could be due to one or more of the three main mechanisms described in section 2.2.7. The reduction in flux could be due to complete pore blocking; the fluid flow in the direction of the membrane has a tendency to bring particles to the pore entrances, which may block them completely (see Figure 7.1). On the other hand, the increase in resistance might be due to the more tortuous route fluid must take to pass through a cake of particles building up on the surface (Figure 7.4). Alternatively, the rise in value may also be due to a combination of the two mechanisms (Figure 7.3). Finally the fouling mechanism may be that of intermediate/incomplete pore blocking, where each particle presented at the membrane may either block a pore or contribute to localised cake formation around a pore Figure 7.2). Hermia (1982) derived a generic equation for all three fouling mechanisms:

$$\frac{\partial^2 t}{\partial V^2} = k_H \left(\frac{\partial t}{\partial V} \right)^n \qquad \textbf{Equation 22}$$

Where:

V = Permeate volume

t = Time

k_H = Constant

The constant n depends on the mechanism involved, where n=0 equates to a cake filtration mechanism, n=1 indicates an intermediate mechanism, and n=2 demonstrates that complete pore blocking is attenuating the flux. The units of k_H depend upon n.

Field *et al* (1995) modified Hermia's equations to allow for crossflow filtration effects. It should be noted that the generic equations of both Hermia (1982) and Field (1995) assume constant pressure filtration.

The generic equation then becomes

$$-\left.\frac{\partial J}{\partial t}\right|_{\Delta P} = k_n (J - J^*) J^{2-n} \qquad \textbf{Equation 23}$$

Where:

J = Flux
J* = Flux at final equilibrium
k_n=filtration constant for modified equation

This modified generic equation is used in all of the following model approaches. The dimensions of constant k again depend on the mechanism involved, as shown in Table 7.1. The values of k all differ from those of Hermia, because Field (1995) chose to use flux rather than volume of permeate collected.

Mechanism	**kn(Field *et al.*)**	**n**
Cake filtration	$\alpha kc/(J_0R_0)=G$	0
Intermediate	1	1
Complete blocking	$-\sigma J_0/\varepsilon_0$	2

Table 7.1 Summary of values for modified cake blocking mechanisms

Where:

α = Specific resistance of cake (m kg^{-1})
k_c = cake filtration constant (kg m^{-3})
J_0 = Initial volumetric flux (m s^{-1})
R_0 = Initial hydraulic resistance (m^{-1})
G = Constant (s m^{-2})
σ = Blocked area per unit volume of filtrate (m^{-1})
ε_0 = Initial membrane surface porosity

True intermediate blocking results only in cells building up randomly on the membrane surface as in Figure 7.2, but sometimes a mixture of pore blocking and cake

filtration can appear to be the same (Figure 7.3), since the combination leads to a numerically similar value of n.

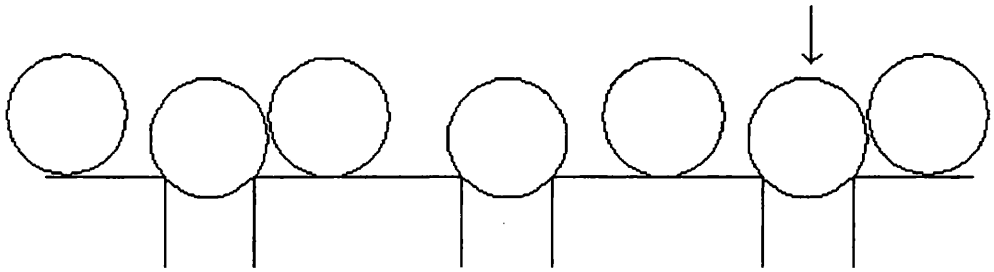

Figure 7.1 Pore blocking mechanism

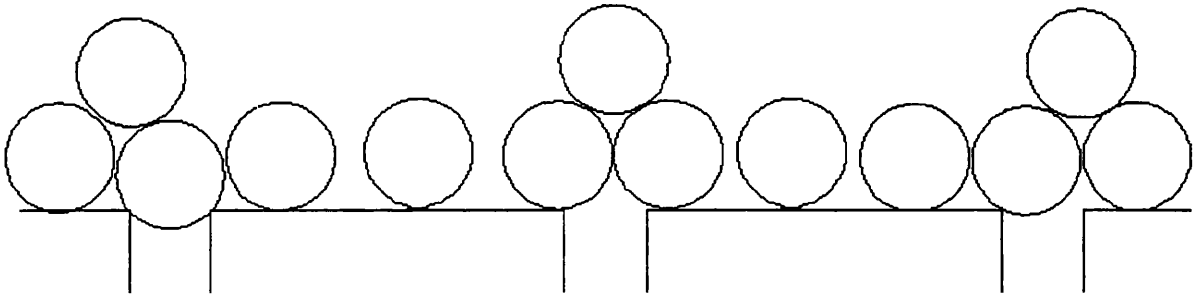

Figure 7.2 Intermediate pore blocking mechanism

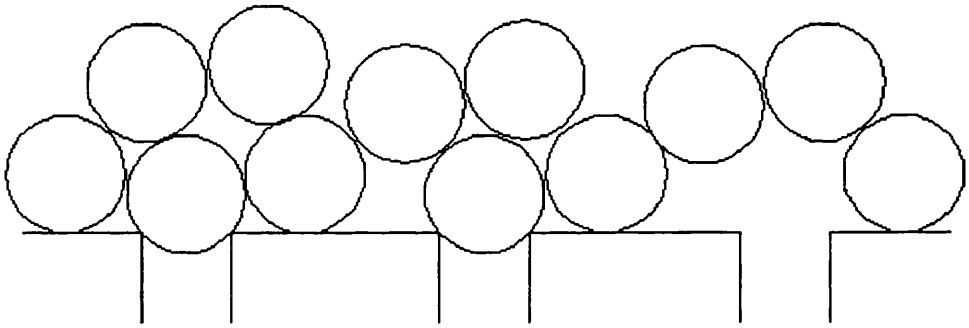

Figure 7.3 Pore blocking + cake filtration mechanism

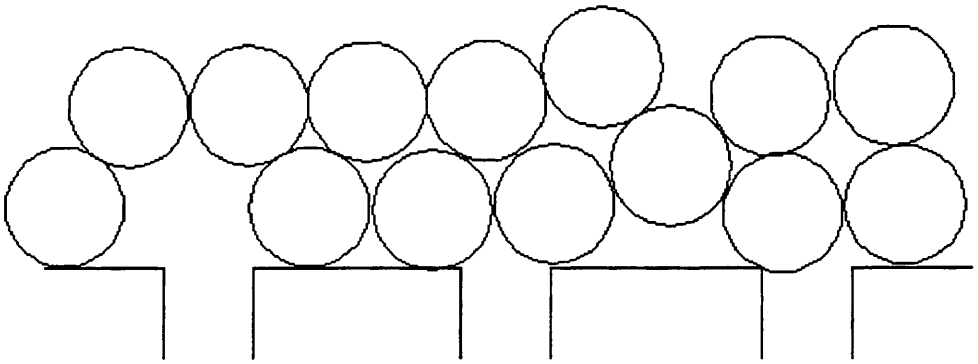

Figure 7.4 Cake filtration mechanism

7.3 Mathematical Basis For Model approaches 1 & 2

In order to determine which fouling mechanism is dominant, the first two model approaches are based upon an analysis of the variation of resistance (due to cell deposition) with time. Starting with Darcy's law,

$$J = \frac{\Delta P}{R} \qquad \textbf{Equation 24}$$

Where:

ΔP = Transmembrane pressure.

R = Resistance.

Rearranging it gives:

$$R = \frac{\Delta P}{J}. \qquad \textbf{Equation 25}$$

Using partial differentiation (required since ΔP and J are not separable), we produce:

$$\frac{dR}{dt} = \frac{1}{J}\frac{\partial \Delta P}{\partial t} - \frac{\Delta P}{J^2}\frac{\partial J}{\partial t} \qquad \textbf{Equation 26}$$

Equation 26 describes the overall temporal increase in resistance with respect to two factors; the temporal rate of change in resistance due to transmembrane pressure (at a constant flux) and that due to temporal change in flux (at a constant TMP).

Rearranging this equation, the change in can be written as:

$$\frac{\partial R}{\partial t} - \frac{1}{J}\frac{\partial \Delta P}{\partial t} = -\frac{\Delta P}{J^2}\frac{\partial J}{\partial t} \qquad \textbf{Equation 27}$$

Substituting in the generic equation of Field *et al.* (Equation 23),

$$\frac{\partial R}{\partial t} - \frac{1}{J}\frac{\partial \Delta P}{\partial t} = \frac{\Delta P}{J^2} k_n (J - J^*) J^{2-n} \qquad \textbf{Equation 28}$$

Finally substituting the Darcy's law equation (Equation 24) to eliminate ΔP from Equation 28 and rearranging, the following is obtained on the basis that the variation of ΔP with t is independent of J.

$$\frac{\frac{\partial R}{\partial t} - \frac{1}{J}\frac{\partial \Delta P}{dt}}{R(J - J^*)} = k_n J^{1-n}$$ **Equation 29**

7.4 Approach 1 (Field et Arnot (1995))

This model approach produces a relationship between resistance and flux, but assumes a constant transmembrane pressure.

If we assume that the transmembrane pressure is constant, then $\Delta P/dt$ is zero.

So with this assumption Equation 29 reduces to:

$$\frac{\frac{\partial R}{\partial t}}{R(J - J^*)} = k_n J^{1-n}$$ **Equation 30**

Taking the logs and rearranging, this becomes

$$\log\left[\frac{\partial R}{\partial t}.\frac{1}{R(J - J^*)}\right] = (1-n)\log J + \log k_n$$ **Equation 31**

If the left-hand side of the equation is plotted against log J, then the fouling mechanism (n) can be simply determined by subtracting the gradient from 1. Examples of this model approach tried on experimental data can be seen in Field & Arnot (1995).

These equations are derived assuming that the transmembrane pressure is constant, which is not the case at the beginning of these experiments. Therefore a model approach allowing for this difference must be derived.

7.5 Approach 2 (R.Field, unpublished)

This approach extends the first model approach by removing the assumption that the transmembrane pressure is constant.

Multiplying Equation 29 by J:

$$\frac{J\frac{\partial R}{\partial t} - \frac{\partial \Delta P}{\partial t}}{R(J - J^*)} = k_n J^{2-n}$$ **Equation 32**

Taking logs,

$$\log\left[\frac{J\frac{\partial R}{\partial t}-\frac{\partial \Delta P}{\partial t}}{R(J-J^*)}\right]=\log k_n+(2-n)\log J \qquad \textbf{Equation 33}$$

By plotting the left-hand side of the equation against log J, the fouling mechanism can be found by subtracting the graph gradient from two.

7.6 Approach 3 (R. Field, unpublished)

Approach 3 is derived by integrating the generic equation of Field *et al.* (1995) (Equation 23). Since this generic equation assumes a constant transmembrane pressure, approach 3 inherits this assumption, which is known to be untrue (see section 7.7). However, this approach is based upon integration, so the plots derived show less scatter than those involving derivatives.

Multiplying Equation 29 by J^{n-2} and integrating with respect to time from time=0 to time=t:

$$\int_0^t -J^{n-2}\frac{\partial J}{\partial t}.\partial t = k_n\int_0^t (J-J^*)\partial t \qquad \textbf{Equation 34}$$

Using $\frac{V}{A}=\int_o^t J.\partial t$, this becomes,

$$-\int_{J_0}^{J} J^{n-2}\partial J = k_n\left(\frac{V}{A}-J^*t\right) \qquad \textbf{Equation 35}$$

Where:

V = Permeate volume.

A = Membrane area

The integration of the left-hand side of Equation 35 has a special case at n=1 when the logs are taken.

$$-\left[\begin{array}{l}\frac{1}{n-1}\left(J^{n-1}-J_0^{n-1}\right).....,n\neq 1\\ \log J-\log J_0.....,n=1\end{array}\right]=k_n\left(\frac{V}{A}-J^*t\right) \qquad \textbf{Equation 36}$$

Listing the explicit results for the three regimes,

$$\left[\begin{array}{c} J^{-1} - J_0^{-1} \ldots\ldots, n = 0(cake) \\ \hline \log J_0 - \log J \ldots\ldots\ldots, n = 1(intermediate) \\ \hline J_0 - J \ \ldots\ldots\ldots, n = 2(pore) \end{array}\right] = k_n\left(\frac{V}{A} - J*t\right) \qquad \textbf{Equation 37}$$

For example, if the complete pore blocking mechanism is valid, the plot of J_0-J against V/A-J*t will give a linear plot, with a gradient of k_2 or $-\sigma J_0/\varepsilon_0$ (see Table 7.1).

Table 7.2 gives a summary of the model approach plots to help determine which mechanism is applicable at any given time. In all plots the variable on the abscissa is (V/A-J*t). The model(s) with the most appropriate deposition mechanism(s) (n value) will possess a straight line fit. The complete pore blocking model has the advantage of being less sensitive to background noise than the other two, as there are no inverse relationships in the expression for the y axis.

Mechanism	**n**	**Y axis**
Cake filtration	0	$1/J-1/J_0$
Intermediate or incomplete pore blocking	1	ln(Jo/J)
Complete pore blocking	2	Jo-J

Table 7.2: Parameters for Approach 3 plots

7.7 Results

7.7.1 Relationship between flux shape and transmembrane pressure

There is a direct relationship between the flux shape and the TMP (transmembrane pressure) value at the beginning of the experiments. Examination of a typical flux-transmembrane pressure plot (Figure 7.5), demonstrates that the flux elbow occurs at a similar time to the attainment of the TMP equilibrium value of 0.5 bar. Other plots can be found in appendix C.

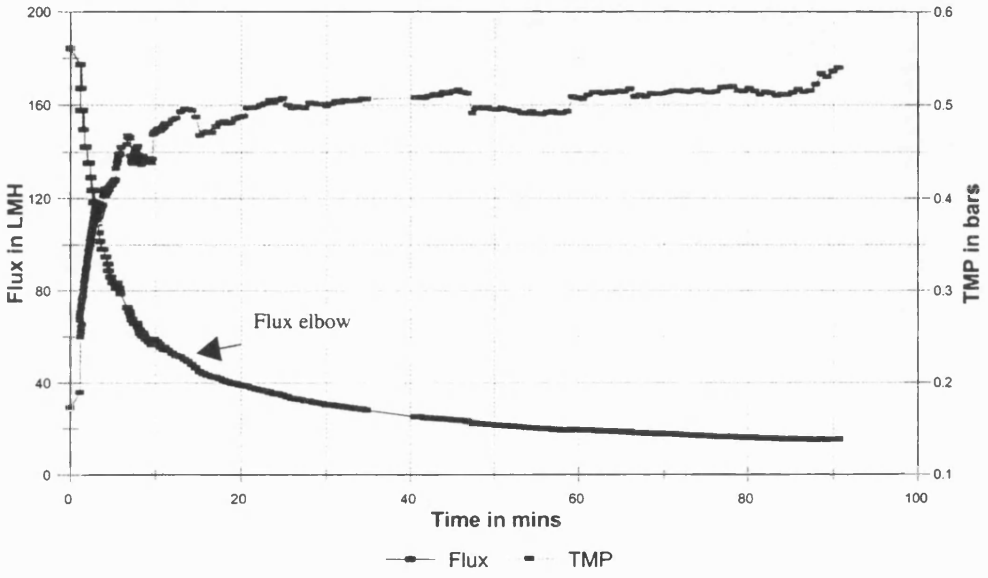

Figure 7.5 Identification of flux elbow using data from a *P.putida* in low NaCl experiment

7.7.2 Model results for all organisms

The results for the three model approaches are summarised in Table 7.3 to Table 7.5. Only some of the results for approach 1 were calculated, since it appeared to be less accurate (and applicable) for the results in this thesis than Approaches 2 and 3. This is not surprising, as the change in TMP is not taken into account. The results for 1/J versus t are also tabulated, since these give an indication of where the intermediate pore blocking mechanism is occurring.

Interpretation of the V/A-J*t graphs (approach 3), reveal that the three types of bacteria display quite different fouling patterns. Typical patterns can be seen in Figure 7.6 -Figure 7.11.

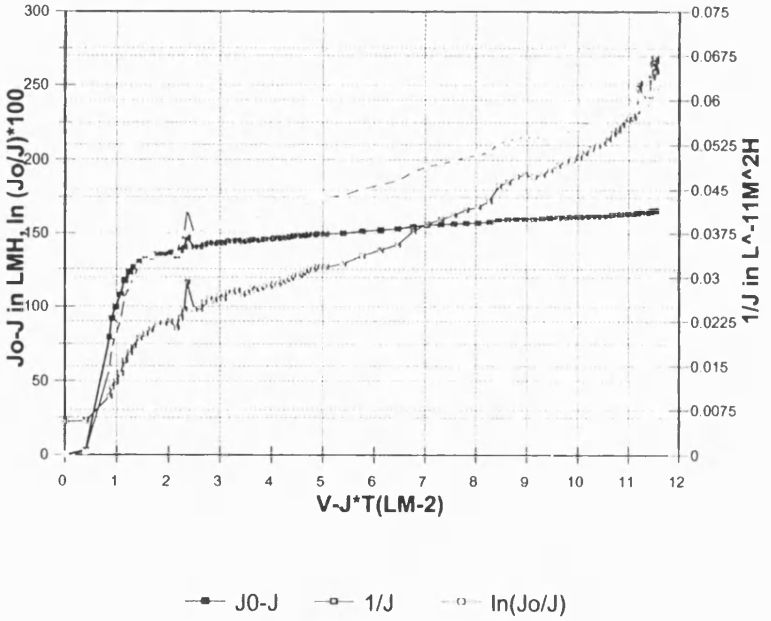

Figure 7.6 *S.multivorum* in high NaCl

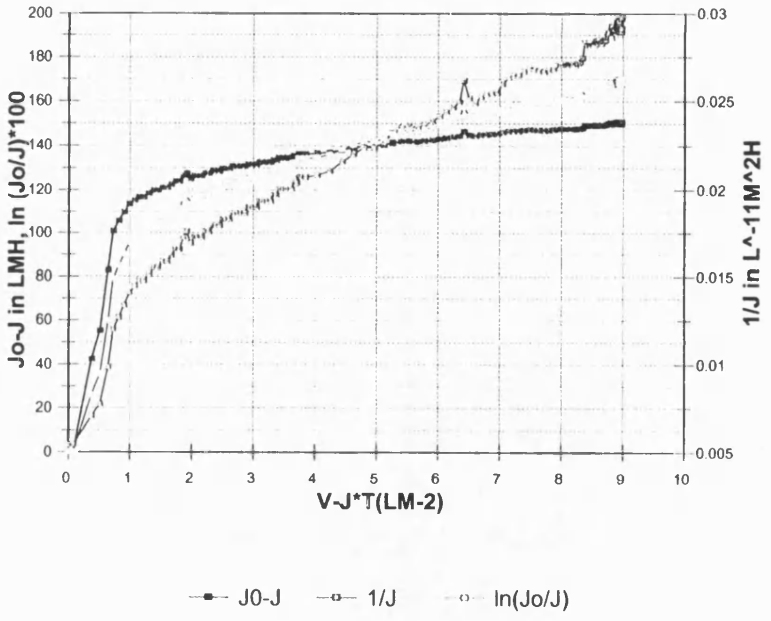

Figure 7.7 *S.multivorum* in low $CaCl_2$

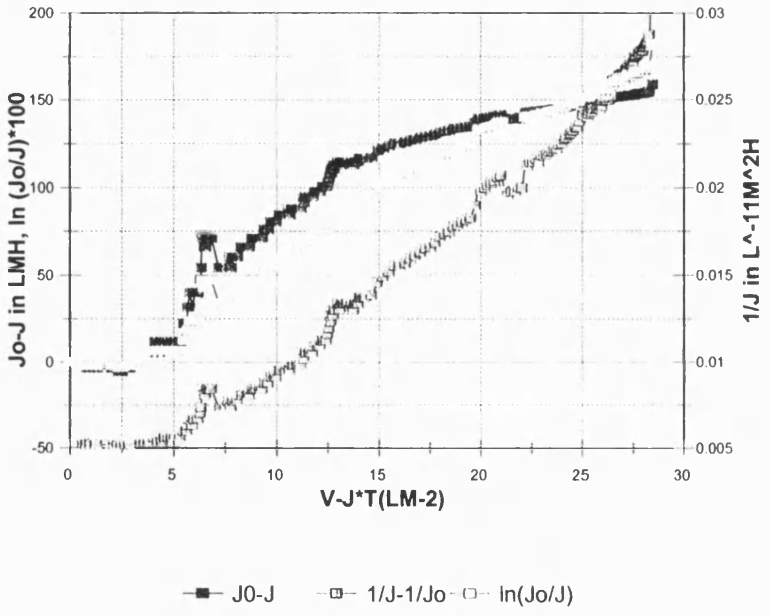

Figure 7.8 *P.elodea* in low NaCl

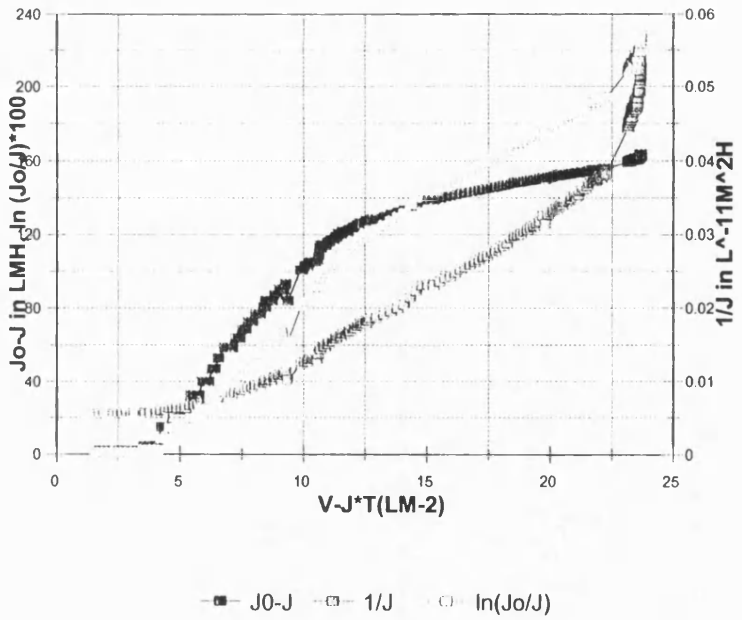

Figure 7.9 *P.elodea* in high $CaCl_2$ and BSA

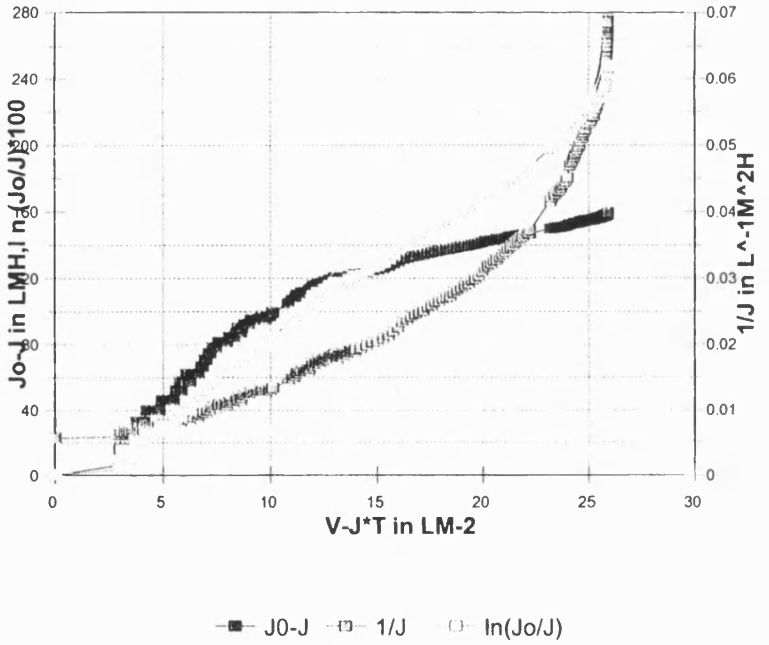

Figure 7.10 *P.putida* in low NaCl

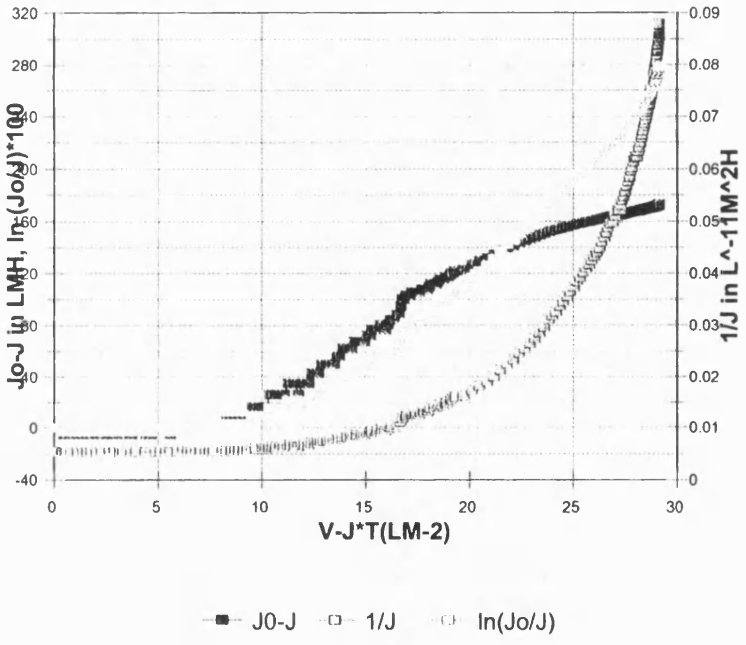

Figure 7.11 *P.putida* in low $CaCl_2$

These graphs illustrate two basic facts:-

- The dominant fouling mechanisms differ according to the organism and the time.
- Different fouling mechanisms can operate simultaneously in a membrane system.

Bowen, Calvo and Hernandez (1995) found that for a single type of protein fouling on a polymeric membrane, no single mechanism operated at one time. They attributed this to the fact that a polymeric membrane had a wide pore size distribution. The different relative sizes of the protein and pore meant different fouling mechanisms operated locally. This may also be a consideration for this study, since here too a polymeric membrane was used.

However in general a single mechanism is expected to dominate at a particular time. Pore blocking always occurs first, either with or without the other fouling mechanisms. Then as the run progresses, cake filtration usually becomes more dominant. Of course the most likely time for pore blocking to occur is when the membrane is clear, and deposition is less than one cell layer thick. A pore may become blocked initially, but then the reduction in hydrodynamic flow may mean the particle is released from the pore (Le and Howell, (1984), only to be covered in cake. This is another reason why the fouling mechanisms can overlap in time.

The sample graphs also demonstrate that there is usually a delay in the start of fouling of varying lengths. This is due to the insensitivity of the flux-measuring device at high flux. The model can only work when there is a detectable difference in starting flux and flux at time t. Therefore the apparent time to start of fouling is actually the time to reach a threshold flux value, i.e. a flux able to be recorded as different to the starting value by the bubble flowmeter (see section 4.4.1.3 for a further explanation).

The experiments that reach this measurable threshold value earliest, indicating the start of pore blocking, are also the ones with the earliest flux elbows. This is inevitable, since the flux elbow value equates to the time it take for the TMP to reach the equilibrium value of approximately 0.5 bar. This observation helps to postulate a general explanation of the shape of a fouling curve. The initial rapid decline of a flux curve is attributed to a phase where pore blocking dominates until the final TMP of 0.5 bar is reached, then the subsequent more gradual flux drop is attributed to domination of the cake filtration mechanism. This contrasts with the explanation of an ultrafiltration

filtration curve shape by Gekas, Aimar, Lafaille and Sanchez (1993). They postulated that for ultrafiltration, the initial steep drop could be attributed to polarisation, whereas the more gradual drop occurs due to fouling. This suggests that the time period during which the most direct attachment of particles to the membrane occurs is later than the theory in this thesis. Therefore the two theories predict very different times to the start of fouling. On the other hand, microfiltration membranes do not act like ultrafiltration membranes until some fouling has initially occurred.

It is also important to note that around the time of the flux elbow, several of the V/A-J*t curves change gradient. This means that even though one mechanism may be effective over a long period of time, the plot is broken into two (or sometimes three) straight lines. It is also interesting to note that this transition usually occurs very rapidly for *P.putida* and *P.elodea*, but for *S.multivorum* there is usually a transition period of several minutes. Periods of transition show up as denser areas in the curves in Figure 7.6 - Figure 7.11. Since the x axis is not time itself, but a function of time, similar model values during a period of transition will cluster. Transition periods for the cake filtration model may also be due to changes in the apparent specific cake resistance (SCR), which is assumed to be constant for cake filtration modelling (see Table 7.1). Section 2.3.9 demonstrates that this assumption is not valid for crossflow filtration of rod-shaped organisms, as the orientation of the rods affects the cake voidage and thus the SCR. For most *S.multivorum* runs there is an early peak before a decline, although the SCR may reach a plateau later on. This is because it is not just the resistance of the cake that is being measured, but also the effects of pore blocking. Therefore the value measured can only be an apparent SCR, unless no pore blocking occurs. Some SCR plots for *P.putida* may also plateau, but not before a steep increase in the first part of the run. Others continue to increase steadily For all *P.elodea* experiments, the SCR increases steadily until the end. The fact that the transition periods are longest for *S.multivorum* correlates with the other evidence that this organism has the greatest tendency to foul by pore blocking.

S.multivorum is also distinguished by the fact that detectable fouling takes place from the very beginning of the experiments, whereas there tends to be a delay for the other two, before any definite fouling mechanisms emerge. This delay varies between 0.43-2.2 minutes for *P.elodea* and 0.7-4.1 minutes for *P.putida*. There is a direct correlation for all these results between how soon the detectable fouling starts and how long the pore blocking phase lasts; the experiments with a slow initial fouling rate have

longer pore blocking phases. The pore blocking phase for *S.multivorum*, usually lasts for the first 30 to 60 seconds of the experiments. After this, cake filtration starts to dominate.

The time period over which the fouling mechanisms are described by these models vary- for *S.multivorum* in low ionic concentration solutions, it is only valid up to 37 minutes. However, it can be seen from the previous chapter that it is usual for the increase in fouling to continue until near the end. All the approaches rely on a difference between the current flux and final flux values. The reason that the mechanisms cannot be discerned from the model beyond a certain time is that the points on the plots are very close together, due to the almost constant flux as the system reaches equilibrium

7.7.3 *S.multivorum*

As mentioned in section 7.7.2, *S.multivorum* exhibits a pore blocking mechanism from the start, whatever the ionic conditions, usually lasting for the first 30 to 60 seconds. After this, cake filtration starts to dominate. The shortest pore blocking time is for cells in high calcium chloride solution, where the pore blocking phase does not last beyond 0.2 minutes.

Bacteria	*S.multivorum*						
		Approach 3-Duration of linearity for each mechanism			**Approach 1**	**Approach 2**	**1/J vs t**
	Flux Elbow (mins)	**Cake (n=0) 1/Jo-1/J (mins)**	**Intermediate (n=1) ln(Jo/J) (mins)**	**Pore blocking (n=2) Jo-J (mins)**	**n value**	**n value**	**Duration of linearity (mins)**
Low Ca^{2+}	1.5	0-1 2.01-36.8	0-1 7.48-55.1	0-0.5	N/A	N/A	None
High Ca^{2+}	1	0.2-1.03 1.03-46.1	0.2-1.03 1.03-52.3	0-0.2	N/A	N/A	None
High Ca^{2+} BSA	1.5	0.23-0.98 7.15-41.7	0.23-0.53 7.15-41.7	0.23-0.53	N/A	N/A	None
High Na^{+}	2	0.46-1 2.9-54	0.15-1 2.9-65.85	0.15-1	N/A	0.279	None
Low Na^{+}	2	#2.86-37	#2.86-26.5	#Start data missing	N/A	N/A	5-15
High Na^{+} BSA	2	0-1 1.7-35.2	0-0.8 3.4-37.35	0-0.48	N/A	N/A	None
Low Na^{+} BSA	2.5	0.1-0.78 1.1-52.4	0.1-0.78 1.1-52.4	0.1-0.78	N/A	0.78	0-1 1-30

Table 7.3: Application of models to *S.multivorum*

The fact that the intermediate, n=1 mechanism is also satisfied is due to the fact that fouling can be attributed to both n=0 (cake) and n=2 (pore) mechanisms occurring simultaneously. If the fouling mechanism were truly intermediate, the plots of 1/flux versus time would also be linear for that time period. This is not the case with the *S.multivorum* data (with the exception of the two low NaCl solutions). The fact that all three lines on the graph tend to display a similar shape at the start (i.e. the timing of their linearity is similar) endorses the likelihood that a combination of the two other mechanisms gives a result of n=1. Field and Arnot (1995) also demonstrate this combinatorial behaviour in their results.

The rapid time to the flux elbow shows that the time to constant TMP arrives early for these micro-organisms.

Since *S.multivorum* starts to foul quickly, it is impossible to make a detailed assessment of the fouling order for this bacterium using the V/A-J*t plots.

7.7.4 *P.putida*

In contrast, *P.putida* shows only equivalent line topology for the pore-blocking and intermediate blocking mechanisms; cake filtration (n=0) does not seem to dominate for this organism. In fact for the two low ionic strength solutions, there appears to be no cake filtration at all, perhaps indicating a physicochemical complication, such as repulsion between the cells. There is also no cake filtration for the high NaCl and BSA solution suspensions, and it exists, but is suppressed until after 12 minutes for the other two suspensions containing protein.

Bacteria	*P.putida*						
		Approach 3-Duration of linearity for each mechanism			**Approach 1**	**Approach 2**	**1/J vs t**
	Flux Elbow (mins)	**Cake (n=0) 1/Jo-1/J (mins)**	**Intermediate (n=1) ln(Jo/J) (mins)**	**Pore blocking (n=2) Jo-J (mins)**	**n value**	**n value**	**Duration of linearity (mins)**
Low Ca^{2+}	12	No	3.5-7.71 10-36.8	3.5-7.71	N/A	1.1	3-20
High Ca^{2+}	12.5	8.25-45.98	2.58-9.93 9.93-69.1	2.58-9.93	N/A	N/A	2-10
High Ca^{2+} BSA	8	12.25-29.21	2.05-15.05	2.05-7.6	N/A	1.64	2.5-7.5
High Na^{+}	8	1.1-8.8 8.8-40.6	0.8-3.8 3.8-8.3 8.3-69	0.8-2.21	N/A	1.86	2-8
Low Na^{+}	12	No	1.61-8.2 8.2-33.8	1.16-5	N/A	1.4	1-9. 9-85
High Na^{+} BSA	10	No	0.7-9.85 9.85-40.58	0.7-4.31	N/A	0.69	0-10 10-32
Low Na^{+} BSA	5	13-32.55 32.55-89.73	0.68-10.18 10.18-26.6 26.6-89.73	0.68-3.13	0.61	0.4	0-10 10-32

Table 7.4: Application of models to *P.putida*

The effects of the feed suspension on the start of fouling are different for *P.putida*. The most noticeable difference is between the type of salt in the suspension. All the $CaCl_2$ suspensions have slower starts to their fouling mechanisms (2.1-3.5 minutes) compared to NaCl (0.7-1.2 minutes). For both $CaCl_2$ and NaCl, an increase in ionic strength and/or addition of protein will decrease the time to fouling.

This organism demonstrates the slowest time to transmembrane pressure steady state, indicated by the high flux elbow values, and thus the longest times before any fouling mechanisms are recorded.

7.7.5 P.elodea

The meaning of the n=1 curves for *P.elodea* are less clear. Looking at Figure 7.6- Figure 7.11, the fouling behaviour for *P.elodea* seems to be in between that of the other two organisms. The pore blocking curve is much more extended in time than that of *S.multivorum,* and cake filtration occurs much earlier and lasts much longer than for *P.putida.* The three plots are not always the same shape at the start, since the onset of cake filtration is sometimes delayed slightly. Figure 7.8 (in low NaCl) exhibits similar fouling times for all three mechanisms, while Figure 7.9 (high $CaCl_2$ & BSA) does not. All the experiments (except for those suspended in the two NaCl & BSA solutions) demonstrate linearity for 1/J versus T plots. In fact, there seems to be a link between a short pore blocking stage at the start of an experiment and the absence of a significant intermediate blocking mechanism. The fouling mechanism seems to go straight from pore blocking to cake filtration. Details of this data can be found in Table 7.5.

Bacteria	*P.elodea*						
		Approach 3-Duration of linearity for each mechanism			**Approach 1**	**Approach 2**	**1/J vs t**
	Flux Elbow (mins)	**Cake (n=0) 1/Jo-1/J (mins)**	**Intermediate (n=1) ln(Jo/J) (mins)**	**Pore blocking (n=2) Jo-J (mins)**	**n value**	**n value**	**Duration of linearity (mins)**
Low Ca^{2+}	12	2.6-6.8 6.8-54.4	2.2-6.8 6.8-54.4	2.2-6.45	N/A	0	2-10
High Ca^{2+}	9	2.5-36	1.13-4.96 6.56-44	1.13-4.96	N/A	0.7	1-8
High Ca^{2+} BSA	7	4.45-47.5	2-7.8 7.8-47.5	1.5-6.05	N/A	1.55	2-8
High Na^{+}	1.5	0.63-4 7-46.5	0.43-1.75 5.46-46.5	0.43-0.63	N/A	0.3	0-4 15-90
Low Na^{+}	12	1.6-39.55	1.6-11.45 11.45-90	0.96-9.2	2	1.075	1.5-7 20-90
Low Na^{+} BSA	5	12-38.55	1-3.95 3.95-22.33 22.33-70	1-1.75	N/A	1.7	None

Table 7.5: Application of models to *P.elodea*

The simplest way to assess the order of fouling is to look at the pore blocking start times detailed in Table 7.5. The exception to this rule is evaluation of the effect of protein addition; the difference between the figures for high $CaCl_2$ and low NaCl with

and without protein are minimal and due in part to the flux measurement device. Therefore a more accurate method of ordering the fouling sequence is by the flux elbows. By this method, it may be deduced that BSA decreases the time to fouling. Therefore the factors increasing the initial rate of fouling are in the order:

a) High ionic strength before low ionic strength

b) Protein before no protein

c) NaCl before $CaCl_2$.

Thus the modelling of the behaviour for *P.elodea* is particularly complex due to the strong influence of physicochemical effects for this type of bacteria. Modelling of *P.elodea* filtration is also complicated by the compressibility of the cake. This could account for the fact that n=1 is satisfied, even when cake filtration predominates. Compressed cake (cell deposition is always early for this species- see section 6.2.4) may act either to block a pore or act simply as a cake with high resistance. This type of pore blocking is more complex than that described by the models detailed in this chapter however.

7.7.6 Approaches 1 and 2

It must be stressed that the results for Approaches 1 and 2 represent fouling models for the first few minutes only, since after that, all the readings become tightly clustered. This is because the models depend on a difference in size between the current flux and the final flux, which quickly becomes small for many experiments, for example, the flux in Figure 7.5. There were three experiments that successfully yielded a plot with an easy to measure gradient. These are illustrated in Figure 7.12 - Figure 7.14. In the first two *P.putida* experiments, the line drops off vertically once the flux difference decreases to a low value. Figure 7.14 is for *P.elodea* (low NaCl with BSA) on the other hand, and clusters around a single value for the y axis as the flux values converge during the experiment.

For the majority of plots for approach 2 however, the oscillations in TMP due to the unsteadiness of the pump prevent a smooth line, even after employing a 6-8 point rolling average technique. One such graph is illustrated in Figure 7.15.

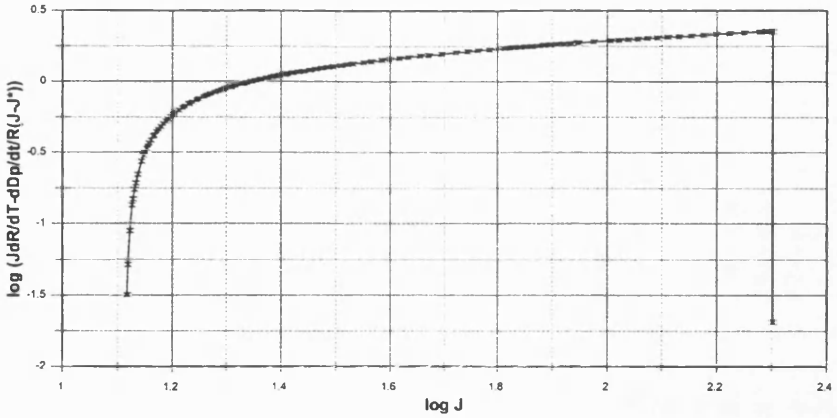

Figure 7.12 approach 2 of *P.putida* in low $CaCl_2$ 1.3-5.1 minutes

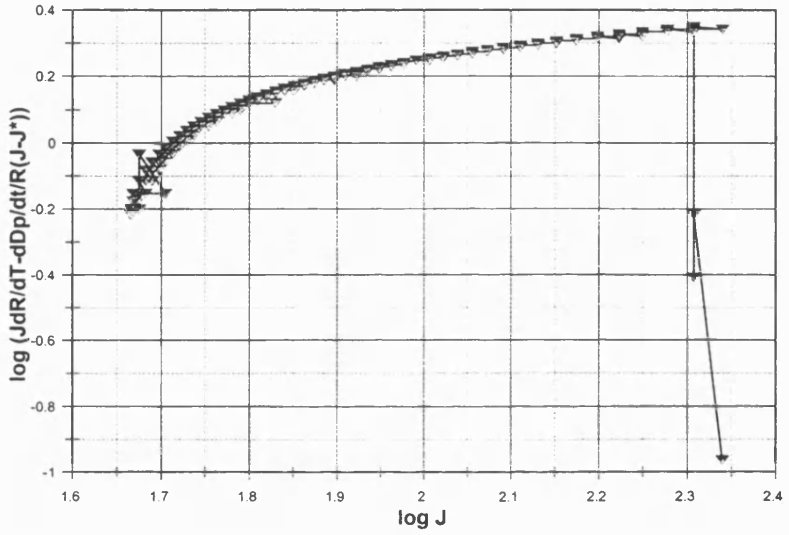

Figure 7.13 approach 2 of *P.putida* in high NaCl with BSA 0.7-12.6 minutes

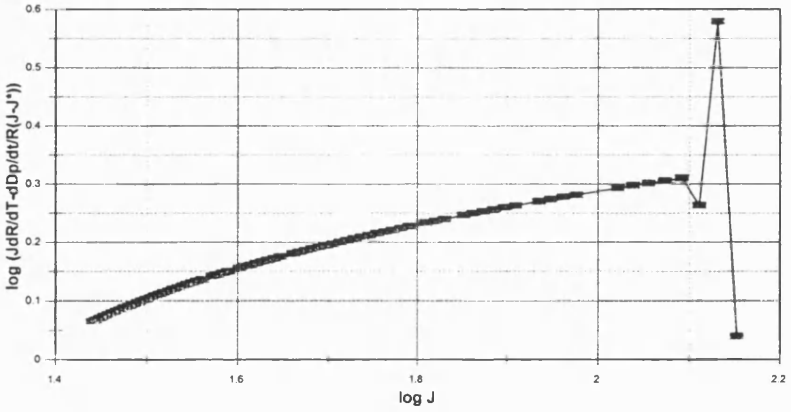

Figure 7.14 approach 2 of *P.elodea* in low NaCl with BSA 0.96-12.5 minutes

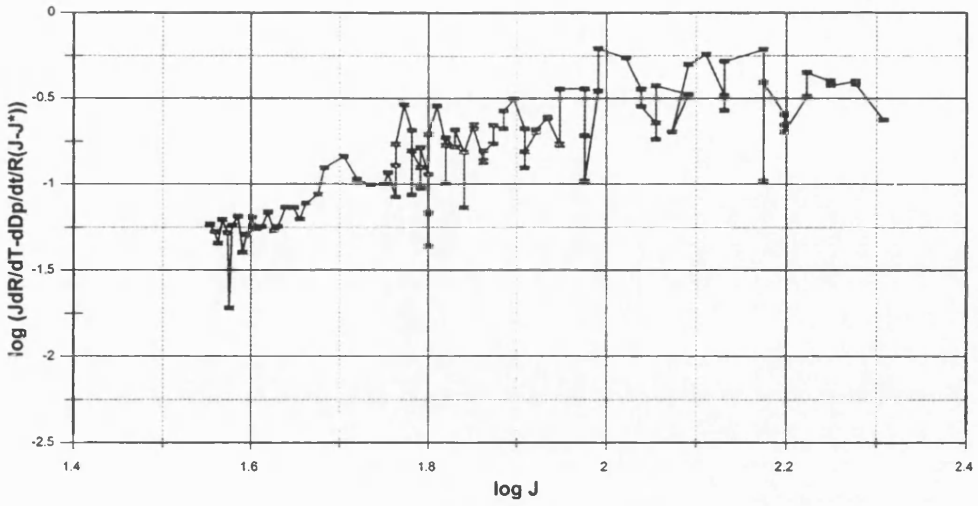

Figure 7.15 approach 2 of *P.elodea* in high $CaCl_2$ 0.9-22.7 minutes

Approach 1 tended to result in graphs that were difficult to interpret due to their variability, so only a few have been calculated. Approach 1 results for *S.multivorum* yielded meaningless values. Although there are a couple of results for *P.elodea* using approach 1, they do not show any correlation with either the approach 2 or approach 3 results. They can therefore be considered inaccurate. On the other hand, the approach 1 results for *P.putida* are more meaningful. This is not surprising, since one of the *P.putida* experiments was also modelled using Hermia's equation without modification for crossflow and a value of n=1 was found (Figure 7.16).

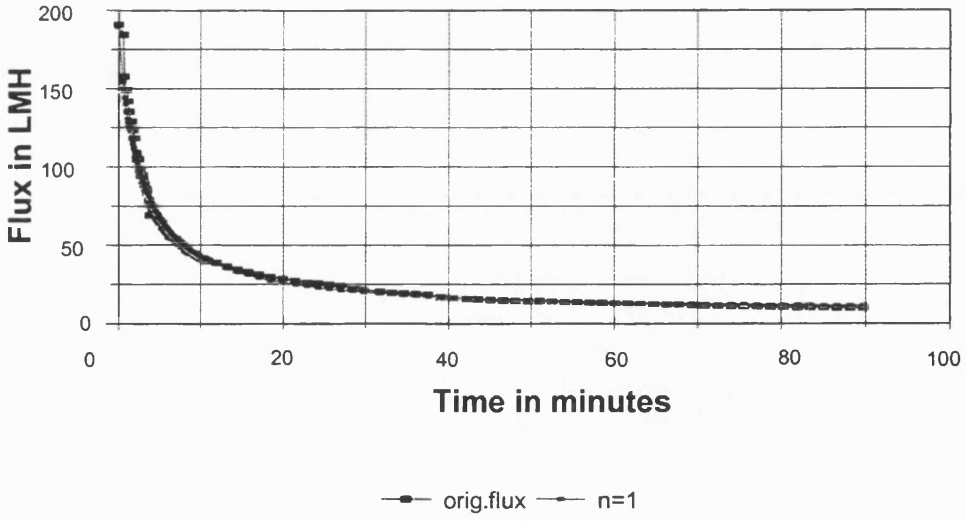

Figure 7.16 n=1 fit for *P.putida* in high NaCl with BSA using Hermia's original equation

There are only two Approach 2 calculations for *S.multivorum* out of a possible seven. Therefore this model approach is not considered very reliable for this organism. The value of n=0.279 for a high NaCl suspension and n=0.78 for the beginning of the experiment correlates poorly with the results for Approach 3 (V/A-J*T plots). The figures for approach 2 indicate that fouling is mainly due to cake filtration (n=0) with some intermediate fouling occurring (n=1). Approach 3 indicates that all three mechanisms are co-existent at the start. However, the figures for approach 3 could be an indication of the brevity of the pore-blocking phase for this cell type, and that cake filtration soon becomes the main fouling mechanism.

For *P.putida*, there is good agreement for the Approach 2 and Approach 3 results for low $CaCl_2$, high $CaCl_2$ & BSA, high NaCl and low NaCl. The two $CaCl_2$ results have a value of n close to 1, indicating intermediate blocking, and the two NaCl results have values between 1 and 2, showing that the fouling mechanism lies between intermediate and pore blocking. These higher n values may indicate a higher probability of pore blocking than the previous two. However for the two NaCl solutions with BSA added, the calculated n values are low. This is very surprising since Approach 3 indicates that cake filtration (n=0) is either delayed or non-existent for these two.

The *P.elodea* results for Approach 2 quite possibly correlate with Approach 3 if it is assumed that the value of n is an indicator of which fouling mechanism is dominant. Analysis of these experiments by Approach 3 indicates that different mechanisms occur concurrently at the beginning, so the lower n values calculated by approach 2 (low $CaCl_2$, high NaCl) indicate that cake filtration is dominant. By the same assumption, high n values (high NaCl or low NaCl with BSA) may indicate that pore blocking is dominant. This agrees with the earlier observation in Chapter 6 that pore blocking dominates at the start, followed by cake filtration. It is also supported by the fact that ninety percent of cell deposition occurs in the first 12-30 minutes of filtration for *P.elodea*, unlike the other two cell types (see section 5.2.4).

It was assumed initially that the reason approaches 1 and 2 did not always produce sensible results was related to the rapidly changing TMP at the beginning of the run. However, this could not be the main cause, as *S.multivorum* has the fastest times to TMP steady state, yet this organism is the most difficult to model for these approaches. It is the time over which the flux differences are large enough to provide a meaningful answer that is the most important factor for successful modelling. Approaches 1 and 2 are only useful at the start of the experiment when there is a high flux difference.

Therefore for experiments with a steep decline in flux at the beginning, such as the *S.multivorum* experiments, or ones with a low data density, modelling is more difficult with the first two model approaches.

Noting the time periods over which the gradients for Figure 7.12-Figure 7.14 are measured, and noting the number of points for each, a clue to why only three plots are entirely successful emerges. Figure 7.15 is erratic partly because there are relatively few points over an extended period of time (22.7 minutes), whereas the other three graphs have many points, even though the time over which the model approach is valid is shorter at 5- 12 minutes. There is a high risk when applying a linear fit analysis to the irregular plots for these model approaches; the irregularity means that it is difficult to ascertain the time at which the model approach is no longer valid. If too many points are included in the calculations, the results may be inaccurate.

Thus it is clear that the results for approach 3 are the easiest and most reliable to interpret with such changeable data. The effect of the fluctuations in TMP as a result of power fluctuations are still evident in approach 3, but do not lead to such swings in the values as for the other two approaches. Approach 3 is the result of integrating Equation 23, while both Approach 1 and 2 are the results of differentiating this equation. Therefore approach 3 is less sensitive to minor variations in the TMP and flux values.

7.8 Repeat experiments

A fuller comparison of the experiments that were repeated can be found in section 6.4.7. Some of these experiments are to test the reproducibility of the experiments, while others were repeated because the specified conditions were not met in some way. Where the cause of the failure is known, a comparison of results can offer an extra insight into the mechanisms occurring.

7.8.1 *S.multivorum* in high NaCl

There were three experiments performed with *S.multivorum* in high NaCl. The approach 3 results for these three experiments can be seen in Figure 7.17 - Figure 7.19. These graphs reveal a close correlation between the experiments for all three parts of approach 3. The offset for repeat experiment 1 (red line) is simply due to a slightly higher starting flux (Jo). Nevertheless, the relative times and gradients for all the fouling mechanisms are well-matched. Since the experimental results for resistance, SCR and final flux are also very similar (see section 6.4.7.1), this is to be expected.

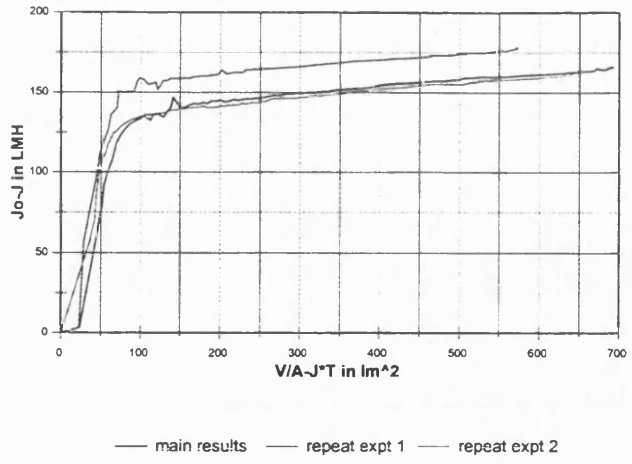

Figure 7.17 ***S.multivorum*** **in high NaCl (Jo-J) repeatability (n=2, pore blocking)**

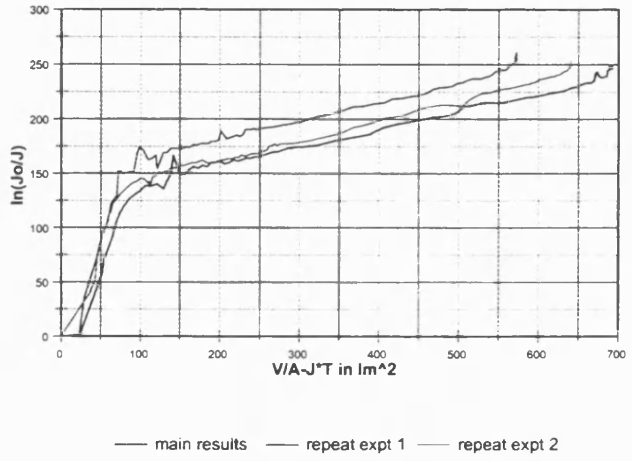

Figure 7.18 ***S.multivorum*** **in high NaCl ln(Jo/J) repeatability (n=1, intermediate blocking)**

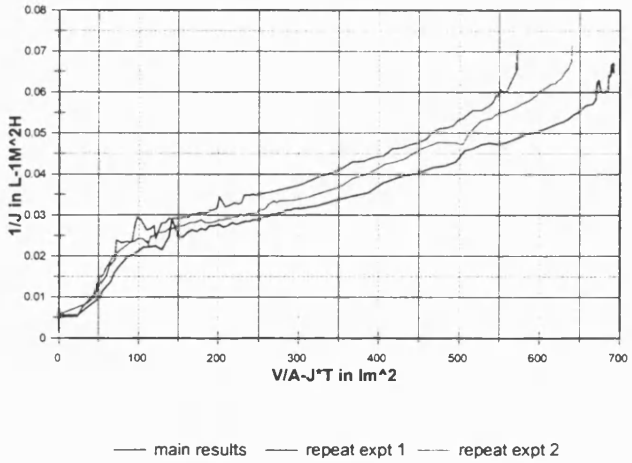

Figure 7.19 ***S.multivorum*** **in high NaCl (1/J-1/Jo) repeatability (n=0, cake filtration)**

7.8.2 *P.putida* in high NaCl

Three experiments were also performed on *P.putida* in high NaCl. Two of the experiments were carried out on the same batch of cells, but the first experiment (blue line) was performed with a cleaner membrane a day earlier than repeat experiment 1 (red line). The approach 3 plots of these two experiments display almost identical behaviour for the first few minutes. Table 7.6 indicates that the main results foul nominally quicker for the first part of the runs. However, the runs soon diverge. Section 6.4.7.2 shows that for the experimental results, after an initial almost identical increase in resistance, the resistance increase paths suddenly diverge dramatically at 8 minutes.

For the modelling results, pictured in Figure 7.20-Figure 7.22, repeat experiment 1 (red line) continues to display linearity for the pore blocking model until close to the end. The main results on the other hand (blue line) favour cake filtration more. This difference in cake filtration dominance is reflected in the cell deposition values; 19 cell layer equivalents are deposited in the main experiment, while only 12 C.L.E.s are deposited for repeat experiment 1.

Repeat experiment 2 displays a similar fouling pattern to the main results, although they occur at a slower rate. For example, the intermediate fouling mechanism occurs up to 12 minutes, then from 17 minutes up until 130 minutes. For the main experiment, the first part of the intermediate mechanism finishes at 9 minutes, and there is a shorter transition period, as linearity occurs again at 12.28 up to 56 minutes.

It seems likely that it is the difference in the cake filtration that is the cause of the divergence in flux or resistance, since the cake filtration model graph for all three experiments is proportional to the inverse of their resistance plots (Figure 7.23).

	Cake (n=0) **1/Jo-1/J** **(mins)**	**Intermediate (n=1)** **ln(Jo/J)** **(mins)**	**Pore blocking** **(n=2)** **Jo-J** **(mins)**
Main result	5.78	8.6	2.5
Repeat experiment 1	8.06	7.13	1.9

Table 7.6 Duration of identical fouling mechanisms for two *P.putida* in high NaCl experiments

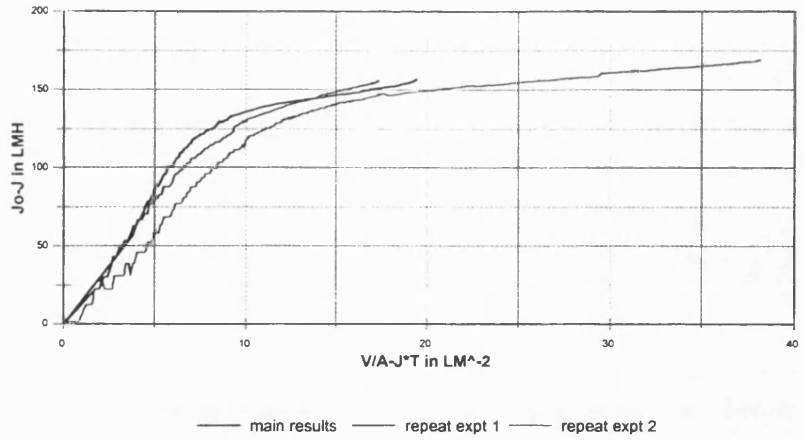

Figure 7.20 *P.putida* in high NaCl (Jo-J) repeatability (n=2, cake filtration)

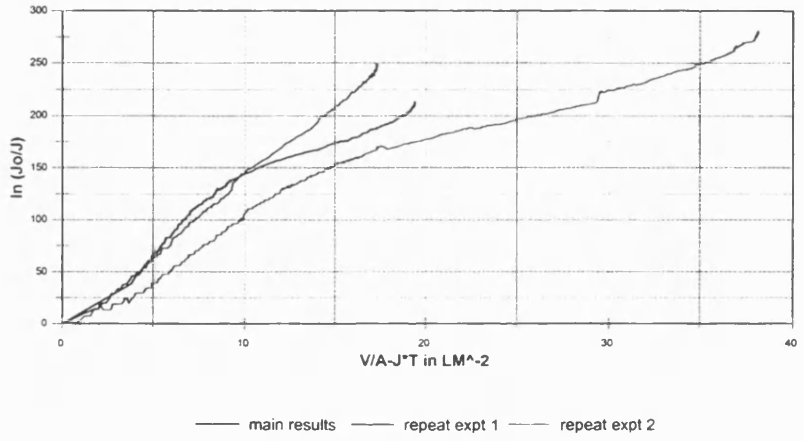

Figure 7.21 *P.putida* in high NaCl ln(J0/J) repeatability (n=1 intermediate)

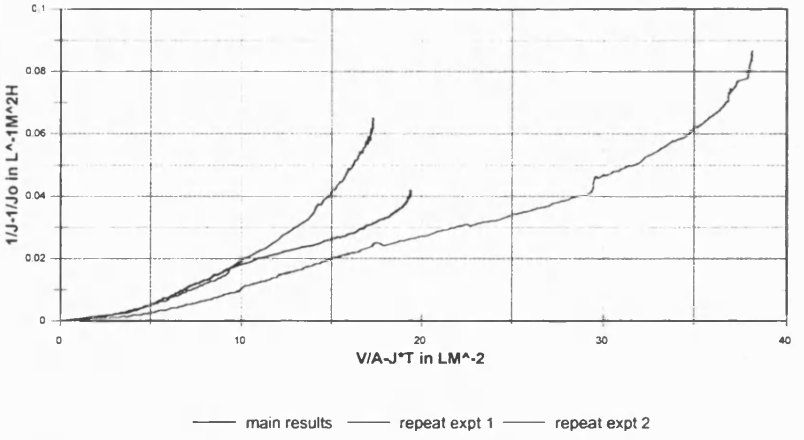

Figure 7.22 *P.putida* in high NaCl (1/J-1/Jo) repeatability (n=0, cake filtration)

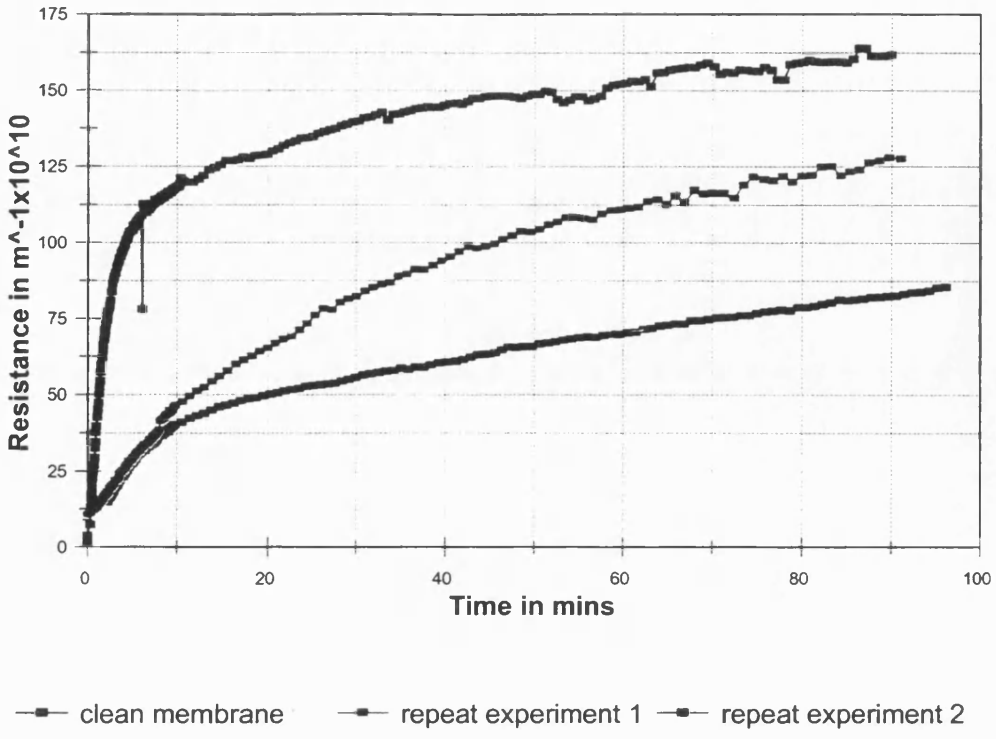

Figure 7.23 *P.putida* in high NaCl repeatability of resistance increase

7.8.3 *P.elodea* in high $CaCl_2$

Two experiments were executed with *P.elodea* in high $CaCl_2$. This time the known difference between them was that the repeat experiment 1 contained cells three days older than the main experiment.

From Table 7.7 and Figure 7.24 - Figure 7.26, it can be concluded that the two runs had similar fouling mechanisms, but the old cells fouled slightly more rapidly.

	Cake (n=0) **1/Jo-1/J** **(mins)**	**Intermediate** **(n=1)** **ln(Jo/J)** **(mins)**	**Pore blocking** **(n=2)** **Jo-J** **(mins)**
Main results	2.5-36	1.13-4.96 6.56-44	1.13-4.96
Repeat experiment 1	0.85-12.56	0.38-3.48 5.65-37	0.38-2.68

Table 7.7 Comparison of approach 3 results for repeat experiments for *P.elodea* in high $CaCl_2$

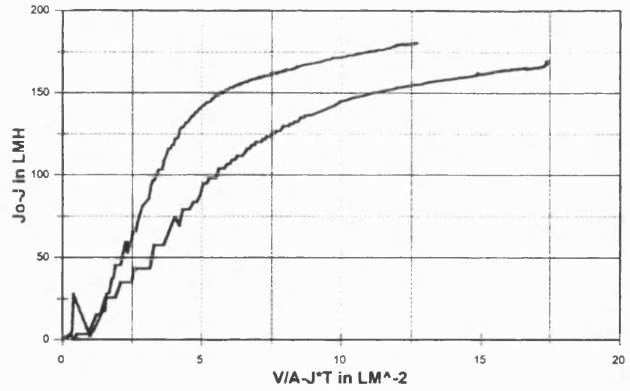

Figure 7.24 *P.elodea* in high $CaCl_2$ (Jo-J) repeatability

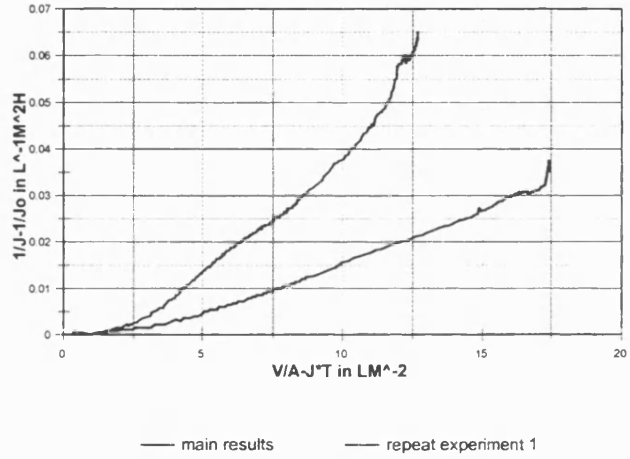

Figure 7.25 *P.elodea* in high $CaCl_2$ (1/J-1/Jo) repeatability

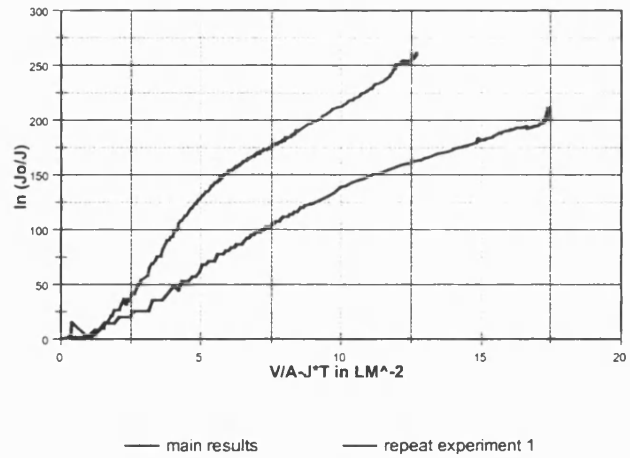

Figure 7.26 *P.elodea* in high $CaCl_2$ ln(Jo/J) repeatability

7.9 Conclusion

An attempt has been made to fit the three model approaches to the experimental data produced in this thesis. The first one is a model approach derived from Hermia's equation and modified for crossflow filtration (by Field & Arnot, 1995 and Field *et al.*, 1995) and then differentiated. The second model approach is a modification of the first one, to take account of the rapid increase in transmembrane pressure at the start of the experiment. The first two model approaches are both differentials of the generic equation 23 and yield only one line for interpretation. The third model approach is an integration of the same equation, with plots of 1/J, $\ln(J_0/J)$ and J_0-J against V/A-J*T. These plots represented n=0 (cake), n=1(intermediate) and n=2 (pore blocking) respectively. A linear correlation indicates the time over which that mechanism was valid. A summary of the findings from these model applications can be found in Figure 7.8.

The three separate plots for approach 3 demonstrate that there is more than one way of satisfying the criteria for n=1. *P.putida* exhibits true intermediate blocking behaviour, fulfilling the assumption that a particle has an equal chance of landing anywhere on the membrane. *S.multivorum* reveals a false positive for pore blocking, since pore blocking and cake filtration occur simultaneously and almost immediately, but without fulfilling the previously mentioned assumption. It is also uncertain if all n=1 results for *P.elodea* are due to intermediate blocking.

Pore blocking for *S.multivorum* only lasts for 30 –60 seconds. This leads to a rapid decline in flux, and the effects of ionic strength, valency and protein on fouling rate are difficult to ascertain for this organism. Fouling occurs more slowly for the other two bacteria, and the effect of varying parameters on the fouling rate can be determined both by the duration of the pore blocking phase and by the position of the flux elbow. Protein increases the rate of fouling for both *Pseudomonas* species, but especially for *P.elodea.* A suspension of a higher ionic strength of a low valency salt will also increase the fouling rate for both *Pseudomonas* species.

Therefore there is much to be gained from analysis of results by model approach 3, whereas the other two models are successful on this data in only some cases. This is because for the differentiative derivations, the importance of a difference in current and final flux becomes much more important. Therefore these model approaches can only reveal significant results if the fouling rate is sufficiently slow to allow the difference for

a long enough period of time. *P.putida* has the slowest fouling rate and thus has the highest chance of a successful result with these models.

	S.multivorum	***P.elodea***	***P.putida***
Fouling trends	Pore blocking demonstrated by SCR trends, rate of resistance increase at beginning and approach 3 results. Intermediate blocking due to a combination of pore blocking and cake filtration-1/J vs t plot not normally linear.	Intermediate blocking may occur, but cake filtration has early onset. Therefore possible that intermediate blocking due to cake collapsing into pores.	Intermediate blocking predicted by approach 2,3 and Hermia.
Success of model approach 1 and 2	Neither	Some success with approach 2	Some success with both approaches

Table 7.8 Summary of the findings for the modelling activity

8 Discussion

8.1 Introduction

The work in this thesis should help answer five main questions for the bacteria selected:-

1) How does ionic strength affect fouling for these types of bacteria?
2) How does fouling in a divalent electrolyte compare with that of a monovalent electrolyte?
3) How does the presence of a protein affect the fouling of the micro-organisms?
4) What are the dominant fouling mechanisms for the three bacteria?
5) From the information gleaned from these questions, how do the properties of an extracellular matrix affect the balance between the hydrodynamic and physicochemical effects that govern fouling behaviour?

8.2 Background to bacterial properties

A summary of the three bacteria selected, together with their characterisation results, are laid out in Table 8.1. Characterisation showed that: -

- Both bacteria and BSA are negatively charged, like the membrane at low ionic strengths, but have a zeta potential closer to 0 at high ionic strengths.
- The cell dimenaions are comparable
- The hydrophobicity tests do not agree 100%, but tend to indicate that *P.elodea* has the highest hydrophobicity, while that of P/.putida is low.
- Although much of the loose polysaccharide on *P.elodea* had been removed by centrifugation, there was still enough gellan gum present to dictate the fouling behaviour and *P.elodea* was the only bacterium with a positive result for loose polysaccharide. The presence of a significant amount of gellan gum is also supported by the higher mass for a *P.elodea* cell.

Parameter	*S.multivorum*	*P.elodea*	*P.putida*
Distinguishing extracellular feature	Smooth polysaccharide capsule	Loose, slimy gellan gum	Long, thin, flagella covering the surface
Zeta potential in low NaCl in mV	Two distinct zones at; -38.19 and -12.35.	One zone at -33.	Three zones close together, between -8.7 and –20.44
Zeta potential in high CaCl2 in mV	Most positive at 3.75.	Most negative at -0.36.	Slightly positive at 0.96
Overall hydrophobicity according to SAT test	The least hydrophobic	The most hydrophobic, but still weak	In between
Site hydrophobicity according to BATH test	High Ca^{2+}/BSA strongly hydrophobic. High ionic strengths moderate, others not hydrophobic	Low ionic strengths and High Na^{+} moderately hydrophobic. Others not hydrophobic	High. Ca^{2+}/BSA moderately hydrophobic. Others not hydrophobic
Overall hydrophobicity according to plastic adhesion test	Low except for High Ca^{2+} (high) and High Na^{+} (medium)	Medium-high except High Ca^{2+}/BSA	Universally low
Dimensions in μm (with SD)	2.39x1.02 (0.7x0.08)	2.28x0.83 (0.65x0.11)	2.42x0.61 (0.88x0.09)
Mass in kg	$2.5x10^{-12}$	$3.2x10^{-12}$	$2.1x10^{-12}$
Polysaccharide detected	No	Yes	No
Viscosity	Highest at high ionic strengths. No effect upon addition of protein except High Ca^{2+}; the highest viscosity for all three was High Ca^{2+}/BSA		

Table 8.1 Summary of cell characterisation experiments

8.2.1 Relevant observations during preparation

An indication of how easily cells can "stick together" at low ionic strengths can be gained from considering how easy or difficult each organism was to centrifuge in a low ionic strength buffer. The relative cell density was not measured, but there seemed to be little difference between the rate organisms settled out, as they all seemed neutrally buoyant. Nevertheless, *P.putida* was very easy to centrifuge; after 15 minutes at 6000 rpm a dense pellet would be formed, which was very hard to resuspend. *P.elodea* needed 25 minutes at 10,000 rpm, after which it needed a gentle shake for resuspension.

S.multivorum however would resuspend with the slightest movement even after 40 minutes at 10,000 rpm.

This behaviour can be explained in terms of the known extracellular characteristics for each organism.

- The smooth highly capsulate exterior of *S.multivorum* means that cell-cell bonding is most difficult for this bacterium
- The negatively charged dispersive gellan gum matrix of *P.elodea* is easily disrupted
- The flagella covering the whole surface of *P.putida* cells encouraged the formation of a tight pellet due to their enmeshment.

P.putida also distinguished itself with respect to membrane fouling by being the hardest to clean chemically, especially if the experiment involved a high ionic strength and/or protein. This may also be because of the flagella. According to the models applied, intermediate blocking dominated for most of the *P.putida* experiments, thus many cells may be partly or fully over the pores. If the flagella enter the pores, the thin, 30-nm strand has a high probability of overcoming repulsion and adsorbing to the pore wall. The forces required to remove it from the cell membrane would be very high. See section 8.8 for a further discussion.

8.2.1.1 Aggregation

Aggregation of particles can change the fouling behaviour of particles quite dramatically.

Most bacterial species exist as individual particles, or small groups of 2 or 3 under milder (e.g. low ionic strength) conditions. For these types of bacteria, changing the conditions to promote aggregation (ionic strength increase or a change in pH) the effective particle size, and thus the specific resistance will decrease, as predicted by the Carman-Kozeny equation. For dispersive aggregates however, a similar change in conditions will reduce the repulsion between the cells in the matrix, thus reducing the permeability of each aggregate, so decreasing the flux. This time the effective particle size will be reduced.

When aggregation makes the effective particle size larger, the voidage should increase accordingly. Ohman & Glatz (1999) had pictorial proof that deposited silica aggregates had wide, deep channels between them to help with the maximisation of flux. Hydrodynamic laws predict a decrease in the deposition of these aggregates of increased

size (see section 2.4.1). However, once an aggregate is deposited on the membrane, the total number of cells deposited will increase dramatically; aggregates have an advantage with regard to attachment possibilities due to their high surface roughness.

Meagher, Klauber & Pashley (1996) pointed out that if under conditions to promote aggregation, cell deposition stayed constant while flux increased, it could be explained in terms of an aggregate having a less regularly ordered cake with larger random voidages. This is due to the existence of increased random cohesive collisions. However, if cell-membrane interaction were important in the overall fouling, the beneficial effects for the flux would be attenuated accordingly.

8.2.2 Prediction of aggregation using hydrophobicity and zeta potential

Ohmon and Glatz. (1999) studied dead end filtration of *C.glutamicum* over a range of pHs and ionic strengths. They concluded that conditions that gave rise to a high hydrophobicity and a low charge encouraged agglomeration.

8.2.2.1 S.multivorum

If only the specific hydrophobicity results are taken, i.e. the BATH test results, they would suggest that the greatest agglomeration of *S.multivorum* should occur in a suspension of high $CaCl_2$/BSA. It should also occur in high $CaCl_2$ and in high NaCl. It was easy to see with the naked eye that the agglomeration in $CaCl_2$/BSA was higher than in $CaCl_2$ alone, although they were the smallest of the three species of bacteria. Agglomeration with NaCl was not visible without a microscope and has not been verified. It does seem likely from the filtration results however that some aggregation occurs in high NaCl. For example, suspensions of high NaCl, like high $CaCl_2$, had a higher cell deposition than the other experiments.

8.2.2.2 P.elodea

Application of the same theory to *P.elodea* results predicts the greatest agglomeration for high NaCl and high NaCl/BSA. Both these suspensions displayed a significant degree of agglomeration. However, as with all of the bacteria species, the conditions that gave the most visible signs of agglomeration were high $CaCl_2$/BSA. This suspension is not predicted to favour agglomeration, but the theory does not take into account the fact that *P.elodea* forms aggregates under all conditions, due to the slimy polysaccharide gellan gum on the outside. Since this is very negatively charged at low ionic strengths (-33mV) it is likely these aggregates are dispersive aggregates. This means their energetic

stability comes from the fact that highly charged bacteria that repel one another are held far apart in the matrix of slimy gum. These aggregates look large, wispy and diffuse.

In high NaCl, the aggregates look tighter and more orange and in high $CaCl_2$, they are an even smaller and a shinier orange. Their tighter looking appearance is predictable from the zeta potential values; at low NaCl, the zeta potential is only -3.2mV while for high $CaCl_2$ it is closer to 0 at -0.36mV. Thus repulsion is reduced and other attractive forces can dominate behaviour.

The theory also ignores the effect of calcium ions on gellan gum (see section 3.2.5.3). Addition of any cation promotes gelation (Burne & Sellen (1994)) but calcium has a particularly marked effect, causing a greater degree of gelation at lower concentrations than other cations (Sutherland, 1994). In fact, all three bacteria exhibited a higher viscosity in the presence of a high ionic strength of calcium, with a slightly lower value for a high NaCl concentration. This contradicts the theory presented in Nazzal and Wiesner (1994) that postulates the apparent viscosity should decrease at high ionic strengths, because the Debye length is smaller.

8.2.2.3 P.putida

The tendency of *P.putida* to aggregate cannot be predicted from the theory of Ohman and Glatz (1999), since all the hydrophobicity measurements are low. The highest hydrophobic value is for high calcium with BSA. However, aggregation in both high NaCl, high $CaCl_2$ and in the presence of BSA with high ionic strengths was easily visible to the eye. The size of the aggregates tended to fall between that of the other two bacteria.

8.3 Operational conditions

The majority of experiments were performed with washed cells in solutions of different ionic strength and valency at pH 6.6. Experiments were performed in these solutions both with and without 1 g/l BSA. See Table 8.2 for details. The cell concentration for each experiment was around $7.5x10^8$ cells per ml, with a deviation of $0.5x10^8$ cells per ml allowed either way.

Their filtration properties were tested at 23 °C using a hydrophilic Optimem 300 membrane module, a crossflow velocity of 0.24 m/s and a steady state transmembrane pressure of 0.5 bars. When pressure transducers were inserted into the rig, it was found that the initial TMP was not at the steady state value of 0.5 bar; it rose rapidly from its

starting value of 0.14 bar to 0.5 bar within the first few minutes of a run. The time taken for this to happen depended on the initial rate of fouling for each experiment. Even when the target TMP was established variations in pump power meant that TMP, flux and resistance all fluctuated slightly. Each run lasted 90 minutes.

	Solution only	**With protein**
Low NaCl	0.1 g/l or (1.71 mmol/l)	& 1 g/l BSA
High NaCl	40 g/l or (680 mmol/l)	& 1 g/l BSA*
Low $CaCl_2$	0.6 g/l or (17.1 mmol/l)	NOT PERFORMED
High $CaCl_2$	29.5 g/l or (680 mmol/l)	& 1 g/l BSA

Table 8.2 Summary of the cell suspension conditions for experiments.

* No results for *P.elodea*

8.4 Methods of experimental analysis

Each type of run was analysed both experimentally and theoretically. Some comments on the main types of analysis are listed below. Details are in chapters 6 and 7.

1) ***Resistance***- this is easier to interpret than flux once the fouling rate becomes low.

2) ***Cell deposition***-cell deposition is expressed in terms of cell layer equivalents or 'CLEs'. These are not accurate estimates of the number of cell layers, since they assume the cells are stacked bricks with no voidage between them. Nevertheless, it is a quick and easy method to compare the cell deposition between experiments.

3) ***Comparison of percentage rates of increase of resistance and cell deposition***- this can help to understand the fouling mechanisms involved for each type of organism, and help to interpret the specific cake resistance results.

4) ***Specific cake resistance or SCR***- this calculation is derived from the total resistance less the membrane resistance, and the cell deposition at a given time. As well as being able to compare the relative rates of change of SCR, it can also help to clarify fouling mechanisms, such as pore blocking and compressible cake. It must be made clear that this is only an *apparent* SCR, since the resistance taken does not differentiate between the resistance due to pore blocking and that due to cake filtration.

5) ***Analysis of repeat experiment data***-some experiments were repeated with a significant degree of success, but others were repeated because the specification

conditions were not met in some way; cells older than normal or with a higher starting crossflow velocity for example. Comparison of these failed experiments with those known to fulfil the criteria can also help to increase understanding of the most critical mechanisms. For example, when experiments were performed on cells 2-3 days older than normal, a greater proportion of fouling was irreversible, and the resistance was generally found to be higher.

6) ***Relationship between final flux and reversible fouling***- the relationship between these two parameters is clear for *S.multivorum* and *P.elodea*. A high final flux correlates with a high percentage of reversible fouling. However, the percentage recoveries for all experiments are clustered close to 100% for the smooth capsulate *S.multivorum*, while the results for the sticky *P.elodea* are more spread out. Below approximately 24 LMH, flux recovery for *P.elodea* is low (less than 60%) but not directly linked to the flux. The relationship between the two parameters for flagellate *P.putida* is less easy to distinguish.

7) ***Protein rejection and loss***- Examining the differences between protein behaviour during filtration can help to understand the interactivity of protein filtration and cell filtration.

8) ***Model approaches to determine type of fouling***- three model approaches based on one generic equation were applied. This equation was a development of Hermia's original equation by Field et al (1995). Approaches 1 and 2 were of limited use, due to the short period of time over which the models could be used, as they were based on a differentiation of the generic equation, with the gradient of just one line determining the fouling mechanisms present. Approach 3 however was based on the integration of the equation and was therefore more robust and applicable for a longer time period (see Figure 7.6 to Figure 7.15). Pore blocking, intermediate and cake filtration were modelled separately, and a straight line represented an active mechanism. Therefore interpretation of approach 3 made it easier to discern where there was an overlap in the existence of different fouling mechanisms.

9) ***1/J vs t***- This model is also based on Hermia's equation. A linear part to a curve determines the period of time over which the intermediate fouling mechanism is active.

10) ***Flux elbows***- a simple way to compare initial rates of fouling is to look at the relative timings of the flux elbows. The flux elbow is where the flux reduction rate starts to

slow. This analysis seems to compare well with the order of the start of the pore blocking mechanisms in approach 3.

8.5 Ionic strength

The importance of ionic strength in filtration behaviour is the result of the reduction in net charge, and therefore repulsion, when the ionic strength increases. This enables other forces such as hydrophobic bonding or specific bonding to take place more easily, allowing tighter packing of cells in the cake or an increase in aggregation. Ionic strength has a distinctive effect on resistance for all three bacteria: it increased resistance for *S.multivorum* and *P.elodea*, but decreased it for *P.putida*.

8.5.1 *S.multivorum*

Experiments performed in low NaCl were found to have the lowest resistances for this bacterium. Not only are the cells very negatively charged in this suspension, but the surface of this capsulate organism is very smooth. Therefore the cells were likely to be repelled both by each other and by the membrane.

Despite the cell deposition for *S.multivorum* in high NaCl being 2.4 times higher than low NaCl, the difference between the apparent SCR values is within the 13% experimental error for these measurements. Therefore, it seems that the main difference between the two is in the cell deposition volume and not the cake properties; each layer of cake for both high and low NaCl has a well ordered similar structure and the fouling due to pore blocking dominates. The additional cell deposition for high NaCL might be due to weak, easily disturbed forces causing enough aggregation to increase the cell number, but not to change the effective particle size.

The difference between high $CaCl_2$ and low $CaCl_2$ is much more significant and the reverse of the NaCl results. This time the SCR is 71% lower for high $CaCl_2$,. This phenomenon can be explained if the greater aggregation in high $CaCl_2$ leads to less pore blocking. The cake itself may have a lower hydraulic resistance if, as in the section above, the voidage is increased and/or the cells in the aggregates are less well ordered and thus the permeability of the aggregates is greater.

Unfortunately the model results were difficult to interpret for *S.multivorum*, due to the rapid intial rate of fouling. although it was noted that the pore blocking phase for high Ca^{2+} is the shortest of all of the experiments.

8.5.2 *P.elodea*

The highest final flux for the broth experiments was for *P.elodea*. It is postulated that the dispersive gellan gum cake must have large gaps allowing high fluxes at a relatively low ionic strength. If this were true, the charge and thus the repulsion would be reduced at high ionic strength and resistance would increase. The zeta potential results demonstrate how much the charge is reduced, but the increase in resistance for higher ionic strengths is even more convincing proof that this hypothesis is valid.

It should be noted that the effect of increasing the ionic strength on *P.elodea* cell deposition is opposite to that for the other two bacteria- the cell deposition ***decreases*** by a factor of 6.3 for NaCl and 4.77 for $CaCl_2$. The SCR on the other hand increases by a factor of 17 and 4.8 times respectively. The difference in SCR increase is reflected in the fouling rates. According to both approach 3 and the flux elbows, the fouling rate increases most dramatically for an increase in NaCl concentration. The flux elbow changes from 12 minutes for low NaCl to 1.5 minutes for high NaCl. On the other hand, the increase is less dramatic for $CaCl_2$, reducing the 12 minute low NaCl elbow by only 3 minutes. The apparent increase in both fouling rate and SCR can be explained if: -

1) pore blocking is much greater for high NaCl than the others. The shape of the SCR time curve supports this theory, which is similar to a typical *S.multivorum* with an early peak, followed by a drop.

2) cake compression and/or rearrangement exists. Judging by eye the high $CaCl_2$ aggregates were much denser than that of any of the others, therefore the potential for rearrangement or compression is much lower. This would account for the less dramatic increase in SCR.

8.5.3 *P.putida*

The number of layers stays around 18 or 19 C.L.E.s, regardless of conditions, except for high $CaCl_2$ at 27 CLEs. The lower resistance value for high NaCl can therefore be attributed to the theory of Meagher et al (1996), that is, the aggregates formed must be irregularly arranged, thus increasing the voidage. This may also be the case for high $CaCl_2$, which has larger aggregates. These larger aggregates can account for the higher cell deposition. They should also have large voidages between them, reducing the resistance even more.

8.5.4 Final flux versus flux recovery

A study of flux recovery versus final flux plots can help reveal some clear patterns of behaviour. All of the bacteria have the highest percentage recovery for low ionic strength solutions; repulsion between all cell species and the membrane is at a maximum at low ionic strengths.

S.multivorum and *P.elodea* also have the highest final fluxes for low ionic strengths. These two have more negatively charged zones than *P.putida*. Therefore more repulsion is likely between cells, thus maximising the final flux.

There is no correlation between high final fluxes and high percentage recovery for *P.putida*, the highest final fluxes are for high $CaCl_2$,. The fact that these two parameters do not correlate for this bacterium indicates that the fouling at the membrane surface is not necessarily the greatest contributor to flux decline in this case.

8.6 Valency

Valency is of interest in this study of fouling for two main reasons. The effect of increasing the valency of an ion is similar in part to increasing the ionic strength; for the same number of atoms around a particle, the effective charge is reduced twice as much. Since the charge on each atom is doubled, the double layer will be more tightly packed (Israelachvili, 1994). Therefore tighter packing, greater aggregation and a possibility of different types of bonding are also likely with an increase in valency. Divalent ions are also known for their importance in helping mechanisms such as polymer bonding (Duddridge and Pritchard 1979). In addition to these general points, calcium is of particular interest because it is known that BSA and the gellan gum on the surface both have a particular affinity for calcium.

8.6.1 High ionic strength effects

The effect of valency on bacterial fouling behaviour depends on whether protein is present or not. In its absence, the high NaCl suspensions have a higher resistance than the high $CaCl_2$ suspensions for all the micro-organisms. This is probably because the most common effect of a divalent ion is to form randomly packed aggregates, while high NaCl brings molecules closer due to weak, easily disturbed bonds, without disturbing regular packing. This theory supports the two observations previously made,

- that the SCR for *S.multivorum* is lowest for high $CaCl_2$

- that the cell deposition decreases more and the SCR increases more for NaCl, when high and low ionic strengths are compared for *P.elodea*.

8.6.2 Low ionic strength effects

The effect of valency on resistance at low ionic strengths is more species specific. The tenfold difference in ionic strength of these solutions ($CaCl_2$ being the stronger one) must be taken into account.

Again the hydrodynamic effects seem to dominate for *S.multivorum*, as neither the change in valency nor ionic strength affects the final resistance, leaving it at around $50x10^{10}m^{-1}$. The cell deposition is only slightly reduced, from around 5.4 to 3.1 CLEs.

The results for *P.elodea* reveal that valency is more important than the ionic strength increase in determining fouling here. An increase in ionic strength with no change in valency increases the resistance. An increase in valency with no change in high ionic strength decreases the resistance. The results for low $CaCl_2$ coincide with the latter trend and concur with the fact that gellan gum has a particular affinity for Ca^{2+}.

The fact that *P.putida* in low $CaCl_2$ has a higher final resistance than in low NaCl does not agree either with the high ionic strength valency trend or with the same valency ionic trend, which both predict that the low NaCl solution should have a lower resistance. This observation may be explained in similar terms to the effects of high ionic strength on resistance. The ionic strength of the low $CaCl_2$ suspension will decrease the charge on the cell and flagella, thus encouraging a tighter cake and higher resistance, without causing aggregation. An increased opportunity for pore blocking should also follow.

8.6.3 Final flux versus recovery

S.multivorum is insensitive to the change in valency for NaCl and $CaCl_2$, with little difference in either final flux or percentage recovery between the experimental results for the two solutions of comparable ionic strength. Reversible fouling lies between 72 and 100% recovery for this organism.

Conversely, the importance of valency when determining either parameter appears more important than ionic strength for *P.elodea*. $CaCl_2$ suspensions always have the highest final fluxes/reversible fouling when experiments of similar strength or with BSA added are compared, once more demonstrating the importance of Ca^{2+} for this organism. Even the increase in ionic strength for low $CaCl_2$ does not reverse this trend. The proportion of reversible fouling for *P.elodea* is less than for *S.multivorum* on average,

the highest being for low $CaCl_2$ at 91% and the lowest at only 48% for high NaCl. Thus the gellan gum appears to promote cell adhesion to the surface of the membrane. It is likely to be on the surface of the membrane, because it was possible to chemically clean the membrane back to its previous clean water flux (CWF), with the help of pulsed flow and the inclusion of bubbles.

For *P.putida*, there is a strong valency effect only when the ionic strength is high; the final fluxes for all high $CaCl_2$ experiments are much higher than for the rest of the experiments (fig 6.27). Low $CaCl_2$ however, has a final flux and percentage recovery similar to that of low NaCl.

Again the spread of recovery figures is wide, with a 96% recovery for low NaCl, but a recovery of only 54% for high $CaCl_2$. Even with the cleaning regime mentioned above, a highly fouled membrane such as this would not be easily cleaned. This would be revealed either by a low CWF or by visible signs of foulant leaving the membrane module upon start up, despite a high CWF. Since these bacteria are of an equivalent size to the others, it is unlikely this is a result of more small bacteria blocking just inside the pores. That type of fouling should be removed by strategies such as pulsing and bubble introduction anyway. Therefore it must have something to do with the unique character of the *P.putida* cell.

The distinctive part of the extracellular matrix is the many flagella on its exterior, made of a homologous proein caled flagellin. These flagella are firmly secured to the inner surface of the cell membrane, and are therefore difficult to remove from the cell. They are very thin, only 0.01-0.2 μm thick, and also very long, up to 10 μm, so they can overcome the secondary minimum of a large surface quite easily. This is especially true in high ionic strengths, when the electrostatic repulsion is reduced. Thus their structure is similar to that of Dextran. Marshall, Munro & Trägårdh (1993) found that Dextran tends to foul ultrafiltration membranes by dangling down into the pores and adhering to the pores in parts along its length. If flagella have similar behaviour, attaching when cells occupy part or all of a space over a pore mouth, the cell s could not be removed by surface cleaning alone.

8.7 BSA

BSA could affect fouling in more than one way. At 11.6x2.7x2.7nm, the protein was significantly smaller than the rated membrane pore size of 0.2 μm. Therefore at low ionic strengths, standard blocking inside the pores was likely, thus affecting the flux if

enough cells were deposited. Adsorption of a monolayer of proteins on the cell surface is also possible. This is called conditioning, and can affect cell-membrane interaction.

However, at high ionic strengths, BSA has a tendency to oligomerise, either by thiol-disulphate cross-links or via surface hydrophobic regions (personal communication, Malcolm Povey, February 2001). Therefore the fouling mechanism for BSA at high ionic strengths was more likely to be on the membrane surface, i.e. pore blocking or gel layer formation. This is particularly true for high $CaCl_2$, as BSA has a special affinity for calcium, as one of the major functions in blood is to store and transport calcium around the body.

The only controls to exhibit any increase in resistance were those of BSA in high NaCl and high $CaCl_2$, but the resistance was at least ten times lower than that obtained in experiments with cells present. All the resistances changed more than 10%. Therefore the resistances were not additive, which agrees with results reported by other sources (Hodgson *et al*, 1993; Foley, 1995 and Field *et al.*, 1995).

The specific cake resistances increased upon addition of BSA, for all bacteria and nearly all electrolytes.

8.7.1 *S.multivorum*

The effect of protein addition is particularly marked in *S.multivorum* where the final resistances are very close (around $80x10^{10}m^{-1}$) which is between the high and low ionic strength values. BSA must therefore ensure that hydrodynamic considerations dominate once more. Therefore it is likely that its effect is evident at the start of the run. This mechanism did not adversely affect the reversible fouling. BSA also has a modifying effect on cell deposition for high NaCl and $CaCl_2$; addition of BSA reduces the final cell deposition values for high ionic strength suspensions down to a similar value as for the low ionic strength suspensions, i.e. below 6 CLEs. In the case of high $CaCl_2$, with BSA, the reduction occurs after an initial deposit of 12 CLEs near the start of the experiment.

In spite of this unifying effect on cell filtration behaviour, neither the protein loss nor the protein rejection figures were similar for the three *S.multivorum* experiments with BSA. This suggests that deposition in the pores may have been different.

8.7.2 *P.elodea*

The presence of protein in a *P.elodea* suspension seems to increase the resistance for all circumstances. Like a biofilm on a pipe, the gellan gum can entrap the protein in its matrix, thus reducing the voidage and increasing the resistance (see section **2.4.4**).

The percentage recovery/ resistances values for all BSA runs for *P.elodea* are in between those of high and low ionic strength suspensions alone, as for *S.multivorum*. However, for percentage recovery only, the low flux values are similar to those of high ionic strength experiments.

Analysis of the modelling results show that the fouling rate in the presence of BSA was much greater, with the flux elbow at 5 minutes, compared to 12 minutes without BSA. Modelling also indicated that this was due to an increase in pore blocking. The increase in pore blocking may also account for the fact that the presence of BSA in low NaCl suspensions increased the apparent SCR by a factor of 7, and decreased cell deposition by a factor of three.

8.7.3 *P.putida*

The effect of BSA on the fouling behaviour for *P.putida* in NaCl suspensions was similar to that for *S.multivorum*; although the resistances in high and low NaCl alone were very different, they were very close when BSA was added. There was a possible slight reduction in cell deposition too, but it is too slight to be statistically significant. Another phenomenon similar to that seen in *S.multivorum* was that addition of BSA also reduced the cell deposition volume for high $CaCl_2$ to a figure similar to that of the other experiments at 19 CLEs.

8.7.4 Protein oligomerisation

For *P.putida*, protein loss and rejection were 55 and 42% higher for low NaCl than high $CaCl_2$. It is likely that agglomerated cells prevented the penetration of the BSA, which would have been polymerised. Since the cake formed by BSA in $CaCl_2$ was only $3.7x10^{10}m^{-1}$, the contribution of a BSA gel layer to the overall flux was likely to be low.

This hypothesis is supported by the results for *P.elodea*; while the resistance increase on addition of protein was 143% in low NaCl (a standard blocking mechanism), it was only 23% for high $CaCl_2$, where oligomerisation would have been occurring.

The protein loss was significant for all species in high $CaCl_2$ (between 9 and 13 % compared to 4.1% in the control). Conversely the transmission was very high for the

Pseudomonas species (99.9% and 99.7%), but not for *S.multivorum* (88%). High protein loss and high transmission concurs with the theory of BSA gel formation.

8.7.5 The effect of BSA on shear

BSA affects the cell deposition behaviour of all three organisms. As previously mentioned, it cancels out the increased cell deposition effect for high ionic strengths in *P.putida* and *S.multivorum*. For *S.multivorum* and *P.elodea* in high $CaCl_2$, it seems to make the cakes more prone to shear. The C.L.E. values for both of these experiments fluctuate over time, with the results for *S.multivorum* being particularly variable. The overall cell deposition may have been evenly spread throughout each of the 40 capillary tubes of the module. Alternatively, some tubes may have become completely blocked, while others were almost free of cells. At the end of some experiments, some tubes appeared to be completely blocked when one end of the module was removed. The cyclical behaviour of cell deposition for *S.multivorum* displayed in figure 6.10 implies that at best, some of the change must be due to the fact that cell deposition narrows the tube, thus affecting the hydraulic diameter. Therefore with a decreased diameter, the shear must increase according to this equation, probably to a critical level for shearing some of the cake away. Shear can be calculated thus:

$$\tau_w = \frac{\Delta P_L D}{4L} \qquad \textbf{Equation 38}$$

Comparing resistance increase with cell deposition shows that for the experiments with variable cell deposition, only some of the cells contributed to the resistance, since the resistance did not change with cell deposition variation for these experiments. This phenomenon supports the theory of some cells in all capillary tubes were swept away, rather than some tubes being blocked and others free. Since it becomes harder and harder for cells to deposit as the flux drops, a totally blocked capillary must occur within the first two minutes for *S.multivorum*, as that is when the greatest drop in flux occurs. For *S.multivorum* in high $CaCl_2$, the pore blocking phase lasted only for 12 seconds out of the 2 minutes to a flux elbow, so it is likely that the main part of the resistance for *S.multivorum* in high $CaCl_2$ and BSA is attributable to cake filtration rather than pore blocking.

8.8 Fouling mechanisms

A comparison of the relative levels of cell deposition and resistance in terms of percentage of their final value, and the changes over the course of an experiment, can

help in the comprehension of bacterial fouling. This is discussed below. A summary of the pertinent observations can be found in Table 6.29.

For the *Pseudomonas* bacteria, the percentage of the final total cell deposition tends to be above that of resistance at any given time before the end. For *S.multivorum* however, the opposite trend occurs, and the percentage resistance was found to be higher.

8.8.1 *S.multivorum*

A higher percentage resistance to percentage cell deposition may occur if pore blocking is the dominant mechanism at the beginning. The hypothesis that pore blocking dominates the fouling behaviour for this bacterium is supported by the specific cake resistance (SCR) results, where there is generally a peak early on in the runs before a subsequent decline, and the values tend to be relatively high. Even for high $CaCl_2$, where the SCR plot for is very variable, it can still be demonstrated that it is the cells closest to the membrane that dominate fouling, since although the cell deposition varies wildly, the resistance continues to increase.

This proves that the measured specific cake resistance is an ***apparent*** SCR for these experiments, since it is difficult to determine how much of a resistance can be attributed to cake filtration and how much to pore blocking at the start. The decline in flux for *S.multivorum* is much more rapid at the beginning than for the other two, and the pore blocking mechanism reveals itself within the first 30-60 seconds of the runs when modelled. This behaviour is commensurate with a significant proportion of pores becoming blocked, leading to a rapid increase in resistance. The rapid fall in flux may be the reason that the final cell deposition is usually relatively low. As the flux is low for almost the entire run, the amount of convection to the surface is also low. The intermediate pore blocking mechanism was tested by plotting 1/J against T, as well as by approach 3. Comparison of these models seems to indicate that intermediate blocking for approach 3 may not be true intermediate blocking, but merely cake filtration and pore blocking existing simultaneously; generally the three model lines are parallel at the start with the same starting time.

Even in high $CaCl_2$ where the cells are visibly aggregated, there is evidence that pore blocking makes a notable contribution to the overall increase in resistance. Comparing the apparent SCR and cell deposition values for low and high $CaCl_2$, the cell deposition for the latter is ten times higher while the apparent SCR is just four times lower. A comparison of the same parameters for high and low NaCl indicates a similar SCR for

the two, even though the cell deposition is different. Both these observations suggest that it is pore blocking that is making the greatest contribution to increase in resistance. The theory that pore blocking is the dominant fouling mechanism also concurs with the fact that fouling reversibility is highest for this organism. Once the pressure difference ceases across a blocked pore, it will be released from the pore entrance and can easily be flushed away (Howell & Aimar, 1984).

8.8.2 *P.elodea*

For *P.elodea*, 90% or more of the cells were deposited in the first 12-30 minutes for all experiments. Meanwhile the resistance continued to increase steadily until the end of the run. Therefore percentage cell deposition was always higher than percentage resistance.

This behaviour for *P.elodea* can be interpreted using either or both of the following theories:

- The cells rearrange themselves once deposited
- The cells or their ECM are compressible.

Fu and Dempsey (1998) found that particles, especially small ones, could navigate through a cake and tend to concentrate at the membrane surface, thus lowering the flux. They found that this activity favoured a well coagulated, permeable cake. When the *P.elodea* cake is diffuse, as in the low ionic strength solutions, the cells may be able to work their way through the cake, especially the smaller, more rotund ones of approximately $0.6\mu m^2$.

On the other hand, the compressibility of gellan gum is high, as there is a high degree of water present (Shimuzu et al, 1993) and therefore the second theory is possible for all of the experiments. Compressible cake also allows parallel alignment of cells next to the membrane. This decreases the voidage and hence increases the resistance. This compressibility would also help to explain why *P.elodea* displays evidence of intermediate pore blocking for approach 3, although its graphs are of a different shape to that of *P.putida*. When a cake is compressible, some cake may collapse into the pores, thus simulating pore blocking.

8.8.3 *P.putida*

The graphs for *P.putida* reveal that there is also usually a steady increase both in resistance and cell deposition until the end of the run (see appendix C), but for this bacterium the percentage cell deposition is always higher. This behaviour can be

explained if the first cells to deposit do not contribute as much to resistance as the later cells, and the SCR increases over the course of an experiment. It is possible that for some of the runs, the cells are laid down as in the experiments described by Tanaka et al, (1994, 1996), who also found the SCR increased during the run. Examination of the cake formed throughout a run gave a clue to what was happening. At the start of operation, when the flow towards the membrane was high, the cells were deposited randomly, as they would be in a comparative dead end filtration experiment. The next phase of deposition occurred when the drag force of the crossflow velocity started to become comparable to the lift force. This effect aligned new cell deposition parallel to the membrane. The final phase of arrangement occurred when cells nearest to the membrane also became aligned to the membrane surface. This last observation might be an effect of compressibility, occurring only when pore blocking was negligible. However this last phase seems unlikely for many of the *P.putida* experiments, because intermediate pore blocking exists and some cakes are incompressible.

8.8.4 Reversible fouling factors

The importance of the first few minutes in determining fouling is emphasised by the graphs obtained when comparing the resistances and cell deposition rates of three *S.multivorum* experiments. It seems clear that the more rapid the rate of increase in resistance during the first 12 minutes, the greater the final value for either parameter.

A comparison of the specific cake resistance, cell deposition and fouling rate for *P.elodea* in low NaCl reveals an interesting correlation. When BSA was added, the SCR increased from $1.4x10^{10}mkg^{-1}$ to $9.8x10^{10}mkg^{-1}$ with a commensurate increase in fouling rate. The flux elbow was at 12 minutes without BSA, but only 5 minutes when BSA was added. Approach 3 predicts cake filtration occurring soon after the start of the run for low NaCl alone. When BSA is present however, the cake filtration model only began to work 12 minutes into the experiment. Therefore the increase in fouling rate shortened the time for cake deposition and thus the total cell deposition was lower and the SCR was higher. This is similar to that of *S.multivorum*, whose fouling behaviour it partly mimics

8.9 Hydrodynamic versus physicochemical effects

For *P.putida* and *S.multivorum*, cell deposition seems independent of BSA addition and electrolyte composition, apart from conditions where a degree of aggregation is likely, i.e. for high ionic strengths. For *S.multivorum*, the only

experiments to have a deposition of more than 6 CLEs are in high NaCl and high $CaCl_2$. For *P.putida*, the cell deposition is only increased in high $CaCl_2$. The presence of protein seems to ensure that aggregation is reduced and hydrodynamic rather than physicochemical effects dominate for all experiments, regardless of ionic complexity. This means that the cell depositions for high ionic strengths are reduced to figures similar to low ionic strengths once more. It is likely that since pore blocking is known to exist in both organisms (pore blocking dominates for *S.multivorum*, while intermediate blocking is common for *P.putida*), it is the rate of pore blocking that determines cell deposition. This is determined predominantly by hydrodynamic factors.

P.elodea on the other hand produces aggregates under all conditions; it is just the type and size that differs. Therefore the consistency of the cake formed is important, and the significance of physicochemical parameters for cell deposition determination is high for this organism. The highest cell deposition occurs when the aggregates are large and diffuse. The cell deposition results for *P.elodea* correlate with both the times to fouling predicted by approach 3 and the flux results, with the exception of the two lowest fluxes, which are close in value. To clarify:

- The slower the fouling rate, the higher the final cell deposition
- The higher the final flux, the higher the cell deposition.

The order of importance of these parameters, from the highest to the lowest values, is

- Low ionic strength
- Presence of BSA
- Increase in valency.

The correlation between these three parameters is less clear for the other two organisms. Cell deposition is hydrodynamically determined, with a common value particular to the species. The only values to differ significantly are those that encourage aggregates, i.e. high ionic strength only, especially high $CaCl_2$. The presence of BSA increases the fouling rate of *P.putida*, as it does for *P.elodea*. Valency and ionic strength also change the fouling rate for *P.putida* in a similar way to *P.elodea*. *S.multivorum* on the other hand fouls rapidly whatever the conditions, due to the dominance of the pore blocking mechanism.

8.9.1 Repeat experiments

Old cells created a greater proportion of irreversible fouling than the cells of a standard age for all species. This may be due to an increase in leakiness of the cells, thus increasing the opportunities for conditioning of the membrane or perhaps due to cell breakdown creating smaller particles. See section **2.3.6** for more details.

Approach 3 was applied to the results for one successful experiment and one repeat experiment with old cells for *P.elodea* in high $CaCl_2$. It was found that the increase in resistance and decrease in cell deposition could be accounted for by an increase in fouling rate for the old cells.

9 Conclusions and Future Work

Three species of gram negative bacteria of similar rod dimensions were selected for their different extracellular matrix properties.

1) *S.multivorum* NMIB 12558 with its smooth polysaccharide capsule

2) *P.elodea* NMIB 31461 with its slimy, loose polysaccharide (gellan gum) covering

3) *P.putida* NMIB 9494 covered with long flagella.

All experiments carried out were performed under similar operating conditions; a crossflow of 0.23 m/s and steady state transmembrane pressure of 0.5 bar at 23 °C. The initial experiments were performed in broth. From the initial broth experiments, it could be seen that all three organisms had high reversible fouling, with *S.multivorum* having the highest. P.elodea exhibited the highest final flux. Both these phenomena concurred with the subsequent filtration experiments. These were performed with washed cells in NaCl and $CaCl_2$ salt solutions of different strengths in a weak phosphate buffer of pH 6.6. Further experiments were performed with BSA added to all the types of cell suspension (except low $CaCl_2$), in order to help to understand the effect of protein on cell filtration performance.

Table 9.1 Summarises the main observations made on the filtration behaviour of the three species of bacteria.

	S.multivorum	*P.elodea*	*P.putida*
Compressibility	Always incompressible	Always compressible	Depends on conditions Incompressible with protein
Cell deposition	Constant low figure except for high ionic strengths	Depends on ionic conditions	Constant high figure. Increases with high $CaCl_2$
Linkage	Flux and reversible fouling	Final flux, fouling rate and cell deposition	Flux and fouling rate
Change in resistance With ionic strength increase	Increase due to more cell deposition of similar SCR	Increase due to tighter cake	Decrease due to more random aggregate packing
Factor governing cell deposition	Hydrodynamic except for high ionic strengths alone	Physicochemical	Hydrodynamic except for high $CaCl_2$ alone
Factors governing resistance	Presence of protein Hydrodynamic at low ionic strengths	Physicochemical	Presence of protein for NaCl only Physicochemical
Fouling mechanism	Pore blocking very important	Intermediate and cake filtration important	Intermediate blocking common
Reversible fouling range	89-100	65-100	72-100
Cleanability	High	Medium	Low

Table 9.1 Summary of trends for all three bacteria

9.1 Common trends for all bacteria

While the sensitivity of different bacteria to changes in valency of low ionic strength suspensions is variable, high calcium solutions have a dramatic effect on all cells; fouling is always governed by physicochemical effects in these suspensions, due to the existence of aggregates.

Addition of protein will always change the resistance,

- to a similar value independent of ionic conditions in the case of all *S.multivorum* suspensions or *P.putida* in NaCl (i.e. hydrodynamic effects dominate)
- to a value in between that of high and low ionic strength suspensions only for *S.multivorum* and *P.elodea* (i.e. physicochemical effects are modified).

9.2 S.multivorum

Interaction with the membrane and other particles seems to be the lowest for this organism; its smooth capsule with highly negatively charged sites at low ionic strengths means that bonding is most difficult to achieve for *S.multivorum*. This results in the highest mean percentage of reversible fouling of the three bacteria, and all cakes being incompressible.

S.multivorum tends to foul predominantly by blocking pores. The rapid rate of this fouling mechanism at the start means that cell deposition (with the notable exception of high Ca^{2+}) tends to be low-below 6 CLEs- apart from in high ionic strength only suspensions. Thus at low ionic strengths and with protein, fouling is affected mainly by hydrodynamic forces. Although weak forces between cells increase the cell deposition to 13 CLEs in high NaCl only, the specific cake resistance is similar to that of low NaCl, since the fouling due to pore blocking still dominates. For high $CaCl_2$ however, the cells are in aggregates and the structure of the much larger cake (32 CLEs) becomes more important for determination of resistance, with an increase in ionic strength increasing the resistance. Thus for high $CaCl_2$ alone, physicochemical forces have a significant effect upon fouling.

9.3 P.elodea

P.elodea fouls by forming cake on the membrane surface, aided by its sticky gellan gum extracellular matrix. The high water content of this gum ensures that the relatively thick cakes formed are compressible. The stickiness ensures that there is

greater variation in the reversibility of fouling between suspension types than for *S.multivorum*, although foulant can be easily removed chemically.

The filtration behaviour of *P.elodea* is profoundly affected by the physicochemical conditions of the suspending medium, acting contrary to expectations and the other bacteria's cell deposition behaviour. In low ionic strengths, both flux and cell deposition are at their highest, thus producing ideal conditions for cell recovery. This time it is high NaCl that alters the cell deposition the most. This strong influence of physicochemical forces on both cell deposition and resistance can be explained by the fact that *P.elodea* aggregates under all conditions. Thus the changes in resistance is no longer due to increased aggregation, but a change in the type of aggregation. At low ionic strengths, the aggregates are dispersive, forming diffuse wispy aggregates to keep the negatively charged cells far apart in a stable matrix. At high ionic strengths however, the aggregates appear denser. Thus the increase in resistance is a result of a tighter cake with fewer cells.

This species is also unusual in that all the cells forming the final cake are laid down only within the first 12-30 minutes of the experiment, presumably as a result of their large aggregate size. Nevertheless resistance continues to increase throughout the experiments, due to either compression or cake rearrangement or both.

9.4 P.putida

Even though hydrophobicity is low for this bacterium, the presence of flagella means that opportunities for cell-cell and cell-membrane interactions are increased. For example, the presence of the long flagella of *P.putida* seems to affect the reversibility of fouling for this organism. Although the range of reversibility of fouling might be narrower than that of *P.elodea*, the remaining foulant may be difficult to remove chemically, especially after experiments in high ionic strengths. This may be attributed to the flagella entering the pore mouths and attaching inside the pores at several points along their length. The variable orientation of these flagella may also explain the fact that some of the cakes are compressible and the rate of fouling is usually slower than for the other two micro-organisms, indicating that the flagella are hydrodynamically active. Intermediate pore blocking is dominant for this organism.

The effect of an ionic strength increase on the resistance for *P.putida* is the converse of the other two species because it results in a resistance decrease. This can be attributed to the reduction in ordered packing in the aggregates. Apart from high $CaCl_2$,

the cell deposition is very close for all the experiments; therefore it must be the structure of the cake that is changing. For high NaCl, the SCR is lower than for low NaCl, which endorses this hypothesis.

The fact that *P.putida* has a similar cell deposition level (16-19 CLEs) for all conditions apart from high $CaCl_2$ alone (27 CLEs) shows that with this one exception, this parameter must be hydrodynamically determined. The strong physicochemical effects of the high concentration of the Ca^{2+} ion ensure that the balance is shifted slightly for this case.

9.5 Future work

Although care was taken to find bacteria of similar dimensions, a better understanding of the fouling phenomena would be gained if the size and size distribution of the cells and aggregates in each type of solution were to be measured. Possible methods include video imaging, as for the individual cells in this thesis, or a laser-based method, such as a Zetasizer. Further experimentation should not necessarily be on solutions of different strengths, as research indicates that a wider variety of behaviour can be observed by varying the pH (Cozens-Roberts, 1990). If this is the case, determination of the cells' isoelectric points must be made, by determining the N/P ratio for example. Mozes *et al.*,(1989) pointed out that the nitrogen present correlates to the positively charged amino groups and the phosphorous correlates to the negatively charged phosphates.

Another method to increase understanding of micro-organism fouling is by using a flat sheet membrane. This allows imaging, unlike a capillary membrane. Imaging can help to investigate how cakes change over the course of the run, and help to verify which fouling mechanisms are occurring and if any cake compression is occurring. For example electron microscopy might be employed, and membrane characterisation using techniques such as FTIR can be undertaken, which was not possible with the membrane used in this study.

The fact that addition of BSA to all types of *S.multivorum* and some *P.putida* suspensions modifies the final resistance to a similar number has been observed. To help to find the mechanism responsible, the distribution of the protein deposition must be investigated. Greater protein concentrations that are easier to measure must be used, and tests for protein concentration must be performed on the cells, the supernatant and the

membrane during experiments of varying length. This can show how the protein distribution changes over time.

The hypothesis for the involvement of flagella in irreversible membrane fouling for *P.putida* may be tested by comparing the behaviour of two strains of the same bacteria, differing only in their presence of flagella. Such strains of *P.putida* exist, the strains in Buell *et al.* (1993) for example. The effect of the gellan gum on filtration behaviour could also be tested on the *P.elodea* gellan mutant (Fialho *et al.* (1991)). This is the same strain as the one used in this thesis.

Lastly the phenomena of cyclical shearing may be better understood if the apparatus was set up to allow the retentate line to be diverted via a spectrophotometer, thus allowing constant sampling.

10 Nomenclature

σ = Blocked area per unit volume of filtrate (m^{-1})

ε= Cake voidage

ρ= Density of retentate (kgm^{-3})

θ= Force per bond in N

ϕ= Friction coefficient

γ= Interfacial tension

Π= Osmotic pressure in Pa

α= Specific cake resistance in mkg^{-1}

τ= Torque set up by the fluid in Nm

μ= Viscosity in centipoise

ζ= Zeta potential in mV

ε_0 = Initial membrane surface porosity

δ_C= thickness of layer in m

ΔG= Gibbs free energy (Joules)

ΔP= transmembrane pressure in Pa

ΔP_L= longitudinal pressure drop in Pa

ε_R = relative permittivity to a vacuum

τ_w*= critical erosion shear stress in Nm^{-2}

τ_w= wall shear stress in Nm^{-2}

τ_{weff}= effective shear stress in Nm^{-2}

A= area of membrane surface in m^2

a= area of one cell in m^2

C= Cell concentration of suspension in cells/ml

C_a= Cell concentration in aqueous phase after hydrophobicity test in cells/ml

C_b= Cell concentration in aqueous phase before hydrophobicity test in cells/ml

C_d= Cells lost from retentate in cells per ml

c_i= Ion concentration in moles/l

D= Hydraulic diameter in m

D_p= Particle diameter in m

F(f)= Friction force in N

$F(x_1)$= Drag force due to crossflow in N

$F(x_2)$= Normal force in N

$F(y_1)$= Convective force due to flux in N

$F(y_2)$= Lift force in N

F= Force in N

f= Fanning friction factor

G = Constant ($s\ m^{-2}$)

J*= Flux at final equilibrium in LMH

J= Flux in LMH

J_0= Initial flux in LMH

K= Binding constant

k_c = Cake filtration constant ($kg\ m^{-3}$)

K_H= Hermia's filtration constant

K_n= Filtration constant for Field and Aimar's generic equation

k_s= Filtration constant

L= Length of filter in m

M_C= Mass of one cell in kg

M_T= Total dry mass in kg

P_1= inlet pressure in Pa

P_2= outlet pressure in Pa

R= resistance in ms^{-1}

R_0 = Initial hydraulic resistance (m^{-1})

R_c= Resistance due to cake in ms^{-1}

R_l= Resistance due to particle layer in ms^{-1}

R_m= Resistance of membrane in ms^{-1}

r_p= Particle radius in m

R_p= Resistance due to pore blocking in ms^{-1}

R_T= Total resistance in ms^{-1}

S= Separation distance in m

t= Elapsed filtration time in minutes

u_E= Electrophoretic mobility

v= Crossflow velocity in ms^{-1}

V= Filtrate volume in ml

v_0= Initial crossflow velocity in ms^{-1}

v_J= Velocity of permeate in ms^{-1}

V_s= Suspension volume in ml

W= Weight of cake deposit in kg

z_i= Valency

11 Glossary

Ampiphilic-a molecule with both a hydrophobic and a hydrophilic part.

Antibody-a specific protein that attaches to a specific antigen to render it harmless

Antigen- a specific protein or carbohydrate, often found on a cell surface which can generate production of antibodies, to which it bonds specifically.

Conditioning-a thin layer of macromolecules, especially proteins, covering a surface. Conditioning often affects cell adhesion to a surface.

Couple-two equal and opposite forces acting upon a body

Extracellular matrix- a general term to cover all macromolecules attached to the surface of a micro-organism

Gellan gum- slimy polysaccharide covering the surface of *P.elodea*

Ligands-Specific donors of electrons to receptors

O side chains-Long polysaccharide part to a lipopolysaccharide antigenic determinant

Peritrichous- covering the whole surface.

Proteolytic- able to break down proteins for an energy source

Receptor-specific receivers of electrons from ligands, antibodies etc.

Specific bonding-the bonding of a specific receptor-ligand pair. It also includes identical ligand-ligand and receptor-receptor bonding.

Stochastic- containing an element of probability

Polymer bridging- the joining together of two bodies, or a body and a surface by attachment of sections of polymer to both entities.

Glycocalyx-layer of carbohydrates and glycoproteins surrounding the cell surface

Taxis- Use of motile equipment such as flagella to move towards a stimulus

11.1 Abbreviations

CF- crossflow

CFMF-crossflow microfiltration

CLE- cell layer equivalents

CWF- clean water flux

CSH- cell surface hydrophobicity

CWF- clean water flux

ECM- extracellular matrix

GMP- good microbiological practice

LMH- $lm^{-2}h^{-1}$

MF- microfiltration

SCR- specific cake resistance

SD- standard deviation

SEM- scanning electron microscopy

TEM- transmission electron microscopy

TMP- transmembrane pressure

12 References

Advisory Committee on Dangerous Pathogens (1990). Categorization of pathogens according to hazard and categories of containment. H.M.S.O., Second Edition.

Aimar P., Howell J.A, and Turner M. (1989), Effects of Concentration Boundary Layer Development, *Chemical Engineering Research & Design*, 67, May, pp. 255-261.

Airey, Yao, S., Wu, J., Chen, B., Fane, A.G., Pope, J.M. (1998). An investigation of concentration, polarization phenomena in membrane filtration of colloidal silica suspensions by NMR micro-imaging. *Journal of Membrane Science*, 145, pp. 145-158.

Altmann, J. and Ripperger, S. (1997). Particle deposition and layer formation at the crossflow microfilration. *Journal of Membrane Science*, 124, pp. 119-128.

Andrade, J.D. ed.(1985). *Surface and Interfacial Aspects of Biomedical Polymers. Volume II*, Protein Adsorption, Plenum Press: New York and London. pp.4-19.

Areekul,S., Vongsthongsri, U., Mookto, T. and Chettanadee, S. (1996). *Sphingobacterium multivorum* Septicaemia : A Case Report. *Journal of the Medical Association of Thailand*, 79, (6). p.395.

Belfort, G. (1989). Fluid Mechanics in Membrane Filtration: Recent Developments, *Journal of Membrane Science*, pp.123-147.

Bell, G. I. (1978). Models for the Specific Adhesion of Cells to Cells. *Science*, 200, May pp.618-627.

Bell, G.I., Dembo, M.& Bongrand (1984). Cell Adhesion: Competition between Non-specific Repulsion and Specific Bonding., *Biophysical Journal*, 45, June, pp. 1051-1064.

Bergey's Manual of Systematic Biology. volumes 2 and 3. (1989). J. G. Holt editor, Fifth Edition. London: Williams and Wilkins Co. pp. 93-97.

Bergey's Manual of Determinative Biology. (1994) . J. G. Holt editor, 9th Edition. London: Williams and Wilkins Co. p.p. 256-265.

Bishop, J.T. and Sanders, N. (1989). Bubble Flowmeter for Measurement of Low Permeate Flows in Ultrafiltration. Biotechnology Techniques, 3, (2),.

Bowen, W. R., Calvo, J.I. and HerƷandez, A. (1995). Steps of Membrane Blocking in Flux Decline during Protein Microfiltration. *Journal of Membrane Science*, 101, pp. 153-165.

Bowen, W. R. and Gan, Q. (1991a). Properties of Microfiltration Membranes: Adsorption of Bovine Serum Albumin at Polyvinylidene Fluoride Membranes. *Journal of Colloid and Interface Science*, 144, (1), pp. 189-200.

Bowen, W. R. and Gan, Q. (1991b). Properties of Microfiltration Membranes: Flux Loss during Constant Pressure Permeation of Bovine Serum Albumin. *Biotechnology and Bioengineering*, 38, (1), pp. 688-696.

Bowen, W. R. and Gan, Q. (1992). Properties of Microfiltration Membranes: The effects of Adsorption and Shear on the Recovery of an Enzyme. *Biotechnology and Bioengineering*, 40, pp. 491-497.

Bowen, W. R. and Gan, Q. (1993). Microfiltration of Protein Solutions at Thin Film Composite Membranes. *Journal of Membrane Science*, 80, pp. 165-173.

Bowen, W. R. and Hall, N.J. (1995). Properties of Microfiltration Membranes: Mechanisms of Flux Loss: the Recovery of an Enzyme. *Biotechnology and Bioengineering*, 45, pp. 28-35.

Bowen, W. R. and Hughes, D.T. (1990). Properties of Microfiltration Membranes part 2: Adsorption of Bovine Serum Albumin at Aluminium Oxide Membranes. *Journal of Membrane Science*, 51, pp. 189-200.

Bowen, W. R. and Jenner, F.(1995). The calculation of Dispersion Forces for Engineering Applications. *Advances in Colloid and Interface Science*, 56, pp. 201-243.

Bowen, W.R, Mongruel, A. and Williams, P.M. (1996). Prediction of the rate of Crossflow Membrane Ultrafiltration: a colloidal interaction approach. *Chemical Engineering Science,* 51, (18), pp.4321-4333.

Bowen, W.R. and Ventham, T.J. (1994), Aspects of Yeast flocculation, size distribution and Zeta potential. *Journal of the Institute of Brewing*, 100, pp.167-172.

Bowen, W.R. and Williams, P.M. (1995). Dynamic Ultrafiltration Model

for Proteins: a Colloidal Interaction approach. *Proceedings of Euromembrane 1995*, 1, pp. 148-151.

Brock T.D. ,(1983), *Membrane Filtration: A user's guide and reference manual*, first edition, Science Tech. Inc.: Wisconsin

Brown D.E. and Kavanagh P.R. (1987), Crossflow Separation of Cells. *Process Biochemistry*, 22 (4) August, pp. 96-101

Buell, C.R., Whetton, R., Tari, P., and Anderson, A.J. (1993). Characterization of Cell Surface Properties in Agglutinable and Nonagglutinable Mutants of *Pseudomonas putida*. *Canadian Journal of Microbiology*, 39, pp. 787-794.

Buffham, B.A. and Cumming, I.W. (1995). Prevention of Particle Deposition in Crossflow Microfiltration. *Transactions of the Institute of Chemical Engineers.*, 73, Part A, pp. 445-454.

Bunt, C.R., Jones, D.S. and Tucker, I.G. (1995). The Effects of pH, Ionic Strength and Polyvalent Ions on the Cell Surface Hydrophicity of *Escherichia coli* evaluated by the BATH and HIC Methods. *International Journal of Pharmaceutics*, 113, pp. 257-261.

Bunt, C R., Jones, D.S. and Tucker, I.G., (1993), The Effects of pH, Ionic strength and Organic Phase on the Bacterial Adhesion to Hydrocarbons (BATH) Test. *International Journal of Pharmaceutics.*, 99, pp. 93-98.

Burne, P. M. and Sellen, D. B.(1994). A Laser Light Scattering Study of Gellan Gels. *Biopolymers*. 34, pp. 371-382.

Chang, D.-J. and Hwang, S.-J. (1995). Unsteady state Permeate Flux of Crossflow Microfiltration : Effect of Particle Size Distribution. *Separation Science and Technology*, 30 (14), pp. 2917-2931.

Charm, S.E. and Wong, B.L. (1970). Enzyme Inactivation With Shearing. *Biotechnology and Bioengineering*, XII., pp. 1103-1109

Chellam, S. and Wiesner, M.R. (1997). Particle Back-transport and Permeate flux Behaviour in Crossflow Membrane Filters., *Environmental Science and Technology,* 31 (3), pp. 819-824

Chellam, S. and Wiesner, M.R. (1998). Evaluation of Crossflow Filtration Models Based on Shear- induced Diffusion and Particle Adhesion: Complications Induced by Feed Suspension Polydispersivity., *Journal of Membrane Science,* 138, (1), pp. 83-97.

Chen, V., Fane, A.G., Madaeni, S.and Wenton, I.G. (1997). Particle Deposition during Membrane Filtration of Colloids : Transition between Concentration Polarization and Cake Formation., *Journal of Membrane Science*. 125, pp. 109- 122.

Chung, Y.C., Huang, C. and Tseng, C.P. (1996). Biodegradation of Hydrogen Sulfide by a Laboratory Scale Immobilized *Pseudomonas putida CH11* Biofilter. *Biotechnology Progress*, 12 (6) pp.773-779.

Collins, C.H., Lyne, P.M. and Grange, J.M. (1995). *Collins' and Lyne's Microbiological Methods*. Arnold: London, Second edition.

Costerton J.W., Geesey G.G. and Cheng K.J. (1978), How Bacteria Stick, *Scientific American* Vol 238., pp. 86-95.

Cozens-Roberts, C., Quinn, J.A. and Lauffenberger, D.A. (1990). Receptor-mediated Adhesion Phenomena. *Biophysical Journal*. 58, July, pp.107-125.

Dahlbäck, B., Hermansson, N., Kjelleberg, S. and Norkrans, B. (1981). The Hydrophobicity of Bacteria- an Important Factor in their Initial Adhesion at the Air-Water Interface. *Archives of Microbiology*, 128, pp. 267-270.

Datar, R. (1985), Studies on the Separation of Intracellular Soluble Enzymes from Bacterial Cell Debris by Tangential flow Membrane Filtration. *Biotechnology Letters*, 7 (7), pp. 471-476.

Davis, R.H. and Leighton, D.T. (1987). Shear-induced Transport of a Particle Layer Along a Porous Wall. *Chemical Engineering Science*, 42, (2), pp. 275-281.

Davison, A.D. and Veal, D.A. (1997). Synergistic mineralization of biphenyl by *Alcaligenes faecalis type II BPSI-2* and *Sphingomonas paucimobilis BPSI-3. Letters in Applied Microbiology*, 25, pp. 58-62.

De Weger, L.A., Van Loosdrecht, M.C.M., Klaassen, H.E. and Lugtenberg, B. (1989). Mutatational Changes in Physicochemical Cell Surface Properties of Plant-growth-stimulating *Pseudomonas spp.* Do Not Influence the Attachment Properties of the Cells. *Journal of Bacteriology*, 171 (5), pp. 2756-2761.

Defrise, D. and Gekas V. (1988), Microfiltration Membranes and the Problem of Microbial Adhesion-a Literature Survey., *Process Biochemistry*. (August) pp.105-116

Dewanti, R. and Wong, A.C.L. (1995). Influence on culture conditions on biofilm formation by *Escherichia coli 0157:H7. International Journal of Food Microbiology*, 26, pp. 147-164.

Doig, P. and Trust, T.J. (1993). Methodological Approaches to Assessing Microbial binding to Extracellular Matrix Components, *Journal of Microbiological Methods,* 18, pp. 167-180.

Drake, D. and Montie, T.C. (1988). Flagella, motility and invasive virulence of *Pseudomonas aeruginosa. Journal of General Microbiology*, 134, pp. 43-52.

Duddridge, J.E.,Kent, C.A. and Laws J.F. (1982), Effect of Shear Stress on the Attachment of *Pseudomonas fluorescens* to Stainless Steel under Defined Flow Conditions., *Biotechnology and. Bioengineering.* 24, pp. 153-164.

Duddridge, J.E., and Pritchard, A.M. (1979). Factors Affecting the Adhesion of Bacteria to Surfaces., in*: Adhesion of Micro-organisms to surfaces.,* (D.C. Ellwood, J. Melling & P. Rutter Eds.) . 24, pp. 153-164. London: Academic Press.

Dudkin. S. (1995). *A study of multistep cleaning.* Ph.D. thesis, Slovak Technical University, Bratislava.

Dyson, R.D. (1978). *Cell Biology: A Molecular Approach.* Second Edition, Allyn & Bacon, Inc. Boston, London, Sydney. pp. 401, 407, 437, 534.

Eberl, L., Givskov, M., Poulsen, L.K. and Molin, S. (1997). Use of Bioluminescence for Monitoring the Viability of Individual *Pseudomonas putida KT2442* Cells. *FEMS Microbiology Letters* , 149, pp. 133-140.

Ennis, J., Zhang, H., Stevens, G., Perrera, J. Scales, P. and Carnie, S. (1996). Mobility of protein through a porous membrane. *Journal of Membrane Science.* 119, pp. 47-58.

Ethier, C.R. and Kamm, R.D. (1989). The Hydrodynamic Resistance of Filter Cakes., *Journal of Membrane Science.* 43, pp.19-30.

Fane, A.G., Kim, K.J., Hodgson, P.H., Leslie, G., Fell, C.J.D., Franken, A.C.M. Chen, C. and Liew, K.H. (1990). Strategies to Minimise Fouling in the Membrane Processing of Biofluids. *Frontiers in Bioprocessing ll*, Boulder, Colorado, June 17-21 pp. 304-320.

Fenton, M. and Jarvis, B.D.W. (1994). Expression of the Symbiotic Plasmid from *Rhizobium leguminosarum biovar trifolii* in *Sphingobacterium multivorum. Canadian Journal of Microbiology*, 40, pp. 873- 879.

Fialho, A.M., Monteiro, G.A., Sa-Correia, I. (1991). Conjugal Transfer of Recombinant Plasmids into Gellan Gum-producing and Non-producing Variants of *Pseudomonas elodea* ATCC 31461., *Letters in Applied Microbiology*, 12, pp. 85-87.

Field, R.W., and Arnot, T. (1995). Fouling Mechanisms and Modelling With Due Allowance for Crossflow and Back Diffusion: Testing of Recent Theoretical Advances With Data on the Membrane Filtration of Yeast Cells. *Proceedings of Euromembrane '95*. 1, (A3), pp. 1-17 to 1-22.

Field, R., Hang, S. and Arnot, T. (1994), The Influence of Surfactant on Water Flux through Microfiltration Membranes, *Journal of Membrane Science*, 86, pp. 291-304.

Field, R.W., Wu, D., Howell, J.A. and Gupta, B.B.(1995). Critical Flux Concepts in Microfiltration Fouling. *Journal of Membrane Science*, 100, pp.259-272.

Foley, G. (1994). Membrane Fouling in Crossflow Filtration : Implications for Measurement of the Steady State Specific Cake Resistance. *Biotechnology Techniques*, 8 (10), pp. 743- 746

Foley, G., MacLoughlin, P.F. and Malone, D.M. (1995). Membrane Fouling during Constant Flux Crossflow Microfiltration of Dilute Suspensions of Active Dry Yeast. *Separation Science and Technology*, 30 (3), pp. 383-398.

Foley, G., Malone, D.M. and MacLoughlin, F. (1995). Modelling the Effects of Particle Polydispersity in Crossflow Filtration. *Journal of Membrane Science.*, 99, pp. 77-88.

Forman, S.M., DeBernardez, E.R, Feldberg, R.S. and Swartz, R.W. (1990). Crossflow Filtration for the Separation of Inclusion Bodies from Soluble Proteins in Recombinant *Escherichia coli* cell Lysate, *Journal of Membrane Science.* pp. 263-279

Fu, F.L. and Dempsey, B.A. (1998). Modeling the Effect of Particle Size and Charge on the Structure of the Filter Cake in Ultrafiltration. *Journal of Membrane Science.*, 149, pp. 221-240.

Gatenholm, P., Fell, C.J. and Fane, A.G. (1988). Influence of the Membrane Structure on the Composition of the Deposit-layer during Processing of Microbial Suspensions., *Desalination*,70, pp.363-378

Gatenholm P.,Paterson S.,Fane A.G. and Fell C.J.D.(1988),Performance of Synthetic Membranes during Cell Harvesting of *E. coli, Process Biochemistry*, June, pp. 79-81.

Gekas, V., Aimar, P., Lafaille, J.-P., and Sanchez, V. (1993). A Simulation Study of the Adsorption- Concentration Polarisation Interplay in Protein Ultrafiltration. *Chemical Engineering Science*, 48, (15), pp. 2753-2765

Gekas, V. and Hallström, B. (1990). Microfiltration Membranes, Crossflow Transport Mechanisms and Fouling Studies., *Desalination*, 77, pp. 195-218.

Göklen, K.E., Thien, M., Ayler, S., Smith, S., Fisher, E., Chartrain, M., Salmon, P., Wilson, J., Andrews, A. and Buckland, B. (1994). Development of Crossflow Filtration Processes for the Commercial-scale Isolation of a Bacterial Lipase. *Bioprocess Engineering*, 11, pp. 49-56.

Goodhue, C.T.and Schaeffer, J.R. (1971). Preparation of L(+) β-Hydroxisobutyric Acid by Bacterial Oxidation of Isobutyric Acid, *Biotechnology and Bioengineering* 8, .pp. 203-214.

Graham, L. L., Harris, R., Villiger, W. and Beveridge. (1991). Freeze-substitution of Gram-negative Eubacteria: General Cell Morphology and Envelope Profiles., *Journal of Bacteriology*, 173, (5), pp. 1623-1633.

Green, G. and Belfort, G. (1980). Fouling of Ultrafiltration Membranes, Lateral Migration and the Particle Trajectory Model. *Desalination,* 35, p. 129.

Güell, C. and Davis, R.H. (1996). Membrane fouling during microfiltration of protein mixtures. *Journal of Membrane Science*, 119, pp. 269-284.

Hadzismajlovic, D.E. and Bertram, C.D. (1998). Flux enhancement in laminar crossflow microfiltration using a collapsible tube pulsation generator. *Journal of Membrane Science*, 142, pp. 173-189.

Hallab, N.J., Bundy K.J., O' Connor, K., Clark R. and Moses R.L. (1995), Cell Adhesion to Biomaterials: Correlations between Surface Charge, Surface Roughness, Adsorbed Protein and Cell Morphology., *Journal of Long Term Effects of Medical Implants*. 5, (3), pp. 209-231.

Hammer, D.A. and Lauffenberger, D.A. (1987). A dynamical Model for Receptor-mediated Cell Adhesion to Surfaces., *Biophysical Journal*, 52, (September), pp. 475-487.

Hammer, D.A. and Apte, S.M. (1992). Simulation of Cell Rolling and Adhesion on Surfaces in Shear Flow: General Results and Analysis of Selectin-mediated Neutrophil Adhesion., *Biophysical Journal*, 63, (July), pp. 35-57.

Harbron, R.S. and Kent, C.A. (1988). Aspects of Cell Adhesion. In: *NATO Fouling Science and Technology*, Algarve: Portugal, May 1987 (L.F.Melo, ed.) pp. 125-140.

Harwood, C.S., Fosnaugh, K. and Dispensa, M. (1989). Flagellation of *Pseudomonas putida* and Analysis of its Motile Behaviour. *Journal of Bacteriology*, 171 (7), pp. 4063-4066.

Hawker, L.E. and Linton A.H. (1971) *Micro-organisms: Function, Form and Environment*, Edward Arnold : London.

Hermia, J. (1982). Constant pressure blocking filtration laws- Application to Power-law Non-Newtonian fluids. *Transactions of the Institution of Chemical Engineers.* 60, pp. 181-187.

Ho, C.S. (1986), An Understanding of the Forces in the Adhesion of Micro-organisms to Surfaces., *Process Biochemistry.* (October), pp. 148-151

Hodgson, P.H., Leslie, G.L., Schneider, R.P., Fane, A.G., Fell, C.J.D. and Marshall, K.C. (1993a). Cake Resistance and Solute Rejection in Bacterial Microfiltration : the Role of the Extracellular Matrix. *Journal of Membrane Science.*, 79, pp. 35-53.

Hodgson,P.H., Pillay,V.L. and Fane, A.G. (1993b). Visual Studies of Crossflow Microfiltration with Inorganic Membranes: Resistance of Biomass and Particulate Cakes. *Sixth World Filtration Congress*, Nagoya, 9b-104, pp. 607-610.

Holdich, R.G., Cumming, I.W. and Ismail, B. (1995). The variation of crossflow filtration rate with wall shear stress and the effect of deposit thickness. *Transactions of the Institute of Chemical Engineering*, Part A, 73, pp. 20-26.

Holmes, B., Owen, R.G. and Weaver, R.E.. (1981). *Flavobacterium multivorum*, a new species isolated from human clinical specimens and previously known as Group IIk, Biotype 2., *International Journal of Systematic Bacteriology*, 31 (1) , 21-34.

Horska, E., Pokorny, J. and Labajova, M. (1993). Changes of surface charge and hydrophobicity of the outer bacterial membrane depending on the cultivation medium. Biologia, 48 (3), pp. 343-347.

Hsu, J.-P., (1988), Stochastic Analysis of Bacterial Adhesion: A Diffusion-layer Mechanism. *Journal of the Chinese Institute of Chemical Engineering*, 19, (4) pp. 235-239.

Huang, L. and Morrissey, M.T. (1998). Fouling of membranes during microfiltration of surimi wash water : roles of pore blocking and surface cake formation. *Journal of Membrane Science.*, 144, pp. 113-123.

Hunter, R. J., (1981). *Zeta potential in Colloid Science.* Academic Press: New York., pp. 69-73.

Isaac, S. and Jennings, D. (1995). *Microbial Culture.* Bios Scientific Publishers: Oxford.

Israelachvili J. (1994). *Intermolecular and Surface Forces.*, Second Edition, Academic Press: London.

Jönsson, A., Jönsson, B. (1991). The influence of Nonionic and Ionic Surfactants on Hydrophobic and Hydrophilic Ultrafiltration Membranes, *Journal of Membrane Science.* pp.49-74

Johri, A.K., Dua, M., Tuteja, D., Saxena, R., Saxena, D.M. and Lal, R. (1998). Degradation of Alpha, Beta, Gamma and Delta- Hexachlorocyclohexanes by *Sphingomonas paucimobilis. Biotechnology Letters*, 20 (9), pp. 885-887.

Jones, D.S., Adair, C.G., Mawhinney, W.M. and Gorman, S.P. (1996). Standardisation and Comparison of Methods employed for Microbial Cell Surface Hydrophobicity and Charge Determination. *International Journal of Pharmaceutics.* 131, pp. 83-89.

Kang, K.S.and Veeder, G.T. (1983). Fermentation Process for its Preparation of Polysaccharide S-60., *U.S. Patent* 4,377,636.

Kawahara, K., Seydel, U., Motohiro, M., Hirofumi, D., Rietschel, E.T. and Zähringer, U. (1991). Chemical structure of Glycosphingolipids isolated from *Sphingomonas paucimobilis. FEBS Letters*, 292, pp. 107-110.

Kawasaki, S., Moriguchi, R., Sekiya, K., Nakai, T., Ono, E., Kume, K. and Kawahara, K. (1994). The Cell Envelope structure of the Lipopolysaccharide-lacking Gram-negative Bacterium *Sphingomonas paucimobilis. Journal of Bacteriology*, 176, (2), pp. 284-290.

Kent, C.A. (1988). Biological Fouling: Basic Science and Models. In: *NATO Fouling Science and Technology*, Algarve: Portugal, May 1987 (L.F.Melo, ed.) pp. 207 –222.

Kim, Keurentjes, J.T.F., Harbrecht, J.G., Brinkman, D., Hanemaaijer, J.H., Cohen, Stuart M.A. and van't Riet, K. (1989). Hydrophobicity Measurements of Microfiltration and Ultrafiltration Membranes. *Journal of Membrane Science.*, 47, pp. 333-344.

Kim, K.J., Fane, M., Nyström, M., Pihlajamak, A, Bowen, W. R. and Mukhtar, H.(1996). Evaluation of Electroosmosis and Streaming Potential for Measurement of Electric Charges on Polymeric Membranes., *Journal of Membrane Science.* 116, pp. 149-159.

Kleizen, H.H., de Putter, A.B., Van der Beek , Huynik, S.J.(1995). Particle Concentration, Size, and Turbidity. *Filtration and Separation.*, 32, (9) , pp. 897-901.

Koltuniewicz, A.B., Field, R.W. and Arnot, T.C. (1995). Crossflow and dead-end microfiltration of oily-water emulsion. Part I : Experimental study and analysis of flux decline. *Journal of Membrane Science.* 102, pp. 193-207.

Kroner, K.H. and Nissinen, V. (1988). Dynamic Filtration of Microbial Suspensions using an Axially Rotating Filter. *Journal of Membrane Science.* 36, pp. 85-100.

Kroner, K.H., Schutte, H., Hustedt, H. and Kula, M.R. (1984). Crossflow Filtration in the Downstream Processing of Enzymes., *Process Biochemistry.* 19, (April), pp.67-74

Kuiper, S., van Rijn, C.J.M., Nijdam, W. and Elwenspoek, M.C. (1998). Development and Applications of Very High Flux Microfiltration Membranes. *Journal of Membrane Science.*, 150, pp. 1-8.

Kuberkar, V.T. and Davies, R.H. (2000). Modelling of fouling reduction by secondary membranes. *Journal of Membrane Science*, 168, (1-2), pp. 243-258.

Kuruzovich, J.N. and Piergiovanni, P.R. (1996). Yeast cell microfiltration: optimisation of backwashing for delicate membranes. *Journal of Membrane Science*, 112, pp. 241-247.

Le, M.S. (1987). Recovery of Beer from Tank Bottoms with Membranes. *Journal of Chemical Technology and Biotechnology*, 37, pp. 59-66

Le Berre, O. and Daufin, G. (1996). Skimmilk Crossflow Microfiltration Performance versus Permeation flux to Wall Shear Stress Ratio. *Journal of Membrane Science.*, 117, pp. 261-270.

Le M.S. and Gollan K.L., (1989). Fouling of Microporous Membranes in Biological Applications, *Journal of Membrane Science*, 40, (2), pp. 231-242

Le, M.S. and Howell, J.A. (1984). Alternative Model for Ultrafiltration. *Chemical Engineering Research and Design,* 62, (6), pp. 373-380.

Le, M.S., Spark, L.B. and Ward, P.S. (1984a). The Separation of Aryl Acylamidase by Crossflow Microfiltration and The Significance of Enzyme/Cell Debris Interaction., *Journal of Membrane Science.*, 21, pp. 219-232

Le, M.S., Spark, L.B., Ward, P.S. and Ladwa, N. (1984b). Microbial Asparaginase Recovery by Membrane Processes, *Journal of Membrane Science*. 21, pp.307-319

Lee, K.-K. and Yii, K.-C. (1996). A Comparison of Three Methods for Assaying Hydrophobicity of Pathogenic Vibrios., *Letters in Applied Microbiology*. 23, pp. 343-346.

Leonard, E.F. and Vassilief, C.S. (1984). The Deposition of Rejected Matter in Membrane Separation Processes. *Chemical Engineering Communications*. 30, pp. 209-217.

Li, H., Fane, A. G. , Kostner, H. G. and Vigneswarin, S, (1998). Direct Observation of Particle Deposition on the Membrane Surface during Crossflow Filtration. *Journal of Membrane Science.*, 149, pp. 83-97.

Liao, C.H. (1989). Antagonism of *Pseudomonas putida* Strain PP22 to Phytopathogenic Bacteria and its Potential use as a Biocontrol Agent. *Plant Disease*, 73, pp. 223-226.

Lindahl, M., Faris, A., Nadström, T. and Hjerten, S. (1981). A New Test based on "Salting Out" to Measure Relative Surface Hydrophobicity of Bacterial Cells., *Biochimica and Biophysica Acta*, 677, pp. 471-476.

Lojkine, M.H., Field, R.W. and Howell, J.A. (1992). Crossflow Microfiltration of Cell Suspensions : a Review of Models with Emphasis on Particle Size Effects. *Transactions of the Institute of Chemical Engineers*, 70, Part C, pp. 149-164.

MacDonald, J.C. and Bishop, G.G. (1984). Spectral properties of a Mixture of Fluorescent Pigments produced by *Pseudomonas aeruginosa. Biochimica et Biophysica Acta*, 800, pp. 11-20.

Mackley, M.R. and Sherman, N.E (1993). Cake Filtration Mechanisms in Steady and Unsteady Flows., *Journal of Membrane Science*. 77, pp.113-121.

Mackley M.R. and Sherman N.E. (1992), Crossflow Cake Filtration Mechanisms and Kinetics., *Chemical Engineering Science*, 47, (12), pp. 3067-3084

Mackley, M.R. (1987). Using Oscillatory Flow to Improve Performance., *The Chemical Engineer*, (February), pp. 18-21

Marshall, K.C., Stout, R. and Mitchell, R.(1971). Selective Sorption of Bacteria from Seawater, *Canadian Journal of Microbiology*, 17, pp. 1413-1414.

Marshall, K. C. (1986). Adsorption and Adhesion Processes in Microbial Growth at Interfaces. *Advances in Colloid and Interface Science*, 25, pp. 59-86.

Martins, L.O. and S>-Correia, I. (1993). Temperature profiles of Gellan Gum Synthesis and Activities of Biosynthetic Enzymes. *Biotechnology and Applied Biochemistry*, 20, pp.385-395.

Meagher, L., Klauber, C.and Pashley, R. M.(1996). The Influence of Surface Forces on the Fouling of Polypropylene Microfiltration Membranes. *Colloids and Surfaces. A.: Physicochemical and Engineering Aspects*, 106, pp. 63-81.

McLoughlin, A.J. (1994). Plasmid stability and Ecological Competence in Recombinant Cultures. *Biotechnology Advances*, 12, pp. 279-324.

Monteiro, G.A., Fialho, A.M., Ripley, S.J. and Sâ-Correia I. (1992). Electrotransformation of Gellan gum-producing and Non-producing *Pseudomonas elodea* Strains. *Journal of Applied Bacteriology*, 72, pp. 423-428.

Moorhouse,R. (1987). Structure/Property Relationships of a Family of Microbial Polysaccharides. *Progress in Biotechnology*. 3, pp. 187-186.

Morris, V. J., Tsiami, A. and Brownsey, G. (1995). Work Hardening Effects in Gellan Gum Gels. *Journal of Carbohydrate Chemistry*, 14, (4 - 5), pp. 667-675.

Mourot P., Lafrance M. and Oliver M. (1989). Aseptic Concentration of Living Microbial Cells by Cross-flow Filtration, *Process Biochemistry*, (February), pp. 3-8

Mozes, N., Amory, D. E., Leonard, A. J. and Rouxhet, P. G. (1989). Surface Properties of Microbial Cells and their Role in Adhesion and Flocculation. *Colloids and Surfaces*, 42, pp. 313-329.

Mozes, N., Marchal, F., Hermesse, M.O., Van Haecht, J.L, Reuliaux, L. Leonard, A.J. and Rouxhet, P.G. (1987). Immobiliziation of Microoganisms by Adhesion: Interplay of Electrostatic and Nonelectrostatic Interactions, *Biotechnology and Bioengineering*, 30, pp. 439-450

Murase, T., Ohn, T., Kimata, K. (1995). Filtrate Flux in Crossflow Microfiltration of Dilute Suspension forming a Highly Compressible Fouling Cake-layer. *Journal of Membrane Science*. 108, pp. 121-128.

Nazzal, F.F. and Wiesner, M. R. (1994). pH and Ionic Strength Effects on the Performance of Ceramic Membranes in Water Filtration. *Journal of Membrane Science.*, 93, pp. 91-103.

Ohmori, K. and Glatz, C. E. (1999). Effects of pH and Ionic Strength on Microfiltration of *C. glutamicum*. *Journal of Membrane Science.*, 153, pp. 23-32.

Parvatiyar, M.G. (1998). Mass Transfer in a Membrane Tube with Turbulent Flow of Newtonian and non-Newtonian fluids. *Journal of Membrane Science.*, 148, pp. 45-57.

Patti, J. and Höök, M. (1994). Microbial Adhesins Recognizing Extracellular Matrix Macromolecules. *Current Opinion in Cell Biology.*, 6, pp. 752-758

.

Paul, F., Morin, A. and Monsan, P. (1986). Microbial Polysaccharides with Actual Potential Industrial Applications. *Biotechnology Advances*, 4, pp. 245-259.

Phillips R.J., Armstrong R.C. and Brown R.A. (1992), A Constitutive Equation for Concentrated Suspensions that Accounts for Shear-induced Particle Migration., *Physics of Fluids A- Fluid Dynamics*, 4, (1), pp. 30-40.

Porter, M. (1972). Concentration Polarisation with Membrane Ultrafiltration. *Industrial Engineering and Chemical Production Research and Development*, 11, pp. 234-248.

Povey, M., Personal Communication from Senior Lecturer in the Department of Food Science, University of Leeds, February 2001.

Powell, M.S. and Slater, N.K.H. (1982). Removal Rates from Glass Surfaces by Fluid Shear. *Biotechnology and Bioengineering*, 24, pp.2527-2537.

Pritchard, M., Howell, J.A. and Field, R.W. (1995). The Ultrafiltration of Viscous Fluids. *Journal of Membrane Science*, 102 , pp. 223-235.

Rautenbach, R. and Schock, G. (1988), Ultrafiltration of Macromolecular Solutions and Cross-flow Microfiltration of Colloidal Suspensions. A Contribution to Permeate Flux Calculations, *Journal of Membrane Science*, 36, pp. 231-242

Read, R.R. and Costerton, J.W. (1987). Effect of Chlorine Injury on Heat- labile Enterotoxin Production in Enterotoxigenic *Escherichia coli*. *Canadian Journal of Microbiology.*, 33, pp. 1080-1090.

Ricq, L., Pierre A., Reggiani J.-C., Zarafoza-Piqueras S., Pagetti, J. and Daufin, G. (1996). *Journal of Membrane Science*, 114, pp. 27-38.

Riesmeier, B. Kroner, K.H. and Kula, M.R. (1987). Studies on Secondary Layer Formation and its Characterization during Crossflow Filtration of Microbial cells. *Journal of Membrane Science.*, 34. pp. 245-266.

Romero, C.A. and Davis, R. H. (1988a). Transient Model of Crossflow Microfiltration., *Chemical Engineering Science*, 45 (1), pp. 13-25.

Romero, C.A. and Davis, R.H. (1988b). Global Model of Crossflow Microfiltration based on Hydrodynamic Particle Diffusion, *Journal of Membrane Science*, 39, pp. 157-185.

Rosenberg, M. (1984). Bacterial adherence to hydrocarbons : A Useful Technique for Studying Cell Surface Hydrophobicity. *FEMS Microbiology Letters*, 22, pp. 289-295.

Rosenberg, M., Gutnick, D.and Rosenberg, E. (1980). Bacterial Adherence of Bacteria to Hydrocarbons : A Simple Method for Measuring Cell Surface Hydrophobicity. *FEMS Microbiology Letters*, 9, pp. 29-33.

Russotti, G., Göklen, K.E. and Wilson, J.J. (1995).Development of a Pilot Scale Microfiltration Harvest for the Isolation of Physostigmine from *Streptomyces griseo fuscus* broth. *Journal of Chemical Technology and Biotechnology*. 63, pp. 37-47.

Samson Wright's Applied Physiology (1982). C.A. Keele, E. Neil and N. Joels Editors. Thirteenth Edition, Oxford Medical Publications: Oxford, New York, Toronto.

Schulz, G. and Ripperger, S. (1989) Concentration Polarization in Crossflow Microfiltration, *Journal of Membrane Science.*, 40, (2), pp. 163-187

Scott, J.A. 1988), Application of Cross-flow Filtration to Cider Fermentations., *Process Biochemistry*, (October), pp. 146-148

Shimuzu, Y., Matsushita, K. and Watanabe, A. (1994). Influence of Shear Breakage of Microbial Cells on Crossflow Microfiltration Flux. *Journal of Fermentation and Bioengineering*. 78, (2), pp. 170-174.

Shimuzu, Y., Shimodera, K. and Watanabe, A. (1993). Crossflow Microfiltration of Bacterial Cells. *Journal of Fermentation and Bioengineering*. 76, (6), pp. 493-500.

Shorrock, C.J. and Bird, M.R. (1998). Membrane Cleaning: Chemically Enhanced Removal of Deposits Formed During Yeast Cell Harvesting. *Transactions of the Institute of Chemical Engineers*, 76, Part C, pp.30-38.

Simpson, D.A., Ramphal, R. and Lory, S. (1995). Characterization of *Pseudomonas aeruginosa* fliO, a Gene Involved in Flagellar Biosynthesis and Adherence. *Infection and Immunity*, 63 (8), pp. 2950-2957.

Sims K.A. and Cheryan M. (1986), Cross-flow Microfiltration of *Aspergillus Niger* Fermentation Broth, *Biotechnology and Bioengineering Symposium.* 17, pp 495-505.

Skierczynski, B. A., Skalak, R. and Chien, S. (1995). Cell Adhesion; Molecular Interpretation. *Proceedings of the ASME Bioengineering Conference.*, pp. 453-454.

Smalley, D.I. (1982). Endotoxin-like Activity in *Pseudomonas paucimobilis* (Group IIK biotype 1) and *Flavobacterium multivorum* (Group IIK biotype 2). *Experientia*, 38, pp. 1483-1484.

Smalley, D.L. and Bradley, M.E. (1983). Lectin-binding and Antibody Response with *Pseudomonas paucimobilis* and *Flavobacterium multivorum. Canadian Journal of Microbiology*, 29, pp. 619-621.

Sonak, N. and Bhosle, N. (1995), Observations on Biofilm Bacteria isolated from Aluminium Panels Immersed in Estuarine Waters. *Biofouling*, 8, pp. 243-254.

Sorongon, M.L., Bloodgood, R.A. and Burchard, R.P. (1991). Hydrophobicity, Adhesion and Surface-exposed Proteins of Gliding Bacteria. *Applied and Environmental Microbiology*, 57, (11), pp. 3193-3199

Stamatakis, K. and Tien. C. (1993). A Simple Model of Crossflow Filtration based on Particle Adhesion. *A.I. Che. Journal*, 39, (8). pp. 1292-1302.

Stanier, R.Y., Adelberg, E.A. and Ingraham, J.L. (1985). *General Microbiology.*, Fourth Edition. MacMillan Publishers Limited: London. pp. 245-246.

Stenström, T.A. (1989). Bacterial Hydrophobicity, an Overall Parameter for the Measurement of Adhesion Potential to Soil Particles. *Applied and Environmental Microbiology*, 55 (1), pp. 142-147.

Stuart, S.T., Payne, A.L., Reyes, D, Ashton, F. and Edgar, J.A. (1994). Detoxification of Annual Ryegrass Toxins by *Sphingobacterium multivorum.* *4th International Symposium on Poisonous Plants*, Chapter 102, pp.451-456.

Sutherland, I.W. (1994). Structure-function Relationships in Microbial Exopolysaccharides. *Biotechnology Advances*, 12, pp. 393-448.

Taddei, C., Aimar, P., Howell, J.A. and Scott, J.A. (1990). Yeast cell Harvesting from Cider using Microfiltration. *Journal of Chemical Technology and Biotechnology,* 47, pp. 365-376.

Tanaka, T., Abe, K.-I.,Asakawa, H., Yoshida, H. and Nakanishi, K. (1994). Filtration Characteristics and Structure of Cake in Crossflow Filtration of Bacterial Suspension. *Journal of Fermentation and Bioengineering*, 78, (6), pp. 455-461.

Tanaka, T., Usiu, K., Kouda, K. and Nakanishi, K. (1996). Filtration Behaviours of Rod-shaped Bacterial Broths in Unsteady-state Phase of Crossflow Filtration. *Journal of Chemical Engineering of Japan*, 29, (6), pp. 973-981.

Tanaka, T., Usiu, K., and Nakanishi, K. (1998). Formation of the Gel layer of Polymers and its Effect on the Permeation Flux in Crossflow Filtration of *Corynebacterium glutamicum* broth. *Separation Science and Technology*, 33, (5), pp. 707-722.

Tarleton, E.S. and Wakeman, R.J. (1993). Understanding Flux Decline in Crossflow Microfiltration: Part 1- Effects of Particle and Pore Size. *Transactions of the Institute of Chemical Engineers,* 71, Part A, (July), pp. 399-410.

Tarleton, E.S. and Wakeman, R.J. (1994) Understanding Flux Decline in Crossflow Microfiltration: Part 1- The Effects of Process Parameters. *Transactions of the Institute of Chemical Engineers,* 72, Part A, (May), pp. 431-440.

Topley and Wilson's Principles of Bacteriology, Virology and Immunity., Volume 2 ,Systematic Bacteriology, and Bacterial diseases. (1990), M.T. Parker and L.H. Collier editors, Eighth Edition, Edward Arnold: London.

Viera, M.J., Oliveira, R., Melo, L. Pinheiro, M. and Martins, V. (1993). Effect of Metallic Ions on the Adhesion of Biofilms formed by *Pseudomonas fluorescens. Colloids and Surfaces B: Biointerfaces,* 1, pp. 119-124.

Watase, M. and Nishihari, K. (1993). Effect of Potassium ions on the Rheological and Thermal Properties of Gellan Gum Gels. *Food Hydrocolloids.*, No. 5, pp. 449-456.

Wilkinson, J.F. (1958). The Extracellular Polysaccharides of Bacteria. *Bacteria Review*, 22, pp. 46-73.

Wu D., Howell J.A. and Field R.W. (1993), Pulsatile Flow Filtration of Yeast Cell Debris: Influence of Preincubation on Performance., *Biotechnology and Bioengineering.*, 41, pp. 998-1002.

Wustman, B.A. (1998). *Extracellular Matrix Assembly in Diatoms.* PhD thesis, Michigan Technological University.

Yabuuchi, E., Kaneko, T., Yano, I., Moss, C.W. and Miyoshi, N. (1983). *Sphingobacterium* gen. nov. , *Sphingobacterium spiritivorum* com. nov. , *Sphingobacterium multivorum* comb. nov., *Sphingobacterium mizutae* sp. nov., and *Flavobacterium indologenes* sp. nov.: Glucose-nonfermenting Gram-negative Rods in CDC Groups II K-2 and IIb. *International Journal of Systematic Bacteriology*, 33, pp. 580-598.

Yamamoto, T., Periasamy, R. P., Donovan, D. Ensor. (1994). Flow Cell for Real Time Observation of Single Particle Adhesion and Detachment. *Journal of Adhesion Science and Technology*, 8 (5) pp.543-552.

Yamasaki, H., Lee, M.-S., Tanaka, T. Nakanishi, K. (1993). Characteristics of Crossflow Filtration of Pullulan Broth. *Applied Microbiology and Biotechnology*, 39, pp. 26-30.

Yoshida, H., Nishihara, H., Kataoka, T. (1993). Adsorption of BSA on Q.A.E.-Dextran: Equilibria. *Biotechnology and Bioengineering*, 41, pp. 280-286.

Zhu, C., Sung, K.P. and Skalak, R.(1990). Mathematical Modeling of Cell Adhesion. *American Society of Mechanical Engineers, Bioengineering Division.* 17, pp.361-364.

Zydney A.L. and Colton K.C. (1986), A Concentration Polarisation Model for the Filtrate Flux in Cross-flow Microfiltration of Particulate Suspensions., *Chemical Engineering Communications.* 47, 1-21.

Appendix A Absorbance calibration curves for the Cecil 1020 spectrotophotometer

P. putida in broth

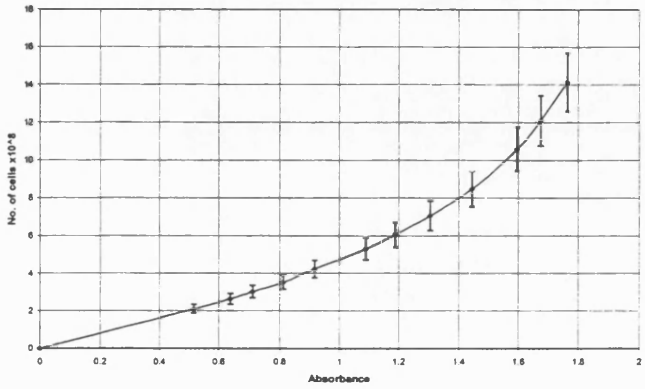

Figure 1 Calibration curve for *P.putida* in broth when wavelength is set to 330 nm

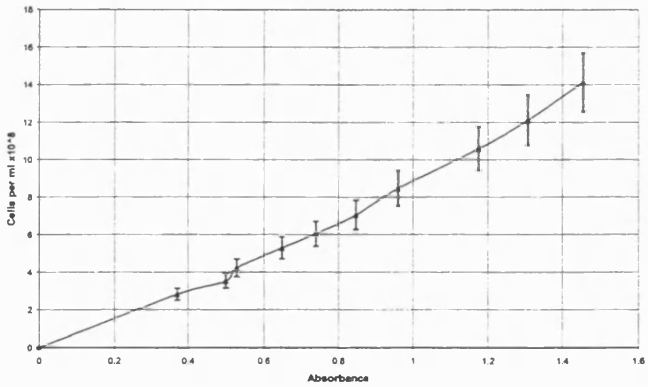

Figure 2 Calibration curve for *P.putida* in broth when wavelength is set to 480 nm

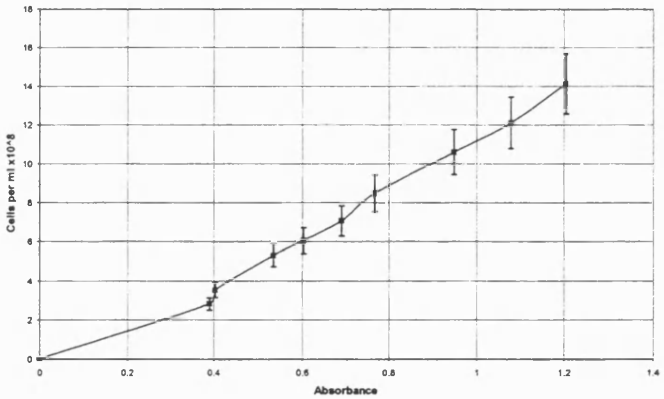

Figure 3 Calibration curve for *P.putida* in broth when wavelength is set to 550 nm

S.multivorum in broth

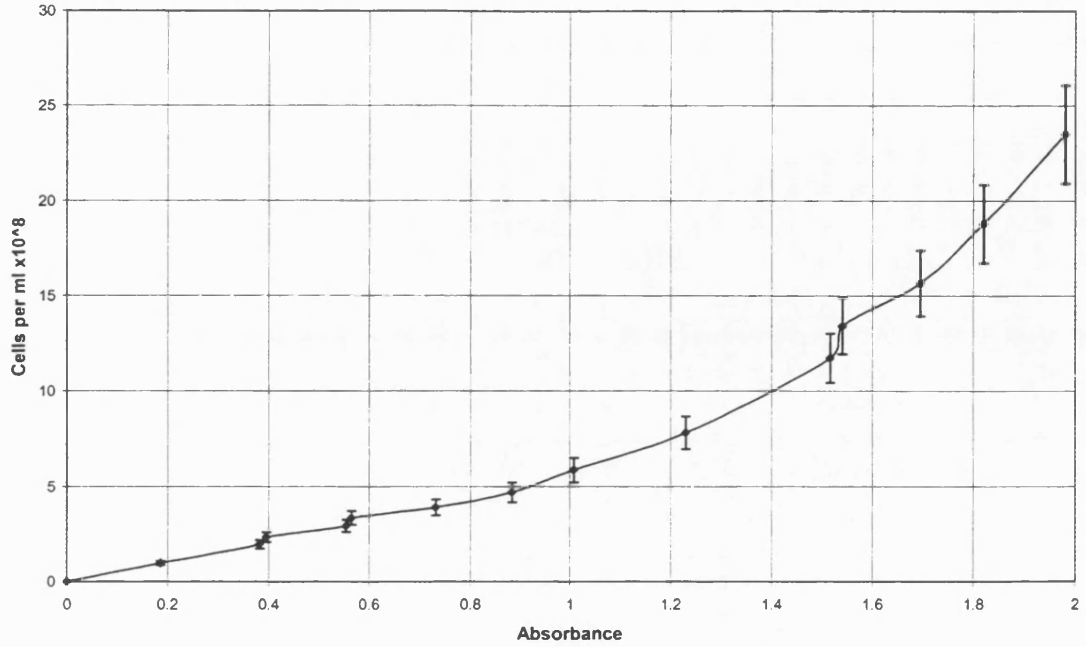

Figure 4 Calibration curve for *S.multivorum* in broth when wavelength is set to 330 nm

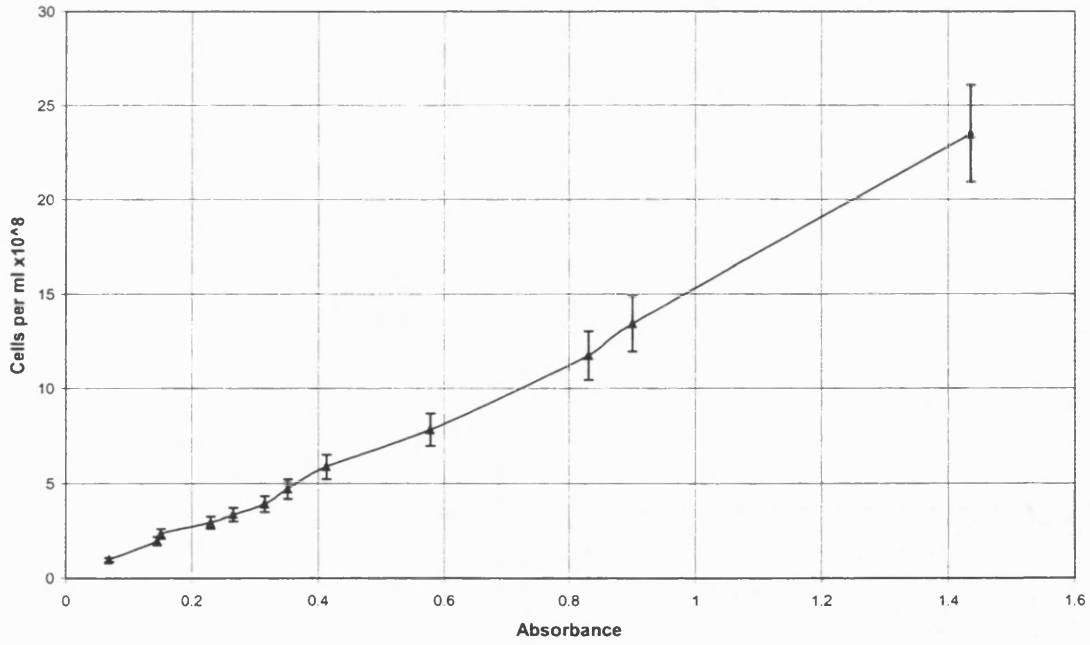

Figure 5 Calibration curve for *S.multivorum* in broth when wavelength is set to 550 nm

P.putida in Ringer's

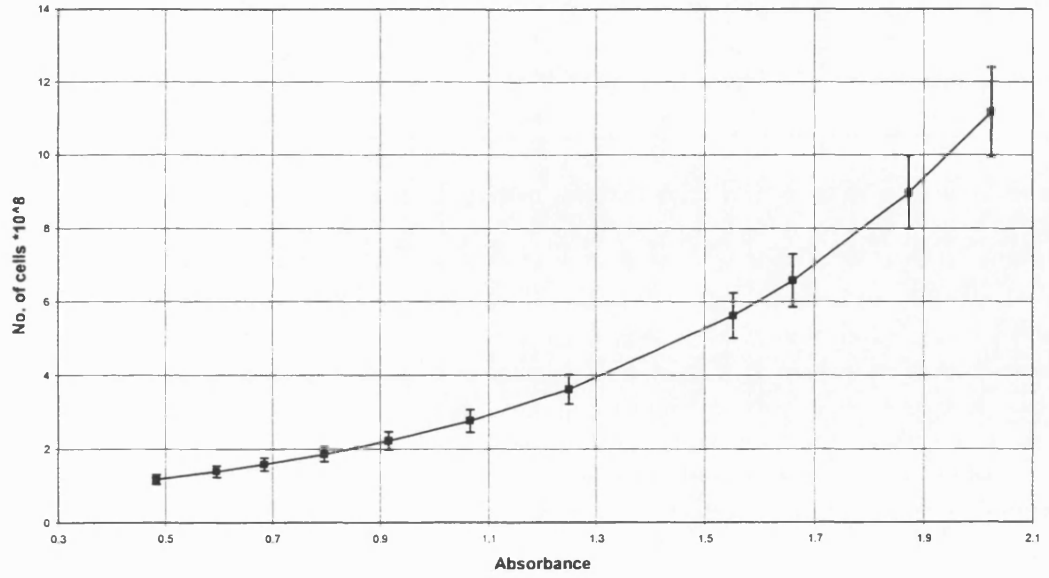

Figure 6 Calibration curve for *P.putida* in Ringer's when wavelength is set to 330 nm

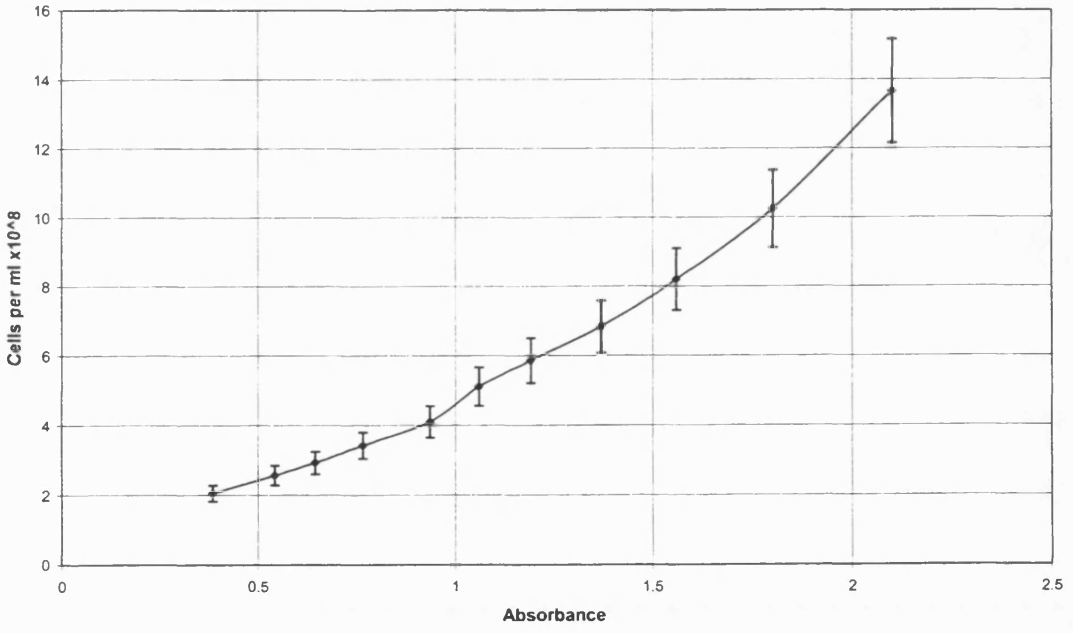

Figure 7 Calibration curve for *P.putida* in Ringer's when wavelength is set to 550 nm

S.multivorum in Ringer's

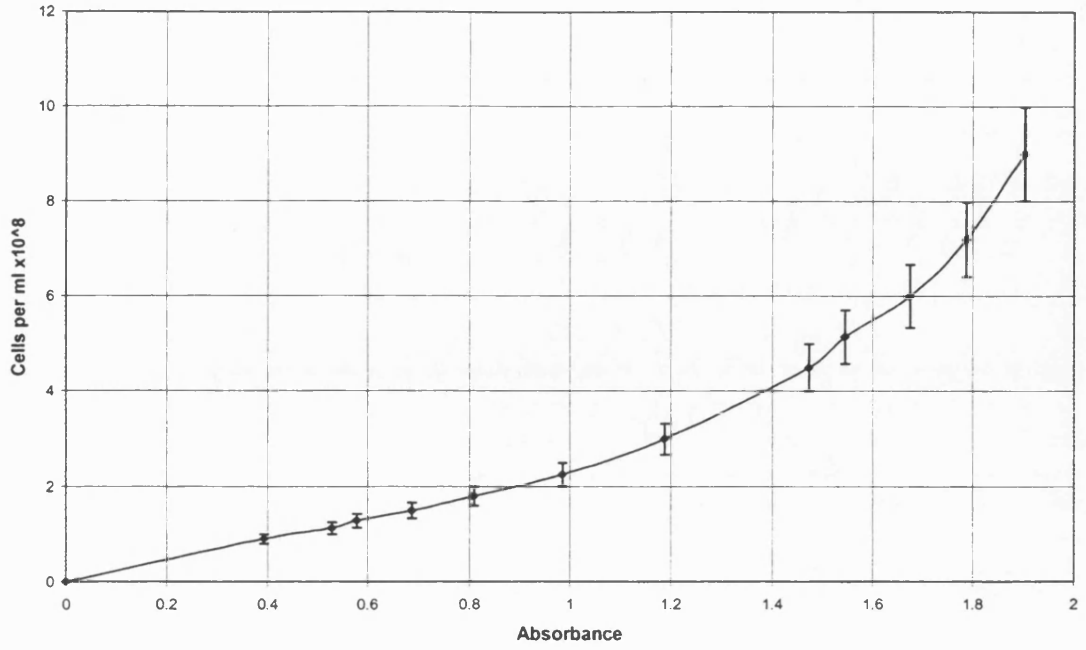

Figure 8 Calibration curve for *S.multivorum* in Ringer's when wavelength is set to 330 nm

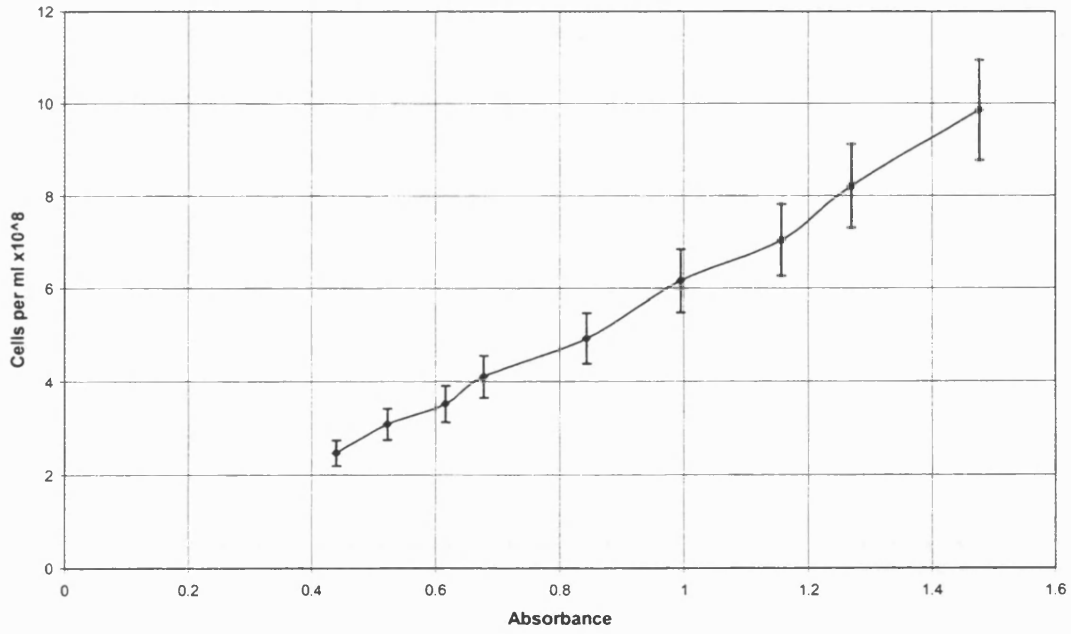

Figure 9 Calibration curve for *S.multivorum* in Ringer's when wavelength is set to 550 nm

P.elodea in Ringer's

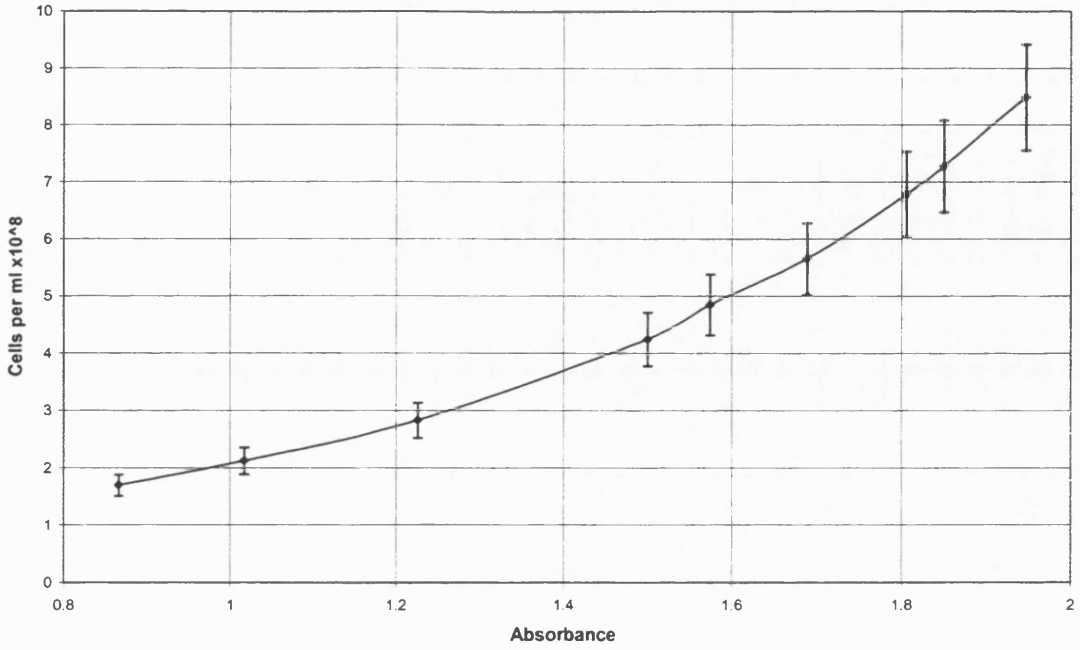

Figure 10 Calibration curve for *P.elodea* in Ringer's when wavelength is set to 330 nm

BSA in Ringer's

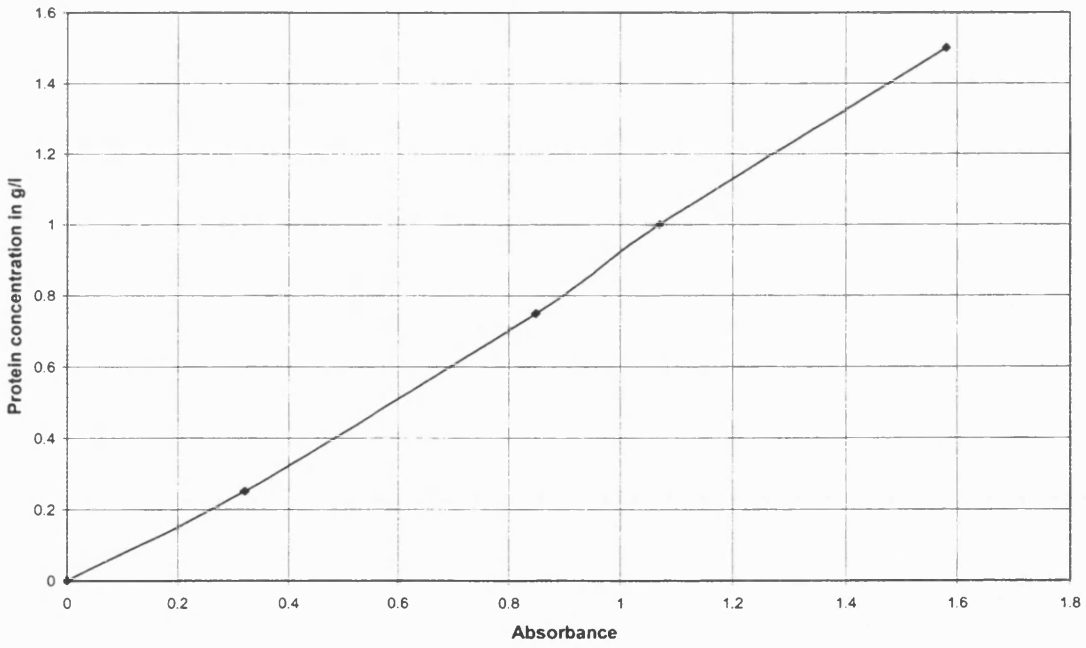

Figure 11 BSA Calibration curve in Ringer's at 330 nm

Appendix B Bubble flowmeter/pressure transducer program

```
DECLARE SUB convertpress ()
DECLARE FUNCTION getbub$ ()
DECLARE FUNCTION pad$ (value%, size%)
DECLARE SUB up.time ()
DECLARE SUB move.on (interval%)
DECLARE SUB average812 (total)
DECLARE SUB ZeroTime ()
DECLARE SUB DoFlowMeter (A$)
DECLARE SUB PrintScreen ()
DECLARE SUB PrintHeader ()

'*********************************************************
'*  Program  : FRANK1.BAS
'*  Revision : 1.00
'*  Date     : 18/10/1996              Frank J.W. Podd
J.T.Bishop
'*=================================================

COMMON SHARED port%, time.now&, time.then&, day.now%, day.then%,
time.last.time&
DIM results(8), averages(8), offset(8), scalef(8), range(8),
pressure(8), SumPressure(8)
COMMON SHARED ElapsedTime, start%, stp%, results(), pressure()
COMMON SHARED SumPressure(), NumPressure, GotFlow%, TimeOffset
COMMON SHARED Flow$, eltim$, transtim$, flux, fluxscale, fluxconst

interval% = 2
average.cnt = 10
filesize% = 50
extension% = 1
fluxscale = 25.834
fluxoffset = 3.77

port% = &H220
REM offsets are in a/d units , Scale factors are in mV, Ranges in bar
offset%(0) = -26: offset%(1) = -1: offset%(2) = -24
scalef(0) = 99.02: scalef(1) = 99.76: scalef(2) = 100.13
range(0) = 1: range(1) = 2: range(2) = 2

start% = 0
stp% = 2
flux = 0

OPEN "COM2:300,n,8,2,CD0,CS0,DS0,OP0,RS,TB2048,RB2048" FOR RANDOM AS #3

CLS
A$ = "a"
PRINT "Priming bubble flow meter, program will continue after the
first"
PRINT "detected bubble."
PRINT "You may have to temporaly turn on the pump to clear the tube of
air."
PRINT "PRESS S to skip or C to continue with priming"
DO: A$ = INKEY$: LOOP UNTIL A$ = "s" OR A$ = "S" OR A$ = "c" OR A$ =
"C"
GotFlow% = 0
IF A$ = "c" OR A$ = "C" THEN
```

```
      PRINT
      PRINT "Awaiting first bubble..."
      DO
            Flow$ = getbub$
            CALL DoFlowMeter(Flow$)
      LOOP UNTIL GotFlow% = 1
      GotFlow% = 0
      DO
            Flow$ = getbub$
            CALL DoFlowMeter(Flow$)
      LOOP UNTIL GotFlow% = 1
END IF

CLS
A$ = "y"
PRINT "input filename for logged data. Do NOT use a file extension."
INPUT filename$
curfilename$ = filename$ + "." + pad$(extension%, 3)
OPEN curfilename$ FOR APPEND AS #1
 IF SEEK(1) > 1 THEN
      PRINT
      BEEP
      PRINT "a file of this name already exists - please use a
different"
      PRINT "filename or delete the file. Then re-run the program."
      CLOSE (1)
      END
 END IF
CLS

REM now set up loop for logging
time.now& = TIMER
time.last.time& = time.now&
time.then& = time.now& + interval%
day.now% = 0
day.then% = 0
flag% = 0

counter = 0

REM *****************************************************
REM MAIN PROGRAM
REM *****************************************************

GotFlow% = 0
NumPressure = 0
FOR n% = start% TO stp%
      SumPressure(n%) = 0
NEXT

CALL PrintHeader

ResetTime = 1
TimeOffset = 0

DO
      DO
            CALL up.time
      LOOP UNTIL ((day.now% >= day.then%) AND (time.now& >=
time.then&))

      CALL average812(average.cnt)
      CALL convertpress
```

```
        Flow$ = getbub$
        CALL DoFlowMeter(Flow$)

        IF GotFlow% = 1 THEN
              IF ResetTime = 1 THEN
                    TimeOffset = ElapsedTime
                    ResetTime = 0
              END IF

              FOR n% = start% TO stp%
                    SumPressure(n%) = SumPressure(n%) / NumPressure
              NEXT

              CALL PrintScreen

              GotFlow% = 0
              NumPressure = 0
              FOR n% = start% TO stp%
                    SumPressure(n%) = 0
              NEXT

              counter% = (counter% + 1) MOD filesize%
              IF counter% = 0 THEN
                    CLOSE (1)
                    extension% = (extension% + 1) MOD 1000
                    curfilename$ = filename$ + "." + pad$(extension%, 3)
                    OPEN curfilename$ FOR APPEND AS #1
              END IF
        END IF

        CALL move.on(interval%)  'this increments day.now and time.now

        A$ = INKEY$: IF A$ = "s" OR A$ = "S" THEN flag% = 1

LOOP UNTIL flag% = 1
CLOSE
END

REM ****************************************************
SUB average812 (total)
SHARED port%, results(), averages(), start%, stp%

OUT port% + 11, 1            'ENABLE SOFTWARE TRIGGER
dummy = INP(port% + 4)        'DUMMY READ, CLEAR DRDY
FOR ch% = start% TO stp%: results(ch%) = 0: averages(ch%) = 0: NEXT

FOR n = 1 TO total  'number of averages
FOR ch% = start% TO stp%
OUT port% + 10, ch%        'SET MUX CHANNEL
FOR wait1 = 0 TO 25: NEXT wait1     'WAIT FOR SWITCHING
OUT port% + 12, 0          'SOFTWARE TRIG

DO
    dh% = INP(port% + 5)       'READ HIGH BYTE DATA
LOOP UNTIL (dh% AND 16) = 0            'CHECK DRDY READY ?

dl% = INP(port% + 4)       'READ LOW BYTE DATA
averages(ch%) = averages(ch%) + (dh% * 256 + dl% - 2048)    'STORE  A/D
DATA INTO ARRAY
NEXT ch%
NEXT n

FOR ch% = start% TO stp%
results(ch%) = averages(ch%) / total
```

```
NEXT

END SUB

REM ************************************
SUB convertpress

SHARED start%, stp%, results(), offset%(), scalef(), range(),
pressure(), SumPressure(), NumPressure
STATIC n%
FOR n% = start% TO stp%
      pressure(n%) = (results(n%) - offset%(n%)) * 100 * range(n%) /
(scalef(n%) * 2048)
'the * 100 bit is to convert to millivolts, since the scale factors are
just
'fullscale delta-V in millivolts.
      SumPressure(n%) = SumPressure(n%) + pressure(n%)
NEXT
NumPressure = NumPressure + 1
END SUB

REM ************************************
SUB DoFlowMeter (A$)

SHARED eltim$, transtim$, flux, fluxscale, fluxconst, ElapsedTime,
GotFlow%

IF LEN(A$) = 9 THEN
      eltim$ = MID$(A$, 6, 4)
      transtim$ = MID$(A$, 2, 4)
      ElapsedTime = VAL(eltim$)
      GotFlow% = 1
ELSEIF LEN(A$) = 3 THEN
    eltim$ = "----"
    transtim$ = "----"
ELSEIF LEN(A$) = 1 THEN
    eltim$ = "----"
    transtim$ = "----"
END IF

IF transtim$ <> "----" THEN
   transtim = VAL(transtim$)
   IF transtim <> 0 THEN
      flux = fluxconst + (fluxscale / transtim)
   ELSE
      flux = -1
   END IF
ELSE flux = -1
END IF

END SUB

REM ************************************
FUNCTION getbub$

'first of all, clear the buffer
WHILE LOC(3) > 0
      A$ = INPUT$(1, 3)
WEND
PRINT #3, "E";
b$ = ""
A$ = ""

DO
```

```
   b$ = b$ + A$
   A$ = INPUT$(1, 3)
LOOP UNTIL A$ = CHR$(13)

getbub$ = b$
END FUNCTION

REM ************************************
SUB move.on (interval%)

time.then& = time.then& + interval%
IF time.then& >= 86400 THEN
   time.then& = time.then& MOD 86400
   day.then% = day.then% + 1
END IF
END SUB

REM ************************************
FUNCTION pad$ (value%, size%)

temp$ = MID$(STR$(value%), 2)
pad$ = RIGHT$("00000000" + temp$, size%)
END FUNCTION

SUB PrintHeader

PRINT "Press S to Stop"
PRINT
PRINT "Elapsed Time   ";
PRINT "Trans Mem(bar)  ";
PRINT "Perm Pres(bar)  ";
PRINT "Pre1 (bar)   ";
PRINT "Flow Rate l/min"

END SUB

REM ******************************************
SUB PrintScreen

SHARED ElapsedTime, TimeOffset, start%, stp%, results(), pressure(),
Flow$, flux, SumPressure()

      PRINT (ElapsedTime - TimeOffset);
      PRINT #1, (ElapsedTime - TimeOffset);

      PRINT TAB(19);
      PRINT #1, TAB(10);
      PRINT USING "+#.###"; ((SumPressure(0) + SumPressure(2)) / 2);
      PRINT #1, USING "+#.####"; ((SumPressure(0) + SumPressure(2)) /
2);


      FOR n% = (start% + 1) TO stp%
            PRINT TAB(n% * 17 + 16);
            PRINT #1, TAB(n% * 12 + 10);
            PRINT USING "+#.###"; SumPressure(n%);
            PRINT #1, USING "+#.####"; SumPressure(n%);
      NEXT

      PRINT TAB(63);
      PRINT USING "##.##"; flux;
      PRINT #1, TAB(52);
      PRINT #1, USING "##.##"; flux;
```

```
      PRINT
      PRINT #1, ""

END SUB

REM ************************************
SUB up.time

time.now& = TIMER
IF time.now& < time.last.time THEN
  day.now% = day.now% + 1
END IF
time.last.time& = time.now&
END SUB

REM ************************************
SUB ZeroTime

'first empty the buffer
WHILE LOC(3) > 0
      A$ = INPUT$(1, 3)
WEND
PRINT #3, "H";
DO
      A$ = INPUT$(1, 3)
LOOP UNTIL A$ = CHR$(13)

END SUB
```

Appendix C Plots for main experimental analysis

S. multivorum in Low NaCl

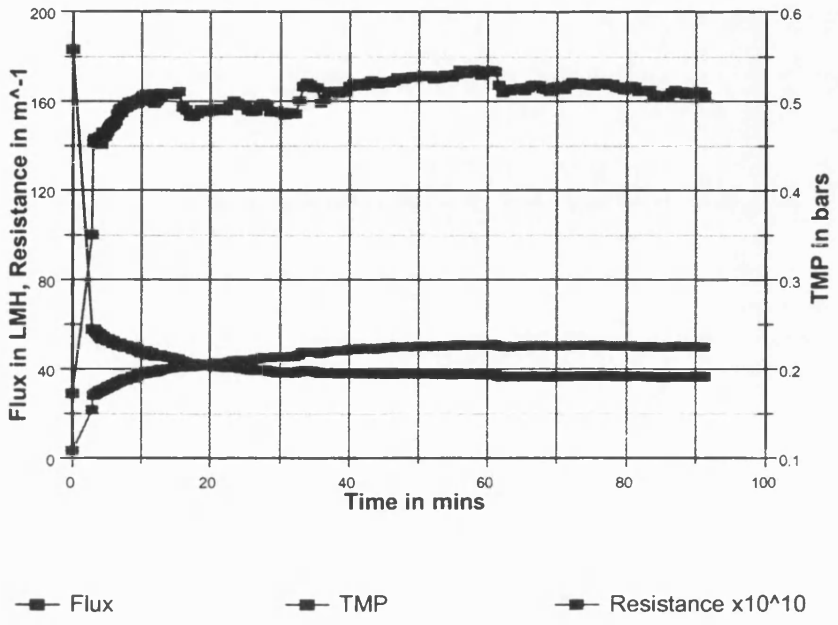

Figure 12 Comparison of TMP, flux and resistance for *S.multivorum* in low NaCl

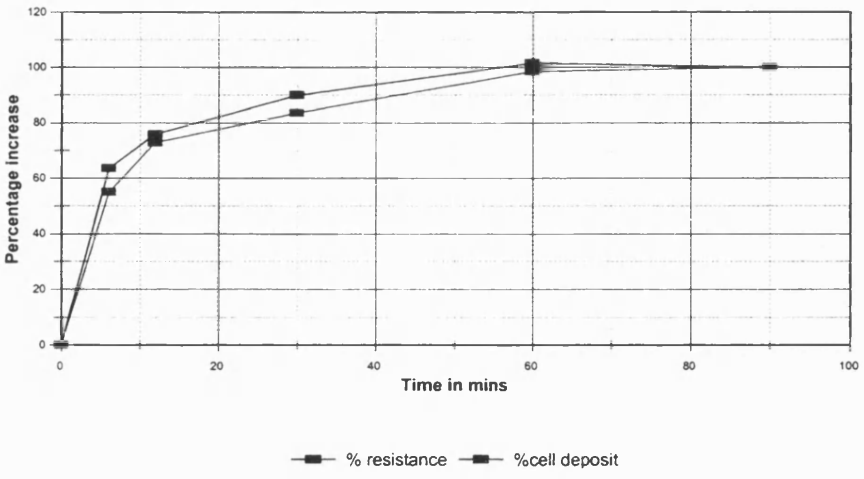

Figure 13 Comparison of percentage increases over time of resistance and cell deposition for *S.multivorum* in low NaCl

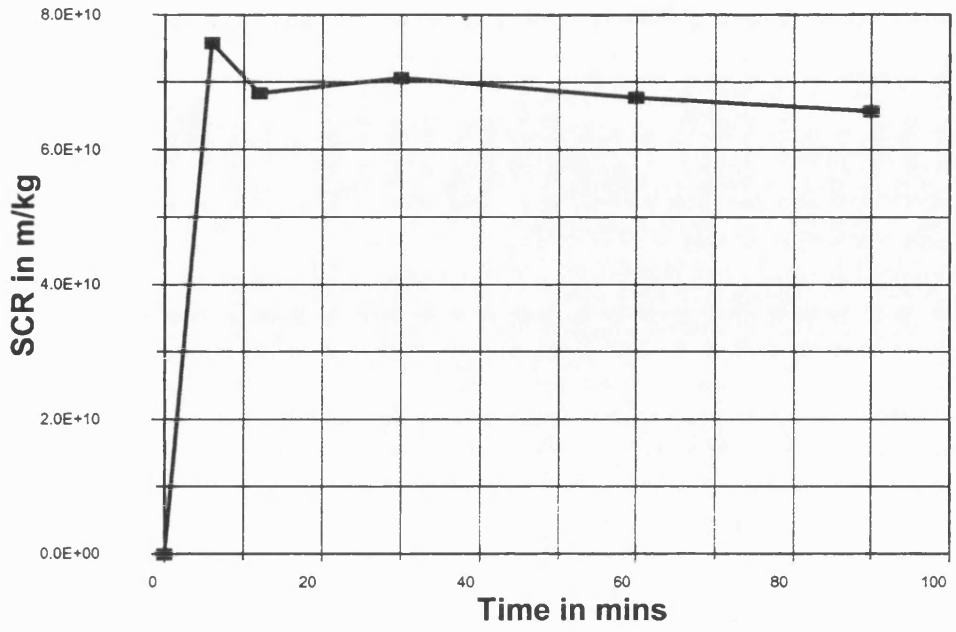

Figure 14 SCR change over time for *S.multivorum* in low NaCl

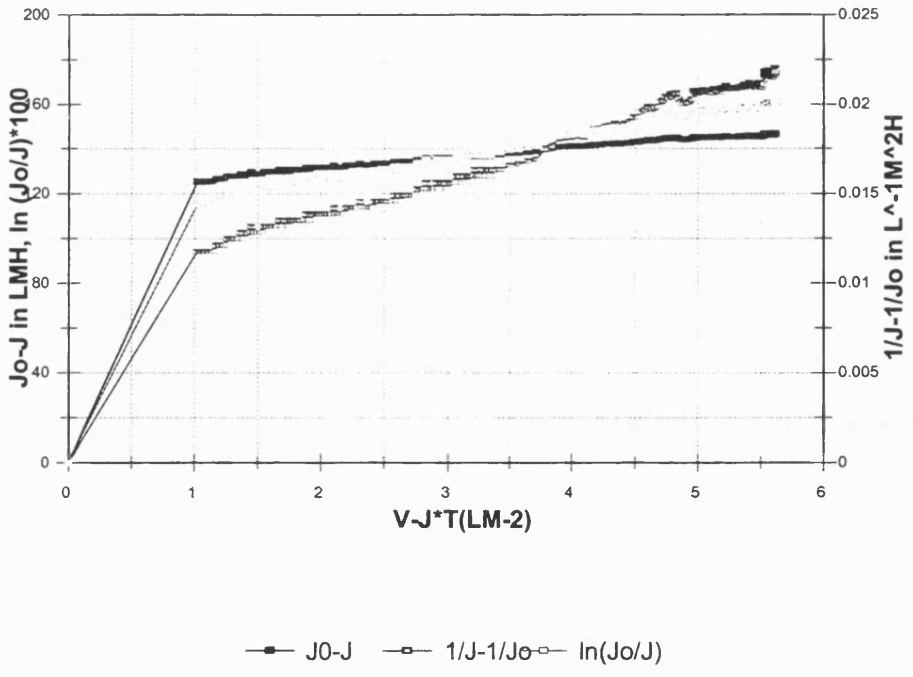

Figure 15 Model 3 results for *S.multivorum* in low NaCl

S.multivorum in High NaCl

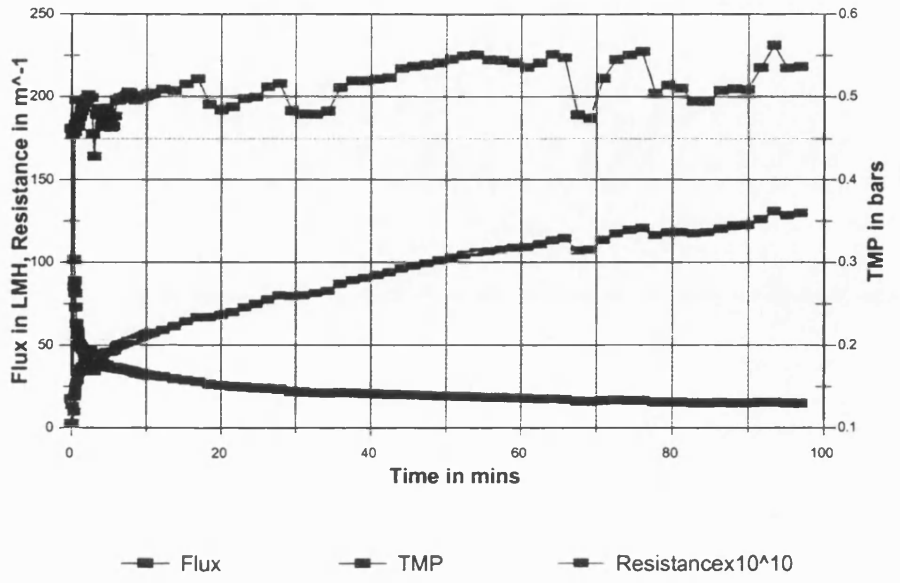

Figure 16 Comparison of TMP, flux and resistance for *S.multivorum* in high NaCl

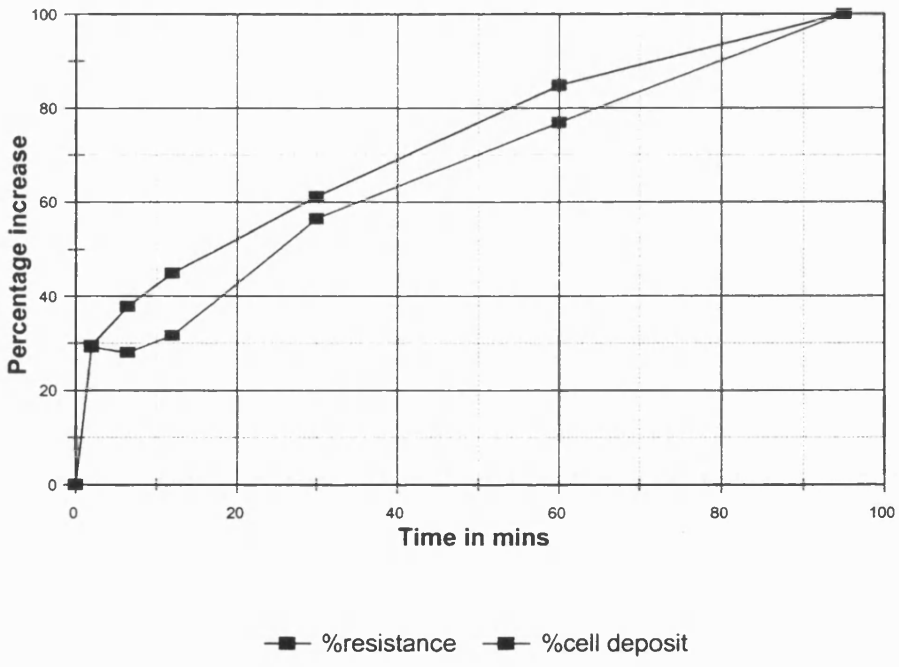

Figure 17 Comparison of percentage increases over time of resistance and cell deposition for *S.multivorum* in high NaCl

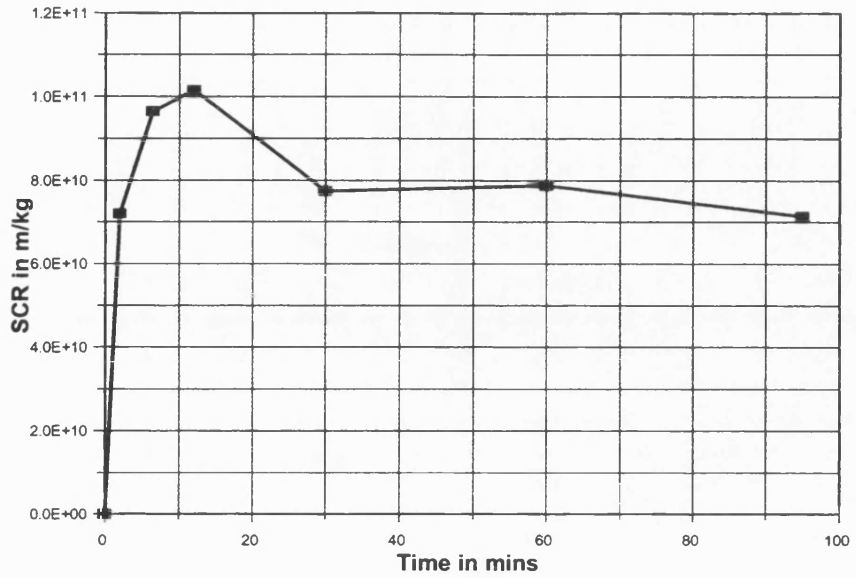

Figure 18 SCR change over time for *S.multivorum* in high NaCl

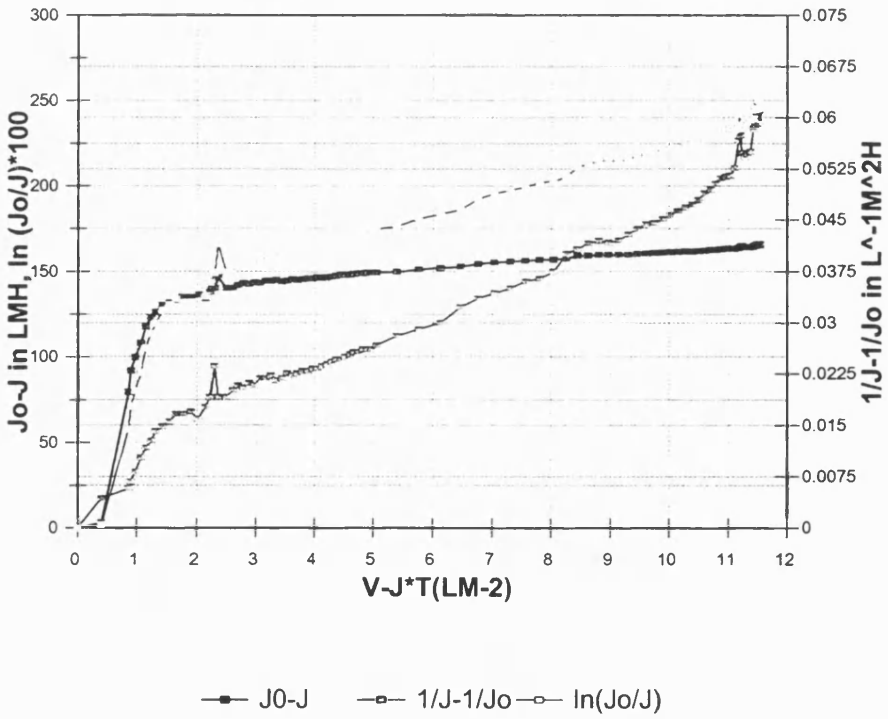

Figure 19 Model 3 results for *S.multivorum* in high NaCl

S.multivorum in low $CaCl_2$

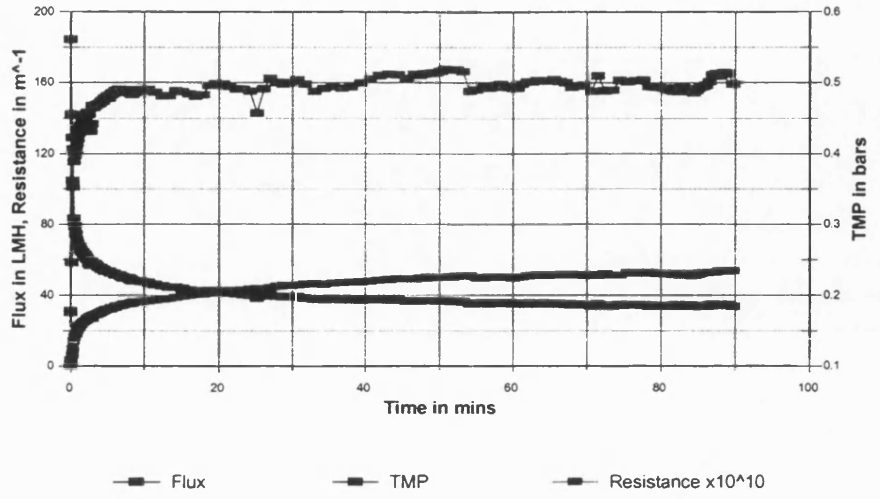

Figure 20 Comparison of TMP, flux and resistance for *S.multivorum* in low $CaCl_2$

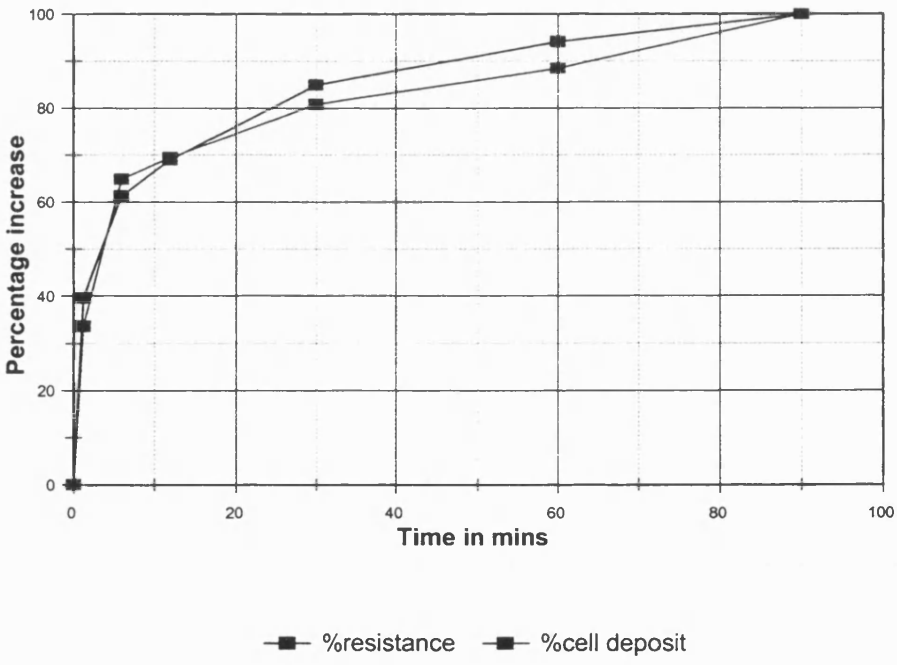

Figure 21 Comparison of percentage increases over time of resistance and cell deposition for *S.multivorum* in low $CaCl_2$

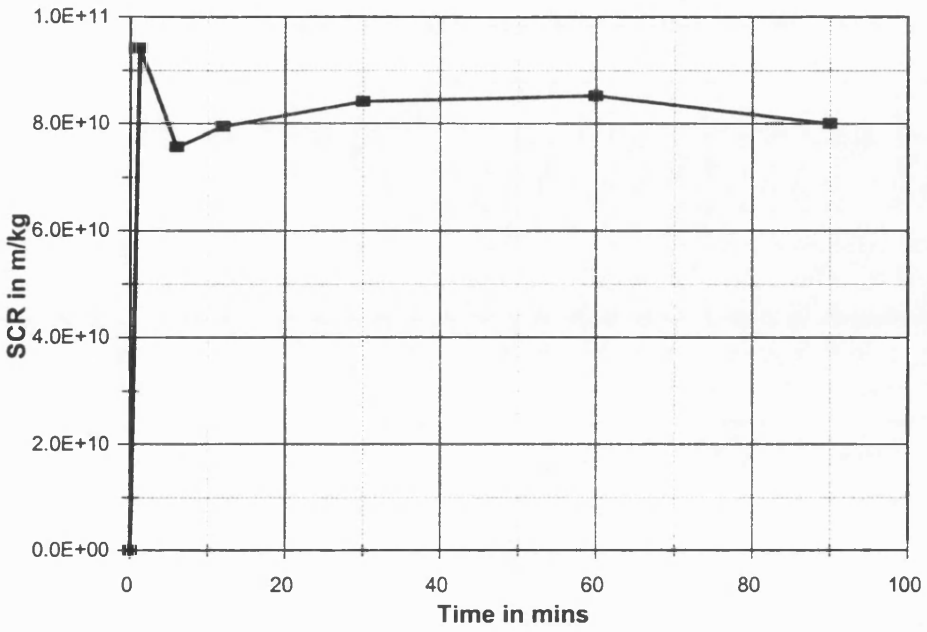

Figure 22 SCR change over time for *S.multivorum* in low $CaCl_2$

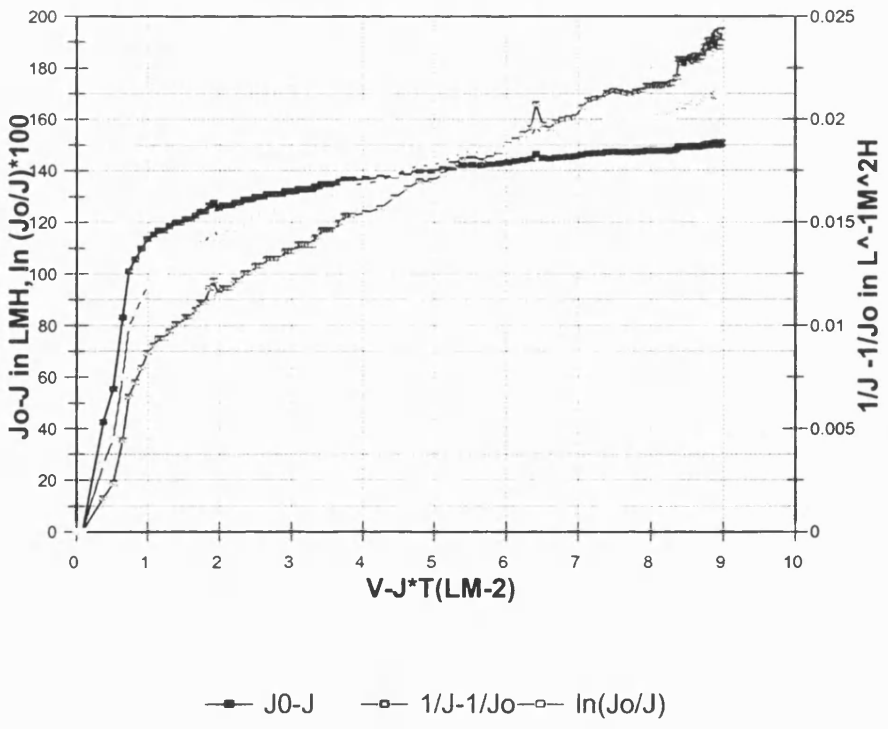

Figure 23 Model 3 results for *S.multivorum* in low $CaCl_2$

S.multivorum in High $CaCl_2$

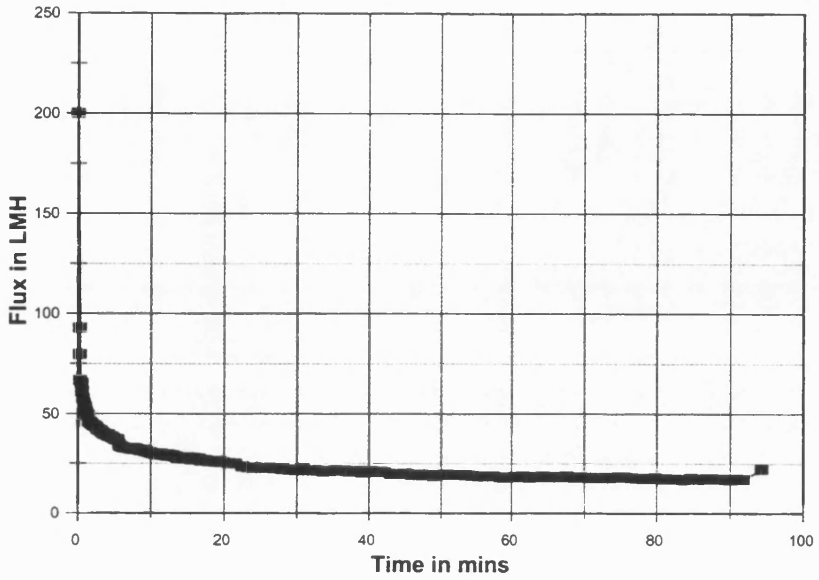

Figure 24 Flux for *S.multivorum* in high $CaCl_2$

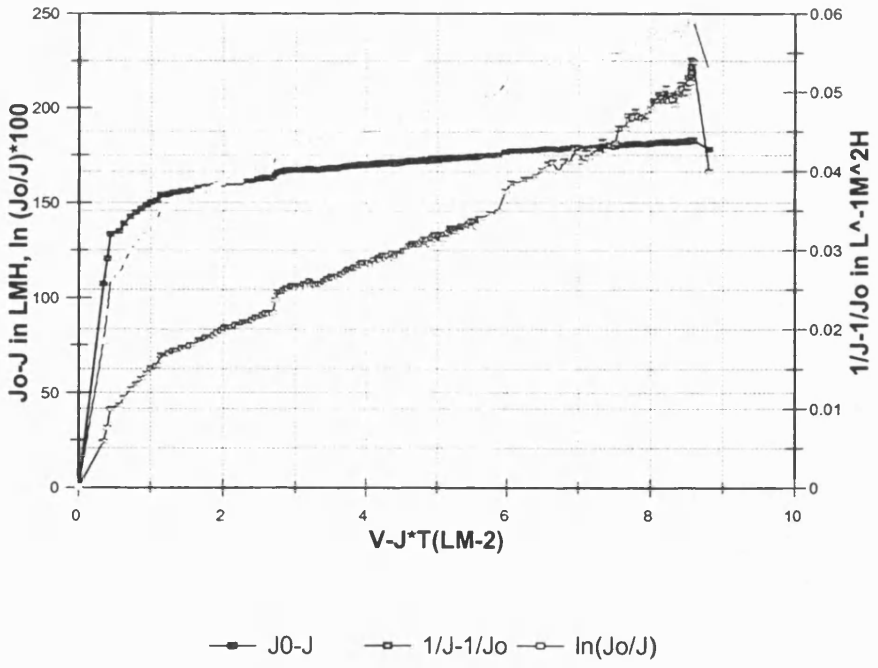

Figure 25 Model 3 results for *S.multivorum* in high $CaCl_2$

S.multivorum in low NaCl with BSA

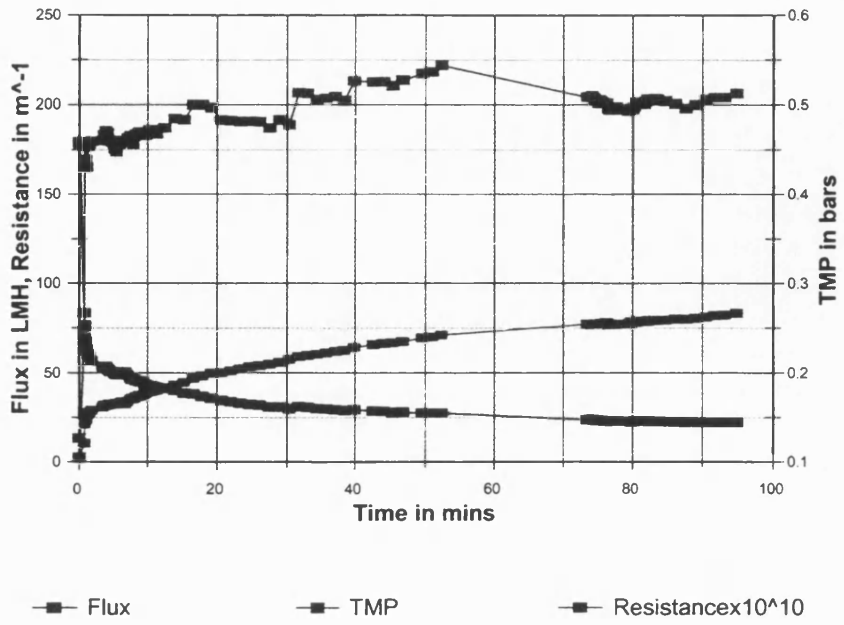

Figure 26 Comparison of TMP, flux and resistance for *S.multivorum* in low NaCl with BSA

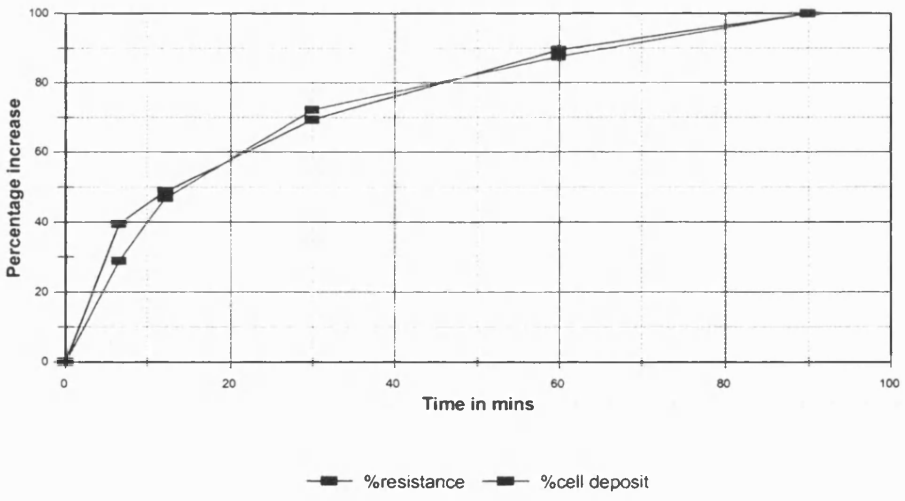

Figure 27 Comparison of percentage increases over time of resistance and cell deposition for *S.multivorum* in low NaCl with BSA

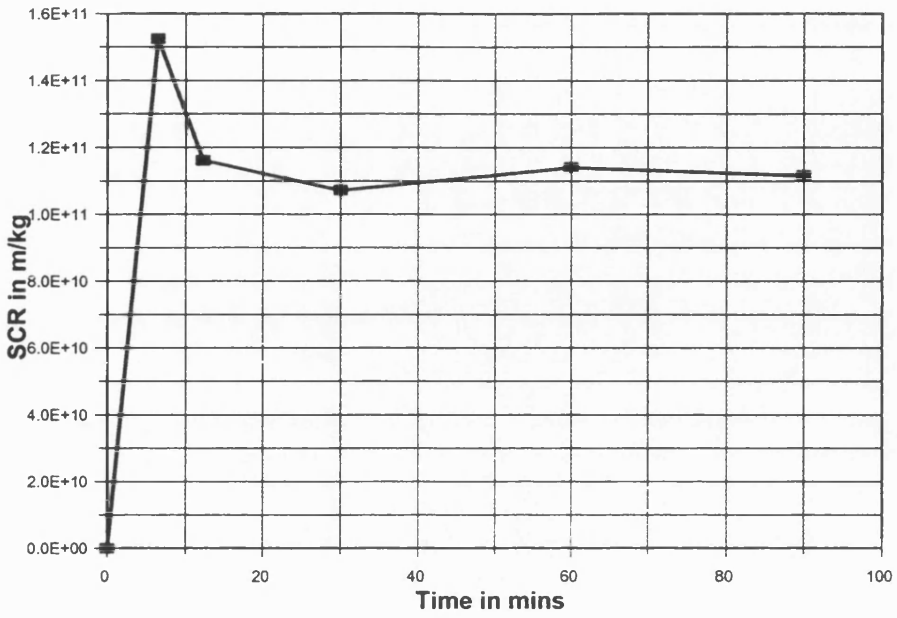

Figure 28 SCR change over time for *S.multivorum* in low NaCl with BSA

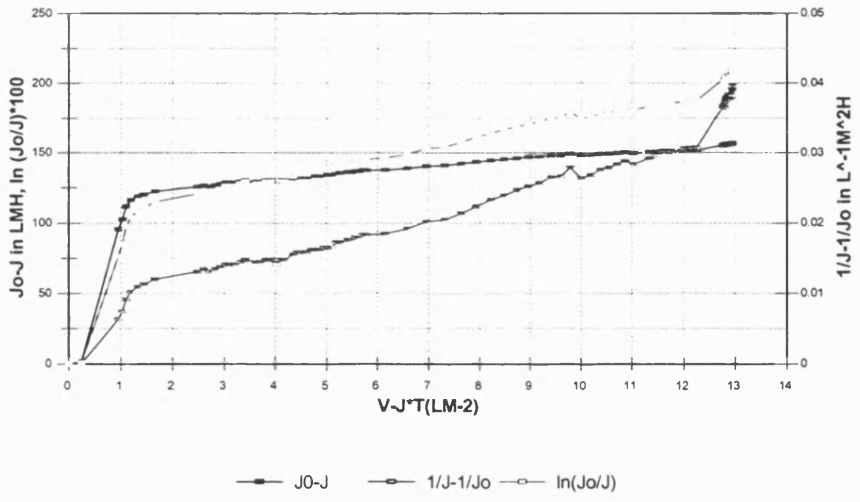

Figure 29 Model 3 results for *S.multivorum* in low NaCl with BSA

S.multivorum in High NaCl with BSA

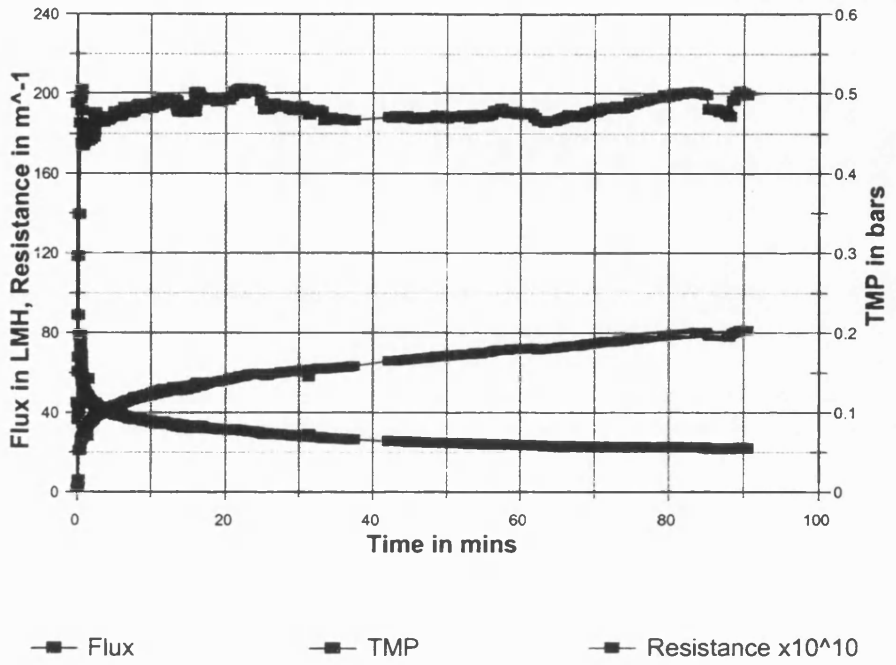

Figure 30 Comparison of TMP, flux and resistance for *S.multivorum* in high NaCl with BSA

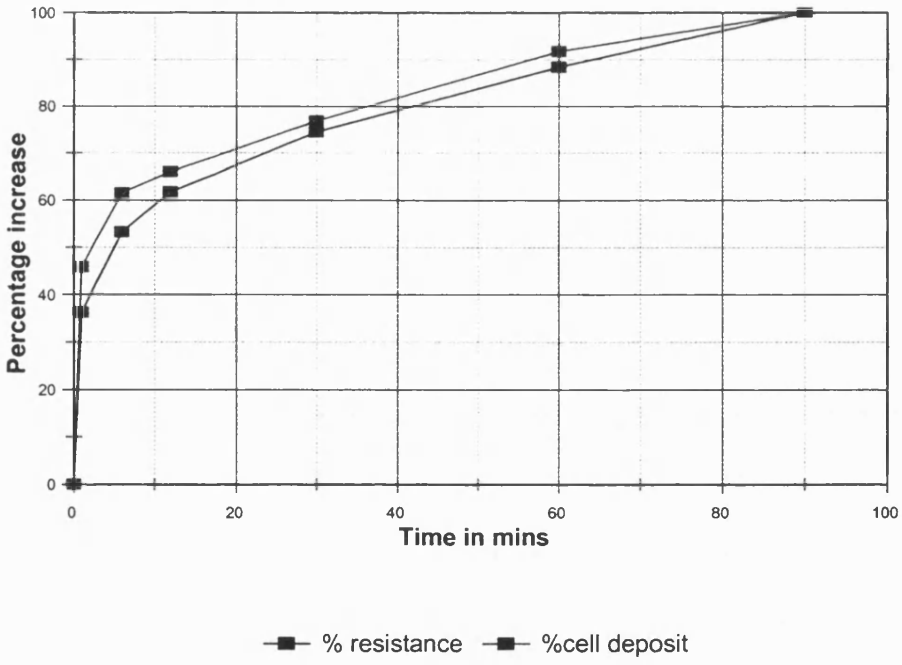

Figure 31 Comparison of percentage increases over time of resistance and cell deposition for *S.multivorum* in high NaCl with BSA

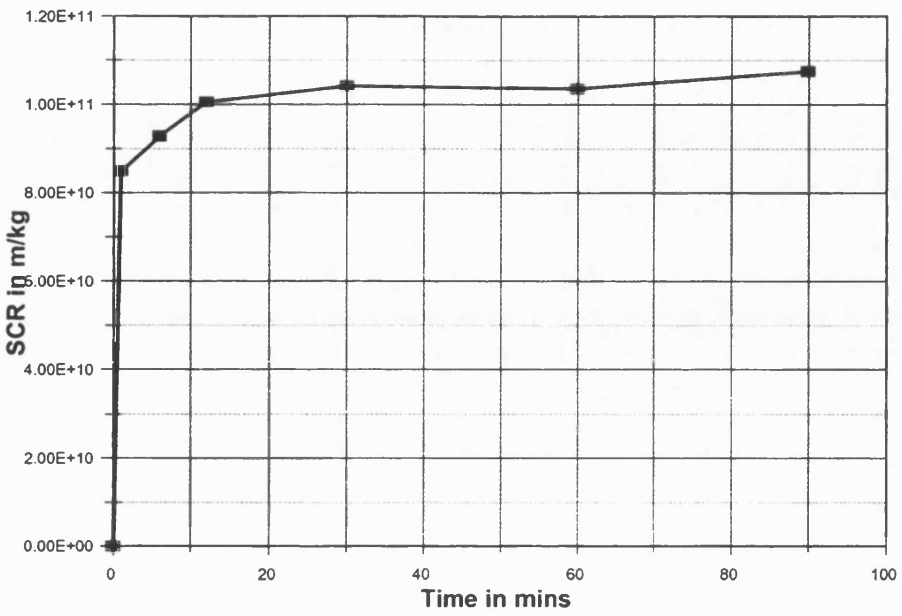

Figure 32 SCR change over time for *S.multivorum* in high NaCl with BSA v

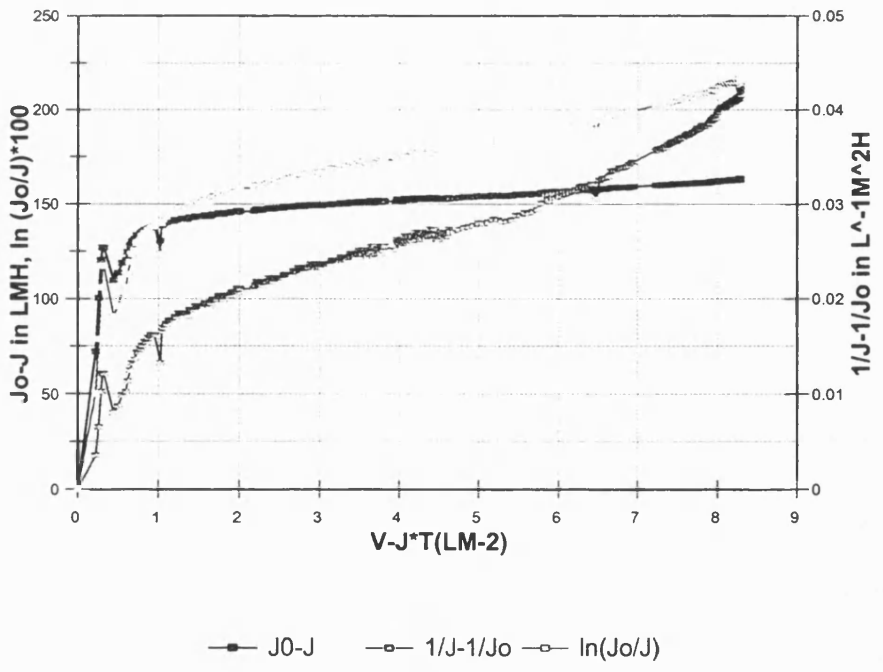

Figure 33 Model 3 results for *S.multivorum* in high NaCl with BSA

S.multivorum in High $CaCl_2$ with BSA

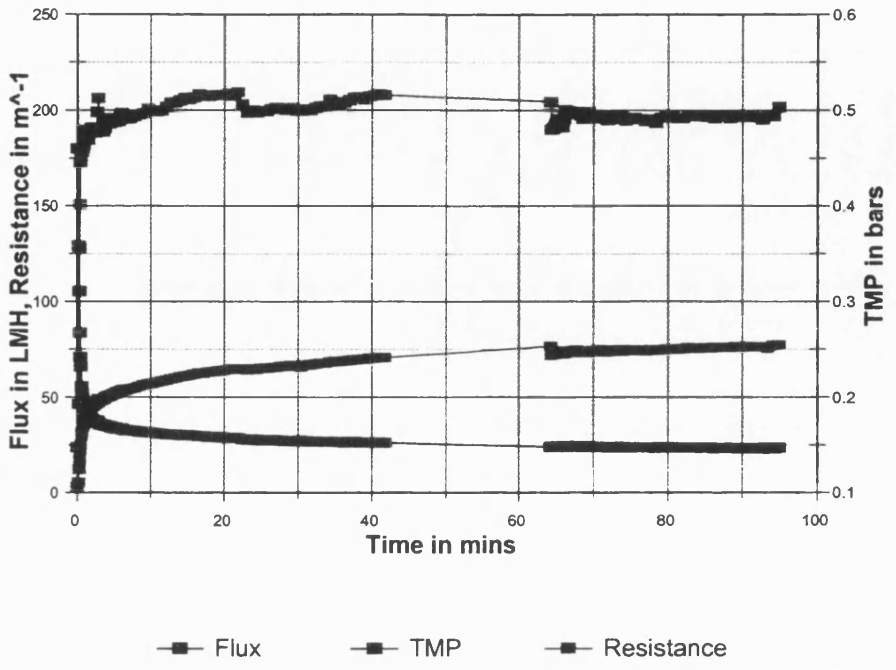

Figure 34 Comparison of TMP, flux and resistance for *S.multivorum* in high $CaCl_2$ with BSA

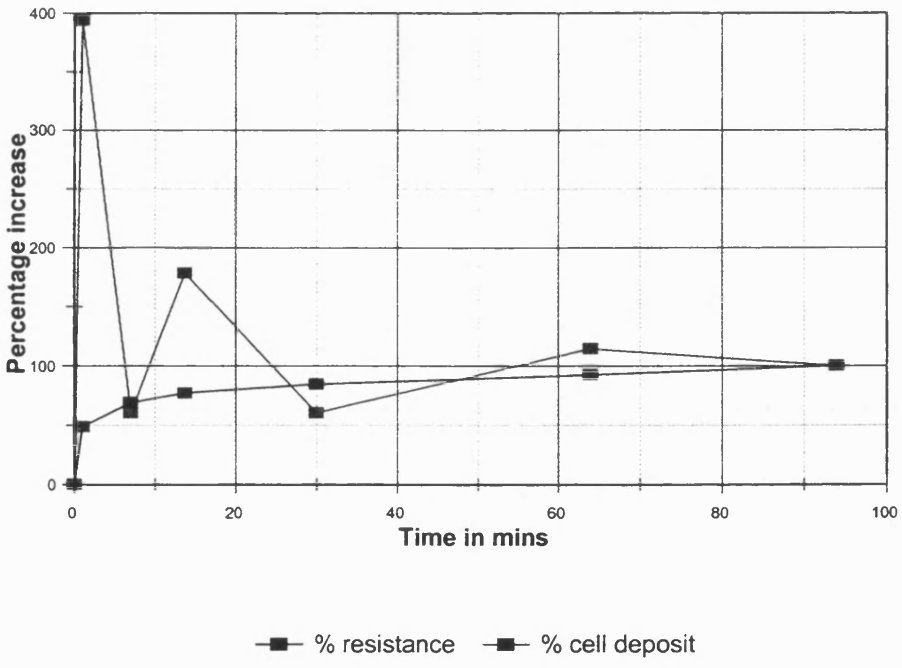

Figure 35 Comparison of percentage increases over time of resistance and cell deposition for *S.multivorum* in high $CaCl_2$ with BSA

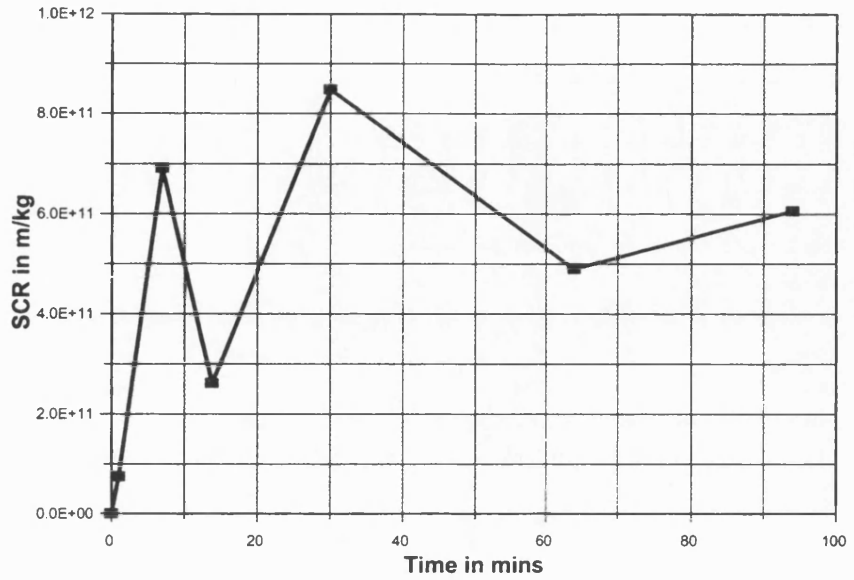

Figure 36 SCR change over time for *S.multivorum* in high $CaCl_2$ with BSA

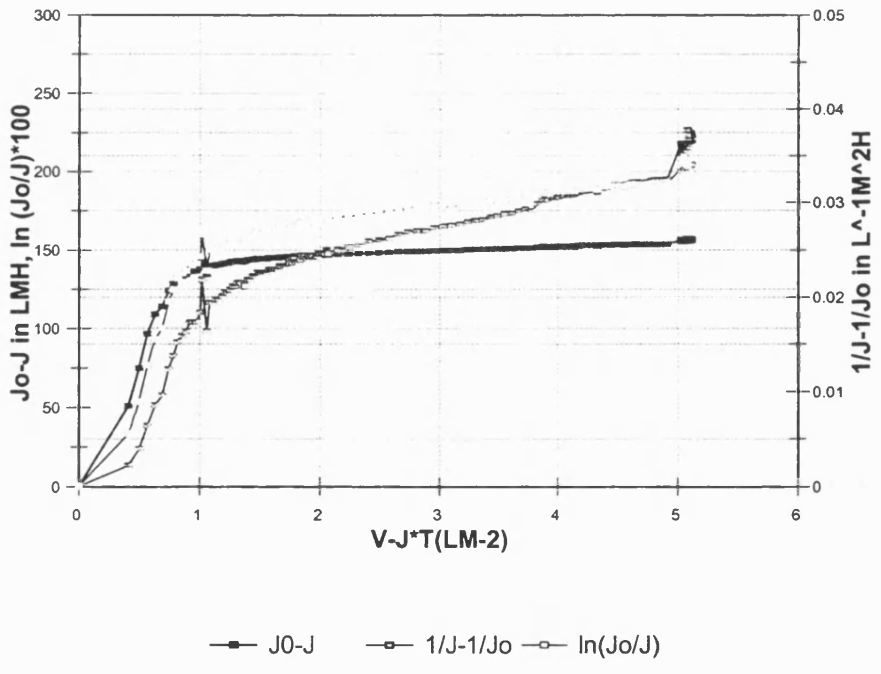

Figure 37 Model 3 results for *S.multivorum* in high $CaCl_2$ with BSA

P.elodea in Low NaCl

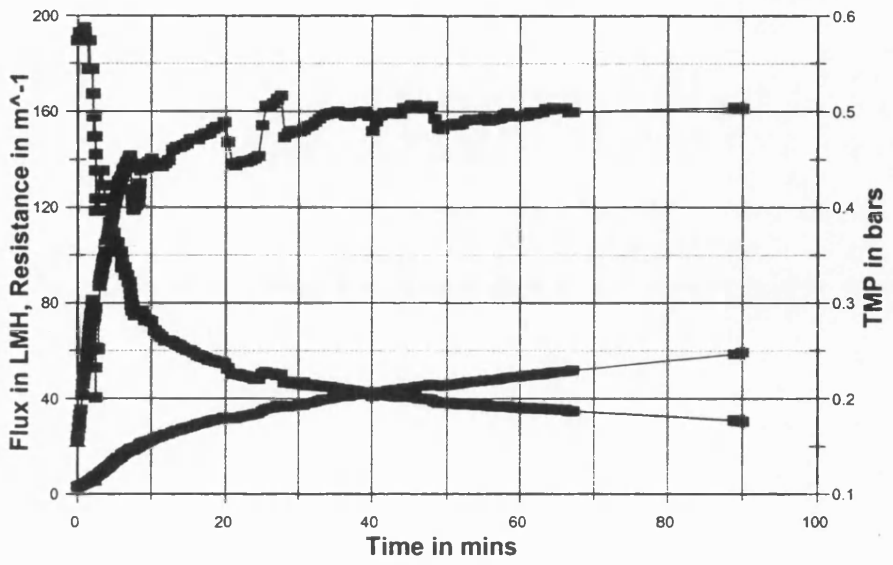

Figure 38 Comparison of TMP, flux and resistance for *P.elodea* in low NaCl

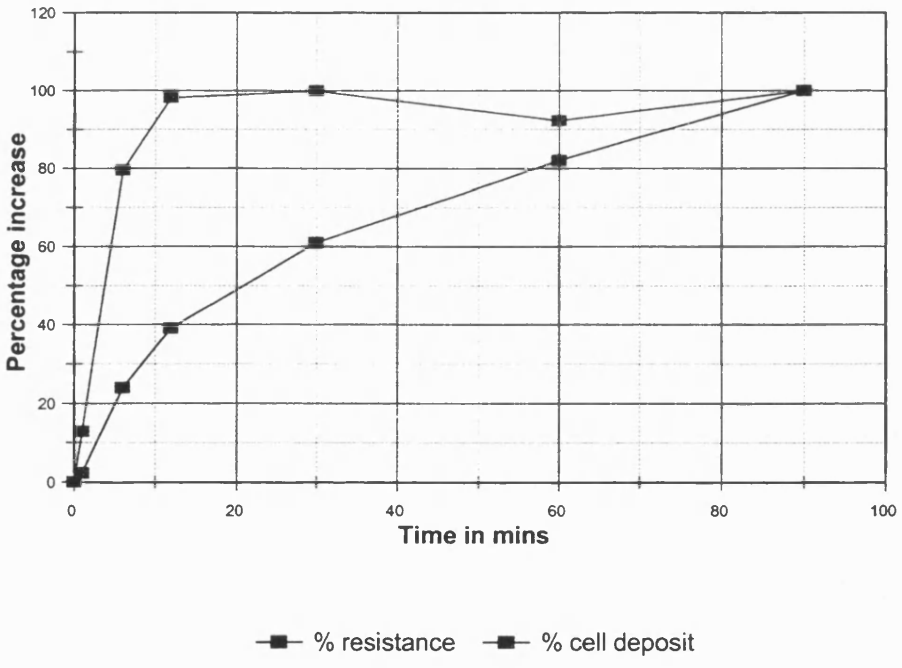

Figure 39 Comparison of percentage increases over time of resistance and cell deposition for *P.elodea* in low NaCl

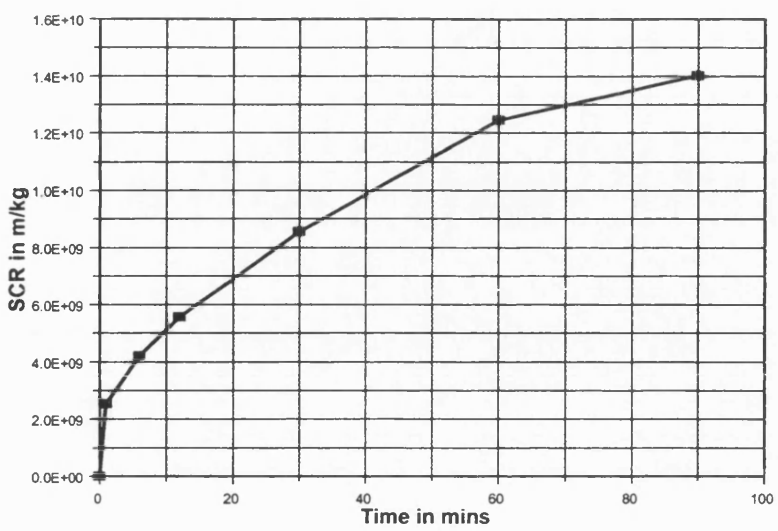

Figure 40 SCR change over time for *P.elodea* in low NaCl

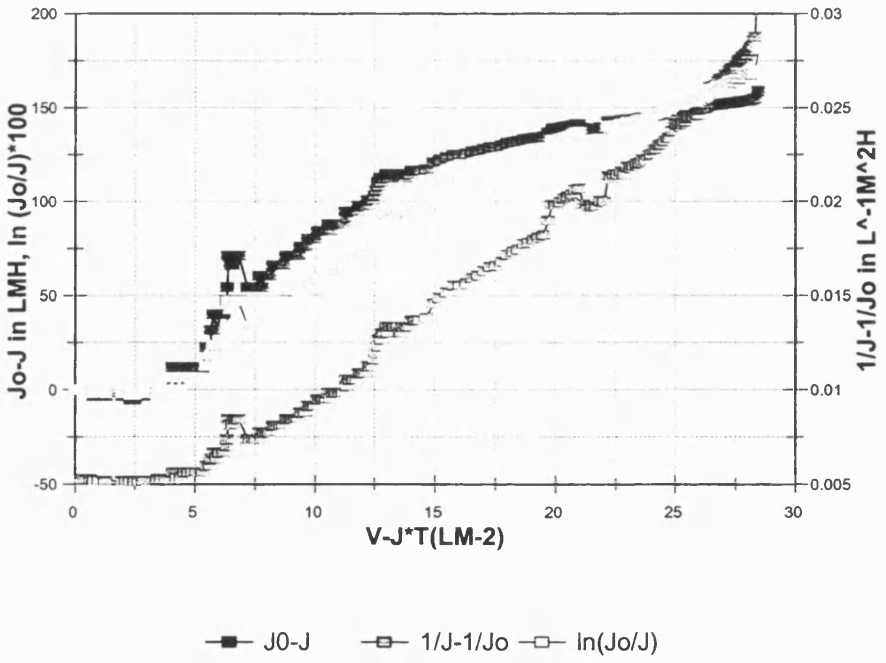

Figure 41 Model 3 results for *P.elodea* in low NaCl

P.elodea in High NaCl

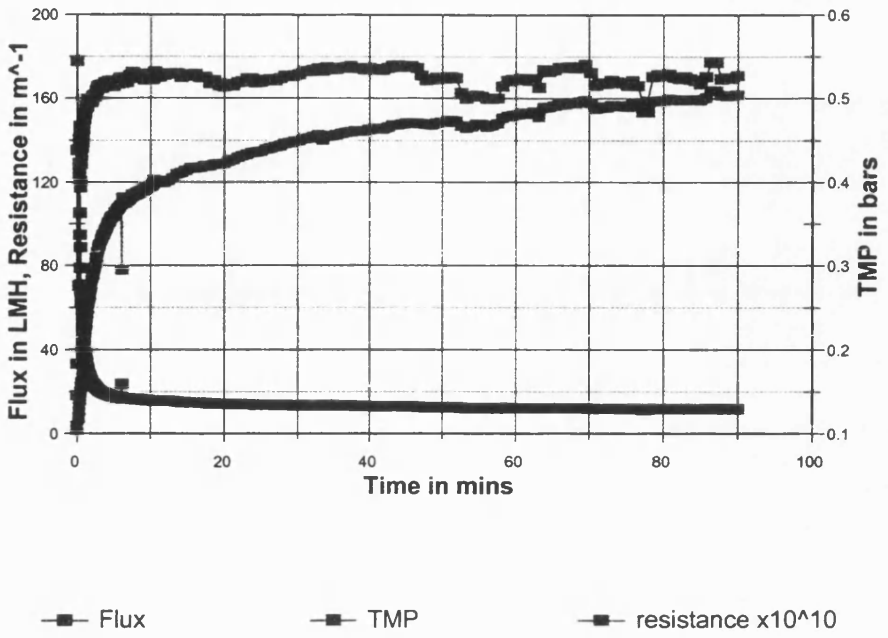

Figure 42 Comparison of TMP, flux and resistance for *P.elodea* in high NaCl

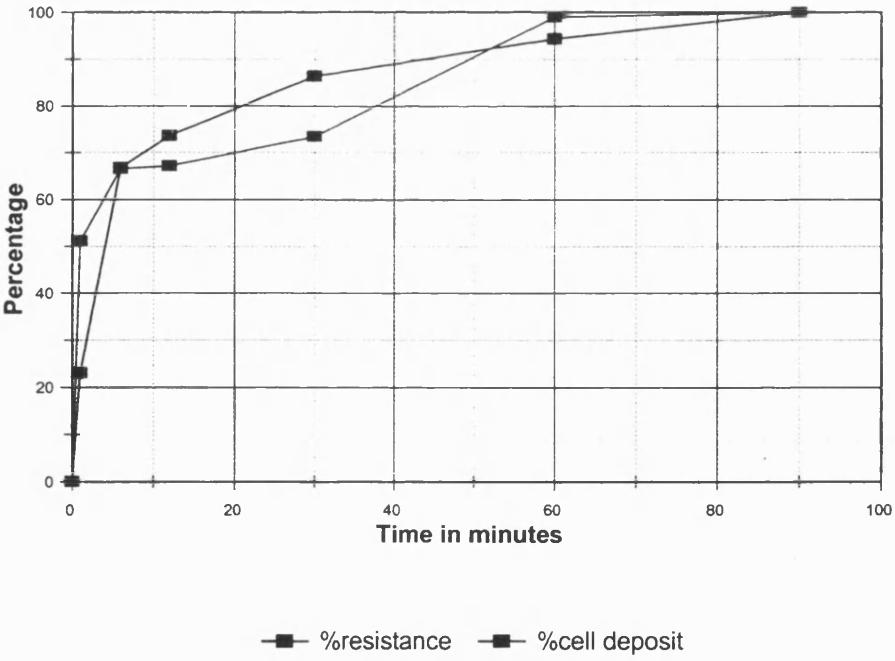

Figure 43 Comparison of percentage increases over time of resistance and cell deposition for *P.elodea* in high NaCl

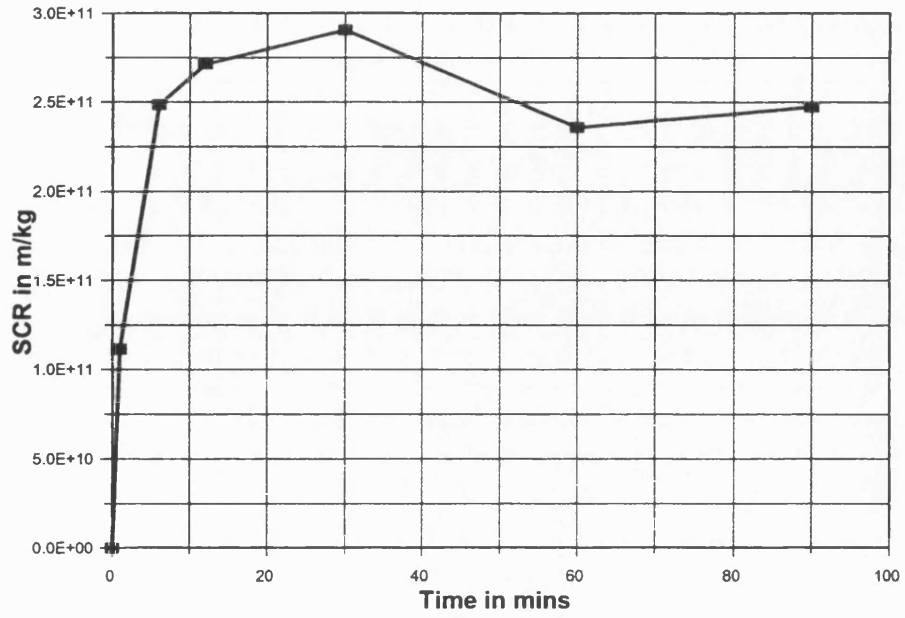

Figure 44 SCR change over time for *P.elodea* in high NaCl

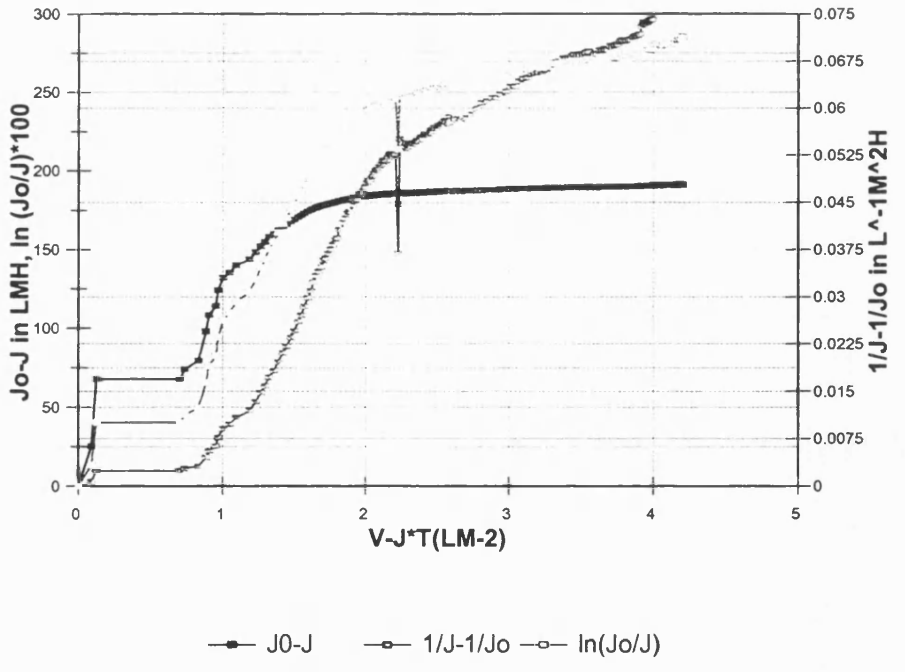

Figure 45 Model 3 results for *P.elodea* in high NaCl

P.elodea in Low $CaCl_2$

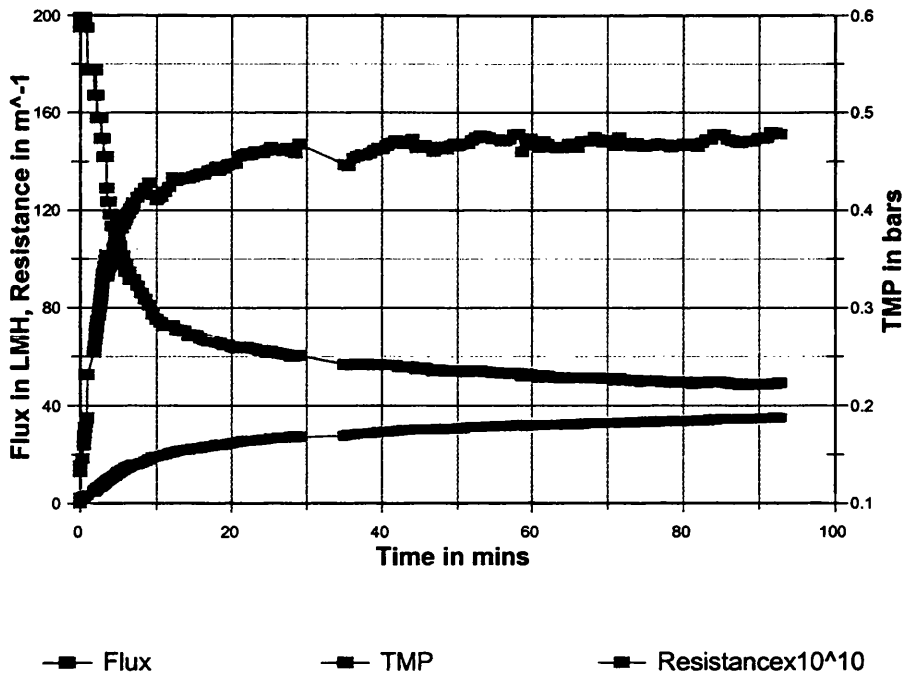

Figure 46 Comparison of TMP, flux and resistance for *P.elodea* in low $CaCl_2$

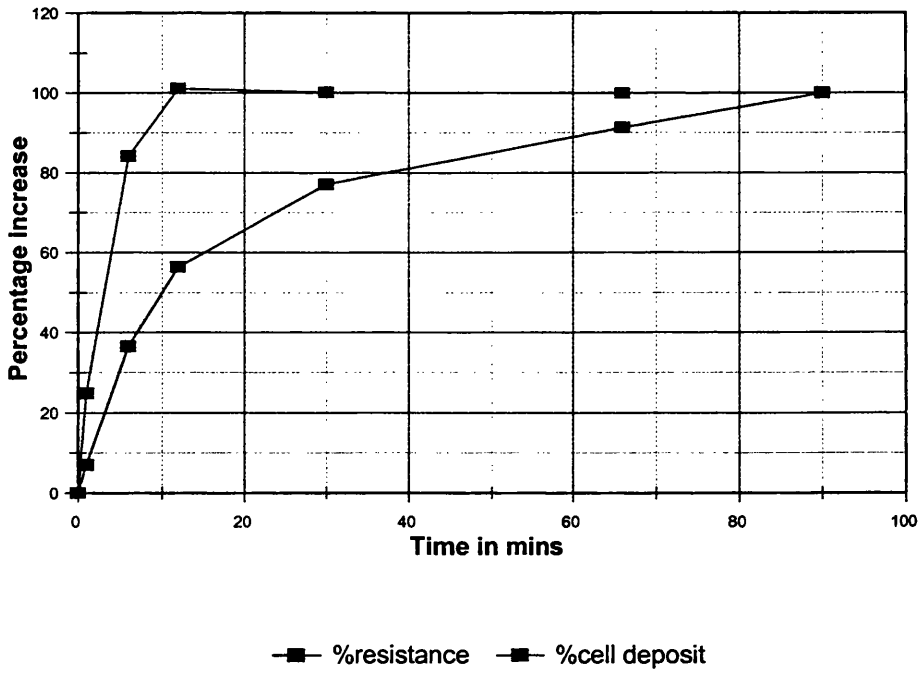

Figure 47 Comparison of percentage increases over time of resistance and cell deposition for *P.elodea* in low $CaCl_2$

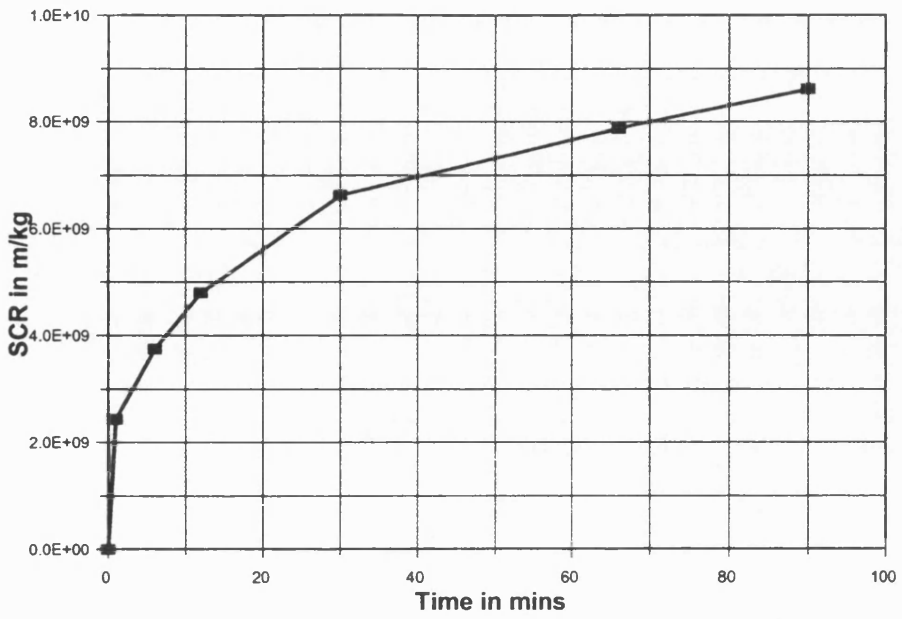

Figure 48 SCR change over time for *P.elodea* in Low $CaCl_2$

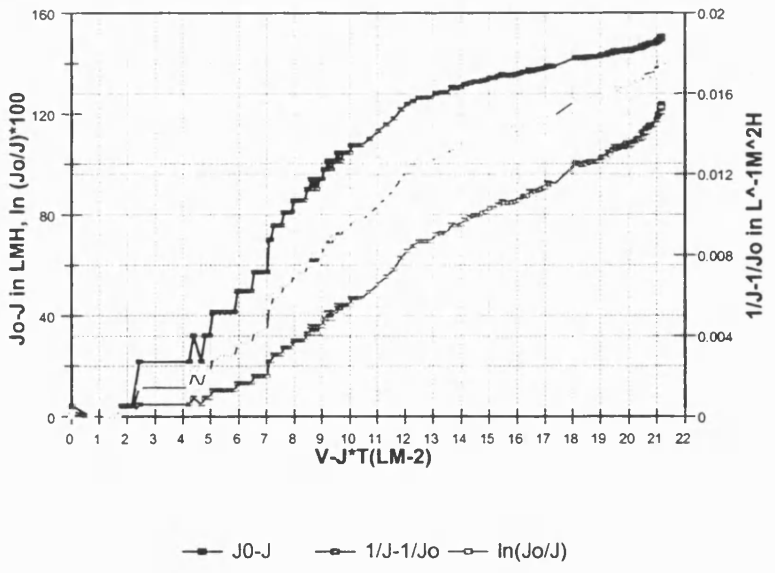

Figure 49 Model 3 results for *P.elodea* in Low $CaCl_2$

P.elodea in High $CaCl_2$

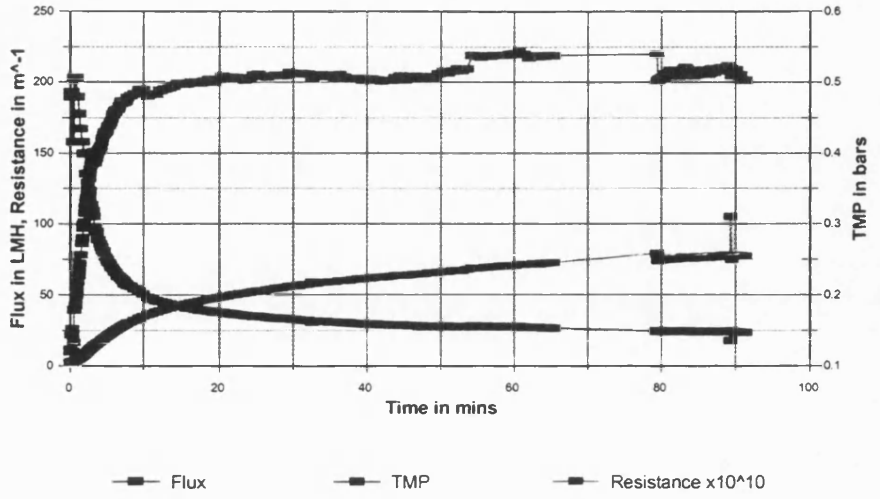

Figure 50 Comparison of TMP, flux and resistance for *P.elodea* in high $CaCl_2$

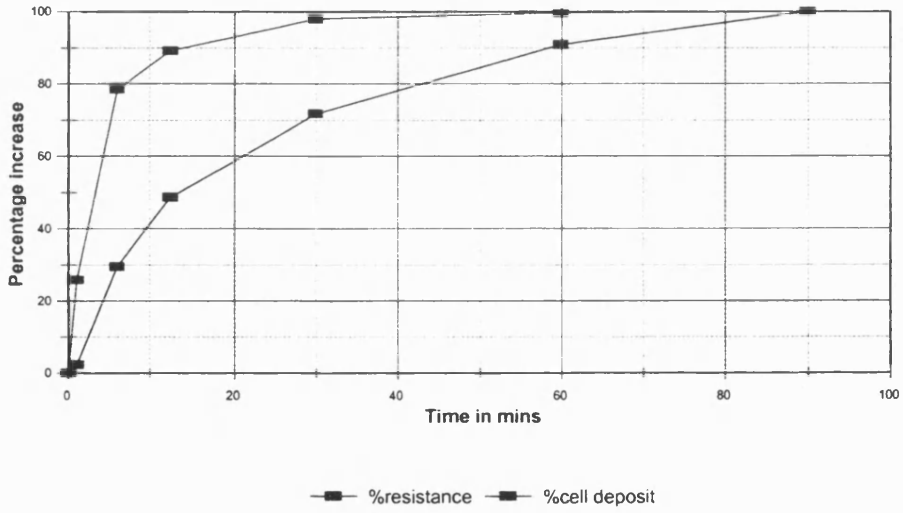

Figure 51 Comparison of percentage increases over time of resistance and cell deposition for *P.elodea* in high $CaCl_2$

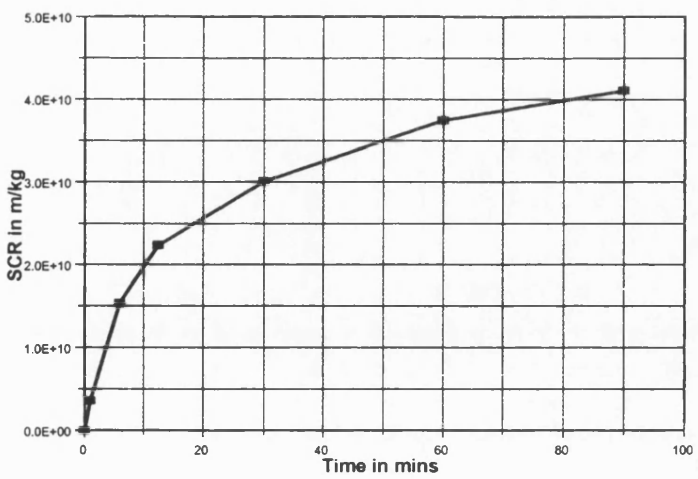

Figure 52 SCR change over time for *P.elodea* in high $CaCl_2$

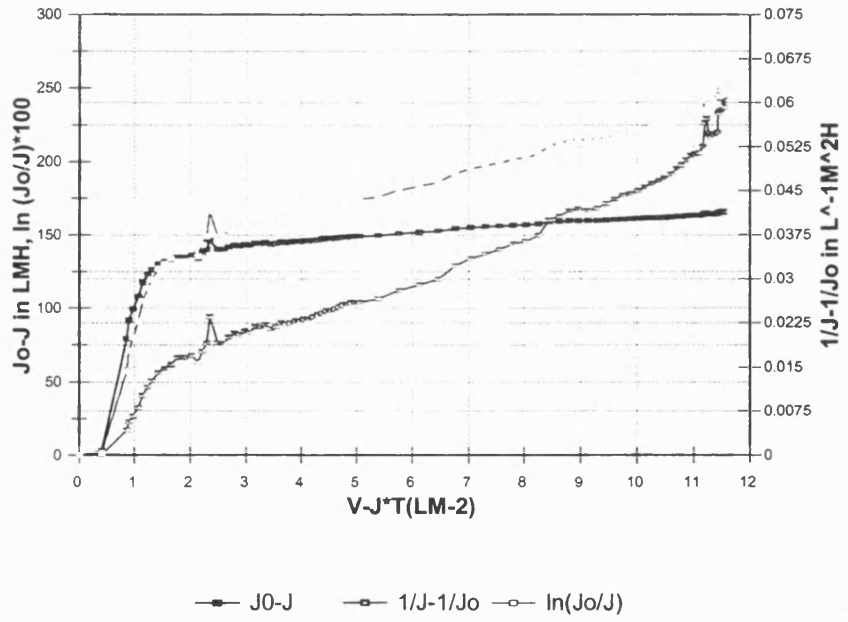

Figure 53 Model 3 results for *P.elodea* in high $CaCl_2$

P.elodea in Low NaCl with BSA

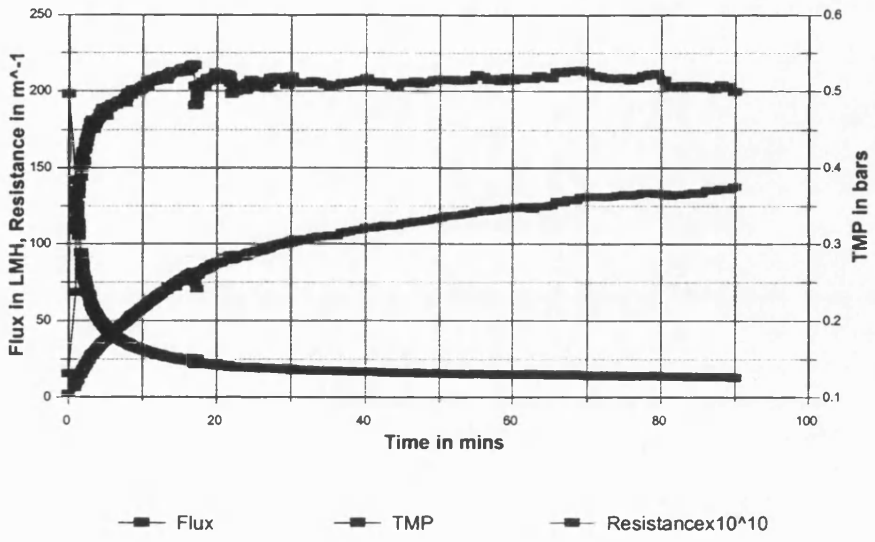

Figure 54 Comparison of TMP, flux and resistance for *P.elodea* in low NaCl with BSA

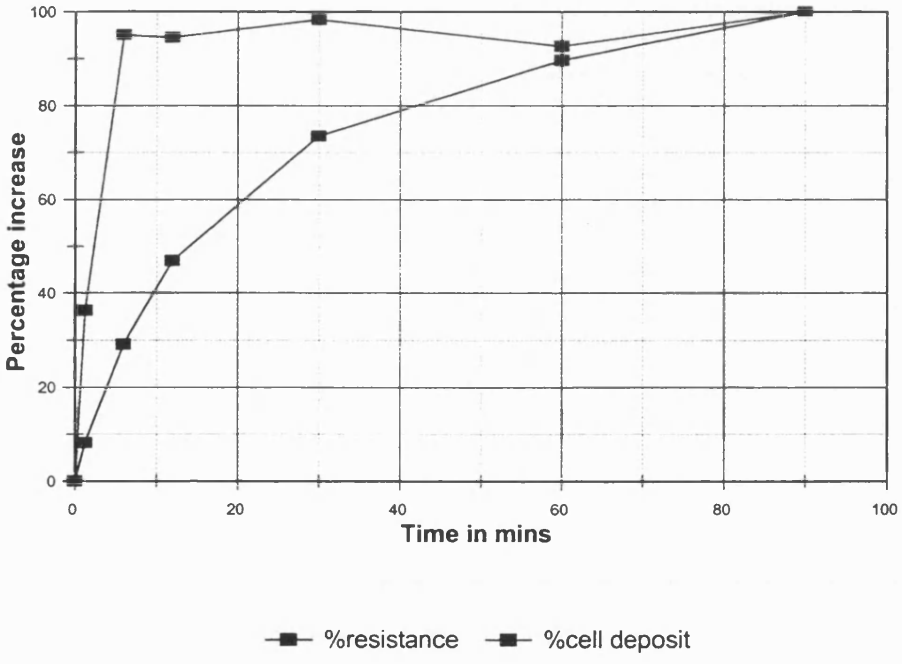

Figure 55 Comparison of percentage increases over time of resistance and cell deposition for *P.elodea* in low NaCl with BSA

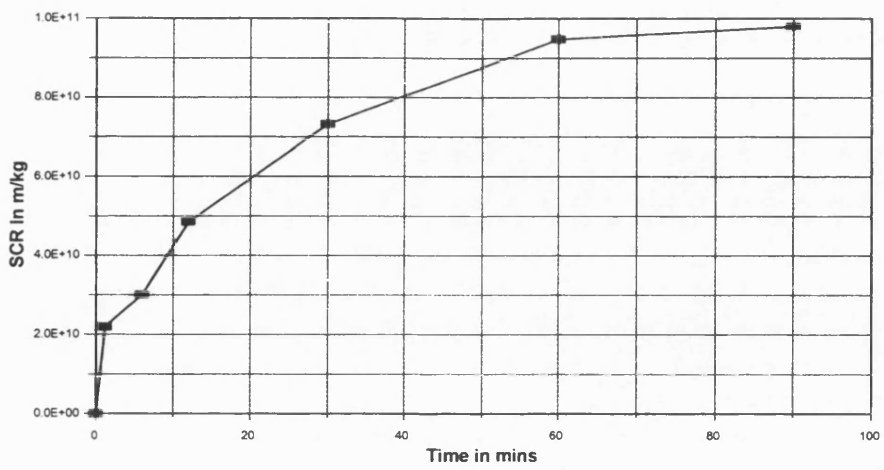

Figure 56 SCR change over time for *P.elodea* in low NaCl with BSA

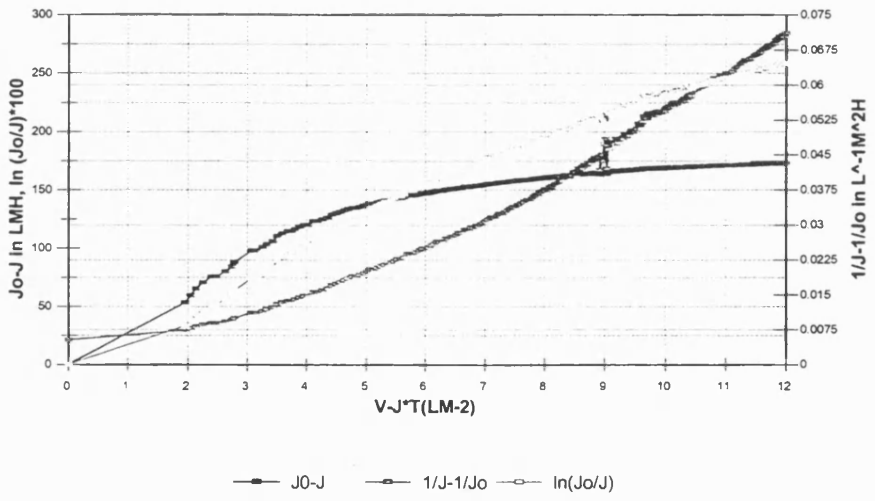

Figure 57 Model 3 results for *P.elodea* in low NaCl with BSA

P.elodea in High $CaCl_2$ with BSA

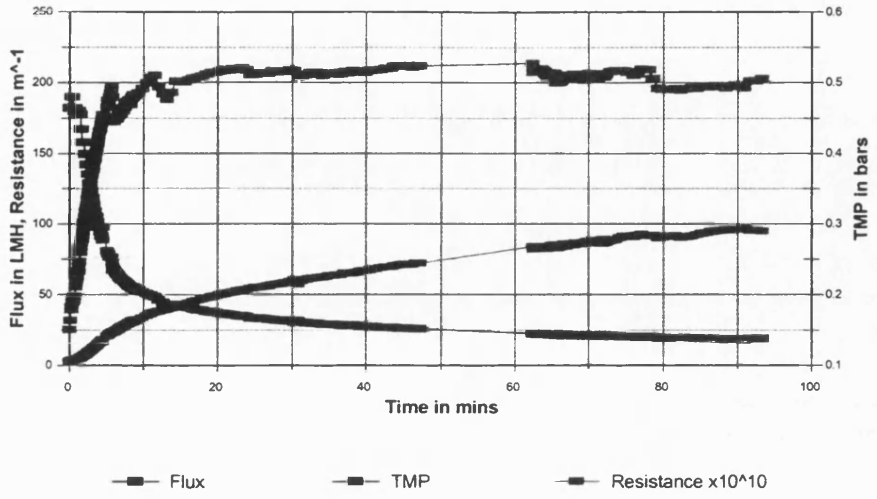

Figure 58 Comparison of TMP, flux and resistance for *P.elodea* in High $CaCl_2$ with BSA

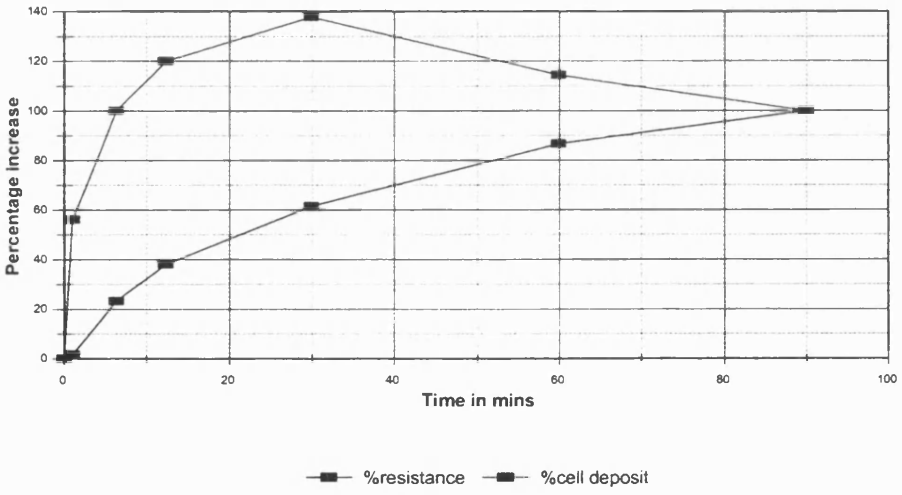

Figure 59 Comparison of percentage increases over time of resistance and cell deposition for *P.elodea* in High $CaCl_2$ with BSA

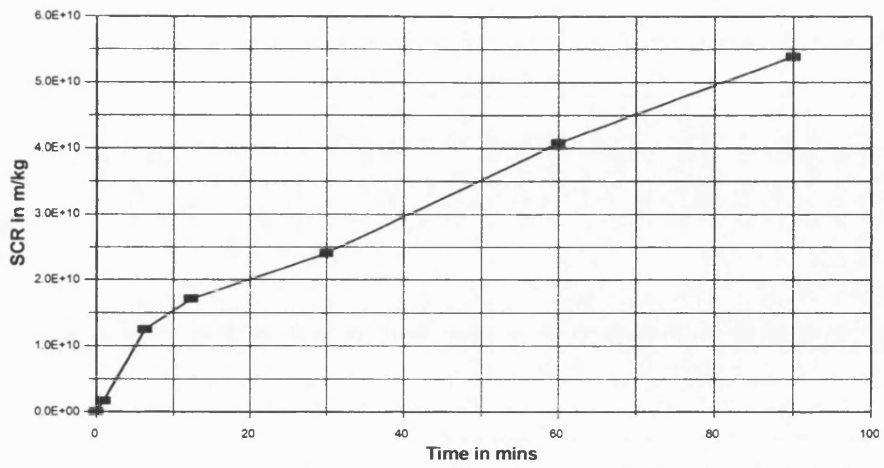

Figure 60 SCR change over time for *P.elodea* in High $CaCl_2$ with BSA

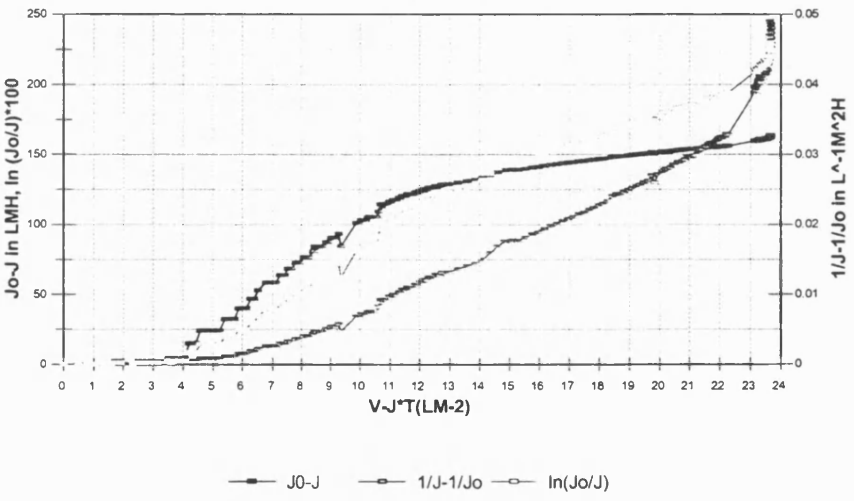

Figure 61 Model 3 results for *P.elodea* in High $CaCl_2$ with BSA

P.putida in Low NaCl

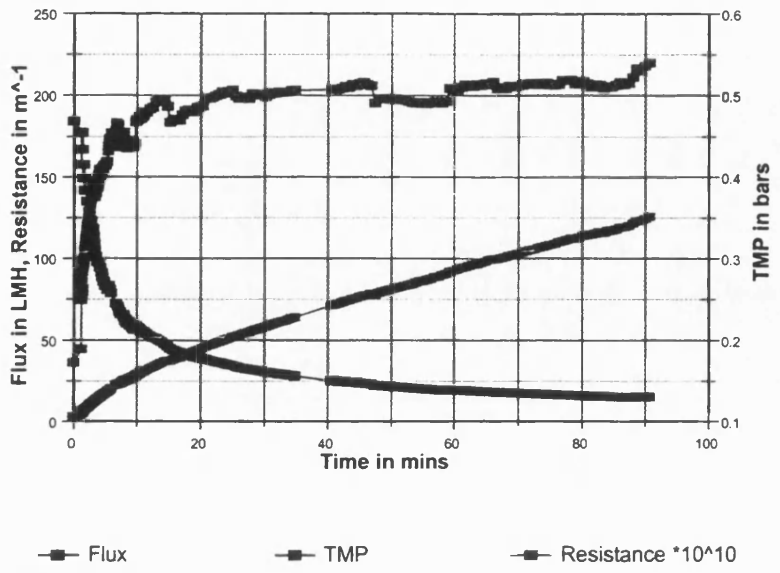

Figure 62 Comparison of TMP, flux and resistance for *P.putida* in low NaCl

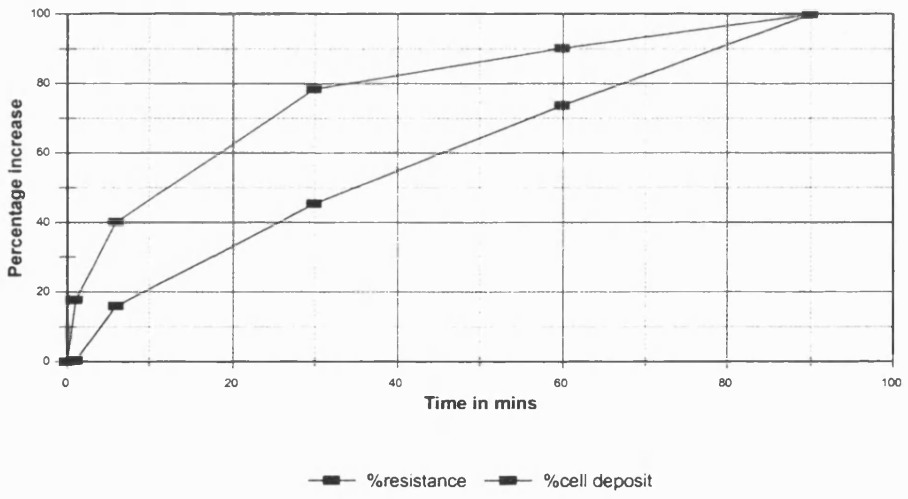

Figure 63 Comparison of percentage increases over time of resistance and cell deposition for *P.putida* in low NaCl

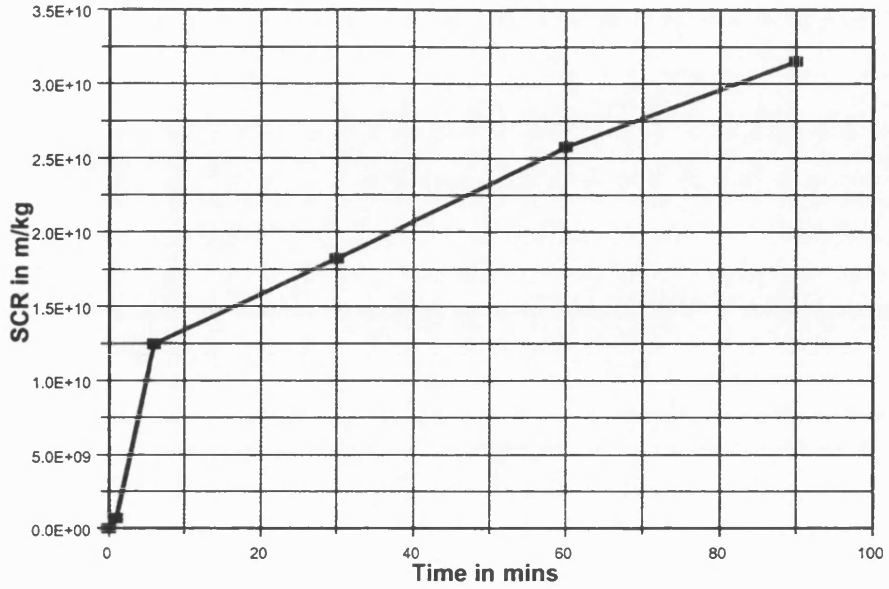

Figure 64 SCR change over time for *P.putida* in low NaCl

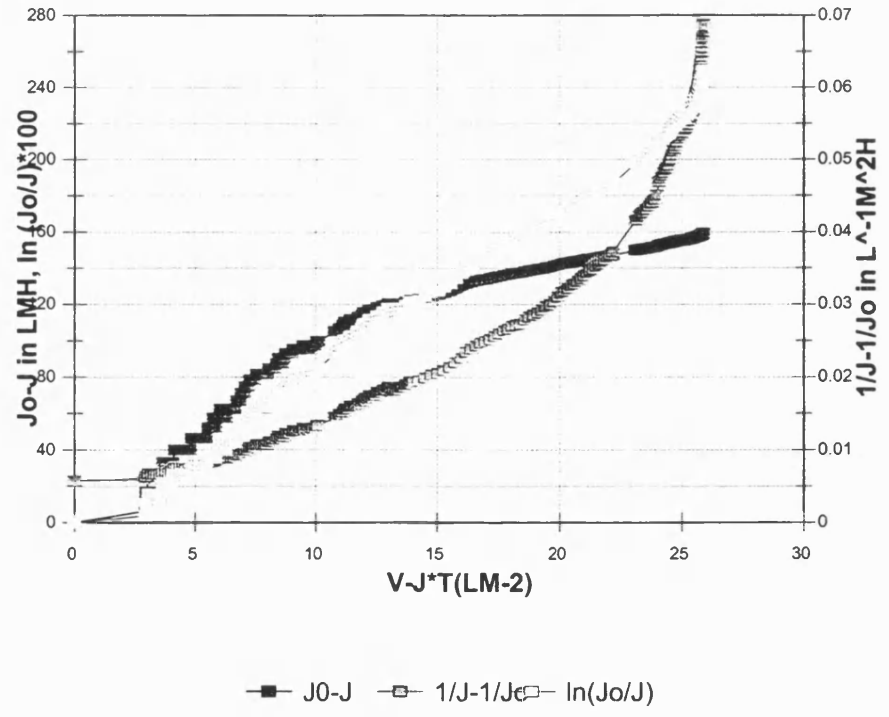

Figure 65 Model 3 results for *P.putida* in low NaCl

P.putida in High NaCl

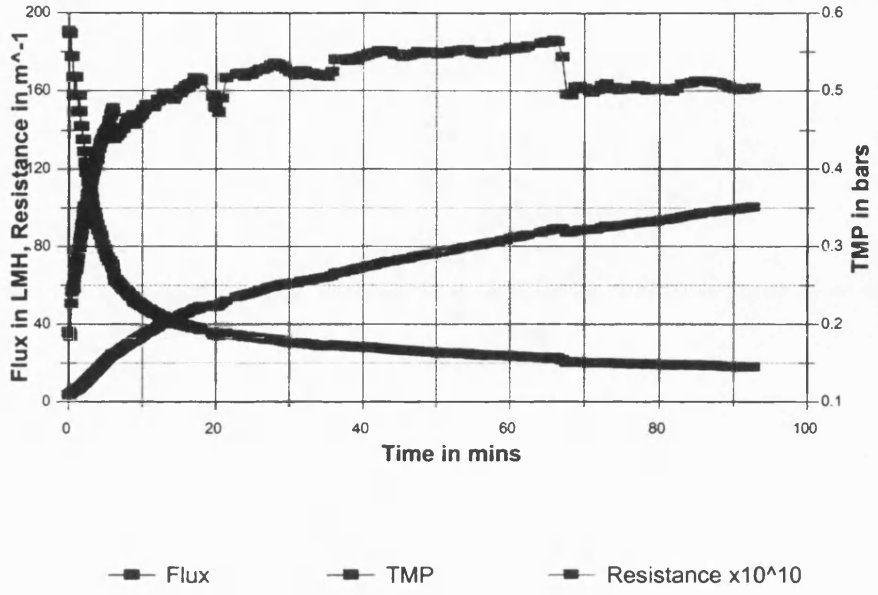

Figure 66 Comparison of TMP, flux and resistance for *P.putida* in high NaCl

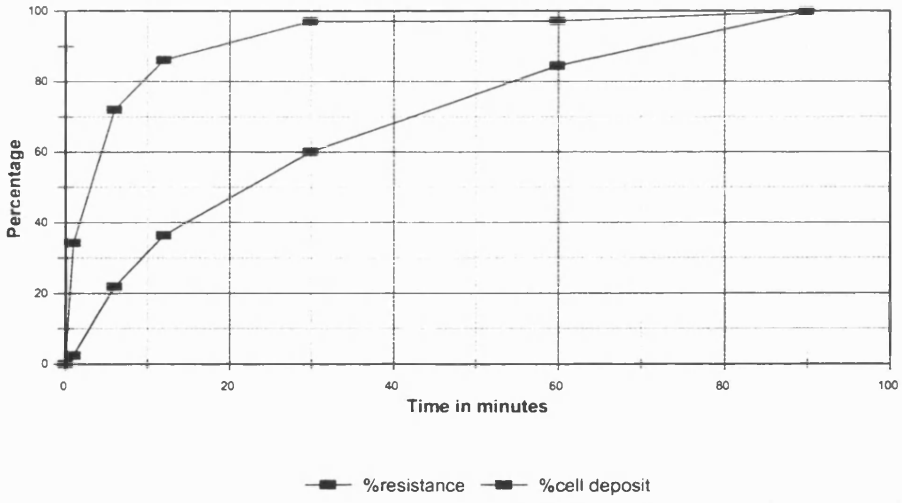

Figure 67

Figure 68 Comparison of percentage increases over time of resistance and cell deposition for *P.putida* in high NaCl

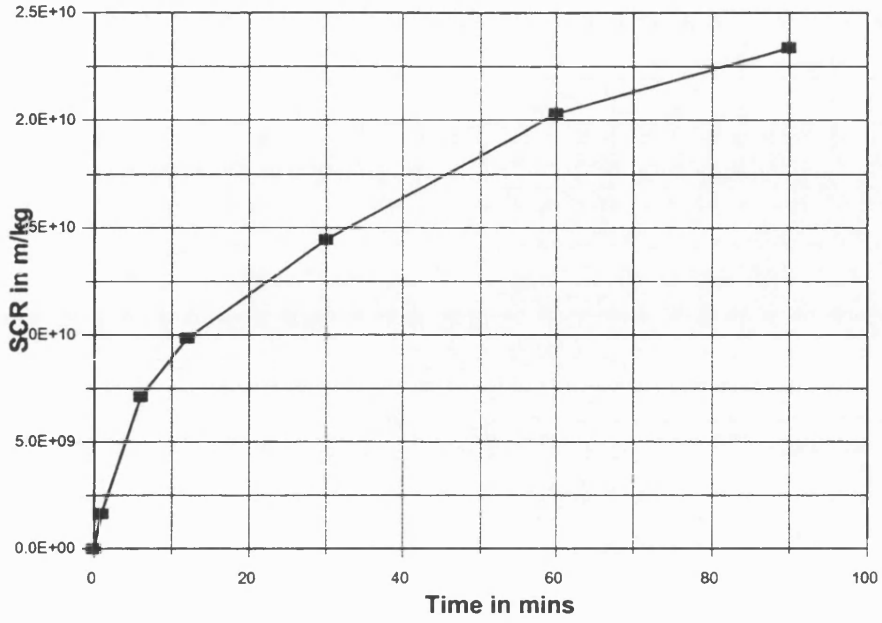

Figure 69 SCR change over time for *P.putida* in high NaCl

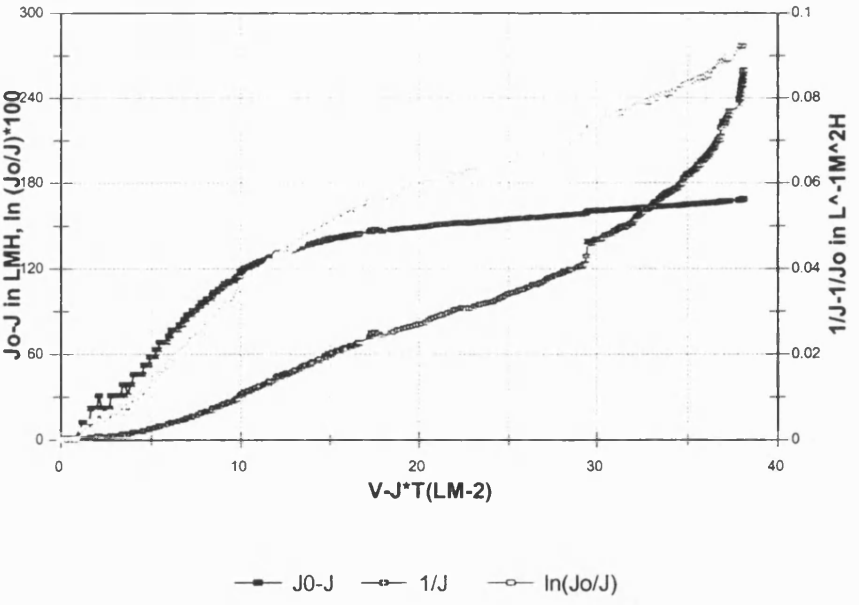

Figure 70 Model 3 results for *P.putida* in high NaCl

P.putida in Low $CaCl_2$

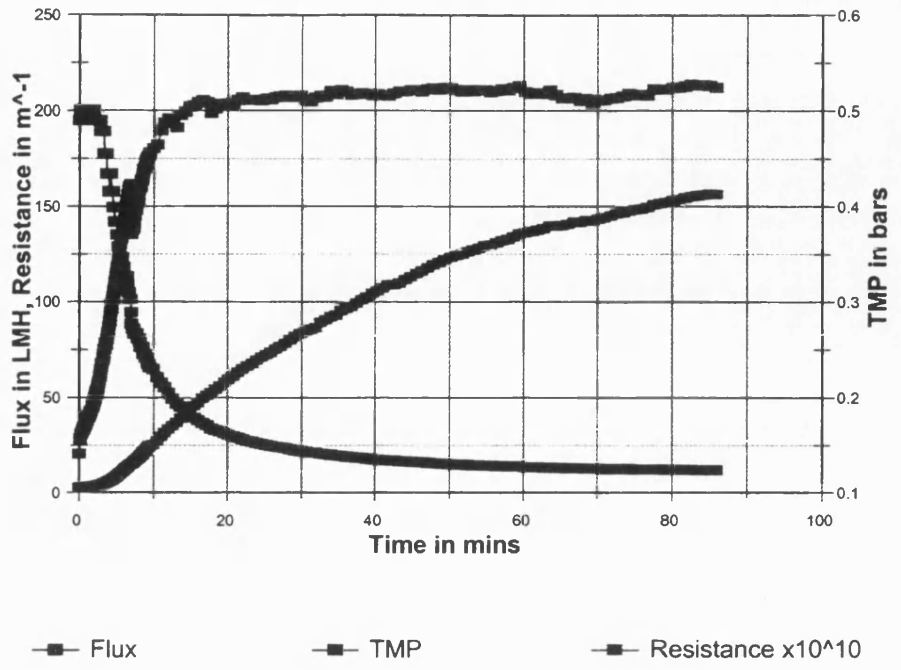

Figure 71 Comparison of TMP, flux and resistance for *P.putida* in low $CaCl_2$

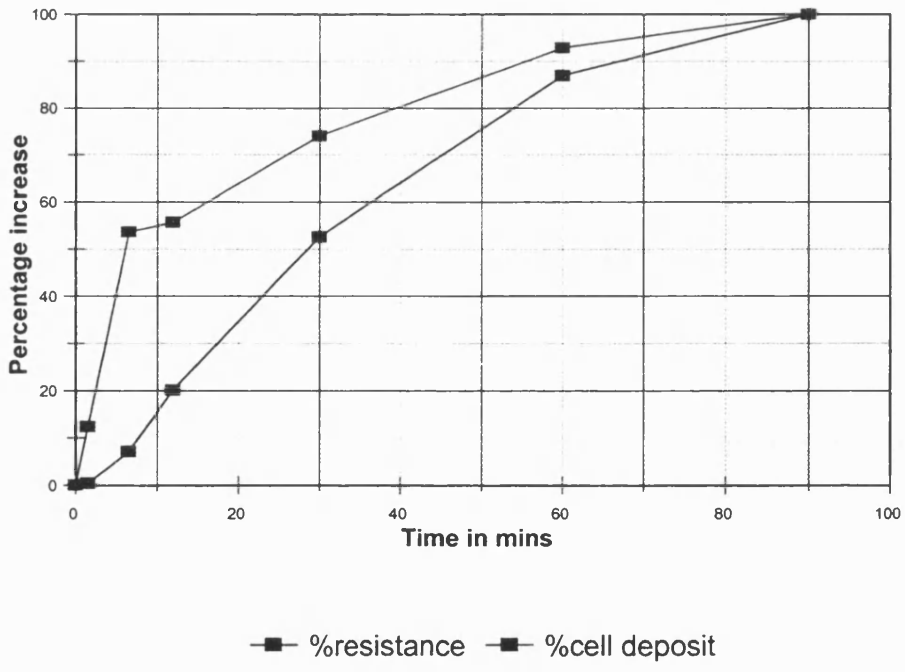

Figure 72 Comparison of percentage increases over time of resistance and cell deposition for *P.putida* in low $CaCl_2$

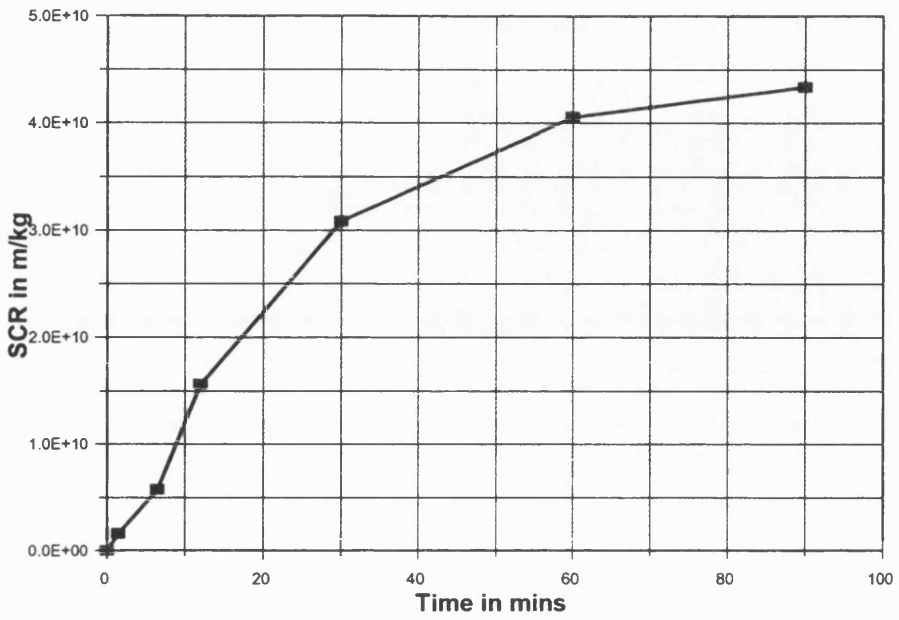

Figure 73 SCR change over time for *P.putida* in low $CaCl_2$

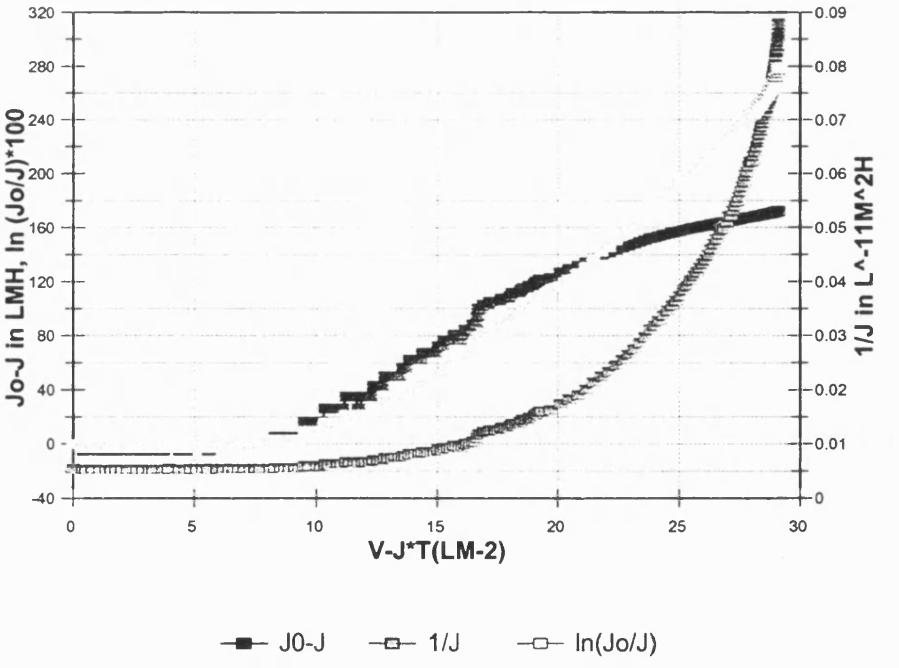

Figure 74 Model 3 results for *P.putida* in low $CaCl_2$

P.putida in High $CaCl_2$

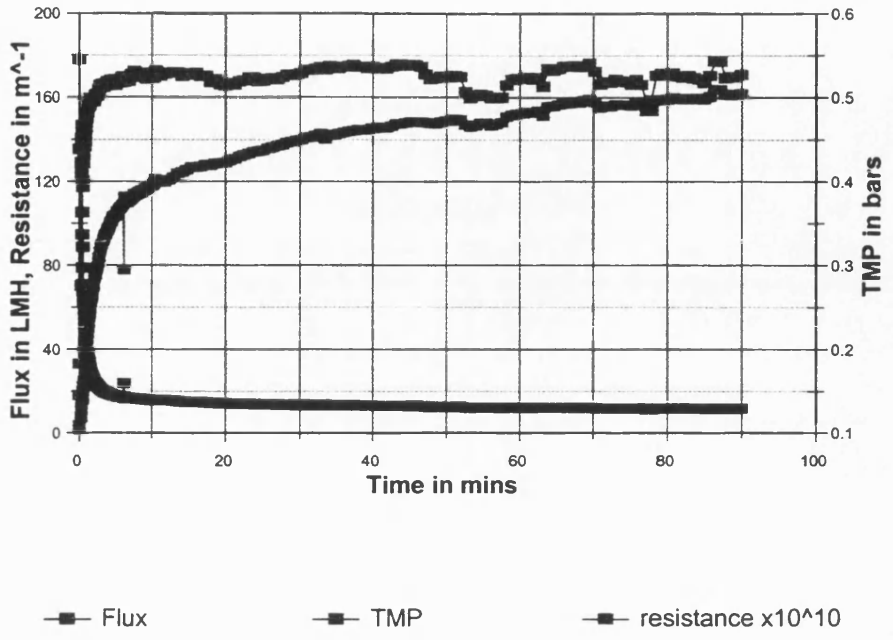

Figure 75 Comparison of TMP, flux and resistance for *P.putida* in High $CaCl_2$

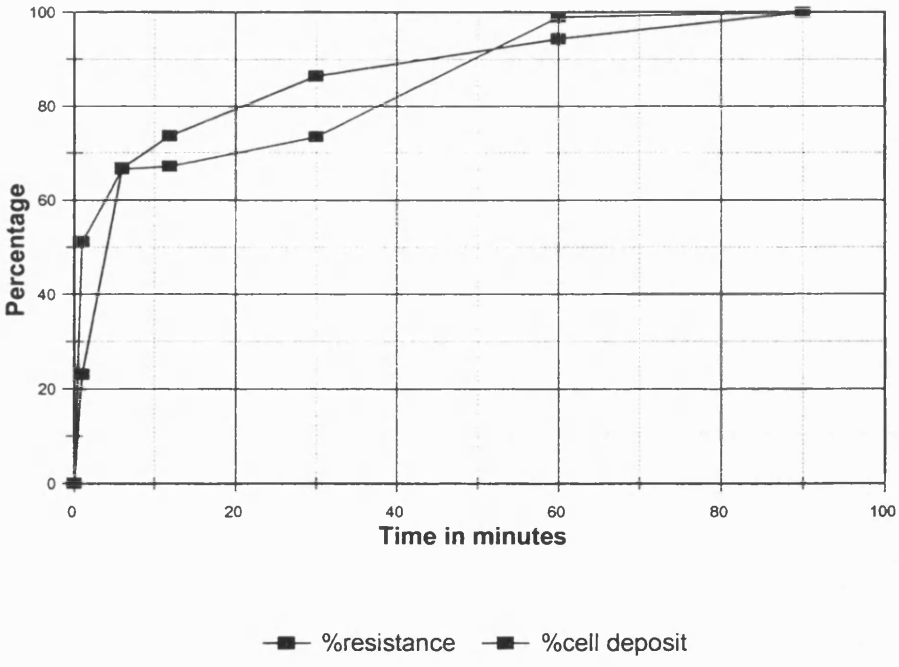

Figure 76 Comparison of percentage increases over time of resistance and cell deposition for *P.putida* in High $CaCl_2$

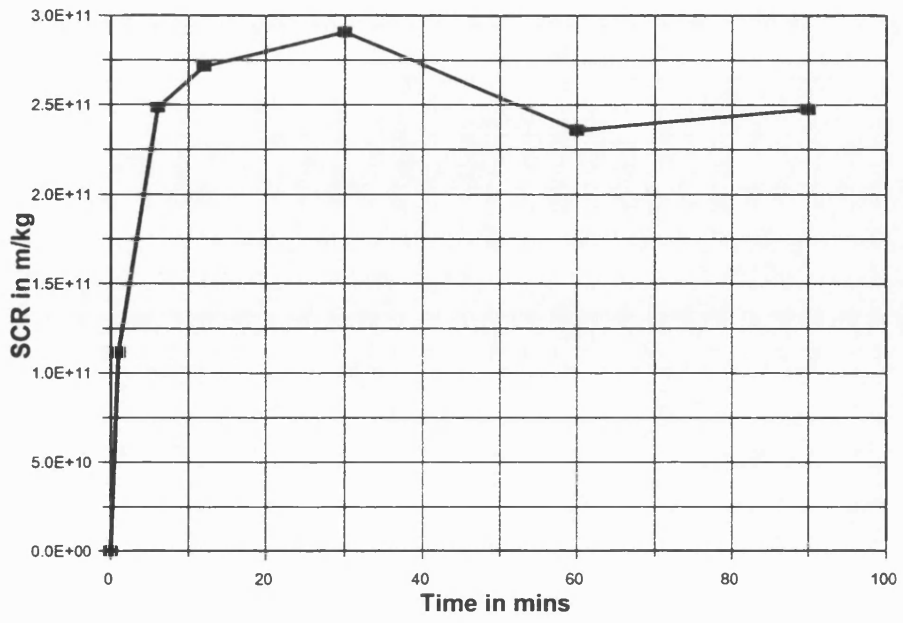

Figure 77 SCR change over time for *P.putida* in High $CaCl_2$

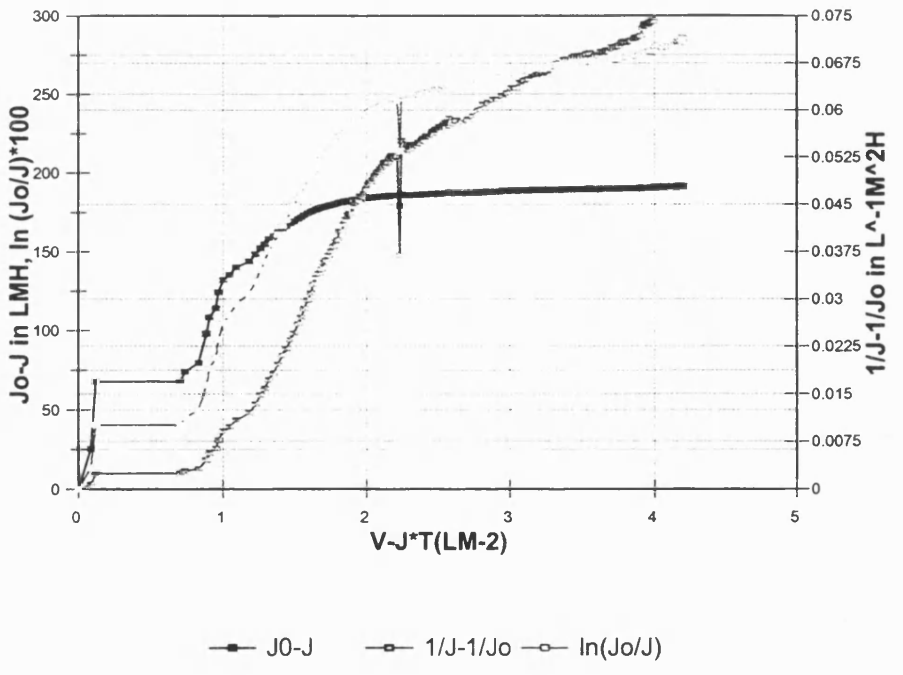

Figure 78 Model 3 results for *P.putida* in High $CaCl_2$

P.putida in Low NaCl with BSA

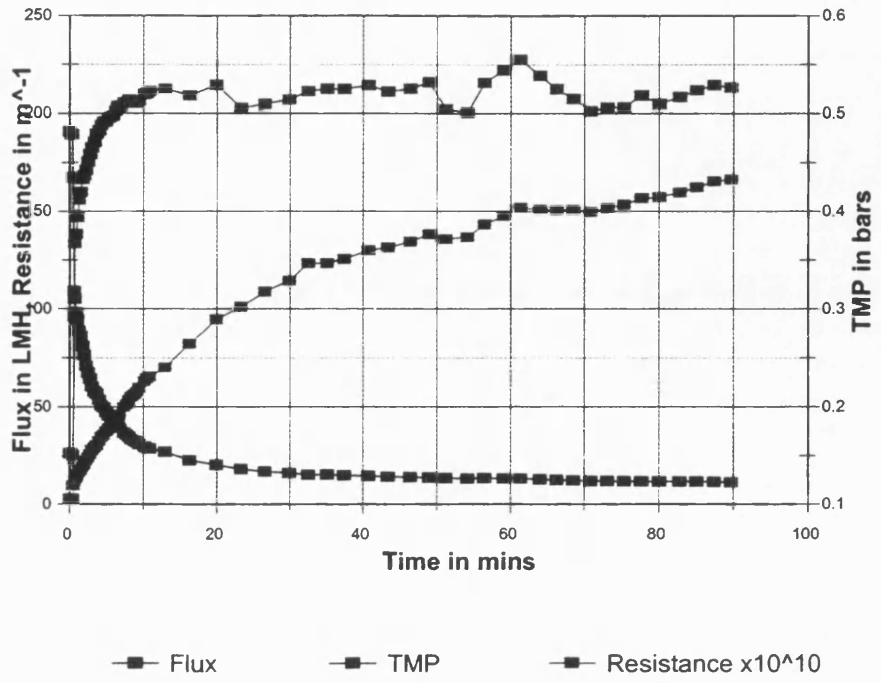

Figure 79 Comparison of TMP, flux and resistance for *P.putida* in Low NaCl with BSA

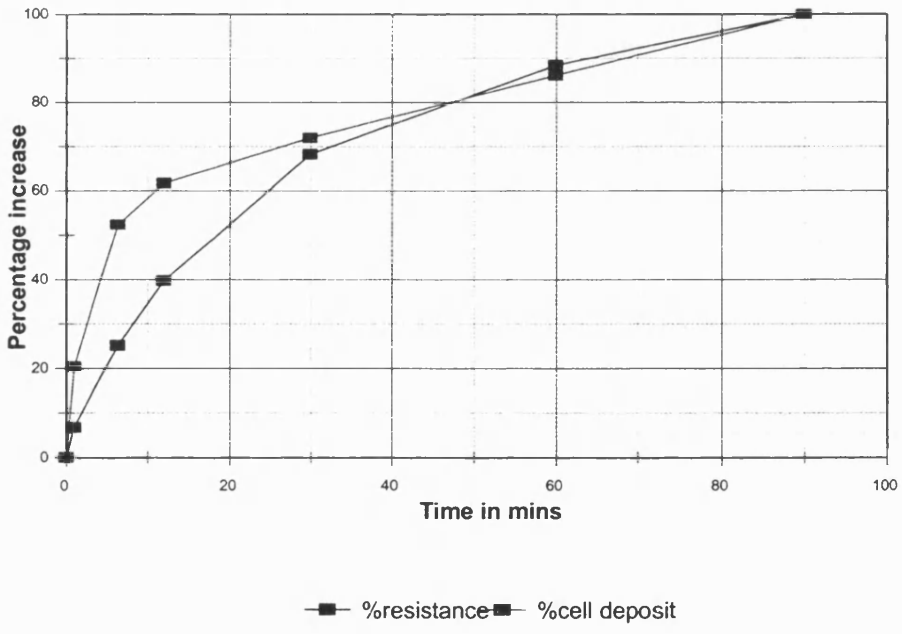

Figure 80 Comparison of percentage increases over time of resistance and cell deposition for *P.putida* in Low NaCl with BSA

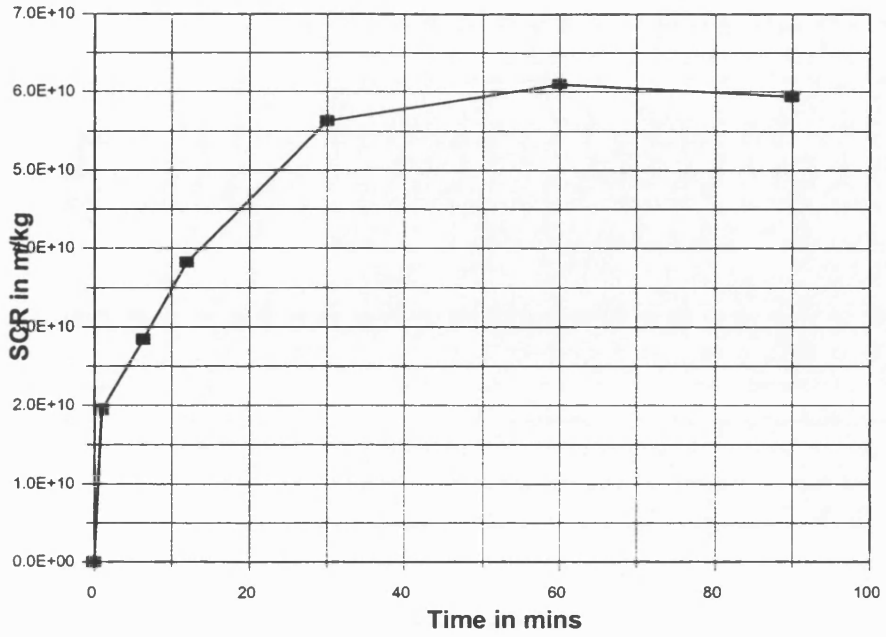

Figure 81 SCR change over time for *P.putida* in Low NaCl with BSA

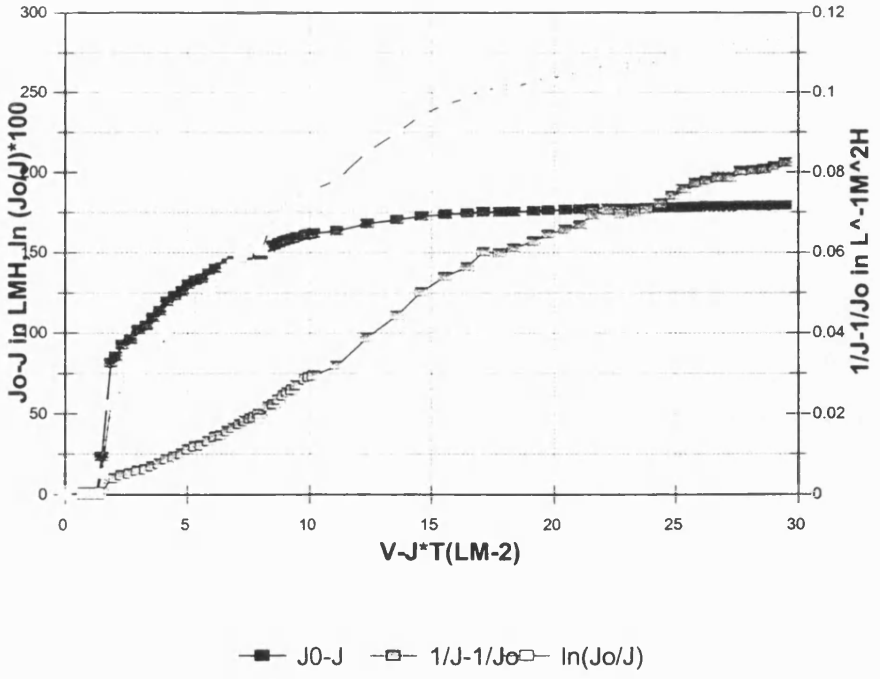

Figure 82 Model 3 results for *P.putida* in Low NaCl with BSA

P.putida in High NaCl with BSA

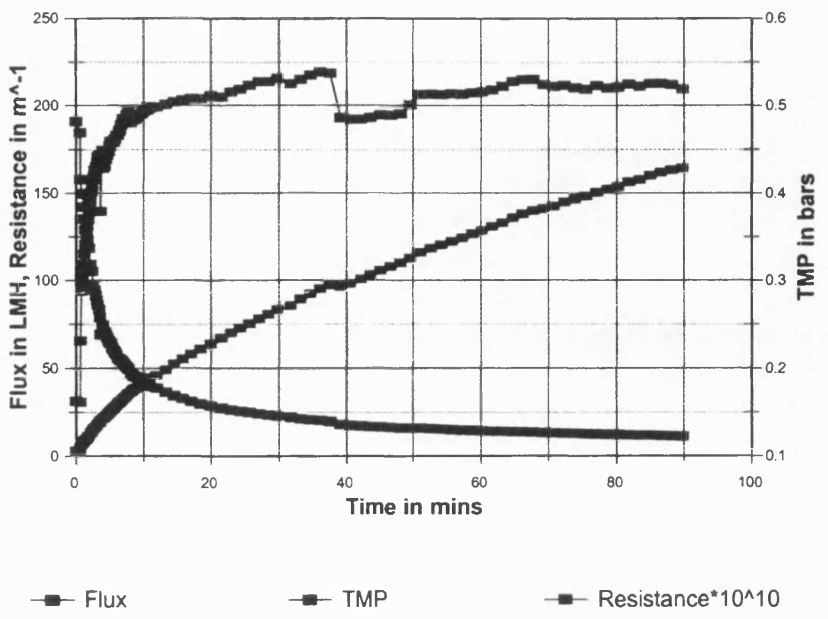

Figure 83 Comparison of TMP, flux and resistance for *P.putida* in High NaCl with BSA

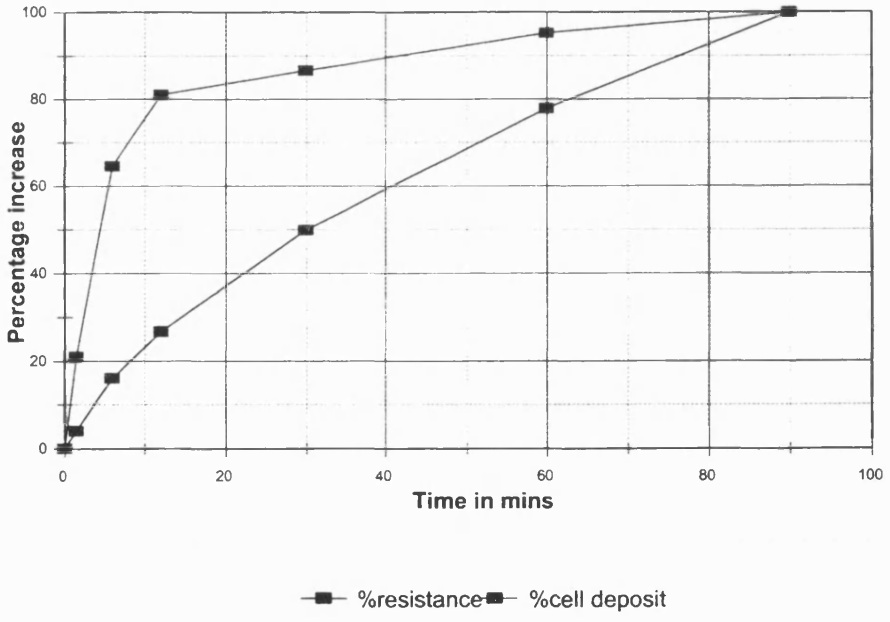

Figure 84 Comparison of percentage increases over time of resistance and cell deposition for *P.putida* in High NaCl with BSA

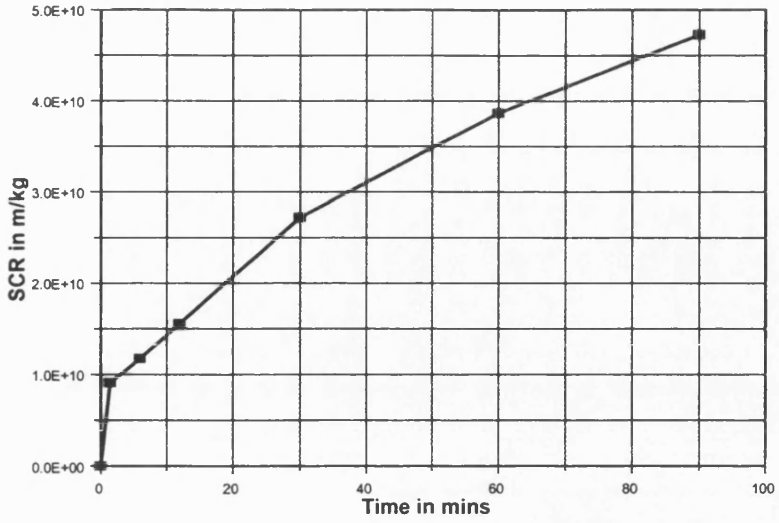

Figure 85 SCR change over time for *P.putida* in High NaCl with BSA

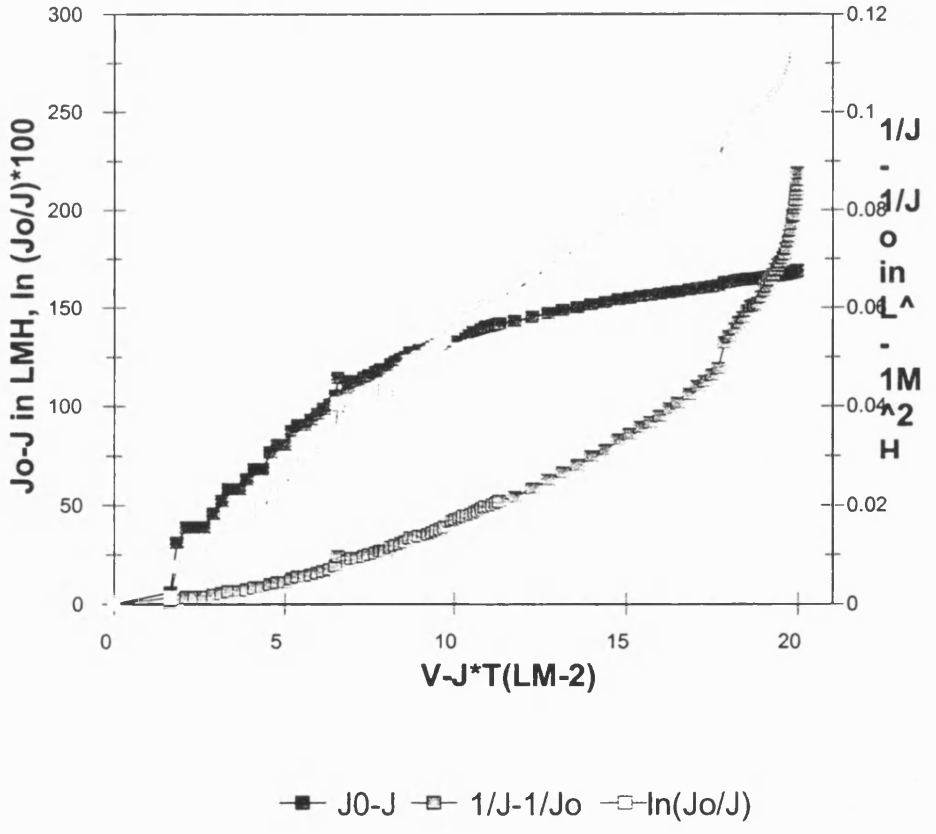

Figure 86 Model 3 results for *P.putida* in High NaCl with BSA

P.putida in High $CaCl_2$ with BSA

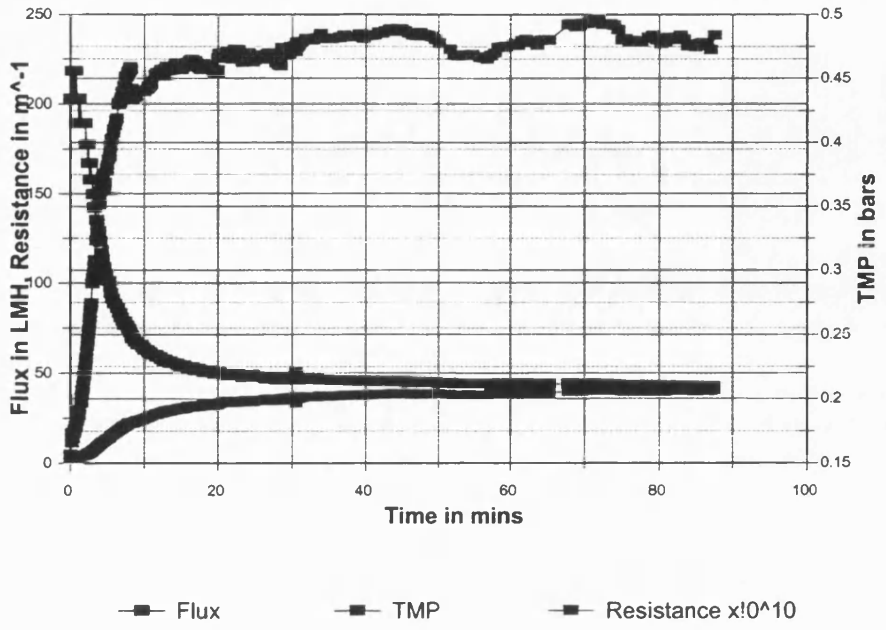

Figure 87 Comparison of TMP, flux and resistance for *P.putida* in high $CaCl_2$ with BSA

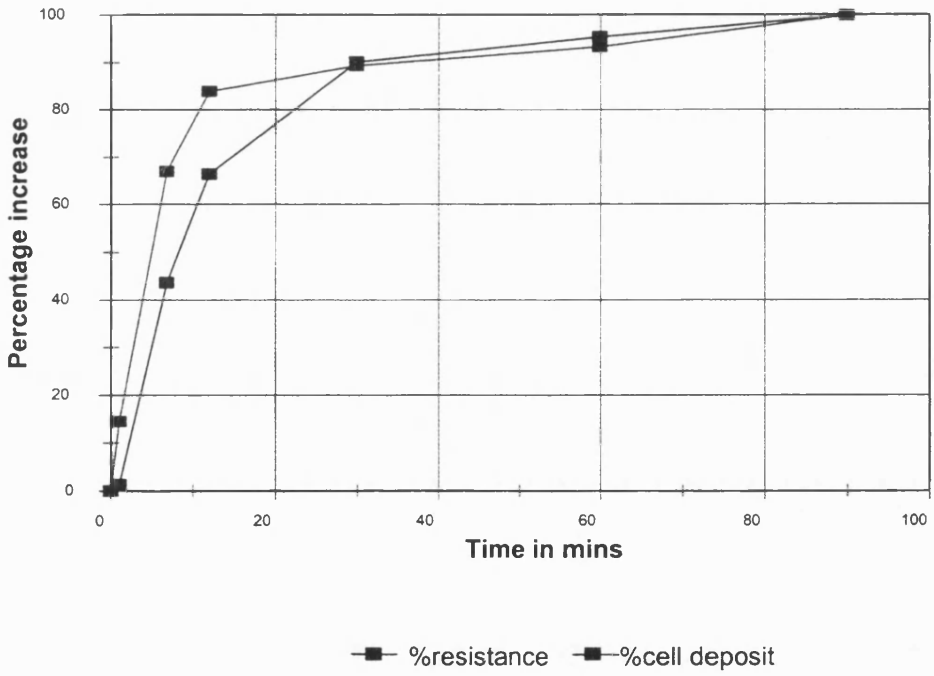

Figure 88 Comparison of percentage increases over time of resistance and cell deposition for *P.putida* in high $CaCl_2$ with BSA

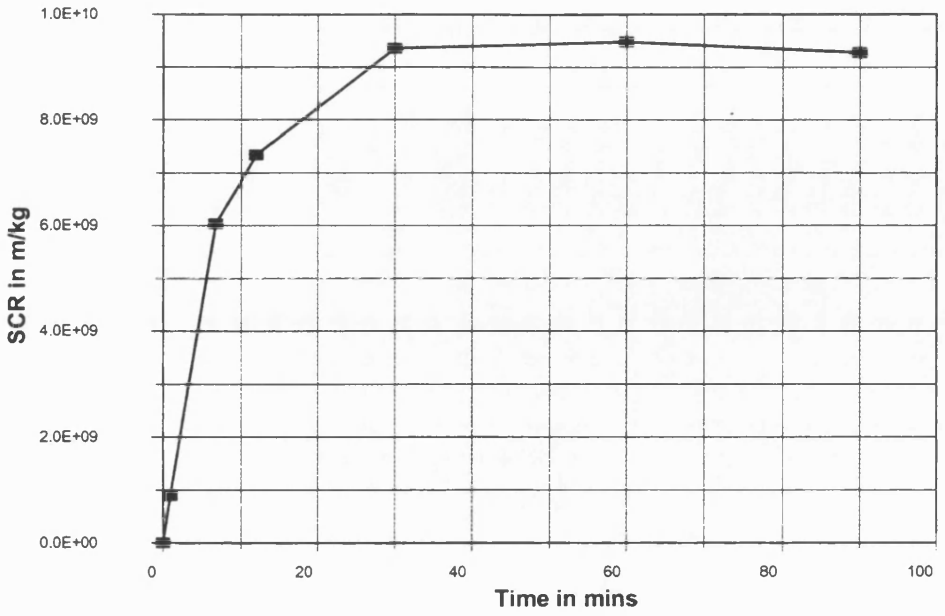

Figure 89 SCR change over time for *P.putida* in high $CaCl_2$ with BSA

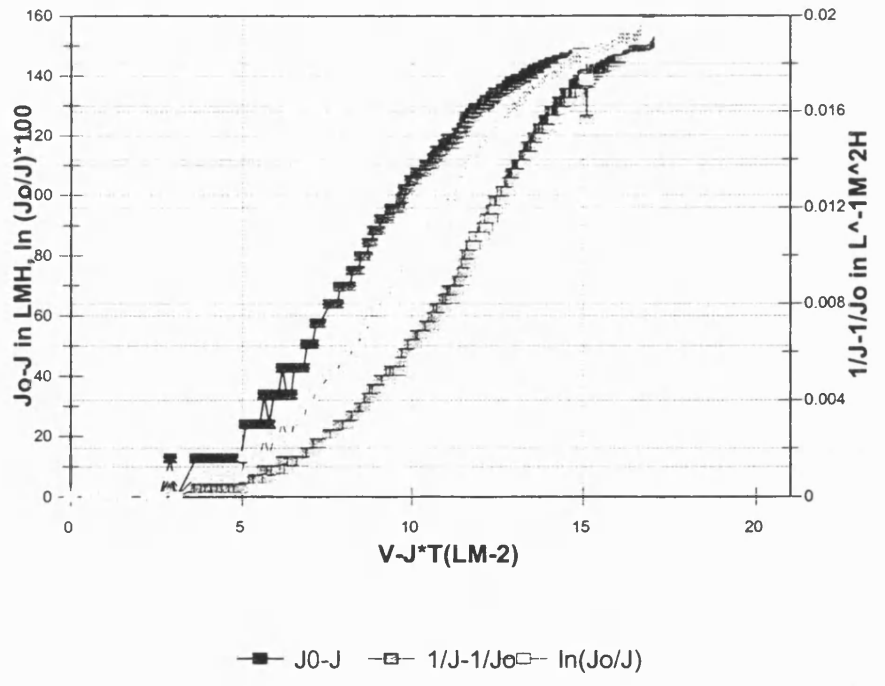

Figure .90 Model 3 results for *P.putida* in high $CaCl_2$ with BSA

Appendix D Calculation of Error for Resistance

According to Darcy's law, Resistance is calculated thus:

$$R = \frac{\Delta P}{\mu J}$$

Where ΔP= Transmembrane pressure

μ= Viscosity of permeate

J = Flux

The error in the estimated resistance measurement is calculated by using the deviations in ΔP and J. The error range in R is (over) estimated by finding the following:

$$Error(R) = \frac{\Delta P + Error(\Delta P)}{\mu J - Error(J)} - \frac{\Delta P - Error(\Delta P)}{\mu J + Error(J)}$$

The error for transmembrane pressure is 5%. The error for flux is taken to be 2%

Using these figures and sample experimental data, the maximum error for the resistance was found to be approximately +/- 7%.

Appendix E Protein and cell concentration changes during experiments

Low NaCl

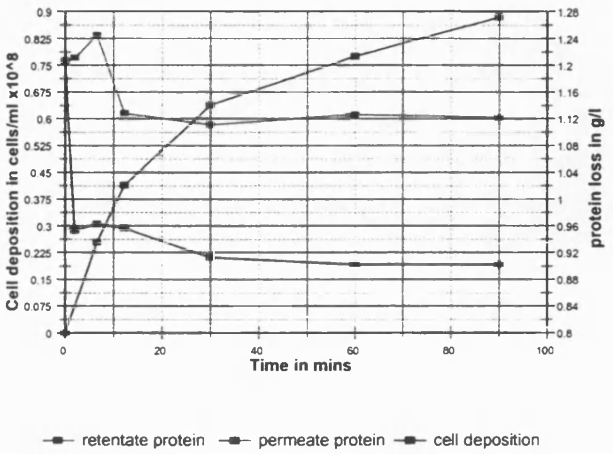

Figure 91 Protein and cell concentration changes for S. multivorum in low NaCl

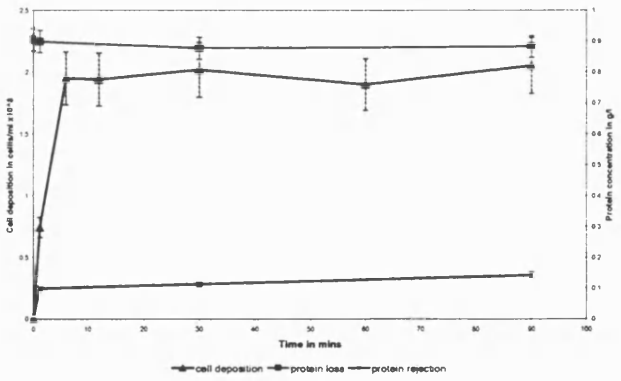

Figure 92 Protein and cell concentration changes for *P.elodea* in low NaCl

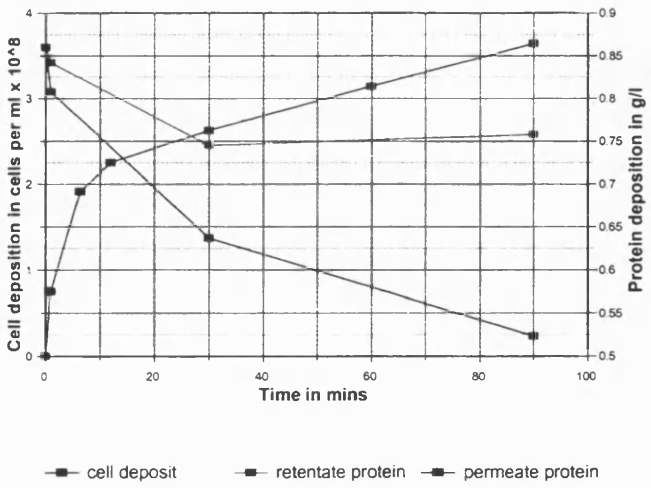

Figure 93 Protein and cell concentration changes for *P.putida* in low NaCl

High NaCl

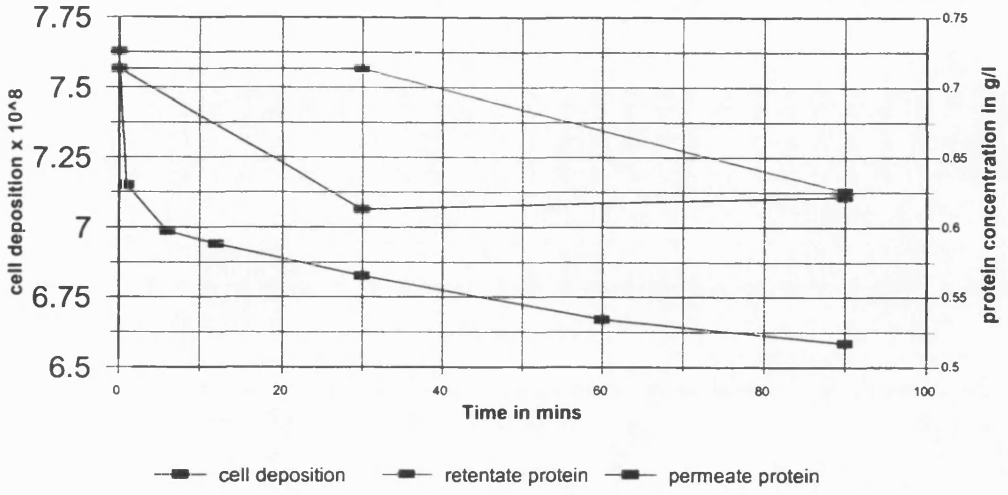

Figure 94 Protein and cell concentration changes for *S.multivorum* in high NaCl

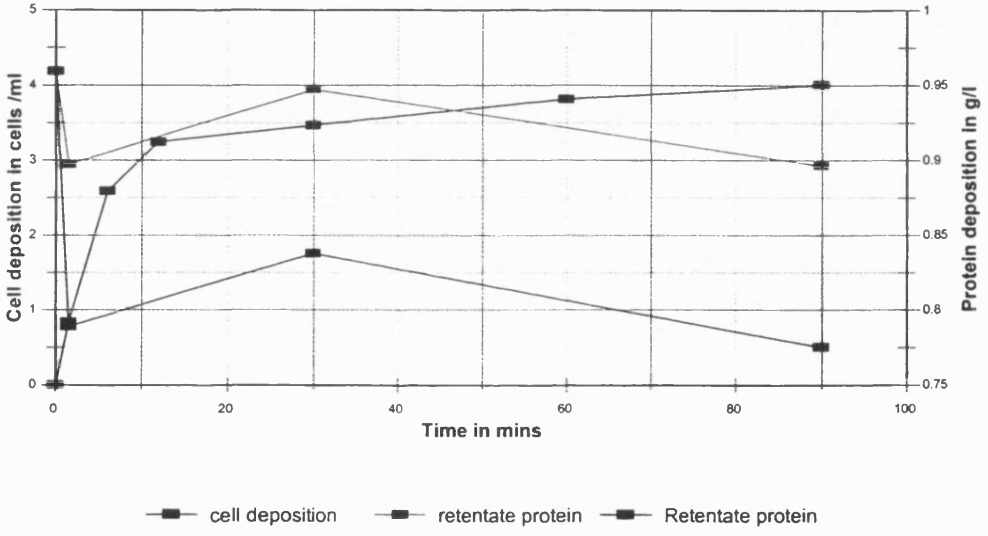

Figure 95 Protein and cell concentration changes for *P.putida* in high NaCl

High $CaCl_2$

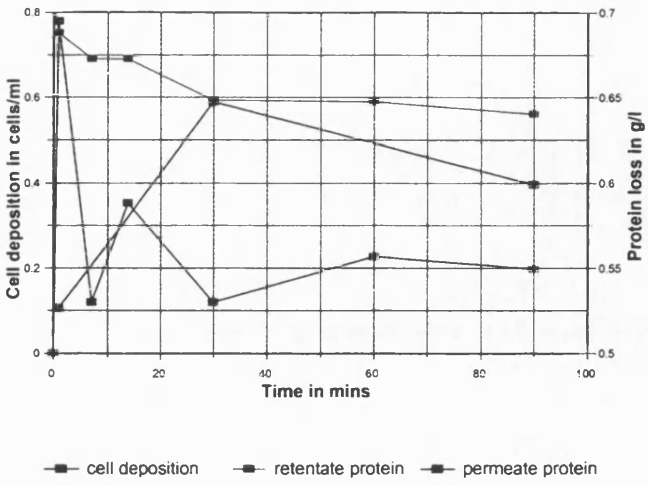

Figure 96 Protein and cell concentration changes for *S.multivorum* in high $CaCl_2$

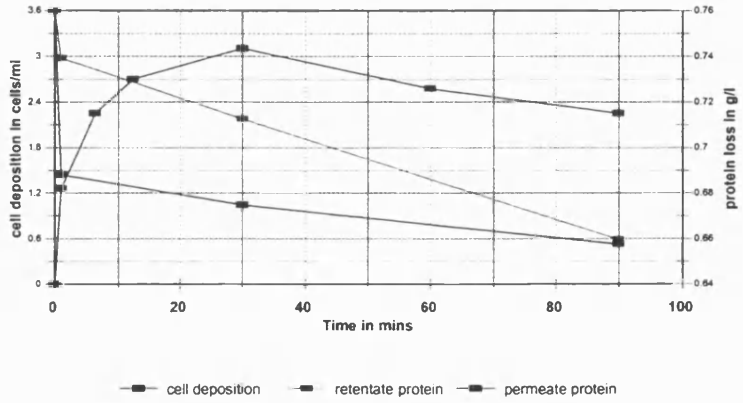

Figure 97 Protein and cell concentration changes for *P.elodea* in high $CaCl_2$

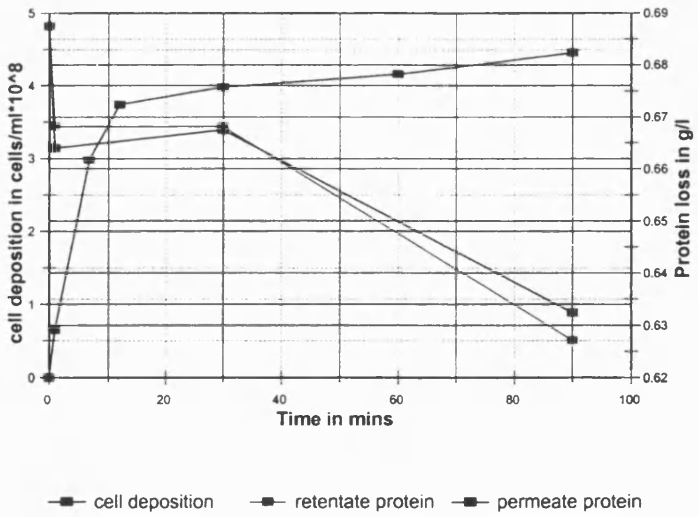

Figure 98 Protein and cell concentration changes for *P.putida* in high $CaCl_2$